



TECHNISCHE UNIVERSITÄT MÜNCHEN

TUM School of Life Sciences

**Turbidity identification in Beer
using Raman micro-spectroscopy (RMS)**

Eva-Maria Kahle

Vollständiger Abdruck der von der TUM School of Life Sciences der Technischen Universität München zur Erlangung des akademischen Grades einer

Doktorin der Ingenieurwissenschaften (Dr.-Ing.)

genehmigte Dissertation.

Vorsitzender: Prof. Dr. Harald Luksch

Prüfer der Dissertation: 1. Hon.-Prof. Dr.-Ing. Friedrich Jacob
2. Prof. Dr.-Ing. Dirk Weuster-Botz

Die Dissertation wurde am 01.10.2021 bei der Technischen Universität München eingereicht und durch die TUM School of Life Sciences am 22.03.2022 angenommen.

Man kann eine Grenze nur erkennen,
wenn man sie zu überschreiten versucht.
(Heinrich Böll)

Acknowledgments

First of all, I would like to thank Prof. Dr.-Ing. Fritz Jacob for providing this outstanding topic, his support throughout the last four years.

Furthermore, I would like to thank Prof. Dr.-Ing. Dirk Weuster-Botz and Univ.-Prof. Dr. rer. nat. Harald Luksch for acting as chief examiner.

A great support throughout this time was my supervisor, Dr. Martin Zarnkow. Thank you for outstanding discussions, great talks, many ideas, reviewing my papers and helping whenever needed.

A big thank you goes to my ex-student and colleague Luis Raihofer for his proofreading and helpful tips. A big thank you goes out to my colleagues Dr. Hubertus Schneiderbanger, Dario Cotterchio, Hubert Walter, Korbinian Haslbeck, Robert Riedl, Florian Mallok, Dominik Stretz, Friedl Ampenberger, Sebastian Hans, Dr. Mathias Hutzler, Tim Meier-Dörnberg, Maximilian Michel and Yvonne Methner, for their collaboration, help and highly valuable discussions.

As this dissertation includes many analyses that would not have been possible without the support of many of the employees of the Research Center Weihenstephan I want to thank all employees for their great support.

Many students supported me during my research with their Diplom, Bachelor's or Master's theses. I would like to offer thanks to Ludwig Gerlinger, Tobias Kretzer, Andreas Laus, Robert Mooser, Luis Raihofer, Joseph Heintges, Claudia Graf, Alice Sawicki und Nils Behnke.

My last thank you is dedicated to Sarah Silva who helped with quality editing of my English when needed.

I want to dedicate this work to my beloved family ♥.

Preface and peer reviewed publications

The results and publications of this thesis were obtained at the Technical University of Munich, Research Center Weihenstephan for Brewing and Food Quality from 2017 to 2020. This thesis includes the following five peer-reviewed publications with first authorship. A list of all the contributed peer-reviewed papers, non-reviewed papers, oral and poster presentations can be found in Chapter 5.

1. Kahle, E.M., Zarnkow, M., Jacob, F. (2020) **“Beer Turbidity Part 1: A Review of Factors and Solutions”** Journal of the American Society of Brewing Chemists, DOI: 10.1080/03610470.2020.1803468
2. Kahle, E.M., Zarnkow, M., Jacob, F. (2020) **“Beer Turbidity Part 2: A Review of Raman Spectroscopy and Possible Future Use for Beer Turbidity Analysis”** Journal of the American Society of Brewing Chemists, DOI: 10.1080/03610470.2020.1800345
3. Kahle, E.M., Zarnkow, M., Jacob, F. (2019) **“Substances in beer that cause fluorescence: evaluating the qualitative and quantitative determination of these ingredients.”** European Food Research and Technology, 245(12), 2727-2737
DOI: 10.1007/s00217-019-03394-x
4. Kahle, E.M., Zarnkow, M., Jacob, F. (2020) **“Investigation and identification of foreign turbidity particles in beverages via Raman micro-spectroscopy”** European Food Research and Technology **247**, 579–591 (2021)
DOI: 10.1007/s00217-020-03647-0
5. Kahle, E.M., Zarnkow, M., Jacob, F. (2020) **“Identification and differentiation of haze substances using Raman microspectroscopy”** Journal of the Institute of Brewing, DOI 10.1002/jib.627

Contents

Acknowledgments.....	II
Preface and peer reviewed publications.....	III
Contents	IV
List of Tables.....	VI
List of Figures.....	VI
Eidesstattliche Erklärung.....	VII
Notations.....	VIII
Summary	- 1 -
Zusammenfassung.....	- 3 -
1 Introduction and motivation	- 5 -
1.1 Raman micro-spectroscopy	- 7 -
1.1.1 History of Raman spectroscopy	- 7 -
1.1.2 Raman effect	- 7 -
1.1.3 Design and function of a Raman spectrometer	- 9 -
1.1.4 Interpretation of Raman spectra	- 11 -
1.2 Fluorescence and Raman.....	- 11 -
1.2.1 Methods of fluorescence avoidance	- 12 -
1.2.2 Further methods	- 14 -
1.3 Turbidity.....	- 15 -
1.3.1 Types and origin	- 16 -
2 Results (Thesis publications)	- 19 -
2.1 Summary of results.....	- 19 -
PART 1	- 20 -
2.2 Beer Turbidity Part 1: A Review of Factors and Solutions.....	- 20 -
PART 2	- 37 -
2.3 Beer Turbidity Part 2: A Review of Raman Spectroscopy and Possible Future Use for Beer Turbidity Analysis	- 37 -
PART 3	- 61 -
2.4 Substances in beer that cause fluorescence: evaluating the qualitative and quantitative determination of these ingredients.	- 61 -
PART 4	- 73 -
2.5 Investigation and identification of foreign turbidity particles in beverages via Raman micro-spectroscopy	- 73 -
PART 5	- 87 -

2.6	Identification and differentiation of haze substances using Raman micro-spectroscopy	- 87 -
3	Discussion	- 97 -
5	Appendix.....	- 107 -
5.1	Oral presentations with first authorship	- 107 -
5.2	Poster presentations with first authorship	- 107 -
5.3	Non-reviewed papers	- 107 -
5.4	Permission of publishers for imprints of publications	- 108 -
	References.....	- 111 -

List of Tables

Table 1 Short overview of the five publications with title of the publication, major objective, applied method and main findings.....	- 19 -
Table 2 Quality of pure substance spectra.....	- 103 -

List of Figures

Figure 1 Emergence of Rayleigh, Stokes, and anti-Stokes scattering	- 8 -
Figure 2 Schematic structure of a Raman spectrometer	- 10 -
Figure 3 Schematic structure of the Raman micro-spectroscopy system used.....	- 10 -
Figure 4 Time course of fluorescence and Raman scattering	- 14 -
Figure 5 Various origins of turbidity and foreign particles that can lead to “visible turbidity”	- 15 -
Figure 6 Dendrogram of all pure substance and beer contact spectra at 532 nm.....	- 102 -

Notations

AFM	Atomic force microscopy
CARS	Coherent Anti-Stokes Raman Scattering
CCD	Charge-coupled device
CDOM	Colored fraction of DOC
DOC	Dissolved organic carbon
DOM	Dissolved organic matter
EEM	Excitation emission matrix
FTIR	Fourier-transform infrared spectroscopy
IR	Infrared spectroscopy
MP	Microplastic particle
NIR	Near-infrared spectroscopy
nm	Nanometer
OC	Organic carbon
PARAFAC	PARAllel FACtor analysis
PVPP	Polyvinylpolypyrrolidone
RMS	Raman micro-spectroscopy
RS	Raman spectroscopy
SERS	Surface-enhanced Raman spectroscopy
TERS	Tip-enhanced Raman spectroscopy
UV	Ultraviolet

Summary

The identification of turbidity particles is an important part of brewery analysis. Beer turbidity can result from different problems or causes throughout the brewing process. To find the origin of the turbidity, it is important to know its composition. Current turbidity analysis are usually based on optical, microscopic or enzymatic methods, which are often inaccurate or costly and time-consuming. Turbidity in beer remains a significant issue in the beverage industry. Many origins of turbidity have already been researched, though it is not always possible to identify the immediate cause. Along with beer foam, gloss fineness is one of the most important visual quality characteristics of filtered beer. Cloudiness, opalescence, or a milky appearance in beverages is usually undesirable and leads the consumer to suspect that the product is of lower quality or even product spoilage. Many different types of formation or introduction of substances can cause turbidity, which can be divided into two main categories:

1. Beverage-specific: ingredients cause an interaction
2. External influences such as process defects or particles interacting with the medium

In this research, Raman micro-spectroscopy (RMS) was used for the first time to detect specific turbidity particles in beer. This method allows the chemical composition of the molecules under investigation to be clearly identified. The main attention in this work was devoted to the particles that can cause the strongest and also the most intense turbidity. As a basic prerequisite for developing a method of turbidity identification via RMS, it was first necessary to investigate the behavior of the medium beer under laser. Since beer contains a large number of fluorescent constituents, an investigation was carried out with the aim of identifying the most intensively fluorescent compounds and bypassing them in further steps. In the subsequent work package, which builds on the fluorescence analysis, foreign particles (e.g. filter aids, stabilizers and various microplastic particles), but also beer's own particles (polyphenols like catechin, proteins like gliadin, β -glucans, calcium oxalate and starch) were detected, evaluated and validated. Appropriate sample preparation allowed membrane filters to be tested and a filtration method to isolate individual particles to be established and implemented. Cluster analyses and similarity matrices were used for identification and validation, respectively, and to better represent the particles. By analyzing the sample components in different media (dry, fluid (water, beer)) the influences could be distinguished.

The filtration residue after membrane filtration has also been analyzed. Two-dimensional image scanning of particles was used to determine particle homogeneity. Raman spectra were recorded by acquiring single point scans. Two different lasers with wavelengths of 532 nm and 785 nm were used to test their applicability for identifying potentially haze-forming particles. The polyvinylpyrrolidone (PVPP) spectra in the different media showed similarities of more than 80 %, usually more than 95 %. The cellulose fiber spectra showed no differences between the various media, but consistently showed high average similarities of 94.5%. The carbohydrates starch, arabinoxylan, cellulose, yeast β -glucan and barley β -glucan, as well as gliadin, ferulic acid, proline, glutamine, calcium oxalate and PVPP were identified at a wavelength of 532 nm. The same substances were analyzed at a wavelength of 785 nm, which resulted in problems with weak carbohydrate spectra of yeast β -glucan, barley β -glucan, and arabinoxylan. All other substances were analyzed with a 785 nm wavelength laser. The β -glucans of yeast and barley could be clearly identified and classified. In addition, catechin, which produced much fluorescence noise when measured at 532 nm, could be identified at 785 nm. The major problem with RMS in relation to beer analysis is the intense fluorescence noise of some beer ingredients. Since beer contains a large amount of fluorescent ingredients, an investigation was carried out in the first research unit (Chapter 2.2) to find out which compounds exhibit the strongest fluorescence in order to be able to process these substances specifically. Special procedures have been used and tested that can circumvent the fluorescence problem. Within the scope of this research work, the enormous potential of RMS for turbidity identification could be highlighted. The developed methods can be adapted in further projects for an extension of RMS to beverage analysis. In this dissertation a method for RMS was established to detect, evaluate and validate foreign beer particles. At the beginning of the work, fluorescent substances were examined by fluorescence spectroscopy. These compounds interfere with the Raman signals and can prevent analysis. A suitable sample preparation was developed, membrane filters were tested and a filtration method for isolating the individual particles was established and implemented. To identify particles with RMS and for better representation, particles were selected and the results validated using cluster analysis and the similarity matrix. The biggest issue with RMS in beer analytics is the intense fluorescence noise of some beer ingredients. Special procedures were used and tested to get around the fluorescence problem. Nevertheless, RMS has enormous potential in haze analytics and throughout the brewery.

Zusammenfassung

Die Identifizierung von Trübungspartikeln ist ein wichtiger Bestandteil der Brauereianalytik. Trübung kann das Ergebnis vieler verschiedener Probleme bzw. Ursachen im gesamten Brauprozess sein. Um den Ursprung einer Trübung zu finden, ist es wichtig, die Zusammensetzung von dieser zu kennen. Derzeit angewandte Trübungsanalytik basiert in der Regel auf optischen, mikroskopischen oder enzymatischen Methoden, die oft ungenau oder aufwendig und zeitintensiv sind. Die Trübung in Bier ist nach wie vor ein bedeutendes Thema in der Industrie, da viele Ursprünge des Trübungsbildes zwar bereits entdeckt wurden, es aber nicht immer möglich ist, die unmittelbare Trübungsursache zu identifizieren. Neben dem Schaum zählt die Glanzfeinheit zu einem der wichtigsten visuellen Qualitätsmerkmale von gefilterten Bieren. Trübung, Opaleszenz oder ein milchiges Aussehen in Getränken ist meistens unerwünscht und lässt den Verbraucher vermuten, dass das Produkt von geringerer Qualität oder verdorben ist. Viele verschiedene Arten von Bildung oder Eintrag von Substanzen können zu Trübungen führen, welche sich in zwei Hauptkategorien differenzieren lassen: getränkesspezifisch, wobei die Inhaltsstoffe eine Wechselwirkung verursachen, und externe Einflüsse wie Prozessfehler oder Partikeln, die mit dem Medium interagieren.

In dieser Forschungsarbeit kam erstmalig die Raman-Mikrospektroskopie (RMS) zur Detektion bestimmter Trübungspartikel in Bier zum Einsatz. Durch diese Methode kann die chemische Zusammensetzung der zu untersuchenden Moleküle eindeutig identifiziert werden. Das Hauptaugenmerk in dieser Arbeit wurde den Partikeln gewidmet, welche die stärksten und auch intensivsten Trübungen verursachen können. Als Grundvoraussetzung für eine Methodenentwicklung der Trübungsidentifikation via RMS musste zunächst das Verhalten des Mediums Bier unter Lasereinwirkung erforscht werden. Da Bier eine Vielzahl an fluoreszierenden Inhaltsstoffen beinhaltet, ist eine Untersuchung durchgeführt worden, mit dem Ziel, die am intensivsten fluoreszierenden Verbindungen aufzuzeigen und diese in weiteren Schritten zu eliminieren oder durch Einsatz spezieller Methoden die Fluoreszenz umgehen zu können.

In anschließenden Forschungsarbeiten, welche auf die Fluoreszenzanalytik aufbaut, sind Fremdpartikeln (bspw. Filterhilfsmittel, Stabilisatoren und verschiedene Mikroplastikpartikeln), aber auch biereigene Partikeln (Polyphenole wie Catechin, Proteine

wie Gliadin, β -Glucane, Calciumoxalat und Stärke) nachgewiesen, bewertet und validiert worden. Eine geeignete Probenvorbereitung ermöglichte es, Membranfilter zu testen und eine Filtrationsmethode zur Isolierung einzelner Partikel zu etablieren und implementieren. Clusteranalysen und Ähnlichkeitsmatrizen dienten zur Identifizierung bzw. Validierung und zur besseren Darstellung der Partikel. Durch Analyse der Probenbestandteile in verschiedenen Medien (trocken, fluid (Wasser, Bier)) konnten die Einflüsse unterschieden werden. Der Filtrationsrückstand nach der Membranfiltration ist ebenfalls analysiert worden. Eine zweidimensionale Bildabtastung der Partikel diente zur Bestimmung der Partikelhomogenität. Die Aufnahme der Raman-Spektren erfolgte durch die Erfassung von Einzelpunkt-Scans. Es wurden zwei verschiedene Laser der Wellenlängen 532 nm und 785 nm eingesetzt, um deren Anwendbarkeit zur Identifizierung von potenziell trübungsbildenden Partikeln zu validieren. Die PVPP-Spektren in den verschiedenen Medien zeigten Ähnlichkeiten von mehr als 80 %, in der Regel mehr als 95 %. Die Cellulosefaserspektren wiesen keine Unterschiede zwischen den verschiedenen Medien, aber durchweg hohe durchschnittliche Ähnlichkeiten von 94,5 % auf. Die Kohlenhydrate Stärke, Arabinoxylan, Cellulose, Hefe β -Glucan und Gerste β -Glucan, sowie Gliadin, Ferulasäure, Prolin, Glutamin, Calciumoxalat und PVPP sind bei einer Wellenlänge von 532 nm erfolgreich identifiziert worden. Dieselben Substanzen sind bei einer Wellenlänge von 785 nm analysiert worden, was zu Problemen mit schwachen Kohlenhydratspektren von Hefe β -Glucan, Gerste β -Glucan und Arabinoxylan führte. Alle anderen Substanzen sind mit dem Laser der Wellenlänge 785 nm analysiert worden. Die β -Glucane der Hefe und der Gerste konnten eindeutig identifiziert und klassifiziert werden. Darüber hinaus konnte Catechin, das bei der Messung mit 532 nm ein starkes Fluoreszenzsignal aufwies, bei 785 nm identifiziert werden. Das größte Problem bei der Raman-Mikrospektroskopie (RMS) in Bezug auf die Bieranalytik ist das intensive Fluoreszenzrauschen einiger Bierinhaltsstoffe. Da Bier eine große Menge an fluoreszierenden Inhaltsstoffen enthält, wurde in der ersten Forschungseinheit (Chapter 2.2) untersucht, welche Verbindungen die stärkste Fluoreszenz aufweisen, um diese Stoffe gezielt verarbeiten zu können. Es sind spezielle Verfahren eingesetzt und getestet worden, die das Fluoreszenzproblem umgehen können. Im Rahmen dieser Forschungsarbeit konnte das enorme Potential der RMS für die Trübungsidentifizierung herausgestellt werden. Die entwickelten Methoden können, in weiteren Projekten, für eine Erweiterung der RMS auf die Getränkeanalytik zielgerichtet adaptiert werden.

1 Introduction and motivation

Haze, cloudiness, blurring, opacity, obfuscation... a lot of names for one big topic: “turbidity”. The sheer number of descriptions shows how complex and multi-layered the topic of turbidity can be. Turbidity in beer and other beverages remains an ever-present, exciting topic in the brewing industry and not least for the analysis institutes.

Purely optical characteristics like gloss fineness or beer color as well as non-visual attributes such as taste, are very important for the appearance of a beer declared to be “filtered beer” [1–3].

Different analysis methods are used in advance to avoid customer complaints and to find out the causes of cloudiness. However, the analysis is normally limited to optical, enzymatic and microscopic analysis for simplicity [4–7]. Turbidity in beer plays a crucial role because it's the primary characteristic to be perceived by consumers and has a decisive influence on their impression of the merchandise [8, 9]. For Pilsner and lager beers, the customer expects a bright beer and unwanted turbidity is perceived as a defect. However, turbidity can even be desirable if the beer is unfiltered or naturally cloudy, such as Wheat beer or cellar beer. Smaller breweries and craft breweries often work without filters to give the impression of naturalness and to differentiate their beers from “industrial breweries”. If the beer has been filtered, gloss fineness is a crucial quality feature and essential for determining the storage period of the merchandise. A beer is considered to be stable to turbidity if no turbidity occurs at a temperature of 25 °C or higher over an extended period of time [10]. Turbidity can have various origins. A basic distinction can be made between non-biological and biological turbidity. Turbidity of non-biological origin is often distinguished as cold turbidity, permanent turbidity and turbidity from foreign substances [3, 11]. Just as in non-alcoholic beverages, turbidity can occur in beer in different ways. Particles already contained in beer or its raw materials can coagulate [11]. Inorganic substances such as filter aids that have penetrated or label residues, can cause small particles in beer [12]. Use of state-of-the-art filtration and filling equipment and implementing comprehensive quality assurance measures therefore ensure that presence of such foreign particles in the finished product is the exception. These particles are often described as “visible turbidity” [3].

Raman micro-spectroscopy (RMS) is a promising tool for the detection of small particles, and is different from current methods. Consequently, in case of unwanted turbidity, it is first

necessary to identify the turbidity particles. Previous applications of RMS can be found in various research areas [13–17]. RMS offers a high information density in the recorded spectra, the so-called "finger print", which represents the chemical structure of the molecule.

Problems with the established methods include the fact that they are usually not very specific and always burdened with the human error factor. In addition, turbidity analysis to date is determined by the judgment of a single person and is thus only statistically validated in the rarest of cases. It can also take a long time and does not always provide conclusive results. Raman micro-spectroscopy is a fast, established method for the high-resolution determination of chemical compositions of a wide variety of particles and is a promising alternative in food analysis [18, 19].

The thesis publications are therefore organized in five parts:

1. Kahle, E.M., Zarnkow, M., Jacob, F. (2020) "Beer Turbidity Part 1: A Review of Factors and Solutions" *Journal of the American Society of Brewing Chemists*, DOI: 10.1080/03610470.2020.1803468
2. Kahle, E.M., Zarnkow, M., Jacob, F. (2020) "Beer Turbidity Part 2: A Review of Raman Spectroscopy and Possible Future Use for Beer Turbidity Analysis" *Journal of the American Society of Brewing Chemists*, DOI: 10.1080/03610470.2020.1800345
3. Kahle, E.M., Zarnkow, M., Jacob, F. (2019) "Substances in beer that cause fluorescence: evaluating the qualitative and quantitative determination of these ingredients." *European Food Research and Technology*, 245(12), 2727-2737 DOI: 10.1007/s00217-019-03394-x
4. Kahle, E.M., Zarnkow, M., Jacob, F. (2020) "Investigation and identification of foreign turbidity particles in beverages via Raman micro-spectroscopy" *European Food Research and Technology* 247, 579–591 (2021) DOI: 10.1007/s00217-020-03647-0
5. Kahle, E.M., Zarnkow, M., Jacob, F. (2020) "Identification and differentiation of haze substances using Raman microspectroscopy" *Journal of the Institute of Brewing*, DOI 10.1002/jib.627

1.1 Raman micro-spectroscopy

In the following chapter, the history of Raman spectroscopy is explained, how the Raman effect was developed and how it works, the structure of the Raman spectrometer is explained and finally how the spectra can be read.

1.1.1 History of Raman spectroscopy

As early as 1923, *Smekal* established the theory of inelastic light scattering. But only *Raman* and *Krishman* could observe the phenomenon experimentally a few years later and published their research in 1928 [20]. They characterized the effect of inelastic scattering as weak compared to ordinary scattering [21–23]. This "weak" phenomenon is now called Raman scattering. Unlike today, no modern technology was available at that time and so *Raman* used sunlight as a source, while a telescope served as a collector. He used his eyes as a detector. Gradually, the components of Raman's equipment were improved [22, 23]. For example, up until the mid-1960s, high-pressure mercury or low-pressure mercury burners were used as light sources, which have now been almost completely replaced by lasers [24]. Furthermore, it turned out that a single monochromator cannot remove stray light as effectively as the double monochromator or even triple monochromator introduced later [22].

Raman spectroscopy (RS) has become one of the most powerful analytical methods in chemical-technical analysis over the last decades. The complementary analytical method of infrared spectroscopy (IR or FTIR) is often used as a comparative method of Raman spectroscopy. Both methods offer advantages over the other and complement each other [25]. Due to the basic physical principles and analysis settings, RS still has some important advantages. The high molecular specificity and the easy implementation into existing systems allows the use of RS systems in many technological areas. In addition to their chemical-analytical and biotechnological relevance, such systems are often used in diagnostic medicine, forensic sciences, and astrophysics [26–29].

1.1.2 Raman effect

The Raman effect is named after the Indian physicist *Chandrasekhara Venkata Raman*. He was able to demonstrate that a small proportion of the photons hitting a molecule are inelastically scattered [20, 30]. If photons of a defined wavelength hit a molecule, a large fraction is reflected or they pass through the molecule unaffected. Only a fraction of about

0.01 % – 0.001 % of the photons are scattered elastically (without changing the energy level) by the molecule in an undefined spatial direction. This scattering is called Rayleigh scattering. An even much smaller fraction of one out of $10^{-6}\%$ – $10^{-8}\%$ is scattered inelastically (with a change in energy level). This Raman scattering can be divided into two different types (Figure 1). In Stokes Raman scattering, a molecule in the ground state is brought into a (virtual) excited state by the exciting photon. When the molecule relaxes again, it emits a photon, but does not completely return to the ground state, instead remaining at a higher energy level. Thus, the exciting photon has transferred some of its energy to the molecule. The emitted photon now has a lower energy and thus a lower frequency than the exciting photon (\rightarrow longer wavelength, redshift). In anti-Stokes Raman scattering, exactly the opposite happens. The exciting photon hits an already slightly excited molecule and lifts it to another (virtual) excited state. If the molecule emits a photon and returns to the ground state it has a lower energy level than before excitation. The energy difference in the molecule is transferred to the emitted photon. This is now more energetic and has a higher frequency than before excitation (\rightarrow shorter wavelength, blue shift). The Boltzmann distribution should also be mentioned. With increasing temperature, more molecules are in the excited state. It becomes interesting from 1000 K, which is why many experimental approaches would not be suitable for this. If the system is in thermal equilibrium, only a few molecules are present in an excited state, which is why the anti-Stokes Raman scattering is much weaker [22, 31].

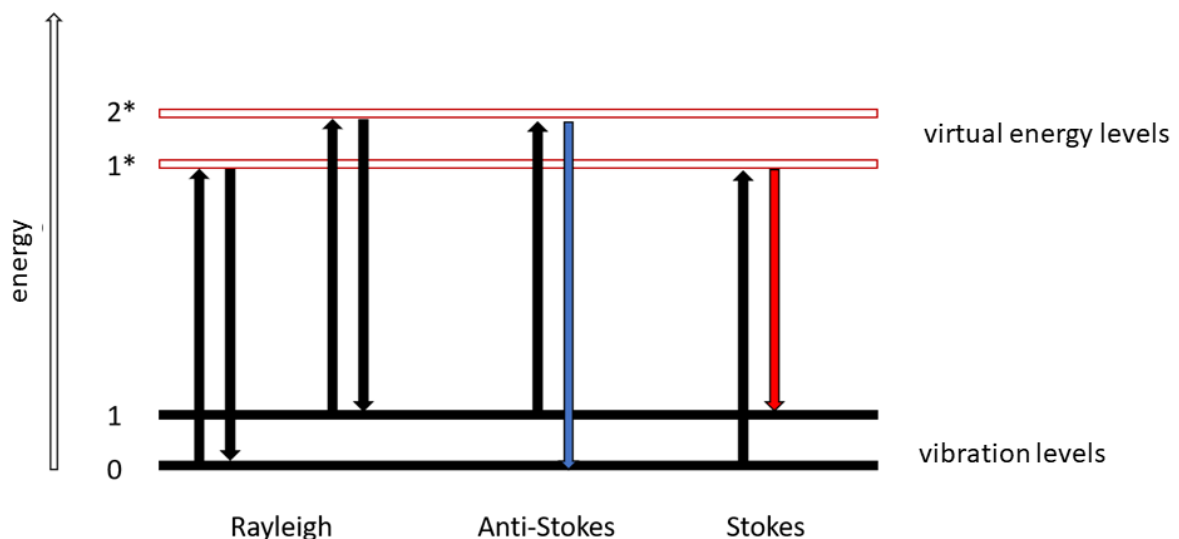


Figure 1 Emergence of Rayleigh, Stokes, and anti-Stokes scattering

In contrast to fluorescence, where a photon actually takes an electron of the excited molecule to a higher energy state, the higher energy state in Raman scattering is considered to be

virtual, since it is not actually a single excited electron that absorbs the energy of the photon, but a much more complex quantum mechanical process [32]. As a result, the photon emitted by Raman scattering can have a broad spectrum of different wavelengths. Compared to the wavelength of the excited photon, the photons emitted in fluorescence can have only the same or a longer wavelength and are thus usually stronger in energy [33, 34].

If a molecule emits photons in the Stokes or anti-Stokes spectrum after excitation by a photon, it is called Raman-active. Each Raman-active substance has a specific Raman spectrum. This means that each molecule of this substance scatters the wavelength of the exciting photon in the same way. This is due to the molecular composition, as well as the types of bonds between the individual atoms, all of which have different but specific scattering behavior. This specificity can be used in analytics to precisely detect and identify simple, as well as highly complex, chemical compounds by comparing with their scattering spectra to databases.

1.1.3 Design and function of a Raman spectrometer

To detect the weak phenomenon of Raman scattering, the substance under investigation is irradiated with monochromatic laser light. This has the advantage of having a higher radiation density than previously used light sources, thus making it possible to concentrate radiation even on very small samples. A laser with photon energies in the UV to almost IR range is used. In order to obtain an increased Raman intensity, the laser beam can be additionally focused, which however implies the risk of damaging the sample. A power reduction of the laser reduces this risk. The light hitting the sample is scattered, resulting in both elastic scattering (Rayleigh scattering) and inelastic scattering (Raman scattering), which is reflected by the mirrors S1 and S2 (see Figure 2) to increase the intensity of the radiation. To avoid masking the Raman scattered light, which has a significantly lower intensity, the Rayleigh radiation, which has the same wavelength as the laser, must be filtered out. The remaining radiation is focused on the entrance slit 1 by means of a lens and then spectrally decomposed in the monochromator by two collimating mirrors and a grating. Finally, the radiation hits the detector through the exit slit 2 to allow analysis [10, 12-14].

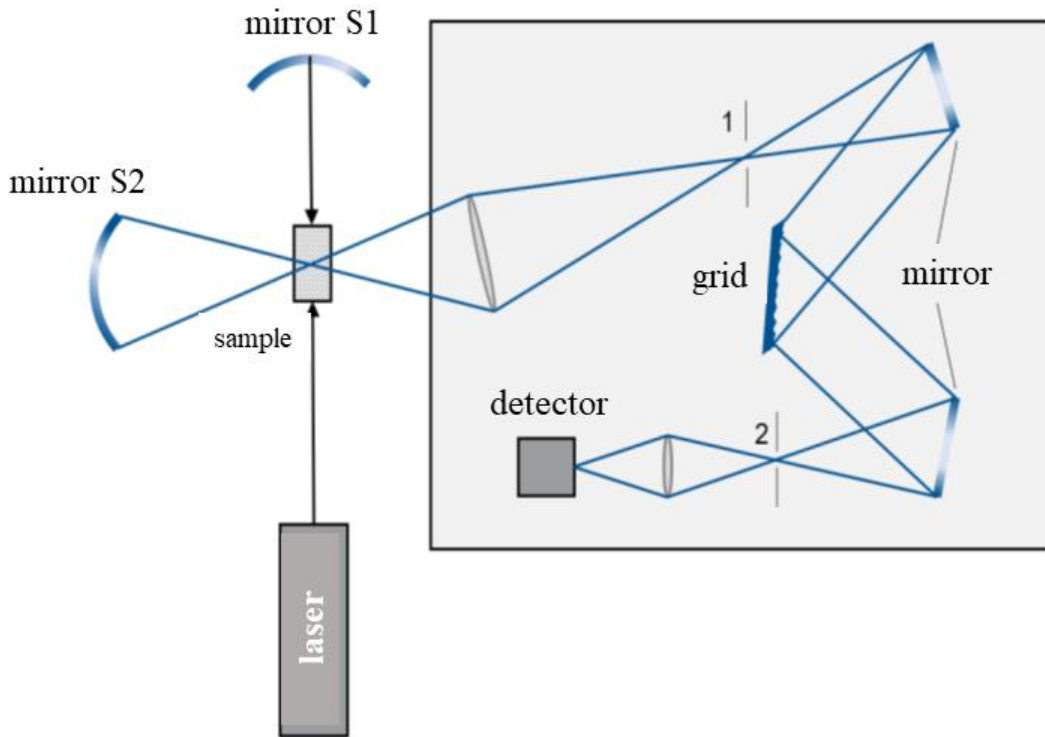


Figure 2 Schematic structure of a Raman spectrometer

Figure 3 shows the schematic structure of the microscope that is used at Research Center Weihenstephan with all the connected peripheral devices.

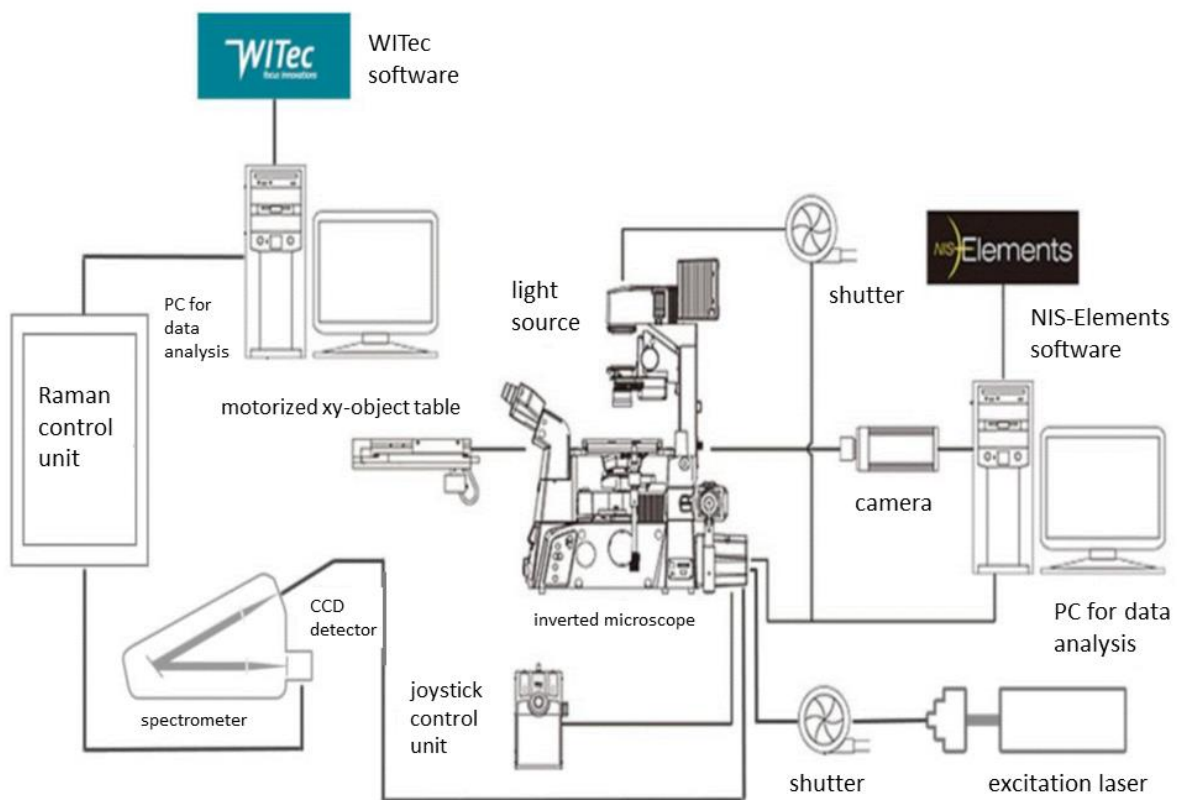


Figure 3 Schematic structure of the Raman micro-spectroscopy system used

1.1.4 Interpretation of Raman spectra

Raman spectra show molecular-specific changes in energy and frequency within the molecule, which can be seen as a series of peaks. These peaks correspond to the individual vibrational energies associated with specific chemical bonds in molecules. Thus, the peaks can be used to draw conclusions about bonds and thus molecular composition [37].

Reference spectra can be used to identify characteristic bands in the individual spectra. Within the spectra, the range 500–1700 cm^{-1} is known as the "fingerprint region". This part contains most of the Raman bands that are used to uniquely identify a particular material. Many of the bands in this region are derived from CH, CH₂ and CH₃ deformation vibrations, which are always present in organic molecules. It is also possible that the positions of the individual bands varied slightly, which may be due to different chemical conditions [38]. Due to the change in energy, different forms of oscillation can occur. Individual atoms can move in three-dimensional space, and this can lead to changes in bond lengths or angles. For example, in a gravitational oscillation only the angle between two atoms changes, whereas in a stretching oscillation the bond lengths change. Different designations are used depending on the movement [39, 40].

1.2 Fluorescence and Raman

Since the Raman signal is very weak, it is also very susceptible to interference. Probably the biggest problem with Raman microscopy is the frequently occurring fluorescence of many organic substances. These problematic substances initially absorb a stimulating photon when irradiated with a laser of sufficient energy. An electron is raised to a real excited state and then falls back to its ground state. A photon is emitted which corresponds at most to the energy of the irradiated photon, but in most cases has a longer wavelength, which corresponds to a lower energy (Stokes rule) [33, 34, 41]. These emitted photons are detected by the CCD detector together with the Raman scattered photons. The main problem is the much higher frequency of fluorescence compared to Raman scattering. Fluorescence signals can therefore completely overlay the Raman signal. The fluorescence of some substances makes the analysis of these substances itself a problem, and that's not the only issue. Even the slightest contamination of a non-fluorescent material with fluorescent substances can make it difficult or even impossible to measure the Raman spectrum [34].

Beer contains a large spectrum of organic and inorganic substances. Among them are some substances that tend to autofluorescence [32, 42–46]. The Raman analysis of beer turbidity particles or particles that have been in contact with beer can therefore lead to fluorescence problems. Therefore, it may be necessary to use methods to avoid fluorescence.

1.2.1 Methods of fluorescence avoidance

An exact recording of Raman spectra is often not possible due to strong fluorescence signals. Therefore different methods to avoid fluorescence have been developed.

1.2.1.1 *Anti-Stokes Raman Spectroscopy*

As already mentioned, fluorescence occurs exclusively on the Stokes side of the Raman spectrum. For this reason it is only possible to view the anti-Stokes side of the spectrum. However, the weak Raman signal is much weaker on the anti-Stokes side. The anti-Stokes signal can be amplified by methods such as Coherent anti-Stokes Raman Scattering (CARS), but these methods require a lot of equipment and are therefore very expensive [47].

1.2.1.2 *Surface Enhanced Raman Scattering*

Another possibility to minimize the fluorescence problem is to amplify the Raman signal very strongly and ideally, weaken the fluorescence signal simultaneously. In Surface Enhanced Raman Scattering (SERS), the analytes are brought into direct proximity to metal nanoparticles. Gold, silver or copper particles are often used for this purpose. The exact mode of action of SERS is not yet known. However, there are assumed to be two dominant effects, a chemical and an electromagnetic amplification. The chemical amplification results from a charge transfer between the analyte and nanoparticle surface, which increases the polarizability and thus the intensity of Raman scattering. The electromagnetic amplification is based on surface plasmon resonance. The irradiated photons excite the charge carriers on the metal surface, which enables them to form a very strong, narrowly limited electric field. This field excites the analyte in addition to the incident light, which greatly enhances the Raman signal. SERS can amplify the Raman signal by up to 10^{15} [48]. However, SERS only takes place if the analyte adsorbs to the nanoparticles and is in sufficient proximity to the surface. In unfavorable cases, the fluorescence of an analyte can even be increased instead of decreased. In addition, spectra recorded with SERS may differ from the normal Raman spectra specific for the substance, which makes it difficult to compare [49].

1.2.1.3 Photo bleaching

In contrast to the Raman signal, which remains almost constant in time with continuous excitation of an analyte, the fluorescence often decreases. This process is called photo bleaching. Due to the repetitive process of excitation and subsequent emission of a photon, the analyzed substance is chemically damaged, resulting in a permanent loss of fluorescence, while the Raman signal is hardly changed [50, 51]. Especially for samples with small fluorescent impurities, photo bleaching can be a simple and inexpensive method to quench fluorescence. However, the time required to bleach different substances varies considerably. Often the bleaching process is completed within a few milliseconds to seconds, making photo bleaching a very useful method in these cases. However, it can also take hours to days until the fluorescence is attenuated. Such long exposure times can be particularly problematic, since some samples can be thermally damaged by long and strong laser irradiation, and this also leads to a change in the Raman signal [52].

1.2.1.4 Use of alternative excitation wavelengths

Another way to avoid the occurrence of fluorescence is to vary the wavelength of the excitation laser. Many substances are only excited to fluoresce by light of certain wavelengths. The critical wavelengths are often found in the visible light range (e.g. $\lambda = 532$ nm) [53]. By using lasers in the ultraviolet (UV) or near infrared (NIR) range, the fluorescence background can often be minimized [54, 55]. Even if fluorescence is emitted after excitation with a UV laser, it is usually not in the range of the observed wave shift [34]. NIR lasers often do not have enough energy to bring the electrons of the analyte to a higher real energy level, which makes fluorescence emission impossible. Unfortunately, UV and NIR lasers also have major disadvantages in analysis. A UV laser can cause lasting damage to the sample by burning even at low power. The problem with NIR lasers can be found in the physics of the Raman effect itself. If the wavelength of the excitation light is increased, the intensity of the Raman scattering decreases to the fourth power [55]. This effect makes the analysis of weakly Raman-active substances in the NIR range very difficult. Another problematic factor of using different wavelengths is the high instrumentation complexity. Several lasers and several detectors are required, which is associated with very high acquisition costs.

1.2.2 Further methods

In addition to the methods already described, there are several other methods of fluorescence avoidance that can be roughly divided into three different categories. The "time-domain methods" make use of the fact that Raman scattering is much faster than fluorescence (Figure 4).

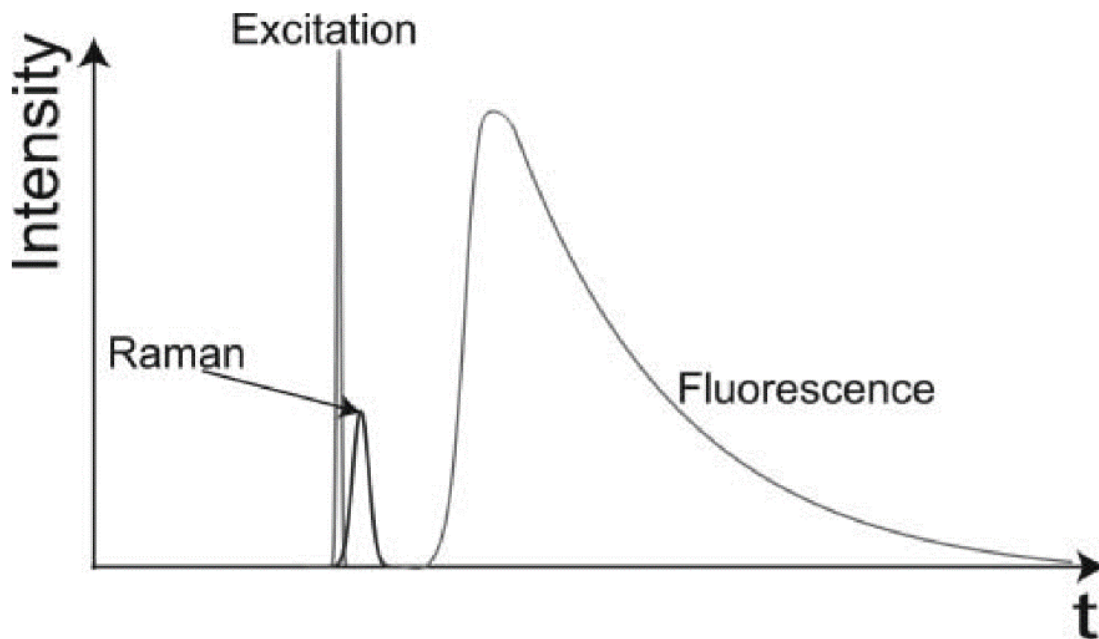


Figure 4 Time course of fluorescence and Raman scattering

While Raman scattering occurs almost simultaneously with excitation, fluorescence emission takes about 10^{-7} to 10^{-9} seconds. If the Raman signal can be detected selectively in this short time, a fluorescence-free measurement is possible. However, this requires a lot of equipment and involves high costs [52]. The "frequency domain methods" are based on a similar principle. Here, too, the fast Raman response or slow fluorescence emission is used. The sample is excited in fast frequency with sinusoidal changing wavelengths. While the Raman signal can follow the sinusoidal excitation, the slow fluorescence obtains a phase shift and an amplitude superposition. Fluorescence and Raman signal can thus be distinguished and evaluated [56]. The "wavelength-domain methods" work with at least two excitation lasers that have a very small wavelength difference. The Raman shift strictly follows the excitation wavelength. This is also the reason why the Raman spectra are very similar at different excitation wavelengths. Fluorescence emission, on the other hand, is wavelength independent. If the sample is irradiated with two slightly different lasers, the fluorescence can be deducted as a constant factor [52].

1.3 Turbidity

Turbidity or foreign particles that can lead to “visible turbidity” of beer and beverages is an almost unwanted phenomenon that can occur immediately or after the beer has been stored for some time. Cloudiness can be caused by a variety of factors (see Figure 5) [3].

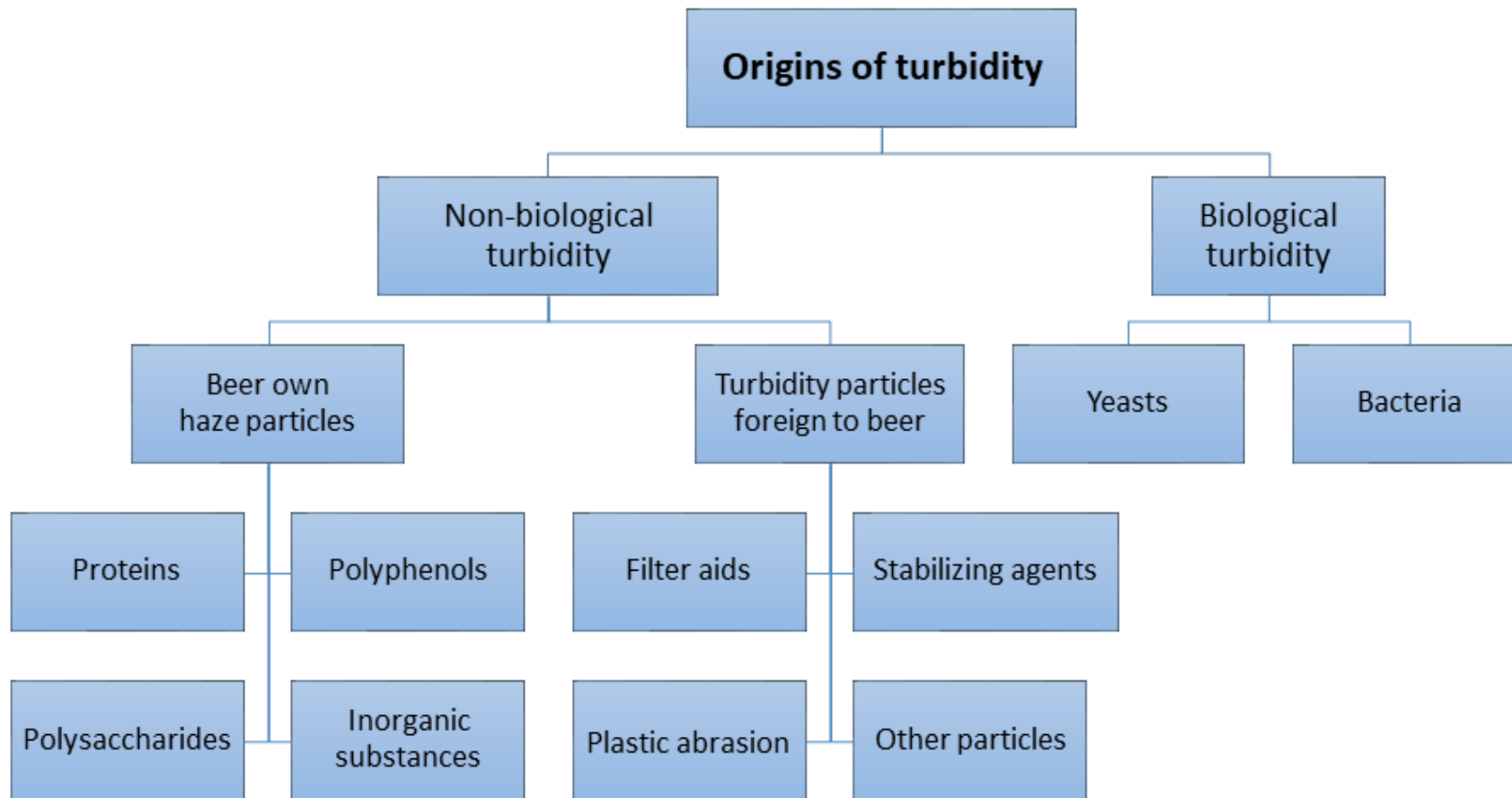


Figure 5 Various origins of turbidity and foreign particles that can lead to “visible turbidity”

1.3.1 Types and origin

The filtration of a beer usually produces a shiny, clear product. Nevertheless, it is possible that the product may experience turbidity after filtration, or that turbidity may develop over time.

1.3.1.1 Protein polyphenol turbidity

In most cases, proteins or polypeptides and polyphenols are responsible for turbidity formation [11]. In the formation of protein-polyphenol turbidity particles, proline-rich protein components are linked together by polyphenols [57]. In brewing practice, this is exploited by using PVPP to stabilize beer, which imitates a polyproline molecule and thus binds and removes polyphenols from the product [58]. In the formation of beer turbidity it is the proline- and glutamine-rich storage proteins of the prolamin fraction that play a primary role. These are called hordeins in barley and gliadins in wheat, but with protein Z there are also proteins that are relevant to turbidity from the albumin fraction [59, 60]. The polyphenols with protein crosslinking properties have at least two o-diphenol groups. In beer, these are mainly the turbidity-causing proanthocyanodins, which usually occur as di- or trimeric catechins [61]. However, in the formation of colloidal particles from proteins and polyphenols, the ratio of the two substances plays a decisive role. It has been shown that a ratio of 2:1 or of 5:1 (gliadin:tannic acid) results in significantly increased turbidity compared to other ratios. The size of the particles also changed significantly at different ratios, which, according to Stokes' Law, has a considerable influence on the sedimentation rate of the particles and thus on the storage and filtration process in the brewery [62–65].

The formation of protein-polyphenol-related turbidity is subject to many influences. Besides the above-mentioned relationships between the two substances, key factors include the temperature and the oxygen content of the beer. Cold storage of beer can cause cold turbidity, which is reversible. During cold storage, polyphenols and proteins clump together but do not form a covalent bond, which is why the clumping is dissolved again when energy is supplied and the turbidity disappears. In contrast, permanent turbidity is favored by high temperatures of the beer. Irreversible covalent bonds are formed between the polyphenols and proteins. This process is accelerated by an increased oxygen content in the beer. The regular turbidity measurement of bottled beer stored at high temperatures can be used to simulate long storage at lower temperatures. In this way, the best before date of the product can be determined as a function of its chemical-physical stability [66–68].

1.3.1.2 Polysaccharide turbidity

In addition to beer turbidity caused by polyphenols and proteins, various polysaccharides can also cause turbidity. The glucans in this group are polysaccharides consisting only of glucose, which are divided into α - and β -glucans. The most common α -glucan in the brewing process is starch derived from malt. This starch consists of amylose of α -1,4-glycosidically linked glucose and as amylopectin of α -1,4-glycosidically and α -1,6-glycosidically linked glucose. As a rule, the starch is almost completely broken down by amylases into maltose and short dextrans during the mashing process. If this does not happen completely or if high molecular weight starch is released again after mashing due to procedural errors, this can lead to turbidity and make filtration more difficult [69]. Yeast cells that are not very vital or dead can excrete glycogen, which is very similar to plant starch as α -glucan and can therefore also cause turbidity [70]. β -Glucan is particularly problematic for the brewing process. This can originate from yeast as well as from malt, with malt β -glucan being much more common. While α -glucans are usually present in the organisms as storage substances, β -glucans are mostly supporting substances and can be found in yeast as well as in grains as a cell wall substance. β -glucans are glucose monomers linked by very stable β -glycosidic bonds. Mainly 1,3- and 1,4-glycosidic bonds are found in cereals and 1,3- and 1,6-glycosidic bonds in yeast. These β -glucans have the property of forming highly viscous gels even at very low concentrations under the influence of shear forces. These gels increase the viscosity of beer, which considerably extends the storage time of beer due to slower particle sedimentation [71]. During malting, β -glucan is broken down in the grain. Highly dissolved malts thus contain less of the problematic substance. However, β -glucan can be released from the grist to a greater extent by an unsuitable mashing program. The yeast β -glucan, like the yeast glycogen, can enter beer through autolysed yeast cells [72, 73].

1.3.1.3 Calcium oxalate turbidity

Another source of turbidity is calcium oxalate. This salt of oxalic acid is formed in most cases by oxalic acid from the cereals and later malt and calcium from the brewing water. Due to its very low solubility, it crystallizes even at low concentrations. In the brewing process the aim is often to precipitate as much of the oxalic acid dissolved from the grain as possible. This can be achieved by ensuring sufficient calcium in the brewing water and a long cold storage of the beer. The salt forms, crystallizes and sediments in the tank. If this does not happen in sufficient

quantities, further calcium oxalate can precipitate in the bottled product and cloud the beer [74]. The crystals are also suspected of triggering gushing - spontaneous effervescence of beer when the container is opened [75].

1.3.1.4 Turbidity due to auxiliary materials

Most beer cloudiness finds its origins in the raw materials used for brewing: malt, water, hops and yeast. However, breakthroughs of filter aids such as diatomaceous earth or bentonites, and stabilizers such as PVPP, can also cause turbidity. Such turbidity often indicates faulty filtration or a police filter that is not working properly [76].

1.3.1.5 Other particles and microbiological contamination

Further particles can get into the beer, especially during the filling process. A malfunction in the bottle washing machine can lead to label residues in the bottles. Glass splinters can enter the product through exploding bottles in the filler or through defective containers that are not recognized by the bottle inspector. It is also possible that various airborne particles or fibers fall into the rinsed bottles and contaminate the product [77]. Culture yeasts, foreign yeasts or beer-spoiling bacteria can also cause turbidity. This can indicate a lack of filtration (culture yeasts) or hygiene deficiencies.

2 Results (Thesis publications)

2.1 Summary of results

The thesis publications are summed up in the following paragraphs 2.2 to 2.6 with a description of authorship contribution followed by full copies of the publications. Table 1 gives an overview of the publications. Publisher permissions for the imprint of publications can be found in paragraph 5.4.

Table 1 Short overview of the five publications with title of the publication, major objective, applied method and main findings

Review Title		Research Title		
Publication 1	Publication 2	Publication 3	Publication 4	Publication 5
Beer Turbidity Part 1: A Review of Factors and Solutions	Beer Turbidity Part 2: A Review of Raman Spectroscopy and Possible Future Use for Beer Turbidity Analysis	Substances in beer that cause fluorescence: evaluating the qualitative and quantitative determination of these ingredients	Investigation and identification of foreign turbidity particles in beverages via Raman micro-spectroscopy	Identification and differentiation of haze substances using Raman micro-spectroscopy
Major objective				
Summary of literature, conference papers and research on turbidity	Summary of literature, conference papers and research on Raman spectroscopy	Finding out which substances in beer are fluorescent and can be avoided concerning Raman	RMS was used to detect, evaluate and validate non-beer turbidity particles	RMS was used to detect, evaluate and validate beer turbidity relevant particles
Applied methods / investigations / devices				
Combining literature of the past decades, critical comparison of outcomes of differing studies.	Combining literature of the past decades, critical comparison of outcomes of differing studies.	Fluorescence spectrometer Aqualog™ of HORIBA Data evaluation using the PARAFAC model	A suitable sample preparation was developed, membrane filters were tested, and a filtration method for isolating the individual particles was established and implemented	Preparation of special slides, Production of turbidity particles from forcibly aged beer, data material was evaluated using BioNumerics software
Main findings / conclusions				
The review examined beer turbidity problems. The various causes and origins of turbidity were discussed.	The different methods of RS were discussed and related to analysis of substances to beer turbidity.	Diverse fluorescing beer ingredients could be assigned using fluorescence spectroscopy. Using the PARAFAC analysis, a specific model was created that identified the three main components of the fluorescing substances.	Different filter aids and stabilizing agents were investigated as well as different polymer samples of the most common types of plastics and some high-performance plastics from food production.	Starch, arabinoxylan, cellulose, yeast β -glucan, barley β -glucan, gliadin, ferulic acid, proline, glutamine, calcium oxalate and PVPP were successfully identified at 532 nm.

PART 1

2.2 Beer Turbidity Part 1: A Review of Factors and Solutions

This review examined beer turbidity in general and the problems dealing with haze. The various causes and origins of turbidity were discussed in detail, starting with the current state of research and human perception and visual opacity. Further classification led to a general definition of turbidity of beer, the distribution by particle size, the general turbidity and more accurately in fluids and in beer. Past and present turbidity measurements were also compared.

The origins of turbidity are discussed in detail:


Origins of turbidity

- Chill haze and permanent haze
- Non-biological turbidity – proteins and polyphenols
- Non-biological turbidity – caused by carbohydrates
- Non-biological turbidity – inorganic substances
 - Filter aids
 - Kieselguhr
 - Perlite
 - Cellulose fiber
 - Stabilizing agents
 - Polyvinylpyrrolidone (PVPP)
 - Silica gel
- Non-biological turbidity – microplastics
- Biological turbidity

Authors/Authorship contribution:

Kahle, E-M.: Literature search, writing, review conception and design; **Zarnkow, M.:** critical review of draft, discussion of data; **Jacob F.:** Supervised the project

Beer Turbidity Part 1: A Review of Factors and Solutions

Eva-Maria Kahle , Martin Zarnkow, and Fritz Jacob

Forschungszentrum Weihenstephan für Brau- und Lebensmittelqualität, Technische Universität München, Alte Akademie 3, 85354 Freising-Weihenstephan, Germany

ABSTRACT

Turbidity in beer will continue to be a major topic as many origins of haze have already been discovered, but it is not always possible to identify its immediate cause. In addition to beer foam, one of the most important visual quality characteristics of filtered beers is gloss fineness. Consequently, in the case of an undesirable haze, it is first necessary to identify the haze particles and how to remove them. The topic is covered in two sections. This review labelled Part 1 and a second review labelled Part 2. Part 1 addresses turbidity in general, the causes and origins of turbidity and the different analytical methods for turbidity identification and removal. Part 2 focuses on Raman spectroscopy and provides a general overview of the physical basics, the areas of application, possible gaps and the challenge for its use for identifying turbidity in beer and beverages.

KEYWORDS

Raman micro-spectroscopy; turbidity; haze; beer; TI-RMS; beverages; identification; particles; fluorescence

Introduction – current state of research

A very important visual quality characteristics of filtered beers is gloss fineness.^[1,2] Anything that impairs the appearance of the beer will reduce acceptance by the consumer and must be prevented.^[3] It is therefore important to be able to identify the composition of haze particles, but analysis is often limited to optical, enzymatic and microscopic analyses.^[4] Raman spectroscopy is one possibility to identify and characterize turbidity particles based on its use elsewhere^[5–8] and is discussed in detail in Part 2 of this review. Part 1 will discuss types of haze and their measurement as well as various removal technologies.

Human perception and visual opacity

Our eyesight helps us to detect visual opacities, but results vary from person to person, making visual opacity a subjective characteristic. Turbidity in fluids or beer can be measured by the naked eye or using analytical methods. The Tyndall effect, which describes the scattering of light by particles, is the basis for the metrological determination and usually correlates with visual perception. An important note: Particles determined in the analysis do not necessarily generate visible turbidity! This is a phenomenon due to the fact that turbidity depends not only on the amount of particles, but also on the particle size and composition.^[9–11] The general definition of turbidity and the classification of the particles is discussed in the following.

General definition of turbidity

According to the standard DIN EN ISO 7027, turbidity is understood to be the “reduction of the transparency of a liquid caused by the presence of undissolved substances”.^[12,13] Turbidity is perceived as a subjective, visual impression, which arises due to refraction of the insoluble particles.^[13] The turbidity measurement and control should satisfy consumer expectations (e.g., cloudy Pils versus the glossy, golden yellow Pils the consumer expects) and also prevent other quality-reducing issues. Turbidity monitoring is thus of great importance for visual reasons as well as for the fact that turbidity is an indicator of more serious contamination.

Turbidity of beer: distribution by particle size

Undissolved solids, which cause turbidity due to light scattering, are divided into three groups based on the particle size (Table 1).

The coarsely dispersed solids are macroscopically well-recognizable particles that can be differentiated by microscopic analysis. Molecularly dispersed solids are already dissolved in the dispersion medium, such as, for example, beer, and are therefore no longer visible as turbidity.^[14] Despite their small particle size, the colloidal dispersed solids, also called colloidal turbidity, are partly visible due to light refraction at the interfaces (Tyndall effect) and are therefore to be investigated first in the course of Raman micro-spectroscopy. In addition to the presence of solids, however, the concentration of available, reactive ingredients should also be mentioned. Furthermore, the temperature,

Table 1. Beer-dyeing solids divided by particle size and examples.^[2,14]

Beer-dyeing solids	Particle size [μm]	Examples
Coarse-particle solids	≥ 0.1	Yeasts, microorganisms
Colloidally dispersed solids	0.001 to 0.1	Proteins, polyphenols
Molecularly dispersed solids	< 0.001	Combine with medium

the contents of turbid metal ions such as iron (Fe) and copper (Cu), the oxygen content and the present pH determine the turbidity reactions.^[15]

Turbidity in general

One of the most important quality features in the beverage industry besides taste, aroma and foam is the chemical-physical stability, which is also called colloidal stability. This describes the property of a beverage to avoid unwanted turbidity – its fineness of gloss. All types of turbidity affect the quality of water and it may be harmful in certain non-alcoholic beverages. However, it could be a welcome characteristic in beer if it were not for consumer perception. Customers expect a clear beverage and any form of turbidity is considered to be a reduction in quality and possibly even a health hazard. However, this particular turbidity has no harmful effects on health. For filtered beverages, chemical-physical stability is an important factor in determining the shelf life of the product. It depends on various factors, such as the type of product, microbiological susceptibility, ingredients, technological factors, etc.^[16]

Turbidity in fluids

The optical impression of turbidity results from the scattering of light by particles finely distributed in the liquid. Colloidal particles can have a size of 1–500 nm and are in a state between microscopically suspended particles and coarsely dispersed suspensions. The Tyndall effect describes the opalescence of this kind of suspended particles and the associated impression of a light veil up to a strong turbidity.^[17] In the Tyndall effect, the size of the distributed particles is approximately equal to the wavelength of the light hitting the liquid. The light is scattered by the particles and directed in all directions. When determining the turbidity, this scattering is measured using nephelometry. In the field of brewing technology, measurement at 90° and 25° angles has proven to be successful.^[17] In the method with 90° angles, the scattered light emerges from the sample perpendicular to the incident light. Here, particles with a size of $< 1 \mu\text{m}$ are measured, which are perceived as opalescence in the liquid. The measurement at an exit angle of 25° measures larger particles ($\geq 1 \mu\text{m}$ – $1.5 \mu\text{m}$) and is particularly suitable for evaluating the condition of the filter elements. It is possible to determine the turbidity using turbidimetry, i.e., a transmitted light measurement based on Lambert-Beer's law.^[18] In brewing, turbidity can be described using the EBC formazin unit, which is based on a standard formazin (formazine) suspension.^[4]

Turbidity in beer

Turbidity in beer plays an important role because it is the first characteristic to be perceived by consumers and has a decisive influence on their impression of the product. In the case of Pils and lager beers, the customer expects a bright beer and unwanted turbidity is perceived as a defect. However, turbidity in beer can also be desirable if the beer is unfiltered or naturally cloudy, such as wheat beer or cellar beer. Smaller breweries and craft breweries often work without filters to create the impression of naturalness and to differentiate their beers from “industrial breweries”. If the beer has been filtered, gloss fineness is an important quality feature and essential for determining the shelf life of the product. A beer is considered to be stable to turbidity if no turbidity occurs at a temperature of 25°C or higher over an extended period of time.^[19]

Turbidity can have various origins. A basic distinction can be made between non-biological and biological turbidity. Turbidity of non-microbiological origin can be distinguished as cold turbidity, permanent turbidity and turbidity from foreign substances.^[19] As in non-alcoholic beverages, turbidity can occur in beer in three different ways. Particles already contained in beer or its raw materials can coagulate.^[20] Inorganic substances, such as filter aids that have penetrated or label residues, can lead to small particles in beer.^[16] Use of state-of-the-art filtration and filling equipment and the application of comprehensive quality assurance ensure that presence of such foreign particles in the end product is the exception. These particles can be referred to as “visible turbidity”. Figure 1 lists various types of turbidity and turbidity particles and shows their origins.

The above overview categorizes the different origins of turbidity and foreign particles.

Turbidity measurement in the past

In the past, the turbidity of a fluid was measured using a transparent container with a viewing panel attached to it (similar to the ophthalmologist's eye test), which could be viewed through the fluid (Figure 2).

The number that was barely legible corresponded to the measured turbidity.^[21] However, this method was very inaccurate and further dependent on the subjective feeling of the subject. One optical analysis method is the measuring technique process for liquids with 90°-scan scattering and 25°-forward scattering (nephelometric measurement). According to Back et al.,^[11] if a beer is considered glossy, the 90° forward spread is < 1.0 EBC-TU and the 25° forward spread is < 0.2 EBC-TU. The 90° side scattering is favorable for finely dispersed colloidal turbidity $< 1 \mu\text{m}$ and the 25° forward scattering for particulate dispersed substances in a size range of ≥ 1 – $1.5 \mu\text{m}$. Table 2 presents the standard values for assessing the turbidity of a beer.

Different units for turbidity measurement

Turbidity values are subdivided into different units depending on the area of application of various liquids to be investigated (Table 3).

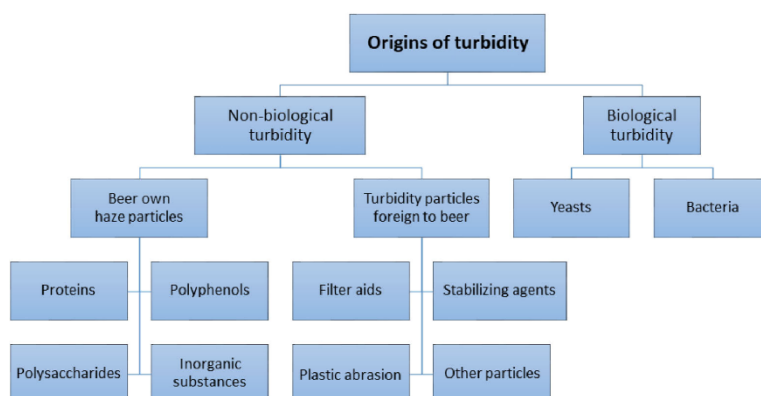


Figure 1. Various origins of turbidity and foreign particles that can lead to "visible turbidity".

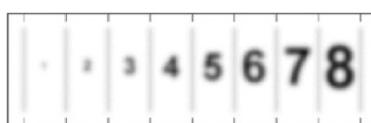


Figure 2. Turbidity synoptic.

For the conversion of the different turbidity values, Table 4 provides an overview of this.

Turbidity measurement in the present

Today, some standardized analysis methods are used, which can also be used in combination. These methods include optical (as already mentioned in the section "Turbidity measurement in the past"), microscopic, and enzymatic methods as well as particle size analysis. Methods have already been mentioned that enable the origin of turbidity to be classified by optical methods. Since only a few turbidifiers can be distinguished from each other by these optical methods, dyes are used. Thus, several substances can be explicitly categorized. The respective dyes are usually specific to a turbidity generator. If a dye stains several different turbidities, these can be determined on the basis of the morphological differences. In addition to the staining methods, the sample is also treated with acid and base in order to limit the possibilities at the beginning of the investigation. A 1 M potassium hydroxide solution (KOH) and a 10% sulfuric acid (H_2SO_4) solution are added to each sample. Solubility of the particles in KOH serves as evidence of compounds that contain protein and solubility in H_2SO_4 would indicate calcium compounds. Optical methods also include staining methods that aim to detect particle material containing carbohydrates, neutral and acidic proteins, starch, etc. With the help of colorants, it is possible to identify turbidities by microscopic examination. Different dyestuffs are used for different components relevant to the turbidity.^[20] For instance, proteins, polyphenols and particles that contain starch can be stained and the cause of turbidity identified. In order to concentrate

the turbidity particles, the sample is first centrifuged or enriched and stained by filtration on a membrane. It is then examined under a microscope using a reflected or transmitted light method.^[20,27,28] The eosin yellow dye is used to identify eosinophilic particles of a proteinic type. Under the microscope, they can be recognized as pinkish-orange-colored skins, flakes, ribbons and fine grains. These particles only occur in small quantities in the finished beer, but multiply as storage time, temperature and mechanical stress increase.^[16,20] Polysaccharides such as starch can be colored and recognized using thionine and iodine. Thionine tints neutral polysaccharides violet and acid ones pink. Iodine, as already known from the iodine test in the brewhouse, colors unglued starch blue and glued starch red. Iodine can also be used to identify the filter aid PVPP, which shows a strong orange color.^[16,20] The polysaccharide glucan can be stained with Calcofluor and made visible with a fluorescence microscope. This allows both β -glucan in yeast, in malt cell walls, and β -glucan in finished beer to be detected, as both fluoresce blue. The same is possible using the dye Congo red instead of Calcofluor. This stains β -glucan red.^[16,20] A thiazine dye, methylene blue, is used to identify fibers, tannins and polyphenols. This is the same dye that is used in yeast viability tests. It colors the particles a strong blue tone. Furthermore, this substance can identify tanning agents in combination with proteins. The microscopic examination of turbidity particles has therefore proved to be a relatively reliable method for determining the origins of some turbidity. However, this is an invasive method that cannot be carried out in a closed container.^[20]

In an enzymatic turbidity determination, the origins of turbidity are identified with the aid of enzymes. This is based on the degradation of turbidity-causing substances using enzymes. This method can be used to determine whether colloidal stability is impaired, by for example, proteins or carbohydrates. Cloudy or opalescent beer samples are mixed with a small quantity of enzymes at room temperature - possibly at 40 °C or 60 °C - and incubated for 24 h. After the reaction time, the turbidity of these samples and untreated zero samples is measured. The cause of this

Table 2. Standard values for the evaluation of beer haze according to EBC, 90° measurement.^[22]

Evaluation	EBC-Turbidity Units [EBC-TU]	ASBC-Turbidity Units [ASBC-FTU]
Bright/brilliant	<0.2	<35
Standard value for a very well-filtered beer	≤0.3	–
Clear/almost brilliant	0.2 to 1.0	35–69
Slightly opalescent/hazy	1.1 to 2.0	69–138
Opalescent	2.1 to 4.0	–
Cloudy/hazy	4.1 to 8.0	138–276
Very cloudy/hazy	>8.0	>276

Table 3. Turbidity units with abbreviation, measurement method, regulation and area of application. (*FTU = NTU*).^[13,22–26]

Name of the unit	Abbr.	Measurement	Regulation	Application area
Formazin Turbidity Units	FTU*	Nephelometer	Regulations according to USA	(Drinking) water treatment
Nephelometric Turbidity Units	NTU*	Measurement is conducted at an angle of 90°	Regulations according to USA, identical to FTU	(Drinking) water treatment
Formazin Nephelometric Units	FNU	Scattered light measurement (angle 90°) Nephelometer with infrared light source	Standard ISO 7027 / EN 27027	(Drinking) water treatment
Formazin Attenuation Units	FAU	Transmitted light measurement (angle 0°)	Standard ISO 7027 / EN 27027	(Drinking) water treatment
Turbidity Unit Formazin	TU/F	Measurement with formazin	Standard ISO 7027 / EN 27027; ASBC and EBC standard methods	(Drinking) water treatment; Beer
European Brewery Convention Formazin Haze units	EBC-TU or FHU	Scattered light measurement /Transmission (angle 90°)	Standard ISO 7027 / EN 27027; EBC standard methods	Beer
ASBC	ASBC FTU	Measurement with formazin	ASBC and EBC standard methods	Beer

Table 4. Conversion of the turbidity units.^[22,24,25]

1 EBC-TU or FHU	1 FNU 1 NTU 1 FTU 1 FAU	1 ASBC FTU	EBC TU or FHU FNU NTU FTU FAU ASBC FTU Nephelo
1	0.25	0.014	
4	1	0.057	
69	17.5 6.7	1	

turbidity can be inferred depending on which sample has lost turbidity due to certain enzymes. Enzymes used include pepsin, amyloglucosidase and lichenase, which can degrade proteins, dextrins and starch, and glucon respectively.^[3,20]

Gel permeation chromatography (GPC) is a process for separating substances dissolved in liquids according to their molecular weight. The separation is carried out by diffusion effects. Molecules of different sizes pass through a separation column at different speeds. This separation column is filled with a porous gel consisting of small beads with a size of 6–10 μm and represents the stationary phase of the chromatograph. The mobile phase - the eluent - consists of one or more solvents in which the particles to be tested are dissolved. If the particles present in the liquid hit the gel, they can penetrate it, depending on their size. Small molecules are able to enter the spaces between the gel beads, which slows their passage through the columns. Large molecules do not interlock in the pores and migrate quickly through the separation column. Depending on the type of gel material, various samples of different molecular masses can be separated and tested with this method.^[29,30] GPC can also be used to identify polysaccharides in beer and wort and assign them to their origin. Beer or wort with a paste

turbidity can be separated by GPC according to the molecular weight and stained with iodine. Subsequently, a photometric iodine sample is taken to analyze the results. This makes it possible to determine whether these are polysaccharides or glucans, and whether they are of vegetable origin or yeast.^[16,20] As with most other analyses for turbidity identification, a disadvantage of using gel permeation chromatography is the invasive nature of the sampling. It is not possible to examine the container unopened. Sample preparation is also relatively time-consuming. The type of turbidity involved must be known in advance so that a suitable column and eluent can be selected. In addition, the liquid must be centrifuged with the GCP before separation in order to obtain a turbidity residue. Before chromatography, this residue must be dissolved again in the eluent.^[20,29]

Origins of turbidity

Haze particles in beer can be further distinguished between foreign particles and those derived from the beer or its raw materials. Turbidity colloids, as they occur in cold and permanent opacification, are composed of turbidity-active substances derived from beer or its raw materials. Table 5 gives an overview of the composition of beer turbidity compounds from different authors' studies.

Here, too, it can be seen that the proteins, together with the polyphenols, make up the major part of the turbidity colloids. The variations in the data can be explained by the use of different raw materials in the production of the beers. In addition, the stabilization measures also have a significant effect on the composition of the beer turbidity, depending on whether the tanning or protein side is stabilized.^[36] The individual components of the beer's own haze builders are further characterized below.

Table 5. Percentage composition of beer turbidity compounds according to different literature data.

	GRAMSHAW ^[31]	WAINWRIGHT ^[32]	Rehmanji et al. ^[33]	NARZİD ^[34,35]
Proteins	58–77 %	40–77 %	40–75 %	40–75 %
Polyphenols	17–55 %	15–75 %	~17 %	30–45 %
Polysaccharides	2–12 %	0–13 %	3–13 %	2–15 %
Inorganic substances	2–14 %	1–14 %	1–5 %	1–14 %

Chill haze and permanent haze

Non-biological turbidity is categorized as chill haze or permanent opacity. Chill haze is reversible, forms at a temperature of 0 °C and dissolves when heated to 20 °C again, whereas the permanent opacity is irreversible. Chill haze is considered to be the precursor of the persistent cloudiness, as it steadily increases with repeated heating and cooling and can finally turn into a perpetual opacity. The reversibility of the cold turbidity results from the rather weak bond types (hydrogen bonds, hydrophobic bonds) between the components that form haze in beer. In contrast, the formation of permanent opacification usually requires oxidation as well as the formation of covalent bonds, which usually involves the formation of larger particles. The most important and common cause of such colloid formation results, according to unanimous opinion in research, from the interaction between proteins and polyphenols.^[2,11,31,36–40] Figure 3 gives an overview of the particle diameter of turbidity particles in cold and permanent opacification.

In the following sections, the various turbidifiers will be discussed in more detail, their origins and interrelations explained.

Non-biological turbidity - proteins and polyphenols

The most important type of beer turbidity in the category of organic substances of non-biological origins is the reaction of proteins and polyphenols. These form complexes which precipitate in the finished beer and affect its colloidal stability.^[3,41] A distinction is made between cold cloudiness and permanent cloudiness. Cold turbidity consists of particles of 0.1–1.0 μm in size and is formed at –8 °C to 5 °C when proteins and polyphenols form non-covalent bonds. This type of turbidity is not permanent and is reversible at 20 °C or higher.

Permanent turbidity with a particle size of 1–10 μm begins with a cold turbidity, but the proteins and polyphenols form covalent bonds and form insoluble complexes that are irreversible, even at higher temperatures. This type of turbidity occurs when the beer temperature changes more often between warm and cold.^[11] Certain inorganic constituents can also favor cold or permanent turbidity. These include calcium, particularly as calcium oxalate, magnesium and manganese, which as induction nuclei can increase the cold haze. These metals and salts were found in increased amounts in the residues of cold haze. More and more metals such as aluminum, iron, nickel, copper, tin and lead have been found in the residues of permanent opacities.^[35] They serve as catalysts for oxidation reactions and increase the tendency to turbidity.^[19] Permanent turbidity can also be

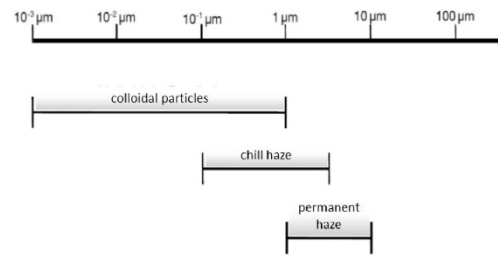


Figure 3. Diameter of colloidal particles in chill haze and permanent haze.^[32]

stimulated and intensified due to ageing processes, oxidation, prolonged shaking, or pasteurization.^[19] Complex formation of proteins and polyphenols is the most common type of undesired impairment of colloidal stability.^[19] Beer contains approx. 500 mg/L proteins, with only 2 mg/L being sufficient to cause turbidity. The proteins in beer are mainly introduced by the malt and hops, a minor role is played by the yeast origin. Since approximately 80% of the proteins in the malt are insoluble in water, they do not pass into the wort or the finished beer but are removed from the process by the spent grains or hot trub. The water-soluble proteins are resistant to proteolysis during mashing, do not coagulate during wort boiling, and are not removed with the hot trub. They remain unchanged or remain as degradation products in beer.^[20,42,43]

There are various stabilization measures but since protein also plays an important role in foam stability, proteins must not be completely removed from the beer. Silica gel has proven itself in practice because it can selectively remove turbidity-forming proteins without influencing the foam.^[44] Silica gel adsorbs proteins and protein-polyphenol complexes. These are then removed from the brewing process by filtration or sedimentation. Since silica gel is not water-soluble and no residues remain in beer, this process conforms to purity requirements. Silica gel acts selectively, only proteins, their precursors and complexes are adsorbed that impair colloidal stability. The removal of foam-positive proteins from beer can be prevented, for example, by adjusting the pore size of the silica gel. The foam properties of the beer therefore do not change.^[44,45]

There are different types of classification and fractionation for proteins, which can be carried out by different solvents. According to Osborne, barley proteins can be divided into four groups, namely albumins, globulins, glutelins and prolamins (hordeins).^[46] According to Asano et al., proteins responsible for cold turbidity can also be differentiated according to their molecular weights.^[47] The different fractions have different effects on the colloidal stability of beer. Albumins and globulins in particular seem to have a major influence on the formation of cold cloudiness. There are numerous different studies in the field of fractionation according to molecular weight. These are concerned with associating proteins of different weights with turbidity. However, the results are unclear, and several studies show that both low and high molecular weight proteins can cause turbidity. In addition, proteins with an isoelectric point in the acidic range

Table 6. Protein fractionation with proline content and turbidity potential.^[47]

Fraction	I	II	III	IV
Molecular weight [Da]	1–1000	19000	16000	40000
Proteins	Hordein	Hordein	Albumin/ Globulin/ Hordein	Albumin/ Globulin/ Hordein
Content of proteins [%]	69	76	65	75
Content of carbohydrates [%]	7	23	12	17
Content of proline [mol %]	5.5	19.9	10.3	8.7
Turbidity potential [EBC]	6.7	23.3	13.2	10.2

appear to have a turbidity-active effect.^[17,27,36,37,47] The hordein fraction of barley has the greatest influence. Hordeins are rich in the amino acid proline and for this reason have a higher affinity for polyphenols than low-proline proteins,^[47] as can be seen in Table 6.

In this work,^[47] samples of the protein fractions were mixed with beer in combination with the polyphenol catechol and the resulting turbidity was then measured nephelometrically. The higher the proline content in the proteins present, the greater the turbidity. Due to a pyrrolidone ring contained in the proline, hydrogen bonds cannot form at these sites and the secondary structure of the protein is impaired. It is also not possible for pyrrolidone to form hydrogen bonds with the oxygen atoms of peptide bonds. This not only disrupts the structure of the protein, but also prevents the binding of other proteins at the proline sites. These free sites and structure impairment prevent the formation of a helix. For this reason, the hydroxy groups of polyphenols can attach to the free oxygen atoms of the carbonyl groups of proteins by hydrogen bonds and form complexes with other proteins. The hydrophobic nature of proline allows them to bind to polyphenols via the hydrophobic effect and cause cold haze.^[37,39] This property is exploited in the stabilization of beer in accordance with the purity requirements by using PVPP (polyvinylpyrrolidone) for polyphenol stabilization. This can be added at the same time as the filter aid before filtration or as a running dosage and serves to stabilize the beer on the tanning agent side. Polyphenols accumulate on the surface of PVPP, i.e., they are adsorbed. Since PVPP, like the silica gel used for protein-like stabilization, is not water-soluble, it can be separated out again after filtration and therefore conforms to purity requirements. The mode of action of this process is similar to the mechanism of complex formation of proteins and polyphenols. PVPP imitates a proline-rich protein to which polyphenols can easily bind. Thus, up to 81% of proanthocyanidins (procyanidin B3, prodelfphinidin B3) and 78% of flavan-3-ols (catechin, epicatechin etc.) can be removed from beer or wort.^[36] As already mentioned, polyphenols are an important building block in the formation of cold haze and a possible permanent haze. They bind to proteins and thus enable the formation of large agglomerates. Polyphenols serve as connecting pieces between proteins.^[48] This is shown schematically in Figure 4.

The ratio of polyphenol and protein concentrations plays an important role. If the polyphenol content is high and the protein content low, all the linking sites are occupied by polyphenols and no further proteins can participate in the complex formation. With a high protein content and low polyphenol content, a few polyphenols bind, but the

probability is low that other proteins are involved in this process. Thus, the complexes remain small and only slight turbidity occurs. If the protein and polyphenol contents are in equilibrium, i.e., if the number of binding sites is the same, colloidal stability is most severely impaired. Significant turbidity occurs.^[48] In addition, the alcohol content and pH of the beer also have an influence on the linking of proteins and polyphenols. Ethanol plays only a minor role. The tendency to turbidity initially decreases slightly with increasing ethanol content and then increases again with increased alcohol content. The pH value, on the other hand, has a stronger effect. If the proteins and polyphenols links are in equilibrium, the turbidity increases rapidly when the pH rises from below 3 to above 4. If the pH value is further increased, the turbidity decreases again. However, this is irrelevant, since the pH value of beer is approx. 4.25–4.6.^[27,48,49]

Up to 30% of the polyphenols contained in beer come from hops, with the rest coming from malt.^[49] They can be divided into three categories that distinguish between monomeric, oligomeric and polymeric polyphenols as shown in Table 7. The flavonoids such as the flavan-3-ole catechins, epicatechins and gallo catechins and their condensed products, the proanthocyanidins such as procyanidin B3 and prodelfphinidin B3, are of great importance. The latter are dimers from the combination of catechins or catechins and gallo catechins.^[36,50–52]

The values in Table 7 do not correspond to the values of real beer. The polyphenols were first removed from the wort with the aid of PVPP and then mixed again with 100 mg/L turbidity-forming polyphenols. This shows which of these polyphenols reach the finished beer. Real values for catechin are 0.15–4.0 mg/L, for procyanidin B3 up to 3.6 mg/L and for prodelfphinidin B3 up to 4.5 mg/L, depending on the type of beer and the raw materials used.^[53,54] In this study, the various polyphenols were dissolved in a sodium phosphate buffer and proteins were added. The resulting turbidity could then be measured nephelometrically. As can be seen from Table 7 and in accordance with Asano et al.,^[50] the two most important polyphenols for turbidity formation are catechol and procyanidin B3. The others form protein-polyphenol agglomerates during wort boiling, which are removed with the hot trub in the whirlpool. The polyphenols that are converted in the finished beer do not seem to have a high affinity to proteins at first. Catechin and procyanidin B3, which consists of two catechin molecules, are therefore not responsible for turbidity, but are important precursors of turbidity.^[50] According to Siebert,^[39] the dimer prodelfphinidin B3, which results from the

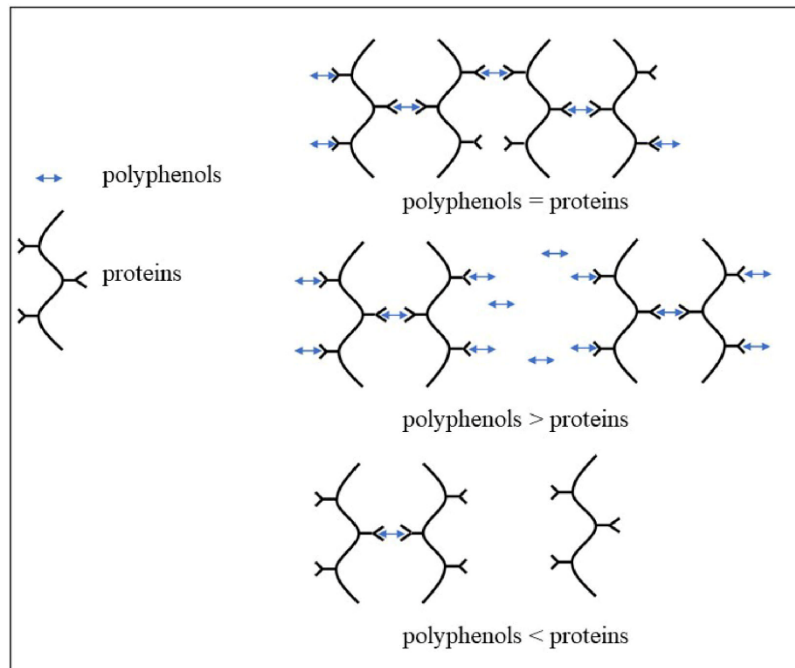


Figure 4. Mechanism of protein-polyphenol complex formation; influence of protein and polyphenol concentration on turbidity formation.^[48] [adapted].

Table 7. Polyphenols and their turbidity potential with hordein.^[50]

Category	Polyphenols	Turbidity potential with hordein [EBC]	Content after wort boiling [mg/L]	Content after storage [mg/L]
Monomeric	catechins	0.02	54	46
	epicatechins	0.42	0	0
Oligomeric/polymeric	procyanidin B ₃ (Dimer)	5.5	11	10
	prodelphinidin B ₃ (Dimer)	18.2	traces	0
	procyanidin C ₂ (Trimer)	79.3	0	0
	proanthocyanidin (Tetramer)	26.5	0	0
	proanthocyanidin (Pentamer)	38.2	0	0

combination of catechin and gallic acid, is also present in higher amounts in finished beer.^[39]

In addition to these flavonoid polyphenols, phenolic acids from the group of hydroxybenzoic acids, such as gallic acid, and from the group of hydroxycinnamic acids, such as ferulic acid, can also influence the colloidal stability of beer. While it is possible to remove the above-mentioned polyphenols from beer using stabilizing measures, this is not the case for phenolic acids. They pass almost unchanged into the finished beer. Phenolic acids are also desirable to a certain extent in beer. Ferulic acid is the precursor for 4-vinyl guaiacol and is responsible for the clove aroma in wheat beer. However, too much of this acid in combination with proteins can lead to undesired turbidity. While gallic acid only occurs in very small amounts - in the microgram range - in beer, it is possible that ferulic acid reaches a content of up to 3.13 mg/L.^[54,55] It was found^[56] that a certain content of ferulic acid can positively influence the turbidity stability.

This is probably due to the blocking of polyphenols that cause strong turbidity, such as pro-cyanidin B₃ and prodelphinidin B₃. The reason for this is that ferulic acid has only one binding site with which it can attach itself to proteins. In this respect it can be said that although ferulic acid has a positive effect on the colloidal stability of beer, it is always present in significant amounts in the residues of turbidity.^[56] The degree of polymerization plays an important role in the formation of turbidity. The higher the polymerization of polyphenols, the higher their affinity to other substances and the deterioration of colloidal stability.

The potential for turbidity formation is increased by ageing processes and in particular by an increased oxygen load during production and in bottled beer. This leads to an increased oxidative polymerization or condensation and thus to substances with a higher molecular weight.^[50] Monomers such as catechins oxidize and polymerize to higher

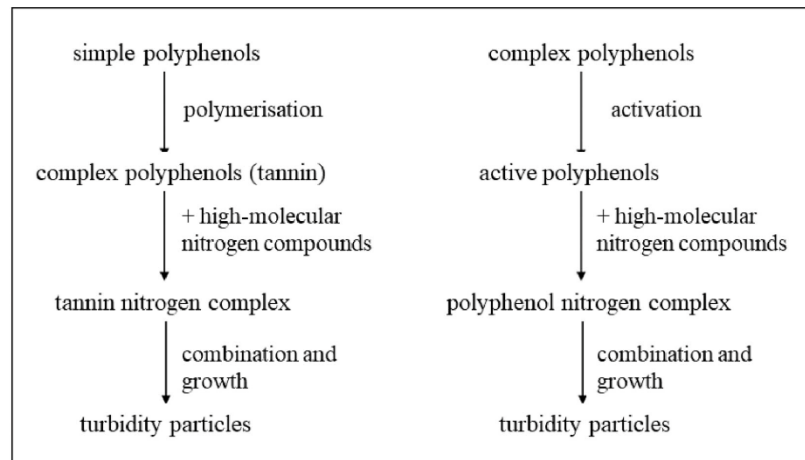


Figure 5. Theories on the formation of turbidity by polymerization or reactivation.^[36] [adapted].

molecular weight phenols, to protein-precipitating polyphenols, which are called tanning agents. This means that another ring is attached to the single molecule. They increase in size as a result. A dimer is formed first, such as procyanidin B3 or prodelphinidin B3. Further polymerization produces oligomers and polymers. The monomers catechin and epicatechin are precursors of turbidity, and only the increased occurrence of dimers and oligomers due to polymerization leads to an impairment of colloidal stability.^[36,50] There are two theories how this complex formation in beer can lead to turbidity. These are described in Figure 5.

The first possibility is the most widely accepted theory. As already mentioned, a polymerization of polyphenols occurs, resulting in the formation of more complex polyphenols. Through the reaction with high-molecular nitrogen compounds, i.e., proteins agglomerate and turbidity particles are formed. The second theory is similar to the first, but here the complex polyphenols are already present and are only activated. The next stage in which turbidity particles are formed is identical to that of the first theory.^[36]

Non-biological turbidity – caused by carbohydrates

A non-biological, organic haze, which occurs far less frequently than a cold or permanent haze, is caused by carbohydrates. Polysaccharides or glucans impair the colloidal stability of beer. Most of these come from malt, but they can also originate from yeast as glycogen.^[20] Glucans consisting of α -(1-4)- and α -(1-6)-glycosidically bound glucose units are present in the endosperm of the malt as amylose and amylopectin and are the carbohydrates that are converted into useful sugars for the yeast during mashing. If these glucans are not sufficiently broken down during mashing, they remain as long-chain dextrans and cannot be used by the yeast. With increasing fermentation and thus increasing alcohol content, the solubility of the dextrans is further

and further reduced, and a gray veil, which is referred to as paste turbidity, appears.^[27] Reasons for a poor degradation of the α -glucans can be a lower quality of the raw materials or can also be based on technological causes. It is possible that the malt has a high all-glass or gelatinization temperature, which makes degradation difficult or impossible. Technological reasons can be an inadequate mashing process with too short rest periods or incorrect temperatures. Wort that are too hot during refining after enzymatic degradation also dissolve glucans from the malt. These dextrans, especially amylopectin, cause turbidity that is difficult or impossible to remove from diatomaceous earth and membrane filters.^[57] Glucans interact with protein-polyphenol complexes via hydrogen bonds and thus additionally increase the tendency to form cold turbidity. By adding a malt extract, enzymes are reintroduced, which cleave α -glucans and degrade them in such a way that they become usable for the yeast. This can counteract clouding of the paste and dissolve it.^[37,57,58] More rarely, α -glucan turbidity occurs. Glucans are α -(1-3)- and α -(1-6)-glycosidically bound glucose units that are present as structural molecules in the cell wall of barley and can enter the finished beer through the complete malting and brewing process. They may cause filtrate disturbances as a β -glucan gel. It is also possible, however, that they pass through the filter at higher temperatures or high pressures during filtration and impair the colloidal stability of the beer. The higher the molecular weight of the α -glucan, the more noticeable the turbidity. The molecular weight is between 31 and 443 kDa. From 300 kDa they can cause turbidity after filtration.^[23] Yeast can also release carbohydrates in the form of glycogen, glucan or mannan during yeast autolysis or under stress conditions. As with α -glucan from malt, turbidity from yeast-glucan rarely occurs. Even rarer is a paste turbidity due to yeast mannan.^[59] Glycogen is a reserve substance from α -(1-4) glycosidically bound glucose units of yeast and can be released under cell autolysis or stress conditions such as high-gravity

Table 8. Turbidity tendency of carbohydrates in beer; (++) = very strong; + = strong, - = weak; -- = very weak).^[45,57,58]

Carbohydrate	Amylose	Amylopectin	Arabinoxylan	β -Glucans	Glycogen	Mannan
Origin	Malt	Malt	Malt (wheat)	Malt / Yeast	Yeast	Yeast
Turbidity tendency	-	++	-	+	+	+

brewing or high fermentation temperatures. Like α -glucan from malt, it can cause paste clouding in beer.^[60] Hemi-celluloses, such as pentosan, are another group of substances that may cause turbidity. These include arabinoxylan, which occurs in the cell walls of both barley and wheat, but it plays a greater role in wheat. This can enter into the finished beer due to poor mashing and can cause turbidity in connection with proteins.^[20,45] Table 8 lists the carbohydrates discussed above according to their origin and cloudiness.

Inorganic turbidity

Turbidifiers or foreign particles of inorganic origin are substances that do not originate from the raw materials but are introduced into the beer by other means. These include filter aids that break through during filtration and enter the finished beer, or residues in containers such as label residues or other substances. The former can be avoided by post-filtration, the latter usually occur only occasionally and are difficult to detect and prevent. Such particles can only enter the beer if process errors occur during bottle cleaning and inspection problems.^[39,61] Stabilizers such as PVPP and silica gel can also occur to some extent in beer and affect colloidal stability.^[16] As already mentioned, by using modern filtration and filling equipment and implementing comprehensive quality assurance, the occurrence of foreign particles in the end product can be considered an exception.

Non-biological turbidity – inorganic substances

Larger substances, such as label residues or objects in containers, do not cause turbidity, but do reduce the quality of the beverage to a lower level for the consumer. Products contaminated in this way must not be placed on the market. Very small particles, such as aluminum residues from bottle cleaning, are often not detected by a bottle inspector and may be responsible for turbidity.^[16]

Filter aids

Filter aids are powdered, chemically inert substances that support filtration both physically and mechanically. There are different principles of action depending on the filter aid used. Either they promote the formation of a filter cake in suspensions with only a small amount of dissolved solids, form a fine-pored filter layer through their own mass or loosen too firm a filter cake. However, filter aids always require a filter medium upon which their alluvium takes place.^[1]

Kieselguhr

Diatomaceous earth, also known as kieselguhr, is the name given to the fossils of unicellular diatoms that have been deposited on the sea floor in a layer of up to several

hundred meters thick approximately 15 million years ago. Dehydration of the water and shifts of the tectonic plates have brought these layers to the surface of the earth, where today they are mined in an open pit. The largest deposits are in the US, Mexico, Chile, China, France and Spain.^[62] There are three different types of diatomaceous earth. Depending on the permeability, a distinction is made between fine (permeability <0.1 Darcy), average (permeability 0.1–0.5 Darcy) and coarse (permeability > 0.5 Darcy) kieselguhr. The preparation of the raw material happens accordingly in three different variants. For the dried kieselguhr, the raw material is crushed, ground and then dried in a rotary kiln at 300–400 °C. At this stage, the natural shape of the diatom shells, as well as their porosity is retained, so that it can be produced from fine diatomaceous earth. The Gur dried in this way usually contains less than 1% crystalline silica. For the preparation of fast-filtering diatomaceous earth, the so-called calcined kieselguhr (medium diatomaceous earth), the dried kieselguhr is heated again up to 800 °C. At these temperatures, the surfaces sinter together diamond shells, thereby increasing the particle size. It is essential that the inner, porous structure and thus the filtration activity is retained as far as possible in this process. The so-called flux-calcined kieselguhr varieties have even faster filtration properties. In order to produce these, the raw siliceous earth in the rotary kiln is added with 2–5% of a flux (sodium chloride or sodium carbonate) and then calcined at 800–900 °C. This process step lowers the melting point of the silica from which the diatom atoms mainly consist. This has the effect of enhancing the sintering of the diatoms, resulting in even larger conglomerates. Inorganic impurities, such as iron and aluminum oxides are thereby converted into barely soluble mixed silicates. This gives the coarse, flux-calcined diatomaceous earth an almost white appearance.^[62] The calcination process increases the content of crystalline silicic acid (SiO₂), in particular in the form of cristobalite. While the cristobalite content of the raw siliceous earth is still below 1%, it increases to 10–40% for calcination and 40–90% for flux calcination. The most important feature of kieselguhr is its large internal porosity. The inner surface is up to 20 m²/g, whereby kieselguhr has only a very low adsorption capacity, but is largely responsible for the formation of a fine-pored filter cake. Both the particle size and the shape of the diatomaceous earth particles have a decisive influence on the clarification effect and the filtration rate. Fine kieselguhr has a higher clarifying effect, but at the same time a lower filtration rates. This applies in the opposite sense for coarse diatomaceous earth.^[14,62] Diatomaceous earth dosages may range from 90–180 g/hl, depending on the prevailing conditions, e.g., the initial turbidity of the unfiltered or the desired degree of clarification.^[63]

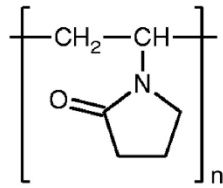


Figure 6. Structural formula of polyvinylpyrrolidone (PVP).^[74]

Perlite

Perlite is a glassy rock of volcanic origin and consists predominantly of aluminum silicates composed of approximately 72% silica (SiO₂) and 13% aluminum oxide (AlO₃).^[64,65] The raw material is annealed at 800 °C, which expands the trapped water and causes the perlite to puff and burst. The resulting glassy particles are ground to a light and fluffy powder, which is 20–40% lighter in weight than diatomaceous earth. Perlites are insoluble in water and largely chemically inert both in beer and in wort. Perlites are considered to be particularly economical due to their long filter life and high flow rates. A disadvantage is the strong abrasive effect of perlites with piping, pumps and fittings. The degree of clarification of perlites is also inferior to kieselguhr.^[66]

Cellulose fiber

The use of kieselguhr is causing increasing problems in the beverage industry. Firstly, the disposal of kieselguhr sludge is very expensive and elaborate. Secondly, the kieselguhr deposits are finite and even if kieselguhr regeneration methods are now available, regenerated kieselguhr can be reused a maximum of five times.^[14] In addition, the inhalation of cristobalite powder holds a potential medical hazard. Not only does the dust lead to silicosis, it is also classified as a carcinogen for humans (cancer risk class 1) when inhaled, according to the International Agency of Research on Cancer (IARC).^[67–69] Due to this, alternative filter aids are gaining more and more attention.^[14] Cellulose fibers have been used since the beginning of industrial filtration as a regenerable filter media in what are called mass filters. In some cases, 1% asbestos was added to the filter mass to increase selectivity.^[63] The mass filter disappeared from breweries, not the least because of the prohibition of asbestos in Germany in 1993, as well as the high workload. However, cellulose fibers are still added today as a supplement to other filter aids. The fibers thereby cause a loosening of the filter cake, a mechanical stabilization against pressure surges and help to detach the filter cake from the filter medium. However, filtration with cellulose fibers requires extensive primary treatment. Cellulose is a biopolymer of β-1,4-glycosidically linked D-glucopyranose units. The cellobiose units form the backbone of the cellulose. In addition to the hydrocarbon chains, wood pulp cellulose contains a carboxy group every 100–1000 glucopyranosyl units.^[70] Cellulose fibers are obtained from both deciduous trees and conifers. It is therefore a renewable resource that is completely biodegradable. Ingredients such as lignin and

hemicelluloses must be removed in order to obtain high-purity, taste-neutral α-cellulose fibers. Cellulose fibers are available in different lengths. Long fibers form a compressible support fabric for the filter cake but have only a low clarification. Short fibers are suitable for fine filtration but reduce the permeability of the filter cake. Fibrillated fibers have numerous partial splits or splits on the surface, as a result of which the filtration activity also increases.^[14,67,71]

Further filter aids

In addition to the above filter aids, there are several other established filter aids in the beverage industry. Since these also have a turbidity potential in the transition to the filtrate, they should also be mentioned at this point. BASF has developed a pebble-free filter aid called Crosspure. It is a synthetic exudate of 70% polystyrene and 30% polyvinylpyrrolidone (PVPP). The PVPP content allows simultaneous tanning agent stabilization.^[63] Another alternative to kieselguhr-free precoat filtration are cellulose-based viscose fibers. The diameter, length, cross-section and shape of the fibers can be varied as required. Furthermore, the fibers can be provided with functional groups and additives. In this way, synthetic fibers can be produced for filtration that are especially suited to a specific beverage.^[72,73]

Stabilizing agents

With the help of stabilizing agents, the formation of colloidal turbidity can be significantly delayed, but not completely prevented. The effect of stabilizers is based on the adsorption of reactants involved in the formation of colloidal turbidity. In practice, breweries today mainly use PVPP or silica gel preparations. These two stabilizers can also be used in combination.^[63]

Polyvinylpyrrolidone (PVPP)

PVPP is a high polymer and water-insoluble stabilizer. It is synthesized by polymerization or condensation from water-soluble polyvinylpyrrolidone (PVP), giving it a three-dimensional structure and becoming insoluble.^[2,63] Figure 6 shows the structural formula of PVP.

The structural formula of PVP has a cyclic amide, also called lactam ring. The lactams are derived from the lactones because they contain an amide group instead of the intramolecular ester group. These monomeric ring structures are connected to each other via hydrocarbon compounds.^[74] PVPP is a white powder and has a melting point of 220 °C. Due to the amorphous structure, PVPP has a high internal surface area of approx. 1.2 m²/g.^[75] The dosage recommendations range from 10 to a maximum of 50 g/hl.^[76] PVPP has a binding site that is complementary to proline segments as found in opacifying proteins. Because of this property, PVPP is able to specifically adsorb polyphenols such as catechol or proanthocyanidins from the unfiltrate. They can then be retained in the filter. Thus, PVPP is a protein dummy and beers can be stabilized on the tanning agent side, as shown in Figure 7.^[2,63,75,78]

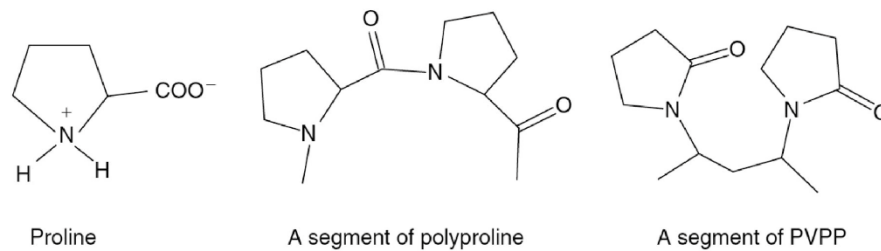


Figure 7. Structural similarities between the amino acid proline, a section of polyproline and a section of PVPP.^[37,77]

PVPP adsorbs polyphenols by hydrogen bonding, which form between the carbonyl groups of the PVPP and the OH groups of the phenols of the polyphenols.^[63] The formation of these bonds is pH dependent, which is why they dissolve again in an alkaline environment. This fact is based on the principle of PVPP regeneration. After stabilization, the PVPP is rinsed with a 0.9% NaOH solution to dissolve the hydrogen bonds. Subsequently, after an intermediate rinsing step with hot water, a second regeneration takes place with sodium hydroxide solution. Finally, it is rinsed again with water and gassed with CO₂ in order to lower the pH again to a value below 7.0. The PVPP regenerated in this way can be used for renewed beer stabilization. In contrast, the so-called “lost” PVPP dosage is the PVPP that is discarded and disposed of after filtration. For a satisfactory stabilization, a contact time of 4–5 min is needed between PVPP and the unfiltrate.^[2,66]

Silica gel

Silica gels, in contrast to PVPP, serve to stabilize beer on the protein side. They cause a selective adsorption of turbidity-relevant proteins and protein-polyphenol complexes and barely reduce the amount of foam-active proteins. Silica gels are odorless and tasteless, as well as chemically inert. There are three different silica gel preparations on the market - xerogels, hydrated xerogels and hydrogels.^[44] The distinguishing feature is the water content of the respective preparations (Table 9).

Hydrogels and hydrated xerogels are less dusty due to their higher water content, making them easier to handle. The use of xerogels, however, is more economical, as they have a better stabilizing effect compared to hydrogels. Silica gel preparations do not swell and so beer losses are very low.^[66] Silica gels consist of cross-linked silica molecules (SiO₂). The preparation of silica gels is carried out by reacting silicates in the form of water glass with mineral acids such as sulfuric acid. This results in an intermediate step to generate first silica sol and then silica gel. By washing, the same hydrogel is formed, which can then, depending on the drying intensity, be processed into xerogel or hydrated xerogel.^[2,44,66] Compared with PVPP, silica gel preparations with 300–700 m²/g have a much larger internal surface area. In addition, there are reactive silanol and silanediol groups,

Table 9. Overview of the various silica gel preparations and their water contents.^[22,44,66]

Silica preparations	Water content [%]
Xerogels	5–25
Hydrated xerogels	25–40
Hydrogels	50–60

which is why silica gel preparations are characterized by a high adsorption capacity.^[66]

Further stabilizing agents

Table 10 gives an overview of other stabilizers, as well as their corresponding effect.

However, with the exception of bentonite, the use of the stabilizers listed in Table 10 is prohibited in Germany due to the purity requirement.^[36] Bentonite is natural aluminum, calcium or magnesium silicates, which have a non-specific adsorption capacity towards nitrogen compounds.^[2] The protein adsorption by bentonite is therefore less selective and thus, for example, foam-active protein fractions are also removed.^[49,80,81] In addition, its strong swelling capacity increases beer loss. Due to these facts, silica gels are usually preferred in breweries for stabilization on the protein side.^[82]

Non-biological turbidity – microplastics

Organic contamination, which is not microbiological or vegetable in nature, is due to contamination with microplastics. Plastics that are not properly recycled or reused can accumulate in water and pollute it. Small plastic particles are formed by decomposition processes, triggered by, for example, UV radiation or mechanical stress. These particles are called microplastics with a size between 1 μm and 5 mm. Primary microplastics are produced directly in this size for use, and secondary microplastics, which reach a size of less than 5 mm through decomposition processes.^[83] Microplastics in water bodies can enter and contaminate drinking water and process water through the public water supply. According to a study by OrbMedia,^[84] 93% of bottled water is contaminated with microplastics. Although no damage to human health has been proven, indigestible particles smaller than 150 μm can penetrate and remain in the body after consumption.^[83]

Table 10. Overview of other stabilizers and their corresponding effect.^[2,22,79]

Stabilizing agents	Effect
Bentonite	Adsorption of proteins
Tannin	Precipitation of proteins
Papain, proteinases	Enzymatic protein degradation
Amylase, glucanase	Enzymatic carbohydrate degradation
EDTA	Complexation of metals
Ascorbic acid	Oxygen reduction

Depending on the container, different concentrations as well as different types of microplastic have been found. Water filled into returnable plastic bottles had a concentration of 118 ± 88 particles/L, 14 ± 14 particles/L in disposable plastic bottles, 11 ± 8 particles/L in cardboard containers, and 50 ± 52 particles/L in glass bottles.^[85] A larger amount of polyethylene terephthalate (PET) and polypropylene (PP) was found in water in plastic bottles, while water from glass bottles had a balanced concentration of different plastics. This is due to the materials into which the water was filled. Reusable plastic bottles are made of PET and screw caps are made of PP.^[85] Products with a higher crystalline content (PET-C) are suitable for use in everyday and consumer articles and can be exposed to higher temperatures (temporarily up to 200 °C). However, due to the higher proportion of semi-crystalline structures, they also tend to become more turbid.^[86] These concentrations of microplastics in water do not cause any visible turbidity. However, due to the increasing health and environmental concerns associated with microplastics, it is necessary to increase the number of analyses of water for plastics.

Biological turbidity

Organic turbidity can have biological or non-biological origins. On the biological side, turbidity can be caused by microorganisms or their metabolic products. Due to the selective properties of beer (low pH value, alcohol content, hop bitter substances, CO₂, etc.), the growth of microorganisms is restricted, and they play a subordinate role in the formation of turbidity. However, poor industrial hygiene can lead to primary or secondary contamination during bottling, leading to contaminated beers that later become cloudy. Microorganisms, such as fungi or bacteria can form turbidity. Some are introduced into production by the raw materials used and can damage the wort or beer.^[28] Only a few types of bacteria and yeasts impair colloidal stability leading to turbidity or sediment. These can be obligatory beer-spoiling species, such as gram-positive bacteria, which belong to the genera of *Pediococcus* and lactic acid bacteria, and gram-negative bacteria such as *Pectinatus* and *Megasphaera*. In yeasts, a distinction can be made between cultivated yeasts and wild yeasts. Culture yeasts include *Saccharomyces cerevisiae* and *Saccharomyces pastorianus* var. *carlsbergensis*, wild yeasts, which can be obligate beer spoilers, potential and indirect beer spoilers such as *Brettanomyces bruxellensis* and *Pichia anomala*.^[27,87,88] *Pediococcus damnosus* can lead to sediment and turbidity in beer. In addition, taste is strongly impaired because the pH value of the beer is lowered, and diacetyl is formed.

Pediococcus inopinatus is another bacterium of this genus that causes damage to beer but occurs to a lesser extent.^[27] There are different types of bacteria that belong to the lactic acid bacteria and occur more often in beer than pediococci. *Lactobacillus brevis* is one of the microorganisms commonly responsible for the microbiological contamination of beer. This type of bacteria is an obligate spoiler and potentially harmful to beer. It leads to a sour taste and turbidity. Another frequently occurring lactic acid bacteria is *Lactobacillus lindneri*, which is also an obligate spoiler and potentially harmful to beer. Contamination with this species leads to a slight clouding of the beer, while taste only changes slightly or does not change. Depending on the selective properties of the beer, other species such as *Lactobacillus coryniformis* and *Lactobacillus casei* can occur. Many other types of lactic acid bacteria can also be found to a lesser extent in beer.^[27,87,88] The gram-negative anaerobic bacteria *Pectinatus* and *Megasphaera* are obligate beer-spoiling microorganisms. They only enter the beverage as secondary contaminants during filling. This is a stray contamination, since only individual bottles are infected during filling. These two types of bacteria are very damaging to beer and lead to beers with an unpleasant odor and bad taste. Both microorganisms cause turbidity, with only a slight fog appearing with *Megasphaera*, while *Pectinatus* forms a strong turbidity, sediment and possibly lumps.^[27,87,88] Table 11 lists bacteria that form a cloud and/or sediment and their route of entry into the beer.

Yeasts can cause beer turbidity by appearing in larger quantities in beer or by impairing colloidal stability through their metabolites. In yeasts, a distinction is made between cultured yeasts used in breweries, wineries, etc. and wild yeasts. Wild yeasts can also be divided into *Saccharomyces* or non-*Saccharomyces* foreign yeasts and into fermenting, low-fermenting and respiratory yeasts.^[91] Culture yeasts cause beer turbidity due to a high cell count in the finished beer. This may be desirable for unfiltered beers such as wheat beer or cellar beers. It is also possible, however, that an undesired increase in the yeast can cause the beer to cloud. This is the case when yeast passes through the filter and there are sufficient nutrients for the yeast due to a low degree of fermentation. Important representatives of wild yeasts that cause turbidity belong to the category of fermentative *Saccharomyces* yeasts. These are very similar to the *Saccharomyces* culture yeasts and can cause other serious defects besides beer turbidity. A yeast of this species is *Saccharomyces cerevisiae* var. *diastaticus*. If beer is infected with this yeast, over-fermentation occurs, i.e., the utilization of dextrins present in the beer. This is not a concern with a regular brewer's yeast. Over-fermentation leads to changes in taste, to subsequent turbidity and to the formation of a sediment. In the worst case, package swelling can also occur. Another representative of wild yeast is non-pitching *Saccharomyces pastorianus*. These are not over-fermenting and at low fermentation can result in issues including turbidity. *Brettanomyces bruxellensis* is an example of a non-*Saccharomyces* wild yeast that can cause turbidity.^[91] Table

Table 11. Cloud-causing, beer-spoiling bacteria; L = *Lactobacillus*; (++) = very strong; + = strong, - = weak; -- = very weak).^[89-91]

Nature	Occurrence	Turbidity	Sediment
<i>L. brevis</i>	secondary, primary if necessary	+	+
<i>L. brevisimilis</i>	primary	-	--
<i>L. lindneri</i>	primary	-	-
<i>L. casei</i>	secondary, primary if necessary	-	-
<i>L. coryniformis</i>	mostly secondary, primary if necessary	-	-
<i>L. plantarum</i>	secondary	-	-
<i>Pediococcus damnosus</i>	primary	--	+
<i>Micrococcus kristinae</i>	-	-	--
<i>Pectinatus cerevisiiphilus</i> / <i>frisigensis</i>	secondary	++	++
<i>Megasphaera cerevisiae</i>	secondary	-	-
<i>Gluconobacter oxydans</i>	-	+	--
<i>Zymomonas mobilis</i>	-	+	+

Table 12. clouding, beer-damaging yeasts; S = *Saccharomyces*; B = *Brettanomyces*; (++) = very strong; + = strong, - = weak; -- = very weak).^[90-92]

Nature	Frequency	Fermentability	Occurrence	Turbidity	Sediment
<i>S. cerevisiae</i>	frequent	fermentative	primary	-	-
<i>S. pastorianus</i> var. <i>carlsbergensis</i>	frequent	fermentative	primary	-	-
<i>S. cerevisiae</i> var. <i>diastaticus</i>	frequent	fermentative, over-fermenting	primary, secondary if necessary	+	+
<i>S. bayanus</i>	from time to time	fermentative	-	-	-
<i>S. pastorianus</i>	from time to time	fermentative	-	-	-
<i>Pichia anomala</i>	from time to time	respiratory yeast	-	--	--
<i>B. bruxellensis</i>	rare	fermentatively weak	-	-	-
<i>B. clausenii</i>	rare	fermentatively weak	-	-	-

Table 13. Overview table of important turbidity types and origins in beer, non-alcoholic beverages (nab) and water.

Turbidity	Origins	Kind	Occurs	Cause / trait
Chill haze	protein polyphenolic complexes	organic; non-biological	Beer, nab	When heated reversible
Permanent haze	protein polyphenolic complexes	organic; non-biological	Beer, nab	irreversible
Turbidity due to carbohydrates	carbohydrates	organic; non-biological/biological	Beer, nab	Caused by malt or yeast; possibly filtration problems, increase in viscosity
Calcium oxalate	calcium, oxalic acid	organic; non-biological	Beer, nab	Small insoluble crystals
Cultured yeasts	microorganism	organic; biological	Beer, nab	Additional taste and/or aroma changes
Wild yeasts	microorganism	organic; biological	Beer, nab	Additional taste and/or aroma changes
Bacteria	microorganism	organic; biological	Beer, nab	Additional taste and/or aroma changes
Dirt particles	Residues in containers, process error	inorganic	Beer, nab	Label remnants, filter aids etc.
Mineral turbidity	Residues from pipes, flocculation	inorganic	water (possibly beer, nab)	flocculation
Microplastics	ubiquitous in waters	organic; non-biological	Beer, nab, water	None or hardly any visible turbidity

12 shows the most important representatives of cultured and foreign yeasts that can occur in beer. This table also indicates the frequency of contamination with these yeasts, their fermentability and their tendency to form turbidity or sediments.

Oxalate turbidity

Oxalate turbidity is an organic turbidity of non-biological origin. It results from the formation of calcium oxalate by the reaction of oxalic acid and calcium. The oxalic acid required for this comes from the malt, whereby wheat malt contains about twice as much as barley malt. The oxalic acid content also depends on the vintage of the respective harvest. If soft water is used for beer production, the calcium content is low during brewhouse work. This leads to

a high content of free oxalic acid in beer, because only a few soluble oxalate salts are produced, which can be separated out during the brewing process. The use of hard or poorly treated water for rinsing filtration systems or for re-dilution in high-gravity brewing means that calcium can be reabsorbed into the beer and lead to the formation of virtually insoluble calcium oxalate.^[27] Calcium oxalate precipitates in the form of various crystals and forms turbidity from a concentration of more than 20 mg/L or leads to sediments.^[93] This type of turbidity can easily be prevented by careful water treatment or it can be precipitated by a sufficiently long storage time. It must be ensured that sufficient calcium is present in the brewing water in the hot area of the production and that only a small amount is introduced and dissolved in the subsequent process steps.^[20,27,75]

Overview of turbidity types

Table 13 gives an overview of all the important types and origins of turbidity in beer, non-alcoholic beverages (nab) and water. It is divided into origin, source, appearance and the causes or properties.

Economic consequences

For the large retail chains, the longest possible best before date (BBD) of a product is an important factor to include in their product range and makes economic sense. The product does not have to be disposed of if the shelf life is longer, which ensures that almost the entire stock can be sold. For many breweries, however, long shelf-life requirements are a problem. Beer is a fresh product with chemical and physical properties that change over time and impact taste.^[94] However, it is in the breweries' interest to sell a flawless, high-quality product that is visually consistent and has a consistent taste for the end consumer. The end consumer should associate the brand with the quality desired and supplied by the brewery to establish customer loyalty. However, in order to be listed by various retail chains, often a shelf life of 9 months or more is required. Realistically speaking, such a long shelf life is hardly possible without changes in the product's taste. In addition, most beers are stored at room temperature in retail stores, transported in warm trucks or, in extreme cases, exported for several weeks in warm shipping containers, which greatly accelerates the ageing process. The ageing stability of a beer can be divided into three different categories: The chemical-physical stability, the microbiological stability, and the taste stability. The best before date of a beer can be determined on the basis of these three factors. Microbiological stability is particularly important. If this is not guaranteed, the product may spoil within a few days. However, microbiological stability can be ensured by using flash pasteurization or pasteurization. As already mentioned, it is almost impossible to achieve the taste stability of a warm stored beer for its entire shelf life. However, the change in taste can be minimized by selecting suitable raw materials and adapting the brewing process. The chemical-physical stability is the stability against the formation of colloidal turbidity particles. The majority of consumers demand a filtered, glossy beer and associate turbidity, which can also occur with microbial contamination, with spoilage. As long as this is the prevailing view, a beer should have no turbidity until the best before date is reached. Guaranteeing this is an expensive endeavor for many breweries. The most frequent measure to avoid colloidal turbidity is the use of PVPP. In addition to polyphenol stabilization, stabilization is also possible by removing proteins that cause turbidity. In addition to the high costs associated with stabilization, the use of stabilizing agents is subject to increasing criticism in society. Media interest is very high, which is accompanied by damage to the reputation of many breweries that constantly advertise the naturalness of their beer in their marketing material. Clouding of the beer can have other causes than proteins and polyphenols. The prevention of turbidity requires the entire process

to be considered. Potential turbidifiers can be influenced at every stage of the brewing process. It is also important to reliably identify and trace any turbidity that has occurred in the product.

Outlook

Part 1 of the review examined beer turbidity problems. The various causes and origins of turbidity were discussed. Part 2 will deal with Raman spectroscopy (RS) and the complex medium of beer and show possible approaches to how it could be implemented for turbidity analysis in beer and other beverages.

Disclosure statement

No potential conflict of interest was reported by the author(s).

ORCID

Eva-Maria Kahle  <http://orcid.org/0000-0001-8371-3361>

Literature cited

- [1] Back, W. *Ausgewählte Kapitel Der Brauereitechnologie*; Hans Carl Fachverlag: Nürnberg, 2008.
- [2] Narziß, L.; Back, W.; Gastl, M.; et al. Das Fertige Bier: Abriss Der Bierbrauerei. In *Abriss Der Bierbrauerei*; Wiley: Wienheim, 2017; pp 361–414.
- [3] Steiner, E.; Gastl, M.; Becker, T. Die Identifizierung Von Trübungen in Bier (1). *Brauwelt* 2011, 151, 161–166.
- [4] MEBAK (ed). Würze, Bier, Biermischgetränke (Band 2): Methodensammlung der Mitteleuropäischen Brautechnischen Analysenkommission, 2012.
- [5] Dele-Dubois, M.; Dhameincourt, P.; Poirot, J.; Schubnel, H. Differentiation between Gems and Synthetic Minerals by Laser Raman Microspectroscopy. *J. Mol. Struct.* 1986, 143, 135–138. DOI: 10.1016/0022-2860(86)85222-X.
- [6] Gremlich, H.; Yan, B. *Infrared and Raman Spectroscopy of Biological Materials*; Marcel Dekker: New York, 2001.
- [7] Petry, R.; Schmitt, M.; Popp, J. Raman spectroscopy—a prospective tool in the life sciences. *Chemphyschem* 2003, 4, 14–30. DOI: 10.1002/cphc.200390004.
- [8] Stöckel, S.; Kirchhoff, J.; Neugebauer, U.; Rösch, P.; Popp, J. The Application of Raman Spectroscopy for the Detection and Identification of Microorganisms. *J. Raman Spectrosc.* 2016, 47, 89–109. DOI: 10.1002/jrs.4844.
- [9] Morris, T. M. The Relationship between Haze and the Size of Particles in Beer. *J. Inst. Brew.* 1987, 93, 13–17. DOI: 10.1002/j.2050-0416.1987.tb04468.x.
- [10] Fries, G.; Ganzlin, G. Beurteilung Von Biertrübungen. *Brauwelt* 1969, 454–456.
- [11] Bamforth, C. W. Beer Haze. *J. Am. Soc. Brew. Chem.* 1999, 57, 81–90. DOI: 10.1094/ASBCJ-57-0081.
- [12] Diniz, P.; Menzel, V.; Nüter, C.; et al. Trübungsanalyse: Aktuelle Methoden Und Neue Möglichkeiten. *Brauerei Forum* 2013, 12–15.
- [13] ISO. 2016. DIN EN ISO 7027(Norm ISO 7027).
- [14] Narziß, L.; Back, W.; Gastl, M.; et al. Die Filtration Des Bieres: Abriss Der Bierbrauerei. In *Abriss Der Bierbrauerei*; Wiley: Wienheim, 2017; pp 301–323.
- [15] Siebert, K. J.; Lynn, P. Y. Effects of Alcohol and pH on Protein-Polyphenol Haze Intensity and Particle Size. *J. Am. Soc. Brew. Chem.* 2003, 61, 88–98. DOI: 10.1094/ASBCJ-61-0088.

- [16] Hartmann, K. Bedeutung rohstoffbedingter Inhaltsstoffe und produktionstechnologischer Einflüsse auf die Trübungsproblematik im Bier, **2006**.
- [17] Kusche, M. Kolloidale Trübungen in untergärigen Bieren – Entstehung, Vorhersage und Stabilisierungsmaßnahmen, **2005**.
- [18] Schwarz, C. Trübungsstabilität von Weizenbier. Technische Universität München, **2012**.
- [19] Mastanjević, K.; Krstanović, V.; Lukinac, J.; Jukić, M.; Vulin, Z.; Mastanjević, K. Beer-the Importance of Colloidal Stability (Non-Biological Haze). *Fermentation* **2018**, *4*, 91. DOI: 10.3390/fermentation4040091.
- [20] Steiner, E.; Becker, T.; Gastl, M. Turbidity and Haze Formation in Beer - Insights and Overview. *J. Inst. Brew.* **2010**, *116*, 360–368. DOI: 10.1002/j.2050-0416.2010.tb00787.x.
- [21] Trübungssichttafel. <http://deacademic.com/dic.nsf/devwiki/1415534>.
- [22] Annemüller, G.; Manger, H.-J. *Klärung Und Stabilisierung Des Bieres*; VLB: Berlin, **2011**.
- [23] Speers, R. A.; Jin, Y.-L.; Paulson, A. T.; Stewart, R. J. Effects of β -Glucan, Shearing and Environmental Factors on the Turbidity of Wort and Beer. *J. Inst. Brew.* **2003**, *109*, 236–244. DOI: 10.1002/j.2050-0416.2003.tb00164.x.
- [24] American Society of Brewing Chemists. *The ASBC: Formazin Turbidity Standards*, 8th ed. ASBC: Malt, **1992**.
- [25] European Brewery Convention. *Analytische-EBC: Haze*, 4th ed. European Brewery Convention: Zürich, **1987**.
- [26] APHA. *Standard Methods for the Examination of Water and Wastewater*, 18th ed. American Public Health Ass: Washington, **1992**.
- [27] Narziß, L.; Back, W.; Gastl, M.; et al. *Abriss Der Bierbrauerei*. Wiley: Wienheim, **2017**.
- [28] Leiper, K. A.; Stewart, G. G.; McKeown, I. P. Beer Polypeptides and Silica Gel Part II. polypeptides Involved in Foam Formation. *J. Inst. Brew.* **2003**, *109*, 73–79. DOI: 10.1002/j.2050-0416.2003.tb00595.x.
- [29] Malawer, E.; Senak, L. Introduction to Size Exclusion Chromatography. In *Handbook of Size Exclusion Chromatography*. Marcel Dekker, Inc: New York, **2003**; pp 1–24.
- [30] Wu, C-S. *Handbook of Size Exclusion Chromatography and Related Techniques: Revised and Expanded*. Marcel Dekker, Inc: New York, **2003**; Vol. 91.
- [31] Gramshaw, J. W. Beer Polyphenols and the Chemical Basis of Haze Formation. Part II: Changes in Polyphenols during the Brewing and Storage of Beer - the Composition of Hazes. *Tech. Q. Master Brew. Assoc. Am.* **1970**, *7*, 122–131.
- [32] Wainwright, T. Non-Biological Hazes and Precipitates in Beer. *Brewers Digest* **1974**, *49*, 38–48.
- [33] Rehmanji, M.; Mola, A.; Narayanan, K.; et al. Superior Colloidal Stabilization of Beer by Combined Treatment with Silica (Xerogel) and PVPP, Polyclar plus 730®. *Tech. Q. Master Brew. Assoc. Am.* **2000**, *37*, 113–118.
- [34] Knorr, F. Polyphenols in brewing (author's transl). *Z Lebensm Unters Forsch* **1978**, *166*, 228–233. DOI: 10.1007/BF01126549.
- [35] Narziß, L. Chemisch-Physikalische Stabilität Des Bieres. *Brauwelt* **1994**, *134*, 2337–2338.
- [36] Poeschl, M. Die Kolloidale Stabilität Untergäriger Biere-Einflussmöglichkeiten Und Vorhersagbarkeit. Dissertation, Freising-Weihenstephan, **2009**.
- [37] Leiper, K. A.; Miedl, M. Colloidal Stability of Beer. In *Beer: A quality perspective*; Bamforth, C. W., Ed.; Academic Press: Burlington, MA, **2008**; pp 111–161.
- [38] Luck, G.; Liao, H.; Murray, N. J.; Grimmer, H. R.; Warminski, E. E.; Williamson, M. P.; Lilley, T. H.; Haslam, E. Polyphenols, Astringency and Proline-Rich Proteins. *Phytochemistry* **1994**, *37*, 357–371. DOI: 10.1016/0031-9422(94)85061-5.
- [39] Siebert, K. J. Haze Formation in Beverages. *LWT-Food Sci. Technol.* **2006**, *39*, 987–994. DOI: 10.1016/j.lwt.2006.02.012.
- [40] Bishop, L. R. Haze-and Foam-Forming Substances in Beer. *J. Inst. Brew.* **1975**, *81*, 444–449. DOI: 10.1002/j.2050-0416.1975.tb03705.x.
- [41] Steiner, E.; Gastl, M.; Becker, T. Die Identifizierung Von Trübungen in Bier (2). *Brauwelt* **2011**, *151*, 193–205.
- [42] Steiner, E.; Arendt, E. K.; Gastl, M.; Becker, T. Influence of the Maltng Parameters on the Haze Formation of Beer after Filtration. *Eur. Food Res. Technol.* **2011**, *233*, 587–597. DOI: 10.1007/s00217-011-1547-0.
- [43] Steiner, E.; Gastl, M.; Becker, T. Protein Changes during Maltng and Brewing with Focus on Haze and Foam Formation: A Review. *Eur. Food Res. Technol.* **2011**, *232*, 191–204. DOI: 10.1007/s00217-010-1412-6.
- [44] Niemsch, K. Die Renaissance Der Bierstabilisierung Mit Kieselgel. *Brauwelt* **2000**, *140*, 580–587.
- [45] Leiper, K. A.; Stewart, G. G.; McKeown, I. P. Beer Polypeptides and Silica Gel Part I. Polypeptides Involved in Haze Formation. *J. Inst. Brew.* **2003**, *109*, 57–72. DOI: 10.1002/j.2050-0416.2003.tb00594.x.
- [46] Osborne, T. B. *The Proteins of the Wheat Kernel*. Carnegie Institution of Washington: Washington, DC, **1907**.
- [47] Asano, K.; Shinagawa, K.; Hashimoto, N. Characterization of Haze-Forming Proteins of Beer and Their Roles in Chill Haze Formation. *J. Am. Soc. Brew. Chem.* **1982**, *40*, 147–154. DOI: 10.1094/ASBCJ-40-0147.
- [48] Siebert, K. J.; Troukhanova, N. V.; Lynn, P. Y. Nature of Polyphenol-Protein Interactions. *J. Agric. Food Chem.* **1996**, *44*, 80–85. DOI: 10.1021/jf9502459.
- [49] Siebert, K. J. Protein-Polyphenol Haze in Beverages. *Food Technol.* **1999**, *53*, 54–57.
- [50] Asano, K.; Ohtsu, K.; Shinagawa, K.; Hashimoto, N. 2014. Affinity of Proanthocyanidins and Their Oxidation Products for Haze-Forming Proteins of Beer and the Formation of Chill Haze. *Agric. Biol. Chem.* **1984**, *48*, 1139–1146. DOI: 10.1080/00021369.1984.10866300.
- [51] Collin, S.; Jerkovic, V.; Bröhan, M.; et al. Polyphenols and Beer Quality. In *Natural Products: Phytochemistry, Botany and Metabolism of Alkaloids, Phenolics and Terpenes*; Springer: Berlin, **2013**; pp 2333–2359.
- [52] Loch-Ahring, S.; Decker, F.; Robbert, S.; et al. Chill-Haze-Identification and Determination of Haze-Active Constituents by HPLC and Mass Spectrometry. Part I: The Role of Polyphenols and the Astonishing Impact of Hop Components on Chill Haze Formation Monats. *Brauwiss* **2008**, *61*, 32–48.
- [53] Gerhäuser, C.; Becker, H. Phenolic Compounds of Beer. In *Beer in Health and Disease Prevention*; Preedy, V. R., Ed.; Academic Press: MA, USA, **2011**, pp 124–144.
- [54] Zhao, H.; Chen, W.; Lu, J.; Zhao, M. Phenolic Profiles and Antioxidant Activities of Commercial Beers. *Food Chem.* **2010**, *119*, 1150–1158. DOI: 10.1016/j.foodchem.2009.08.028.
- [55] Franz, O. Systematische Untersuchungen zur endogenen antioxidativen Aktivität von hellem, untergärem Bier unter besonderer Berücksichtigung technologischer Maßnahmen beim Brauprozess. Technische Universität München, **2004**.
- [56] Papp, A.; Winnewisser, W.; Geiger, E.; Briem, F. Influence of (+)-Catechin and Ferulic Acid on Formation of Beer Haze and Their Removal through Different Polyvinylpyrrolidone-Types. *J. Inst. Brew.* **2001**, *107*, 55–60. DOI: 10.1002/j.2050-0416.2001.tb00080.x.
- [57] Zeuschner, P.; Pahl, R. Der Jodwert in Der Brauerei. *Brauwelt* **2017**, *2017*, 262–264.
- [58] Letters, R. Haze and Foam Group Origin of Carbohydrate in Beer Sediments. *J. Inst. Brew.* **1969**, *75*, 54–60. DOI: 10.1002/j.2050-0416.1969.tb03183.x.
- [59] Kupetz, M.; Aumer, J.; Harms, D.; Zarnkow, M.; Sacher, B.; Becker, T. High-Throughput(Beta-Glucan Analyses and Their Relationship with Beer Filterability. *Eur. Food Res. Technol.* **2017**, *243*, 341–351. DOI: 10.1007/s00217-016-2748-3.
- [60] Malcorps, P.; Haselaars, P.; Dupire, S. Glycogen Released by the Yeast as a Cause of Unfilterable Haze in the Beer. *Tech. Quart. Master Brew. Ass. Am.* **2001**, *38*, 95–98.
- [61] Siebert KJ (ed). Haze in Beverages. In *Advances in Food and Nutrition Research*. Elsevier: Amsterdam, **2009**.

- [62] Keil, H. Was Genau Ist Kieselgur?: Entstehung, Aufbereitung Und Einsatz Des Filterhilfsmittels. *Brauindustrie* **1997**, 216–218.
- [63] Kunze, W.; Manger, H.-J. *Technologie Brauer und Mälzer*. VLB: Berlin, **2016**.
- [64] Römpp. **2002**. Perlite. <https://roempp.thieme.de/roempp4.0/do/data/RD-16-01088>.
- [65] Römpp. **2010**. Perlite. <https://roempp.thieme.de/roempp4.0/do/data/RD-16-01090>.
- [66] Annemüller, G.; Manger, H.-J. *Gärung und Reifung des Bieres: Grundlagen-Technologie-Anlagentechnik-Qualitätsmanagement*. VLB: Berlin, **2013**.
- [67] Braun, FH. *Auswirkungen des Einsatzes von Zellulose als Filterhilfsmittel in der Bierfiltration*. Diss. Technische Universität München, **2012**, pp 392–395.
- [68] Ruß, W.; Meyer-Pittroff, R. Rechtliche Vorschriften Für Kieselgur. *Brauwelt* **2001**, *141*, 343–346.
- [69] IARC. Silica Dust, Crystalline, in the Form of Quartz or Cristobalite, **1997**.
- [70] Römpp. **2009**. Cellulose. <https://roempp.thieme.de/roempp4.0/do/data/RD-03-00833>.
- [71] Eßlinger, H. M. Filtrationstechnik in Der Brauerei. *Brauwelt* **1992**, *1992*, 611–613.
- [72] Probst, B.; Rogenstein, W.; Scholz, R.; et al. Filter Aid and Filter Layer, **2016**.
- [73] Zacharias, J.; Schneid, R. Viscose Fibres as Alternative Filter Aid-Chance, Limitation and Possible Coexistence with Membrane Filtration. *Proc. 35th EBC P* **2015**, *50*, 117.
- [74] Römpp. **2008**. Polyvinylpyrrolidone. <https://roempp.thieme.de/roempp4.0/do/data/RD-16-03673>.
- [75] McMurrrough, I.; Kelly, R.; Madigan, D. Colloidal Stabilization of Beer. *Ferment* **1995**, *8*, 39–45.
- [76] Erbslöh. **2015**. PVPP Datenblatt. https://erbsloeh.com/product_datasheets/de/PMB_ErbsloehPVPPBier_D_003.pdf.
- [77] Siebert, K. J.; Lynn, P. Y. Comparison of Polyphenol Interactions with Polyvinylpyrrolidone and Haze-Active Protein. *J. Am. Soc. Brew. Chem.* **1998**, *56*, 24–31. DOI: 10.1094/ASBCJ-56-0024.
- [78] McMurrrough, I.; Madigan, D.; Kelly, R. J. Evaluation of Rapid Colloidal Stabilization with Polyvinylpyrrolidone (PVPP). *J. Am. Soc. Brew. Chem.* **1997**, *55*, 38–43. DOI: 10.1094/ASBCJ-55-0038.
- [79] Schur, F. Bierstabilisierung. *Brauerei-Rundschau* **1979**, *90*, 5–12.
- [80] Wackerbauer, K.; Anger, H. M. Bierstabilisierung Unter Besonderer Berücksichtigung Der Polyphenole. *Monatsschrift Für Brauwissenschaft* **1984**, *4*, 153–161.
- [81] Siebert, K. J. Effects of protein-polyphenol interactions on beverage haze, stabilization, and analysis. *J. Agric. Food Chem.* **1999**, *47*, 353–362. DOI: 10.1021/jf980703o.
- [82] Siebert, K. J.; Lynn, P. Y. On the Mechanisms of Adsorbent Interactions with Haze-Active Proteins and Polyphenols. *J. Am. Soc. Brew. Chem.* **2008**, *66*, 48–54. DOI: 10.1094/ASBCJ-2007-1116-02.
- [83] Fath, A. Einleitung: Mikroplastik-Eine Wachsende Gefahr Für Mensch Und Umwelt. In: *Mikroplastik*. Springer: Berlin, **2019**; pp 1–13.
- [84] Tyree, C.; Morrison, D. **2018** Plus Plastic: Microplastics Found in Global Bottled Water. Available at <https://orbmedia.org/stories/plus-plastic/>
- [85] Schymanski, D.; Goldbeck, C.; Humpf, H.-U.; Fürst, P. Analysis of Microplastics in Water by Micro-Raman Spectroscopy: Release of Plastic Particles from Different Packaging into Mineral Water. *Water Res.* **2018**, *129*, 154–162. DOI: 10.1016/j.watres.2017.11.011.
- [86] Kaiser, W. *Kunststoffchemie Für Ingenieure: Von Der Synthese Bis Zur Anwendung*. Carl Hanser Verlag GmbH Co KG: Germany, **2015**.
- [87] Suzuki, K. 125th Anniversary Review: Microbiological Instability of Beer Caused by Spoilage Bacteria. *J. Inst. Brew.* **2011**, *117*, 131–155. DOI: 10.1002/j.2050-0416.2011.tb00454.x.
- [88] Vaughan, A.; O'Sullivan, T.; Sinderen, D. Enhancing the Microbiological Stability of Malt and Beer: A Review. *J. Inst. Brew.* **2005**, *111*, 355–371. DOI: 10.1002/j.2050-0416.2005.tb00221.x.
- [89] Schneiderbanger, J.; Grammer, M.; Jacob, F.; Hutzler, M. Statistical Evaluation of Beer Spoilage Bacteria by Real-Time PCR Analyses from 2010 to 2016. *J. Inst. Brew.* **2018**, *124*, 173–181. DOI: 10.1002/jib.486.
- [90] Hutzler, M.; Müller-Auffermann, K.; Koob, J. Beer Spoiling Microorganisms-a Current Overview. *Brauwelt Int.* **2013**, *1*, 23–25.
- [91] Back, W. *Colour Atlas and Handbook of Beverage Biology*. Fachverlag Hans Carl: Nurnberg, **2005**.
- [92] Hutzler, M.; Riedl, R.; Koob, J.; et al. Fermentation and Spoilage Yeasts and Their Relevance for the Beverage Industry-a Review. *BrewingScience-Monatsschrift Für Brauwissenschaft* **2012**, *65*, 33–50.
- [93] Burger, M.; Becker, K. Oxalate Studies on Beer. *Proceedings. Annual meeting-American Society of Brewing Chemists*, **1949**; Vol. 7, pp 102–115. DOI: 10.1080/00960845.1949.12006272.
- [94] Vanderhaegen, B.; Neven, H.; Verachert, H.; Derdelinckx, G. The Chemistry of Beer Aging-a Critical Review. *Food Chem.* **2006**, *95*, 357–381. DOI: 10.1016/j.foodchem.2005.01.006.

PART 2

2.3 Beer Turbidity Part 2: A Review of Raman Spectroscopy and Possible Future Use for Beer Turbidity Analysis

Beer Turbidity Part 2 focuses on Raman spectroscopy (RS). The review provides a general overview of the physical basics, the areas of application, possible gaps, and the challenge for the use of Raman spectroscopy in beer and beverage analysis. Analysis of turbidity in beer is often limited to optical, microscopic and enzymatic analyses. This review explores in detail how Raman micro-spectroscopy can be used as a way to identify beer turbidity particles and the possibility of establishing it as a future robust beer analysis method.

The aim of this review was to determine whether and how turbidity-relevant substances in beer can be examined with the aid of RS. This paper discussed what effort is involved in spectroscopy with regard to sample preparation and what technical equipment is required. It has been found that most substances that affect the colloidal stability of beer can be identified by Raman spectroscopy. Some substances such as the protein fraction prolamine or the proanthocyanidins procyanidin B3 and prodelphinidin B3 have not yet been investigated. For other substances, spectroscopy is difficult. This is true for glutamic acid. When studying glutamine, fluorescence is strongly excited and covers the Raman bands, which makes it difficult to obtain a meaningful Raman spectrum. The investigated substances were mainly analyzed in their pure form or in solution. Fluorescence makes a direct examination of beer or other beverages difficult. Beverages contain numerous different substances which can strongly hinder the uptake of the Raman spectrum and therefore require complex sample preparation, e.g., by centrifugation and recovery of turbidity residues. While there are very few studies for beer in connection with Raman spectroscopy, wine has already been the subject of many studies in this field. Wine was analyzed for phenolic constituents, which can also cause turbidity in beer. However, no specific substances, such as catechin or epicatechin, could be differentiated in those investigations; a distinction was made only with regard to non-specific polyphenols, anthocyanins and tannins.

Authors/Authorship contribution:

Kahle, E-M.: Literature search, writing, review conception and design; **Zarnkow, M.:** critical review of draft, discussion of data; **Jacob F.:** Supervised the project

Beer Turbidity Part 2: A Review of Raman Spectroscopy and Possible Future Use for Beer Turbidity Analysis

Eva-Maria Kahle , Martin Zarnkow, and Fritz Jacob

Forschungszentrum Weihenstephan für Brau- und Lebensmittelqualität, Technische Universität München, Alte Akademie 3, 85354 Freising-Weihenstephan, Germany

ABSTRACT

Beer turbidity Part 1 focused on beer turbidity, its origins and problems. Beer Turbidity Part 2 focuses on Raman spectroscopy (RS), especially on TI-RMS (Turbidity Identification - Raman Micro-Spectroscopy). The review provides a general overview of the physical basics, the areas of application, possible gaps, and the challenge for the use of Raman spectroscopy in beer and beverage analysis. Analysis of turbidity in beer is often limited to optical, microscopic and enzymatic analyses. This review explores in detail turbidity identification using Raman micro-spectroscopy as a way to identify beer turbidity particles and the possibility of establishing it as a future robust analysis method for beer.

KEYWORDS

Raman micro-spectroscopy; turbidity; haze; beer; TI-RMS; beverages; identification; particles; fluorescence

Introduction – current state of Raman spectroscopy research

In addition to beer foam, one of the most important visual quality characteristics of filtered beers is gloss fineness.^[1,2] Even a slight opalescence impairs the appearance and reduces consumer acceptance. Accordingly, turbidity is given a high level of attention along the entire value-added chain and is ideally prevented via suitable countermeasures.^[3] For undesirable haze, it is first necessary to identify the haze particles. However, the analysis is often limited to optical, enzymatic and microscopic analyses.^[4] In recent years, Raman Spectroscopy has been established as a powerful tool in many research fields such as biology, medicine and archaeology. It offers another possibility to identify and characterize turbidity particles. Previous applications of Raman Spectroscopy can be found in various research areas. The applications range from the characterization of proteins and the rapid identification of pathogenic microorganisms, to the early *in vivo* detection of cancer cells, and the age determination of archaeological finds.^[5–8] The advantage over other methods is that it provides a fast, non-invasive, non-destructive and high-resolution measurement. It also offers a high information density in the recorded spectra.^[9,10] This makes it easy to work with samples in liquid media and requires no laborious sample preparation.^[7, 10,11] A significant exception is complex media such as beer, since the variety of ingredients means these require accurate knowledge of the composition and their Raman spectra.^[9] A multitude of organic constituents (e.g., amino acids, vitamins, phenols, iso- α -acid) can cause fluorescence, leading to drift movements in the Raman spectra that superimpose the actual Raman signals.^[12] Treatment is also more elaborate

in that the samples must first be decarbonated.^[13,14] This article is intended to give a general overview of Raman Spectroscopy, with a focus on Raman Micro-Spectroscopy (RMS) in connection with the turbidity issue and presents the likely problem areas and some possible solutions.

Microscopy

Confocal microscopy

Confocal microscopy is a modification of conventional optical light microscopy. It is characterized by better resolution and the possibility to record optical sections through a sample. These can then be combined into three-dimensional images using imaging software.^[14] In contrast to conventional light microscopy, confocal microscopy detects the pixels from the focal plane individually. Normal light microscopes image all points in the focus at the same time. This method is also used to image points that are not in the focal plane. The overall image is therefore diffuse and lacks the necessary depth of field. The theoretically achievable resolution limit is described by Abbe's formula or the Abbe limit.

$$d = \frac{\lambda}{n \sin \alpha} = \frac{\lambda}{NA}$$

The quotient of the wavelength λ of the light used and the numerical aperture NA of the lens used gives the achievable resolution d . This describes the minimum distance that two lines in a grating must have so that they can still be recognized as separate lines.^[14,15] By connecting pinholes, both the illumination beam path and the detected light beam are selected. Light from outside the focus is blocked by the

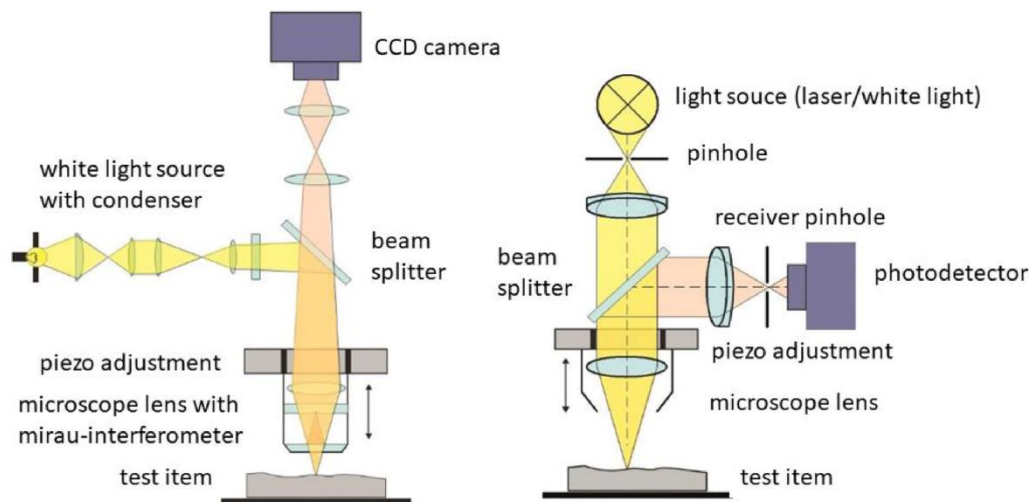


Figure 1. Beam path scheme of a) conventional and b) confocal microscopes.^[17] [adapted].

pinhole.^[13,14, 16] Figure 1 shows a comparison of the functional principles and the design of conventional light microscopes and confocal microscopes.^[17]

Although the optical resolution limit of confocal microscopy is also limited by Abbe's diffraction limit, the resolution theoretically improves by a factor of $1/(\sqrt{2})$. Confocal microscopy allows images with significantly improved resolutions due to the suppression of these non-focal signals.^[15] In order to obtain a complete image of the sample and to achieve the high contrast, the individual pixels are serially illuminated and screened. The resolution of the obtained image plane is determined by the numerical aperture and the magnification of the objective used, as well as by the diameter and the selected distance of the pinhole.^[13,14, 16]

Raman spectroscopy

Raman spectroscopy (RS) has become one of the most powerful analytical methods in chemical-technical analysis in recent decades. The complementary analysis method of infrared spectroscopy (IR or FTIR) is often used as a comparative method of RS. Both methods offer advantages over each other and complement each other. Due to its basic physical principles and analytical settings, RS nevertheless has some important advantages. The high molecular specificity and easy implementation in existing systems allows the use of RS systems in many technological fields. Besides their chemical-analytical and biotechnological relevance, such systems are also often used in diagnostic medicine, forensic sciences or astrophysics.^[18]

Raman effect

The physical principle on which RS is based is called inelastic light scattering. The Austrian physicist Adolf Smekal first

predicted the existence of frequency-shifted scattering lines in 1923. This effect, termed the Smekal Raman effect, was then experimentally proven in 1928 by the Indian physicists C. V. Raman and K. S. Krishnan.^[16, 19,20] This effect is understood as the phenomenon that the scattered light spectrum of a solid, liquid or gaseous chemical compound irradiated with monochromatic light contains various weaker lines (referred to as Raman lines) in addition to the line of exciting light. These are due to energy interactions such as oscillations and rotations, between the scattering molecules and the stimulating radiation.^[16, 19,20] Furthermore, elastic scattering types exist, for instance Rayleigh scattering. Among other things, this is responsible for the blue coloration of the sky during the day. The underlying Tyndall effect describes the transmitted light intensity as a function of wavelength. Accordingly, shorter wavelength blue light is scattered more than red light, with longer wavelengths. Shortly before sunset the angle of incidence is very small and due to the long way through the atmosphere, the blue components of the light are scattered almost completely. What remains are the longer-wave, red light rays, which are commonly referred to as "evening red".^[16]

$$I = \frac{1}{\lambda^4}$$

The Tyndall effect is also relevant for Raman scattering and the Raman spectroscopy based on it, since it plays a decisive role in the selection of suitable laser wavelengths.^[21] Light scattering is a relatively weak phenomenon by nature. On average, only about one in 10^3 photons is scattered by an irradiated sample. The rest of the light passes unhindered through the sample and is therefore called transmitted light.^[22] Of this small number of scattered photons, only a very small proportion of the photons are Raman-active (about one of 106–108 photons) and can be detected for

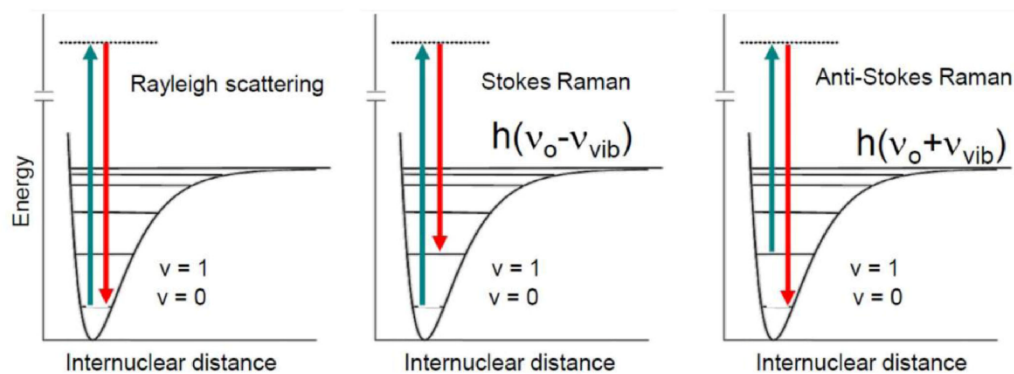


Figure 2. Energy diagram showing the vibrational quantum states of molecules in Rayleigh (left), Stokes (center) and anti-Stokes scattering (right).^[23]

further measurements.^[14] In the original experiment, solar rays were focused with a lens and passed through a sample of purified water. The scattered radiation was then bundled by a second lens and detected by various optical filters. Thus, the frequency shift could be detected. At that time, however, the results were purely qualitative and not yet quantifiable.^[16] Through the development of modern laser and microscope technologies, a sufficiently high photon density can be guaranteed even for very small samples ($< 1 \mu\text{m}$ is theoretically possible). However, this is accompanied by increasing difficulties in parameterizing the measurement, fluorescence interference signals and thermal loading of the sample material.^[16] The correct choice of laser is essential for the analyses and the result.^[14, 16, 21]

Raman spectroscopy is a vibrational spectroscopic analysis method. As in infrared spectroscopy, it can be used to observe energy interactions resulting from movements at the molecular level. The functional principles of infrared (IR) and Raman spectroscopy differ from each other. In IR spectroscopy, the samples are excited with a wide frequency range of infrared energy. The molecules absorb the energy when the frequency of the incident radiation corresponds to the frequency of a vibrational state of the molecules. The frequency decrease is detected and the resulting spectrum can be used to identify the substances.^[14, 16] In Raman spectroscopy, the scattering molecules are excited by radiation sources with a very small frequency range. They reach higher or lower energy levels and then release part of their energy to the irradiated photons. This frequency or energy difference between exciting and emitted radiation is detected and is unique for each group of molecules. Peaks of the respective molecule groups are imaged on the frequency spectra. These "fingerprint" areas can then be used to identify unknown substances.^[16]

The detected Raman-active scattered radiation can be divided into three categories according to their frequency shifts. The Rayleigh scattered radiation has the same frequency as the stimulating output radiation, which is referred to as fully elastic scattering. The irradiated photons only hit the electron cloud in the immediate vicinity of the nucleus. Due to the low electron mass, the frequency shifts and the energy

differences of the scattered photons are so small that they cannot be detected. Therefore, no information can be generated on the scattering molecular groups.^[14, 16] Rayleigh scattering makes up the largest part of the scattered radiation detected and must often be attenuated by suitable optical filters in order not to damage or overload the sensitive CCD (charge-coupled device) detectors.^[14] The relevant Raman scatterings are divided into Stokes scattering and anti-Stokes scattering according to their energy interactions with the scattering molecule. In Stokes scattering, the irradiated photon transfers energy to the scattering molecule. This molecule is raised from its energetic ground state to a higher, virtual energy level and then returns to the next higher vibration-excited state. The emitted photon has a lower frequency and energy than the stimulating photon. In the Raman spectrum, the Stokes lines are detected and imaged in the longer-wave, i.e., redshifted, region.^[14, 16] In contrast, the scattering molecule in anti-Stokes scattering transfers energy to the photon and thus reaches a lower energy level. The emitted photon again has a higher energy and frequency than in its initial state. The anti-Stokes lines are detected in the shorter wavelength, blue shifted range. This means that the scattering molecules must already be in an excited state of vibration in order to enable anti-Stokes scattering at all. Figure 2 shows the scheme of the energy interactions of the individual scattered light types and the virtual energy levels. The variable ν indicates the vibrational quantum state of the sample.

According to the Boltzmann distribution, however, there are significantly fewer molecules in the excited oscillation state at room temperature than in the energetic ground state.^[24] Therefore, the anti-Stokes scattering radiation is basically weaker and thus offers less potential than the Stokes scattering radiation.^[14, 16] Although there are methods to efficiently generate and record Raman signals by means of anti-Stokes scattering radiation, these require a higher equipment investment as well as more complex sample preparation methods. Therefore, adapted spectroscopy methods such as coherent anti-Stokes Raman spectroscopy (CARS) are only suitable for specific analyses.^[14, 25]

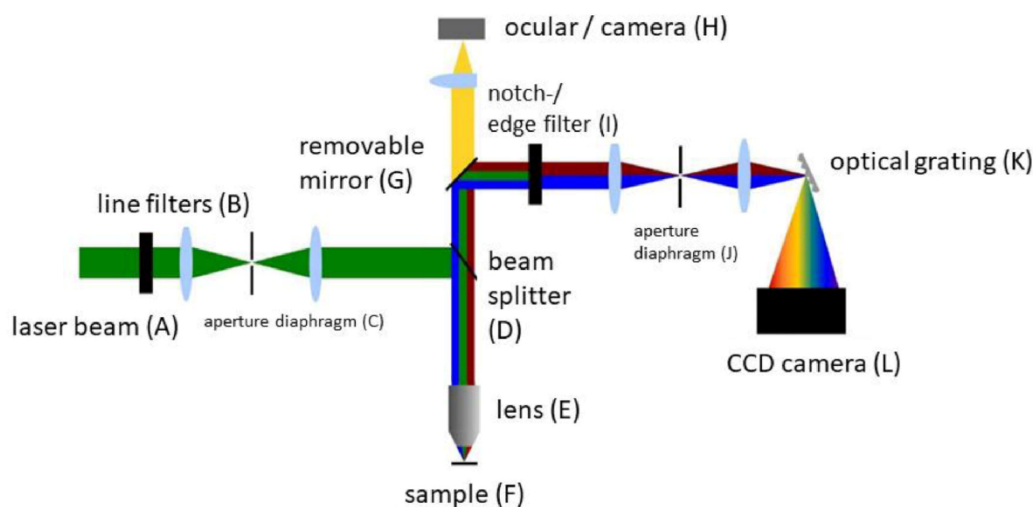


Figure 3. Beam path of a confocal Raman micro-spectroscopy.^[26] [adapted].

Functional principle of Raman spectroscopy

Figure 3 shows the schematic beam path within a confocal RS system.^[26] The laser beam is focused on the confocal plane of the sample via one or more pinholes and a series of filters (A-F). The photons scattered at the sample molecules are guided through the optics of the microscope onto an optical filter (I). This filter only allows light to pass through if its wavelength differs from the wavelength originally irradiated by the laser. A large proportion of the Rayleigh scattered light is filtered out of the beam path, which makes the significantly less intense Stokes and anti-Stokes scattered rays measurable. The filtered scattered light is focused once again with the aid of a pinhole (J) and is then guided via laser fibers into the connected spectroscopy onto a diffraction grating. The diffraction grating splits the light beam according to wavelength ranges and scatters it over the detection surface of the CCD detectors (L). Here the radiation is converted into an electronic signal, which can then be calculated by the respective spectroscopy program using complex algorithms and imaged as a Raman spectrum of the respective substance.^[16, 26]

The time required to analyze the RS depends on several factors. On the one hand, the method requires a more complex sample preparation, depending on the type of scatterer tested. Samples to be examined on the basis of their anti-Stokes scattering tendency must be kept at a higher energy level before and during the measurement.^[16] This is usually performed with the aid of a thermoblock in which the sample holder is located. The choice of laser wavelength also has an effect on the duration of the analysis. Higher wavelengths correlate proportionally with the decreasing intensity of the scattering signals. The use of EM-CCD detectors (electron multiplying charge-coupled device) has a positive effect on the measurement duration. In this relatively new development, weak signals such as Raman signals are routed

over an amplifier path and electronically amplified.^[16] In this way, measurements can be accelerated by a factor of up to 20.^[26]

Laser types of Raman spectroscopy

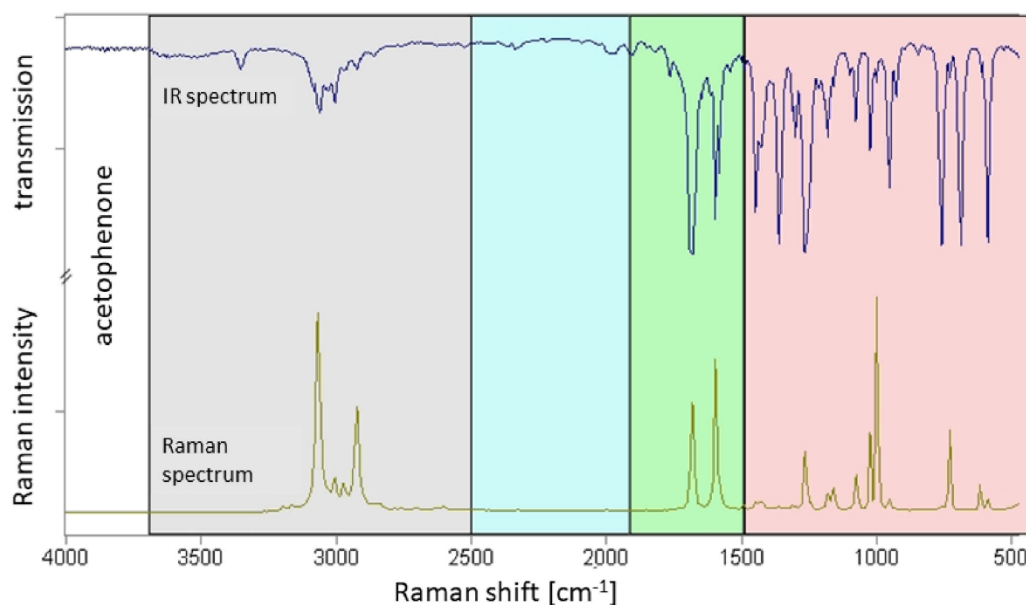
A Raman spectrometer consists of three main components. These are a laser source, a sample irradiation array, and a spectrophotometer. There are different types of lasers that can be used for this procedure. For example, argon ion lasers (454.3–528.7 nm) are used when high sensitivity is required.^[27] Helium neon lasers (611–640 nm) have a lower intensity than the aforementioned laser, but are less expensive. The Nd:YAG laser (1065 nm), which produces less fluorescence at higher wavelengths in the infrared range, is also being used more frequently.^[28,29] Lasers with wavelengths of 532 nm and 785 nm are also often used. The 532 nm is green light, which can be emitted by a Nd:YAG laser. A laser with a wavelength of 785 nm is in the near-infrared range and is provided by Al-GaAs lasers. In addition, there are numerous other types of lasers, but these are less important in the Raman process.^[30] Table 1 lists some lasers commonly used in Raman spectroscopy.

Interpretation of Raman spectra

The spectral ranges of a Raman spectrum can be subdivided according to the excited molecular groups. Figure 4 shows a Raman spectrum of acetophenone. The convergent IR spectrum and the four frequency ranges described below are also shown. In the first wavelength range from 3700 cm^{-1} to 2500 cm^{-1} , mainly monovalent molecular groups such as OH, NH and CH groups of saturated and unsaturated compounds are detected. This peak occurs more or less strongly in all organic compounds and is therefore of little relevance for the identification of unknown substances. The next

Table 1. Laser types for Raman spectroscopy.^[27-32]

Laser	Wavelength [nm]	Spectrum	Field of Application
Argon ions	454.3–528.7	blue to green	inorganic material
Helium neon	630	red	fluorescence suppression
Nd:YAG	355, 532, 1064	ultraviolet to infrared	fluorescence suppression, organic material
Krypton ions	350–800	blue to red	fluorescence suppression, organic material
Diode laser	785, 830	near-infrared to infrared	fluorescence suppression, organic material

Figure 4. Raman spectrum with convergent IR spectrum of acetophenone.^[33] [adapted].

range from 2500 cm^{-1} to 1900 cm^{-1} covers molecular groups with triple bonds or accumulated double bonds.^[33] These include nitrogen compounds such as cyanates, nitriles and isolated thiol compounds. The third range goes from a wavelength of 1900 cm^{-1} to about 1500 cm^{-1} . From carbonyl compounds and $C=C/C=N$ double bonds, through aromatics, ketones, esters to amides and aldehydes, a large number of specific molecular groups can be detected in this range.^[16, 34]

The last area is below a wavelength of 1500 cm^{-1} and is called the fingerprint area. In this area several oscillation spectra of different origins can be found. Examples are deformation oscillations, valence oscillations and framework oscillations, but inorganic and metallo-organic oscillations can also be detected here.^[33] This fingerprint area is substance-specific and characterizes the molecule. An overview of the Raman-active (and infrared-active) molecular groups as well as single oscillations and their respective frequency ranges can be found in Figures 5–9.^[16]

Advantages of Raman micro-spectroscopy (RMS)

In addition to Raman spectroscopy, there are several other quantitative analysis methods for trace and substance

identification. The purely optical identification of microparticles was used in many studies only a few years ago. Even in combination with possible staining methods or optical filters, the results of such studies are not empirically reliable as they may contain a human error factor and are difficult to reproduce.^[26] Due to the development of new, significant analytical methods, this scientific practice was largely abandoned and now only serves as a preliminary microscopic examination. The group of thermoanalytical detection methods comprises various sample preparation and chromatography systems as well as various combinations of these two subgroups. Examples from the subgroup of sample preparation and sampling methods are solid phase extraction (SPE), thermal extraction and desorption (TED) and pyrolysis (Py). The analytical part of the measurement methods is performed using methods such as gas or liquid chromatography (GC/HPLC), mass spectroscopy (MS) or thermogravimetric analyses (TGA).^[16, 26] All of these methods are suitable for the analysis of microplastic particles (MP) and their additives. However, all of these analyses are also invasive methods, i.e., the destruction of the samples prevents all further analyses. They also require a relatively large amount of sample material and can therefore only be used from a certain particle loading or for particle sizes from

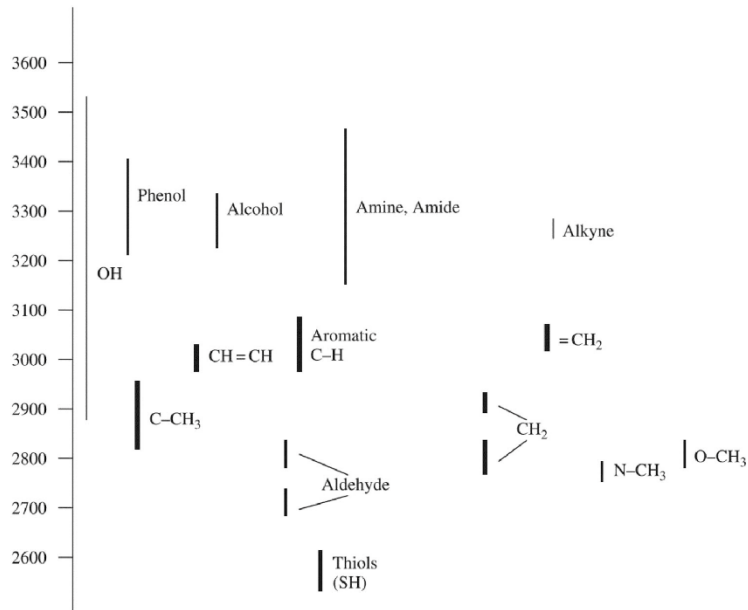


Figure 5. Single oscillation and group frequencies as well as indications of possible intensities of peaks usually identified during Raman scattering ($3600\text{--}2600\text{ cm}^{-1}$).^[16]

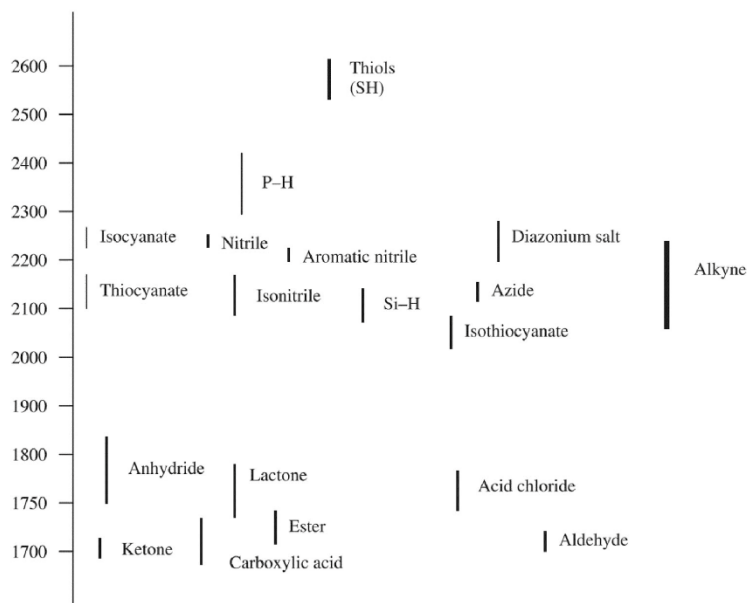


Figure 6. Single oscillation and group frequencies as well as indications of possible intensities of peaks usually identified during Raman scattering ($2600\text{--}1700\text{ cm}^{-1}$).^[14]

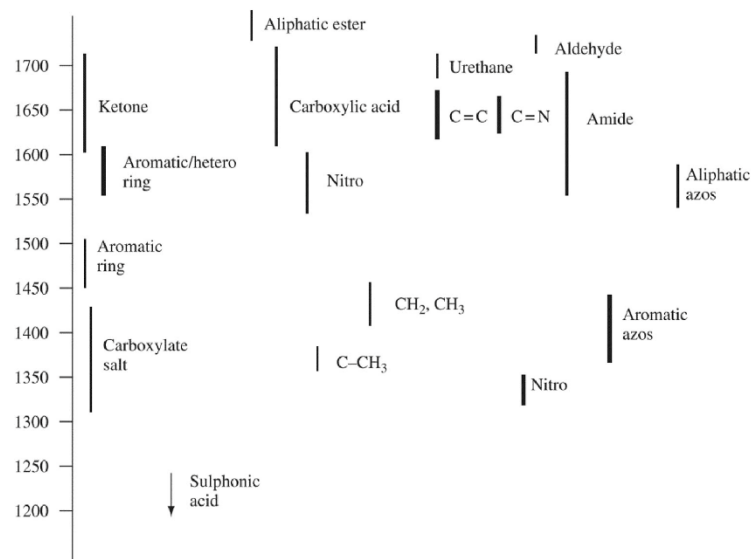


Figure 7. Single oscillation and group frequencies as well as indications of possible intensities of peaks usually identified during Raman scattering ($1700\text{--}1200\text{ cm}^{-1}$).^[14]

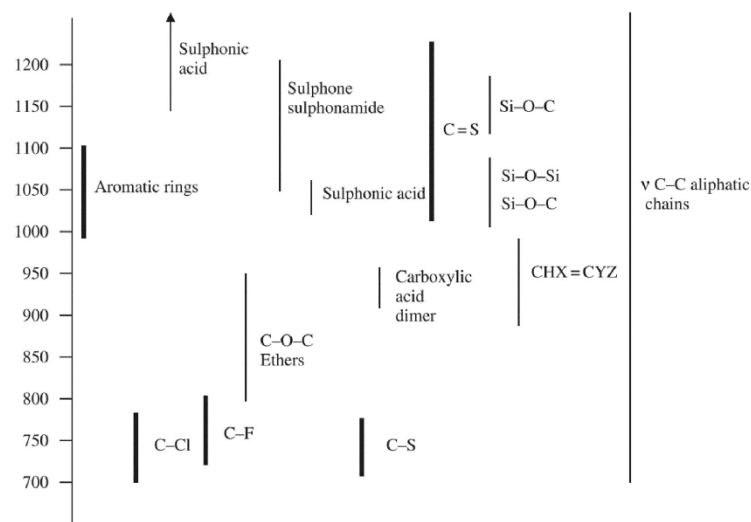


Figure 8. Single oscillation and group frequencies as well as indications of possible intensities of peaks usually identified during Raman scattering ($1200\text{--}700\text{ cm}^{-1}$).^[14]

approximately $100\ \mu\text{m}$.^[21, 26] Accordingly, the thermoanalytical methods, the vibrational spectroscopic methods RS and FTIR are subject to both process engineering requirements and minimum detection limits.

The alternative method of RMS, the complementary analysis method of Fourier transform infrared spectroscopy, is often used for direct comparison with RS due to its

similarity. Both methods generally function according to the same physical principles and differ predominantly in the excitation wave range used. The application areas and possibilities of both methods often overlap.^[16, 26] Nevertheless, there are various differences between the two analysis methods, starting with the minimum resolution limit. The theoretical resolution limit of the FTIR, for example, is between

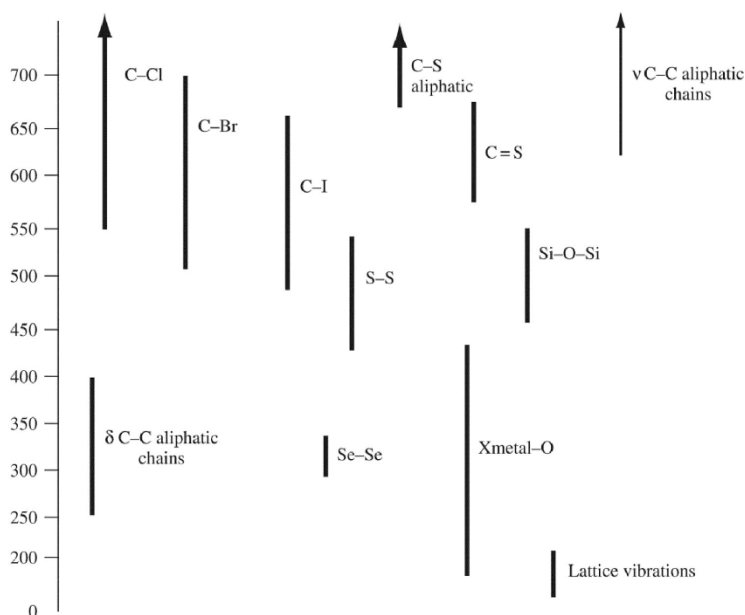


Figure 9. Single oscillation and group frequencies as well as indications of possible intensities of peaks usually identified during Raman scattering ($700\text{--}0\text{ cm}^{-1}$).^[14]

$1.7\ \mu\text{m}$ and $13\ \mu\text{m}$, depending on the exciting wavelength range. The empirically determined minimum resolution limit, however, was determined at about $20\ \mu\text{m}$. Particles smaller than $20\ \mu\text{m}$ can also be detected. However, the identification accuracy decreases with decreasing particle size.^[21, 26]

In contrast, RS is the only non-invasive analysis method that enables the chemical identification of MP particles $> 1\ \mu\text{m}$. Theoretically, the detection limit of the RS is even below $1\ \mu\text{m}$, but the result depends strongly on the magnification and numerical aperture of the objective, the wavelength of the laser, the diameter of the laser dot and matrix effects of the samples themselves.^[21] The minimum resolution that can be achieved using this optical method can be calculated using the Rayleigh criterion.^[16]

$$d_{\text{Rayleigh}} = \frac{0.61 \lambda}{NA}$$

Particle sizes below this diffraction limit can only be detected by non-linear Raman applications.^[16, 21] Another advantage of RS compared with FTIR is the easier sample preparation. Aqueous samples can be analyzed directly without preparation, since water has only a weak tendency to scatter. In addition, the use of sample carriers made of glass or quartz has no effect on the results.^[26] The major drawback of RS is the possibility of interference and fluorescence signals when analyzing environmental samples. A variety of microbiological, organic and inorganic contaminants can significantly influence the identification of such samples and so suitable cleaning steps are usually carried out when analyzing environmental samples. In addition, carefully selecting

the analysis parameters (e.g., λ_{Laser} , λ_{Laser} , NA objective, etc.) can avoid a large part of the fluorescence overlaps.^[16, 26]

Difference: normal to inverse confocal Raman micro-spectroscopy

In addition to normal Raman spectroscopy, in which a sample is analyzed in the gaseous, liquid or solid state, there is also confocal Raman microscopy. Figure 10 schematically illustrates the principle of Raman spectroscopy and Raman micro-spectroscopy. While in the traditional version the substance to be investigated is examined non-specifically in its entirety, a selected particle can be identified in micro-spectroscopy.^[36] Normal Raman spectroscopy aims to analyze a sample quantitatively and qualitatively. This includes, for example, the investigation of mechanical stress, crystallographic orientation and the determination of the concentration of substances in solutions or gases. Raman micro-spectroscopy focuses on qualitative analysis. It serves to identify and investigate substances. These can be of biological origin, such as microorganisms or chromium chromosomes, but non-biological material, such as plastic, can also be examined for its chemical composition.^[36]

Figure 10 shows the difference between normal Raman spectroscopy and Raman micro-spectroscopy. As can be seen on the one side of the image, in the classic version the sample is irradiated with a laser for examination. All substances within the laser beam are excited rather than individual particles. The concentration of the substance can be determined if the samples are gaseous or liquid. If the

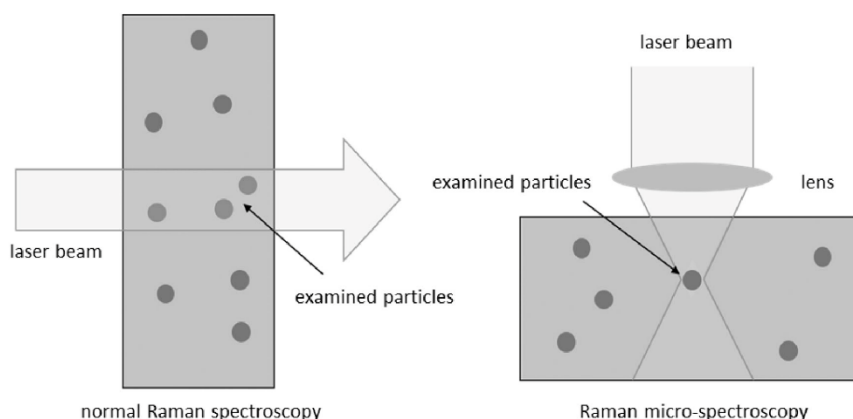


Figure 10. Difference between Raman spectroscopy and Raman micro-spectroscopy.^[35] [adapted].

sample is homogeneous, it is also possible to identify which substance is present. With heterogenic samples, on the other hand, it is difficult to identify individual molecules because they are not excited individually. Due to fluorescence, the Raman bands can be masked. Solutions must also contain a high concentration of the particles to be investigated so that the Raman bands are not falsified by the solvent if a solvent other than water is used.^[26, 30, 35] In contrast to classic Raman spectroscopy, Raman micro-spectroscopy allows the analysis of a single particle. This type of spectroscopy uses light in the visible spectrum up to the near-infrared range. The laser beam is focused to a point through the microscope lens and it is thus possible to excite and examine microscopically small particles in a targeted manner. If a confocal microscope is available, particles in deeper planes can also be analyzed with transparent substances and not only the surface.^[35] In the solid state, substances such as minerals and plastics are analyzed without much sample preparation. In the case of aqueous solutions or dispersions, sample preparation can be more complex. Optical tweezers are required to examine particles in suspension in liquids.^[35] The different methods also require special equipment. The normal Raman spectrometer consists of four important components. These are the light source of the excitation laser, the arrangement for irradiating the probes and Raman probes, a spectrometer and a CCD detector. In addition to these components, a confocal Raman microspectrometer is equipped with an optical microscope. For an axial sample examination, an aperture with perforated plates is required to ensure confocality.^[36] If the microscope is inverted, the design of the instruments is slightly different. With a microscope of this type, the sample is not illuminated from below and viewed from above as usual, but vice versa. The slide is irradiated from above, while the objective is mounted under the specimen. This has the advantage that, for example, samples in aqueous solution, which may form a sediment, can be better examined. While with normal microscopes a thin film of the sample is transferred onto a slide and covered with a cover glass, when using inverted microscopes, a

slide must be turned upside down in order to examine the sample it contains. The distance between stage and illuminator is greater than with conventional microscopes, allowing larger specimens and sample vessels.

Raman microscopy of liquid samples

Raman microscopy of liquids or aqueous solutions can be performed with little preparation, depending upon the nature of the sample. However, in the case of liquids with fluorescent components or impurities, analysis can be difficult and require more complex sample preparation. Since water only weakly triggers the Raman effect, aqueous solutions are well suited for examination by Raman spectroscopy. Therefore, particles that are finely dispersed in water and in suspension - dispersions - can be analyzed. Such samples are usually excited with light in the visible or near-infrared spectrum, which allows the use of a microscope.^[35] Many liquid samples are examined in a glass cuvette or glass tubes at room temperature. The sample containers can also have different colors, which allows, for example, the examination of samples in brown glass bottles.^[16] The sample is irradiated by a laser to a point inside the liquid to create an energy-rich area. In this energy-intensive zone, the scattering of photons is most efficient, and the Raman effect is more likely to occur. In the case of clear liquids, this zone is relatively clearly defined and there is little scattering outside the energy-rich zone. In turbid liquids, the intensity of the laser beam is attenuated, resulting in a lower Raman effect. Light is also absorbed due to turbidity, which can heat and damage the sample. Since in this case the laser only poorly penetrates the sample, the scattering within the liquid is small and is absorbed again by the surrounding areas. The detected scattered photons originate from the surface or the uppermost layers of the liquid.^[13]

The frequency plays an important role in the selection of a suitable laser. The higher the frequency, the higher the Raman sensitivity. Energy-rich ultraviolet radiation is therefore particularly suitable for excitation of scattering.

Although high-frequency excitation has advantages, it is rarely used. UV radiation is often absorbed by the samples and heat-induced damage can occur. Lasers with high-frequency radiation are also more expensive to purchase and more complicated to handle. It is also not possible to use a microscope because the light is in the non-visible range.^[16] For dispersions, it has been shown that Raman microscopy is suitable for examining individual particles in their surrounding medium.^[35] A laser with a wavelength in the visible or near-infrared range is chosen for excitation, which makes it possible to use a microscope. If confocal microscopes are used, the laser can be focused on a small volume, a single particle can be identified and its behavior in relation to directly adjacent substances can be investigated. One difficulty is to keep the confocal focus of the microscope and the laser on the volume with the particle to be examined, since in an aqueous solution it is not possible to prevent molecular movement. This problem is solved by using optical tweezers. The particle to be examined is held in position by the laser beam. If the refractive index of the particle is greater than that of the surrounding medium, it is held in the focus of the laser and overcomes gravitational and thermal forces. In this way, particles in liquids can be examined up to a mass in the femtogram range (10^{-15} g). Depending on whether a particle is smaller or larger than the wavelength of the used light, the effects vary as a particle is held in the microscope's focus. If the object to be examined is larger than the wavelength of the laser, it is kept in the focus of the laser beam due to the transmitted impulse of the light photons.^[35] If it is smaller than the wavelength of the light, a particle induces a larger dipole moment due to its higher polarizability and is pulled into the focus of the laser beam because a force is generated along the field gradient.^[35, 37] This force is stronger than the scattering force that forms when light hits a surface and acts along the radiation of the light. The particle is drawn to the point of greatest light intensity. However, this effect only works for transparent or weakly absorbing particles. If the particles are highly light-absorbing, the scattering force is higher, and they are moved away from the light source. To prevent this, a glass plate can be placed over the focus of the laser. A displacement of the particle from the zone of greatest intensity is thus avoided.^[35] Longer wavelengths are preferred because of the small volume into which the laser beam is focused. These wavelengths are associated with a lower frequency and are therefore lower in energy. This prevents heating and thus damage to the sample. Sensitive samples, such as microorganisms, cannot tolerate an intense laser over a longer period of time without damage. Therefore, lasers with a wavelength in the visible to infrared range (460 nm to 780 nm) are used. The radiation is relatively low in energy, but capable of stimulating the Raman effect. In addition, the fluorescence is reduced at small wavelengths, which improves the results of Raman spectroscopy. Lasers include krypton ion lasers, titanium sapphire lasers or Nd:YAG lasers. Depending on the type of substance to be examined, the laser and its frequency need to be adjusted to avoid fluorescence and damaging the sample.^[38] In addition,

suitable monochromators and filters must be used to filter out Rayleigh scattering. By using spectrometers with CCD detectors, the Raman shift is determined and the sample identified. Even at higher wavelengths, a certain amount of heat is generated, which is why the temperature must be controlled in this type of investigation. The use of a temperature-adjustable cell allows cooling of the sample.^[35]

Raman microscopy of solids

Raman microscopy is also suitable for the examination of solids. These substances can be present in any form (e.g., as powder or crystalline). Sample preparation for solids is simple or in some cases not even necessary. Powdery substances in a solid state are usually filled and analyzed in containers with a small hole or in glass capillaries. For larger non-powdery materials, such as fibers, the sample can be placed directly into a Raman microscope and analyzed. To avoid damaging the product, it is rotated. This means that the laser is not focused on a single point over an extended period of time. Depending on the purity of the substances, a lower-energy frequency with a longer wavelength can be selected to avoid fluorescence excitation.^[39] For solid samples, an argon ion laser is often used with a wavelength of approximately 514 nm in the visible spectrum. This is a laser with green light that is particularly suitable for material of inorganic origin. A laser with a wavelength in the UV range is ideal for organic substances such as proteins, but this spectrum is outside the visible range and therefore not suitable for microscopy.^[38]

In general, Raman spectroscopy is suitable for most solids. An exception are metals in their pure form. Metals are not polarizable, and light is only reflected. Thus no molecular oscillations are excited, which are necessary for the Raman effect.^[40] Even the smallest solid particles from flue gases, including diesel exhaust gases, can be investigated by means of solid phase microextraction (SPME).^[41] First, the exhaust gases are collected in special sample containers with a septum. The protective cannula of the SPME pierces the septum to expose a quartz barrel to which the particles accumulate in the flue gas. This fiber can be examined by confocal Raman microscopy. First, the Raman spectrum of the quartz fiber is determined in its original and enriched state. By comparing the spectra, any influence from the quartz can be excluded. Individual particles smaller than $1 \mu\text{m}$ can be analyzed from the uppermost layer of the quartz fiber. This method does not require optical tweezers, as is the case with the examination of particles in liquids, because the particles are already fixed on the fiber. The laser used for this study was a helium neon laser with a wavelength in the visible spectrum of 632.8 nm.^[41] The use of SPME is not only suitable for the smallest solids from flue gases, it can also be used for liquids. If highly volatile substances are to be investigated, the quartz fiber of the SPME can be held in the headspace of the sample container. If volatility is low, it can also be immersed directly in the liquid.^[41]

Raman microscopy of gaseous samples

Gaseous substances can also be examined using Raman spectroscopy. However, their low density makes the intensity of the Raman bands for gases much weaker than for solids and liquids. To increase the intensity of the bands, special glass cuvettes with integrated mirrors are used to reflect the radiation of the laser and thus excite the sample several times.^[42] Since the Raman effect is not based on the change of the dipole moment but on a periodic change of the polarizability, hydrogen, nitrogen and oxygen molecules can also be identified, which is not possible in IR spectroscopy.^[39] In contrast to the investigation of solid substances, it is not possible to analyze individual molecules in gaseous samples because they cannot be fixed. However, confocal Raman microscopy can be used to identify gas inclusions in transparent media. The gas bubbles in the substance must have a volume of only a few μm^3 . The distance between the inclusion and the surface of the examined object is important. The deeper the bubble, the weaker the signal and thus the Raman intensity. Objects that have not been developed for optical applications contain impurities. These can impede the laser beam and thus be responsible for a weaker Raman effect. The object does not have to be destroyed to identify the contained gas, which is a great advantage of this non-invasive analysis method.^[43] An argon krypton laser, which is located in the visible spectrum with a wavelength of 514.5 nm, can be used.^[43]

Fluorescence

A major topic affecting the efficacy and applicability of the Raman effect is fluorescence. As a background signal, this strongly limits Raman spectroscopy. It is produced as a spontaneous emission of light by the excitation of the material to a higher energy level and can be caused by the sample itself or by impurities in it. Fluorescence superimposes the weak Raman effect and can strongly impede the recording of the Raman spectrum.^[44] Beer contains a wide range of organic and inorganic substances. These include some substances that tend to autofluoresce.^[12, 45] The Raman analysis of beer's own turbidity particles or particles that have been in contact with beer can therefore lead to fluorescence problems. The Stokes and anti-Stokes lines, as already described (Figure 2), which are important for the Raman effect, are caused by inelastic scattering and by the energy exchange between photon and molecule, which results in a change of the energy level of a particle. In fluorescence, however, the incident light is completely absorbed and the molecule remains in an excited energy state for a certain time. The release of photons causes the molecule to return to its energetic ground state, creating fluorescence. The wavelength of the emitted light of fluorescence is always higher and therefore lower in energy than that of the irradiated light. There is no exact wavelength to trigger the Raman effect but a certain wavelength range is necessary for every substance with a tendency to fluoresce. In order not to reduce the effectiveness of Raman spectroscopy, the excitation of fluorescence must be avoided or reduced.^[45-47] Wavelengths in the

infrared and near-infrared range, such as those used in Raman microscopy, can prevent fluorescence because it requires higher energy radiation. It is also possible to use wavelengths in the UV range for Raman spectroscopy. Although this can strongly excite fluorescence, the energy difference to Raman scattering is too high to have a negative influence on Raman spectroscopy.^[45-47]

While in the Raman effect, only one photon of 108 incident light quanta has a change in wavelength and is scattered, and fluorescence produces ten photons with the same amount of light quanta. The Raman spectrum can therefore easily be covered by fluorescence. However, this phenomenon only affects Stokes Raman scattering. Anti-Stokes lines are not affected by fluorescence, and good results can be obtained with special forms of Raman spectroscopy despite the fluorescence and the much weaker intensity of the anti-Stokes shift.^[44] The light emitted by the fluorescence always has a lower wavelength than that of the excitation laser. Only a Stokes shift can occur because the emitted light is less energy efficient. With anti-Stokes scattering, which can occur to a lesser extent with a Raman effect, the wavelength of the emitted light becomes higher. This effect is used for Coherent anti-Stokes scattering spectroscopy (CARS). Here the anti-Stokes scattering is amplified by using a four-wave mixture. This means that lasers interact with different wavelengths to increase the amplitude of the emitted wavelength.^[25] The first laser is a pump laser, which raises the second laser – a Stokes laser – to a higher energy level and produces a coherent beam with the frequency of the anti-Stokes signal. The pump laser has a wavelength of 680–1010 nm and the Stokes laser 1064 nm. If the frequency difference between these two lasers corresponds to the molecular oscillation of a Raman-active substance, the anti-Stokes scattering is amplified and can be measured.^[48]

The problem of fluorescence can also be largely solved by using Fourier transform Raman spectrometers and lasers with low frequencies in the near-infrared range.^[44] NIR radiation is not energetic enough to excite the sample – or impurities in it – to a higher energy level and induce fluorescence. However, low irradiation frequencies are at the expense of the Raman effect. Fourier transform (FT) made it possible to develop more powerful and sensitive spectrometers that also provide results at low frequencies of the light source.^[49] While normal Raman spectroscopy detects different spectra one after the other using a monochromator, FT-Raman spectroscopy detects different spectra simultaneously. Spectra of different wavelengths are measured several times in different combinations. The intensity of the individual wavelengths is then determined by a computer.^[50] This type of spectroscopy often uses an ND:Yag laser in the near-infrared range with a wavelength of 1064 nm. This wavelength excites zero or only minimal fluorescence.^[51]

Findings

Raman spectroscopy of turbidity relevant components

To date, there are no studies dealing with the identification of beer turbidity using Raman microscopy. However, studies

exist in the field of wine production.^[52-57] Although these scientific studies were not designed for turbidity, conclusions can be drawn about turbidity-active components. The main components of turbidity-active substances are polyphenols and proline-rich proteins. There are several studies on these substances for identification by Raman spectroscopy.^[58-60]

Turbidity-relevant proteins

Prolamine/hordein. Prolamine — also called hordein in barley — is the name given to storage proteins of plants. They are a main component of barley and wheat grains and their malts. Prolamines consist of approximately 25% proline and up to 46% glutamine.^[61] Proline, in particular, is the main component of cold and permanent turbidity because it forms complexes with polyphenols such as procyanidin B3 and thus impairs colloidal stability. Prolamines have not yet been investigated in aqueous solutions, only as solids. They were dissolved from rice according to the Osborne principle with 70% ethanol and then analyzed in powder form after freeze-drying.^[62] A confocal Raman microspectrometer and an argon ion laser with a wavelength of 514.5 nm were used. It has been shown that prolamines can be investigated and identified in this way, although they differ only slightly from other protein fractions - albumin, globulin, and glutelin - in terms of wave numbers and intensities.^[63] The analysis of turbidity residues on proline, instead of prolamine, helps to draw conclusions on the formation of beer turbidity. This is the main component of protein-polyphenol complexes and can be investigated and identified in aqueous solutions, even in complex amino acid structures.^[59]

Proline-rich proteins. Proteins consist of complex structures of different amino acids, which make it difficult to investigate specific amino acids. However, Raman Optical Activity Spectroscopy (ROA) has been shown to be able to study unfolded and disordered proteins.^[58] This type of spectroscopy differs from classical Raman spectroscopy in that it measures a small change in Raman shift due to the chirality of molecules. This may be important in the analysis of turbidity-relevant substances. In beer, the formation of protein-polyphenol complexes is mainly responsible for a deterioration in colloidal stability. As mentioned above, proline-rich proteins in particular play an outstanding role, as they have a high affinity to polyphenols, such as catechins and their derivatives, and enter these compounds. The amino acid proline keeps the protein in a rigid configuration and prevents the formation of regular secondary structures. This happens due to the ring structure of proline, the resulting lack of amide hydrogen and the lack of function to form hydrogen bridge bonds with other amino acids. These are partly unfolded molecules.^[64] This type of structure - caused by proline - is called a polyproline II helix. They limit the formation of a secondary structure, a helix or a leaflet, and thus favor the connection with polyphenols. There are already studies dealing with the Raman shift of amino acids.^[59, 65] Since proteins that contain proline are some of the main turbidifiers, it would be advantageous if they could be investigated and identified using Raman spectroscopy.

However, to date, no published work has specifically investigated beer for proline-rich proteins using Raman microscopy. Pure proline can be found and identified by Raman spectroscopy. In 1970, W. B. Rippon spectroscopically identified the monomer proline, its polymers poly-L-proline I and poly-L-proline II and specific Raman bands.^[65] These partly correspond to the results of infrared spectroscopy, but there are also some Raman-specific bands. Thus, it is theoretically possible to identify proline and its polymers from aqueous solutions as contained in beer.^[65] Dissolved L-proline was investigated for a spectral range of 600–1700 cm^{-1} at a wavelength of 785 nm. The amino acids (proline) and proteins (collagen) were present in crystalline form and dissolved in water. In general, they are better analyzed in a solid state. In aqueous solutions, Raman spectra have a poorer resolution because, among other things, Brownian molecular motion makes measurement more difficult.^[66,67] This describes the jerky movements of particles in liquids that vary with temperature. Since beer resembles an aqueous solution, however, only these Raman spectra are discussed here. The following Figure 11 shows the Raman spectrum of proline in aqueous solution and in solid form.^[59]

Some prominent bands of proline appear at a wave number of 1457 cm^{-1} , which is due to a CH_2 deformation oscillation. We can see a weaker peak at 1090 cm^{-1} due to a swinging vibration of CH_2 , stronger bands at 1045, 992 and 921 cm^{-1} due to a ring-breathing vibration and finally a strong peak at 845 cm^{-1} due to a skeletal stretching vibration. These measurements of L-proline were determined in solution with a pH of 6. Here the peaks in aqueous solution are somewhat wider than in solid, but their intensity can still be easily identified.^[59] The pH value in finished beer is between 4.25 and 4.6.^[68] These values were not taken into account in the Raman spectroscopic examination of proline. The wave numbers can therefore deviate from the above. In their work, Culka et al. investigated solutions with pH values of 1, 6 and 11. On average, their wave numbers were about 1–7 cm^{-1} apart.^[69,70] Individual amino acids have already been identified in complexes with animal proteins, such as collagen, using Raman spectroscopy.^[59] Due to its complex structure, collagen is a good indicator of the extent to which individual amino acids can be analyzed from a protein. This is illustrated by the Raman spectrum in Figure 12.^[59]

Figure 12 shows that even in complex proteins the solid form allows a sharper delineation of the bands. The peaks of the aqueous solution are less pronounced. At the wave number of 922 cm^{-1} , a peak with strong Raman intensity can be recognized in the solid colony layer, which is due to the proline located in the protein complex. In the aqueous solution, this band is less intense, but can still be recognized. The intramolecular interactions and the oscillations of the molecules are responsible for the less pronounced bands of the aqueous solution, some of which have high shifts. In addition, molecules collide with each other at will, which increases the movement and thus the temperature. This is not the case in crystalline or solid form. The molecules are rigid in three-dimensional form and only weakly influence each other.^[59] It can therefore be stated that proline - the

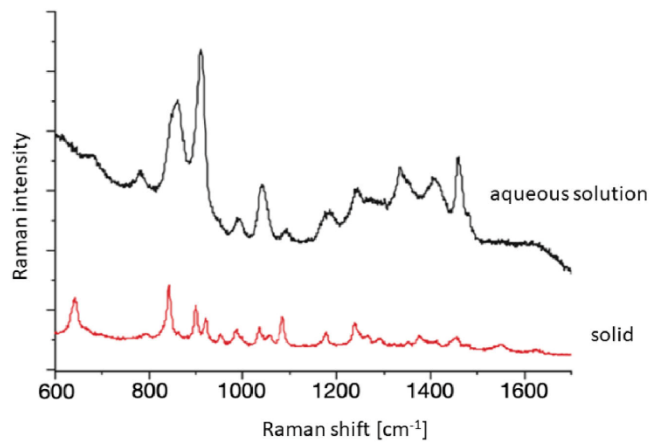


Figure 11. Raman spectra of pure proline in aqueous solution and as solids.^[59] [adapted].

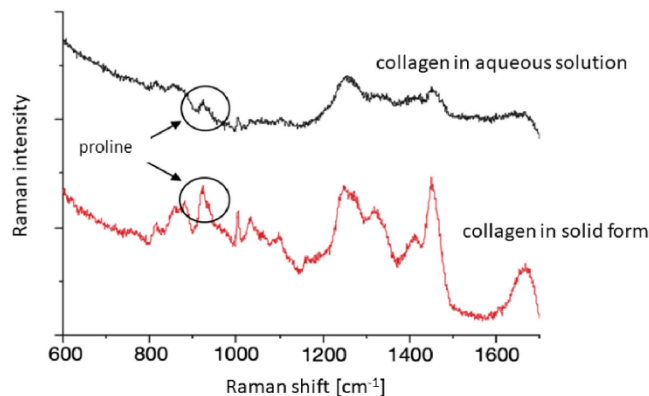


Figure 12. Raman spectra of collagen in aqueous solution and as solid with bands for proline at approx. 922 cm^{-1} .^[59] [adapted].

most turbid protein in beer - can be identified using Raman spectroscopy and also with Raman microscopy. It is not only easy to detect in free form, but also as a component of complex proteins such as collagen. The change of the secondary structure by the proline facilitates the analysis.^[71] If the residue of a turbidity is extracted in beer and analyzed spectroscopically in solid form, proline should be identifiable in complexes. In aqueous solution, such as in beer, problems may occur due to poorer resolution and the tendency of other substances to fluoresce.

Glutamine-rich proteins. Glutamine also appears to have an influence on the colloidal stability of beer, as it could be isolated from cold cloudiness in high concentrations. An actual effect, however, has not been confirmed. According to Siebert, glutamine is often bound to a proline, as Figure 13 shows.^[72]

Figure 13 shows the primary structure (i.e., the amino acid sequence) of a B hordein of barley. As already described, this

is mainly responsible for the complexation with polyphenols and thus for cold and permanent opacities.^[72] It can be seen that the amino acid glutamine, referred to here as Q, is almost exclusively bound to a proline, in this case P. The amino acid glutamine is also known as proline. For this reason, it can be assumed that glutamine only plays a passive role in turbidity formation, and that here too, proline, in combination with polyphenols, causes turbidity.^[72,73] It would be possible to examine beer for glutamic acid using Raman microscopy in order to indirectly deduce proline and turbidity-relevant constituents. As with proline, it would be advantageous to measure turbidity residues and not to analyze beer directly, because solids provide better results. According to Zhu et al., it is possible to analyze free glutamic acid using spectroscopy, as shown in Figure 14. It has already been described that it was examined both in solid form and in aqueous solution at a wavelength of 785 nm .^[59]

Here, too, it is examined both in solid form and in aqueous solution, with the solid form producing better results.

QQQFPQQPIPQQQPQY
 PQQQPYPQQPFPPQQP
 FPQQVPQQQPYPQQP
 FPPQQFPQQPPFWQQK
 PFPQQPPFGLQQPILSQQ
 QPCTPQQTPL-PQ-

P = proline; Q = glutamine

C = cysteine; F = phenylalanine; I = isoleucine; K = lysine;
 L = leucine; T = threonine; V = valine; W = tryptophane;
 Y = tyrosine

Figure 13. Amino acid sequence of a B hordein.^[72] [adapted].

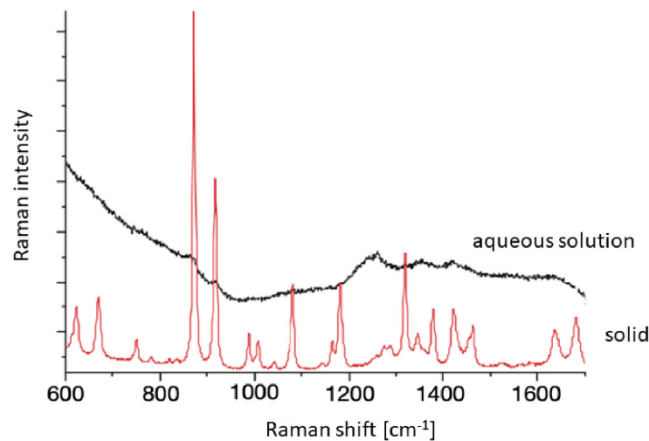


Figure 14. Raman spectra of glutamic acid in aqueous solution and as solid.^[59] [adapted].

The most pronounced peaks are at 873 cm^{-1} and 917 cm^{-1} . The first deflection can be attributed to the deformation oscillation of the COOH group. The second is based on the C–C–N aspect ratio. Due to the low concentration of glutamic acid in the aqueous solution, the intensity bands are very weak.^[59] Raman spectroscopy of glutamic acid shows an increased fluorescence problem. While very strongly defined bands can be recognized in the solid form of glutamic acid, these are hardly recognizable in the aqueous solution. This is not only a consequence of the low concentration and the aqueous aggregate state, it is also related to the strong tendency of glutamic acid to fluoresce. The Raman spectrum is strongly attenuated and it is difficult to perform successful Raman spectroscopy. Unlike proline, glutamic acid cannot be identified from the Raman spectrum for collagen. For this reason, the Raman microscopic examination of beer for glutamine, as a passive turbidifier

alongside proline, does not seem to be in the position to provide meaningful results.^[59]

Relevant polyphenols for turbidity

Catechins. Polyphenols are an essential component of cold and permanent turbidity. The most important polyphenols are catechin, an anthocyanogen, and the oligomer procyanidin B3. Both polyphenols are flavan-3-ols. The Raman bands of catechin, epicatechin and gallocatechin have already been investigated.^[60] Since, as with many Raman spectroscopies, fluorescence is a major problem, FT-Raman spectroscopy (Fourier Transform Raman spectroscopy) was used. This has the advantage that a light source with a high wavelength (1064 nm) can be used, thus avoiding excitation of fluorescence. It was found that catechin could easily be identified with this method, since the wave numbers of the bands of

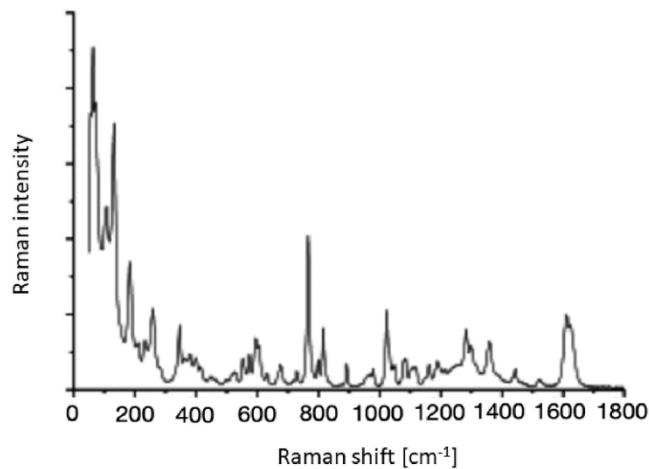


Figure 15. Raman spectrum of catechin as a solid.^[60] [adapted].

different polyphenols differed at a wavelength of 1064 nm. The bands of catechin and epicatechin differ, but at some peaks the difference in wave number is very small, making it difficult to differentiate.^[60] Basically, all these polyphenols are relevant for turbidity, but catechin is one of the most frequently found in finished beer.^[74] Its Raman spectrum can be seen in Figure 15 and was determined for samples in the solid state.

Figure 15 shows the Raman spectrum of catechin when excited by a laser with a wavelength of 1064 nm. Strong deflections can be seen here at 766 nm and 1633 nm, which are due to the oscillations of aromatic carbon double bonds.^[60] It was found that phenolic components in wines can be detected by Raman spectroscopy. The Raman spectrometer used in this study was equipped with a laser with a wavelength of 785 nm and complex sample preparation was unnecessary for the analysis. Various wine samples could be examined after a simple filtration. Polyphenols, anthocyanins and tannins were quantified. However, no individual polyphenols were identified in these studies, only the content of phenolic components in their entirety. The coefficient of determination R^2 of this study was the worst for polyphenols at 0.829, but this was still a good value.^[52,53] In general, it can be said that a reverse phase HPLC in combination with fluorescence detection is better suited to investigating catechins and other polyphenols than Raman spectroscopy.^[55, 75]

Proanthocyanidins. Proanthocyanidins, such as procyanidin B3 and prodelfinidin B3, are polyphenols that play an important role in the formation of turbidity in beverages. They are oligomers of catechins and gallo catechins, which mainly occur as dimers in beer. The higher the polymerization of these polyphenols, the greater their tendency to complex with proteins and affect the colloidal stability of beer. Procyanidin B3 is a dimer consisting of two catechin molecules. Prodelfinidin B3 consists of one catechin and one gallo catechin molecule. These dimers have not yet been

specifically investigated by Raman spectroscopy. Another problem is the tendency of proanthocyanidins to fluoresce. Polyphenols in wine are coloring substances and are easily excited to fluoresce when Raman spectra are recorded. This phenomenon significantly limits the effectiveness of Raman spectroscopy. Important bands for the identification of substances may be covered by this type of radiation.^[57] Reverse phase HPLC in combination with fluorescence detection is more suited to analyzing proanthocyanidins. With such a method, wine can be analyzed directly for these substances with simple sample preparation and minimal time expenditure.^[55]

Ferulic acid. Even though ferulic acid plays a lesser role than catechol and its derivatives procyanidin B3 and prodelfinidin B3 with regard to colloidal stability, it is present in significant amounts (up to 6.8 mg/L depending on the type of beer) in the residues of cold or permanent opacity.^[74] Ferulic acid has already been investigated in various studies using Raman spectroscopy and clearly identified.^[60, 76,77] Figure 16 shows the Raman spectra of pure ferulic acid, of the cell wall of the endosperm of wheat and of arabinoxylans. The samples were analyzed using a confocal Raman microscope. The three substances are present in crystalline form and not in aqueous solution. They were excited with a helium-neon laser in the red spectrum and examined confocally, i.e., also in an axial direction.^[76]

As can be seen from the spectrum in Figure 16 of ferulic acid, the most intense peak shows a double band at 1601 cm^{-1} and 1630 cm^{-1} , which can be traced back to the symmetrical valence oscillation of the aromatic ring in ferulic acid. Slightly weaker bands are detected at 1176 cm^{-1} and 1271 cm^{-1} , which occur due to deformation oscillations of the CH groups present in the ring.^[76, 78] This can also be identified by Raman spectroscopy in more complex systems, such as in the cell wall of the endosperm of wheat and in arabinoxylan and ferulic acid. It can be assumed that the

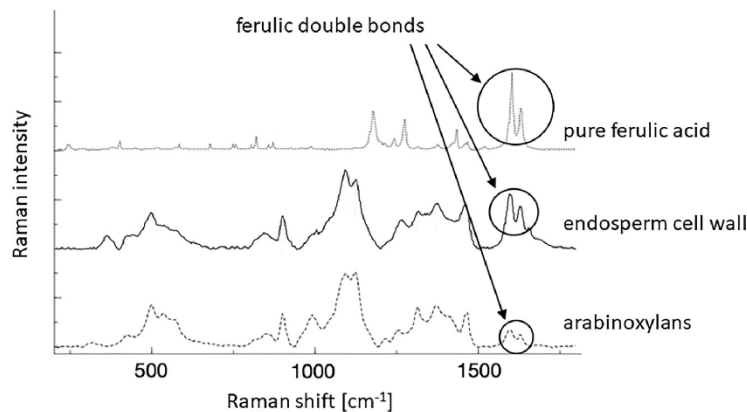


Figure 16. Raman spectra of ferulic acid/endosperm/arabinoxylans as solids.^[76] [adapted].

bands become somewhat blurred in aqueous solutions since measurement becomes more difficult here too due to Brownian molecular movement and therefore requires a higher concentration. However, it should still be possible to identify ferulic acid in beer when the turbidity residue is extracted and investigated. However, a sufficient amount of this phenolic acid is positive for colloidal stability and would cause hardly any noticeable turbidity.^[79]

Microbiological opacifiers

Microorganisms such as bacteria and yeasts may cause turbidity in clear beverages. Different microorganisms may be responsible for impairing the colloidal stability of different types of beverages. However, there are also overlaps, as certain types of yeasts, for example, infect and damage both beer and non-alcoholic beverages. Microorganisms are easily identified by Raman spectroscopy. Species of lactobacilli, pediococci etc. were analyzed and distinguished in wine.^[56] A ND:YAG laser with a wavelength of 532 nm was used. An inoculation solution of each of the different microorganisms was treated in phosphate-buffered salt solution and dissolved, pipetted in glass cuvettes and then investigated with spectroscopy. The bacteria were not analyzed directly in the wine, but rather in samples of bacteria grown on Petri dishes.

In order to examine an infected wine - or beer - the bottle would first have to be opened and the sample incubated on a culture medium for four days at $\sim 30^\circ\text{C}$. Then the bacteria were analyzed in samples of wine. With this method it is possible to identify the different bacteria correctly at a high probability and to distinguish them from microorganisms of the same genus.^[54]

Table 2 shows turbidity-relevant, drink-spoiling microbes and their sensitivity as well as the positive predictive value of the identification. Sensitivity describes the proportion of correctly identified samples from all samples of the genus or species. The positive predictive value indicates the

percentage of correctly identified samples of all analyzed and correct samples.^[80]

Genera such as *Lactobacillus* or *Pediococcus* can be distinguished correctly with very high probability. Depending on the specific species, the results may be lower. As shown here, *Lactobacillus plantarum* has the highest sensitivity at 95.8% and the highest positive predictive value at 100%. The identification of the important beer and beverage contaminant *Lactobacillus brevis* is more difficult. Here the sensitivity is 84.2% and the positive predictive value is only 72.7%.^[54] Different bacteria have similar structures and cell components, which makes investigation and identification difficult. However, different genera of microorganisms have different compositions of carbohydrates, lipids, proteins, etc. This results in a unique fingerprint for Raman spectroscopy, so that microorganisms can be distinguished. It is therefore relatively easy to identify genera. However, problems with the differentiation of bacterial species can occur.^[54] Raman spectra have also been recorded for yeast in connection with wine. Within the scope of one study, the yeasts *Saccharomyces cerevisiae*, *Brettanomyces bruxellensis* and *Zygosaccharomyces bailii*, which are harmful to wine and may also infect beer and non-alcoholic beverages, were investigated (Table 3). The top-fermented *S. cerevisiae* is a cultured yeast that is used in beer production but can also occur as a spoiler in bottom-fermented beer or if it enters bottled clear beer. It can cause problems in soft drinks by causing post-fermentation clouding and fermentation. The yeast *B. bruxellensis* is used in Belgian beers as a culture yeast, but is usually considered to be an undesirable yeast, which among other issues, reduces colloidal stability. *Z. bailii*, on the other hand, does not occur at all or only very rarely in beer, but is a feared contaminant in products such as fruit juices.^[56, 81, 82]

As in the previous analyses, a Raman spectroscope was used with a ND:YAG laser with a wavelength of 532 nm. The yeast samples, previously incubated on a culture medium (Petri dish) were selected with an inoculation loop,

Table 2. Probabilities of the identification of turbidity-forming bacteria in wine by Raman spectroscopy.^[54]

Genus / Species	Sensitivity	Positive forecast value
<i>Lactobacillus</i> (genus)	0.946	0.963
<i>Pediococcus</i> (genus)	0.928	0.908
<i>L. brevis</i>	0.842	0.727
<i>L. casei</i>	0.958	0.958
<i>L. plantarum</i>	0.958	1.0
<i>P. damnosus</i>	0.826–0.875	0.840–1.0
<i>P. inopinatus</i>	0.917	0.880

Table 3. Probabilities of identification of turbidity-forming yeasts in wine by Raman spectroscopy.^[56]

Kind	Sensitivity	Positive forecast value
<i>Saccharomyces cerevisiae</i>	0.986	0.940
<i>Brettanomyces bruxellensis</i>	0.938	0.958
<i>Zygosaccharomyces bailii</i>	0.923	0.949

dissolved in a phosphate-buffered salt solution, and then spectroscopically examined. Yeast samples were examined for the possibility of identification and distinctness, sensitivity, and the positive predictive values were determined.

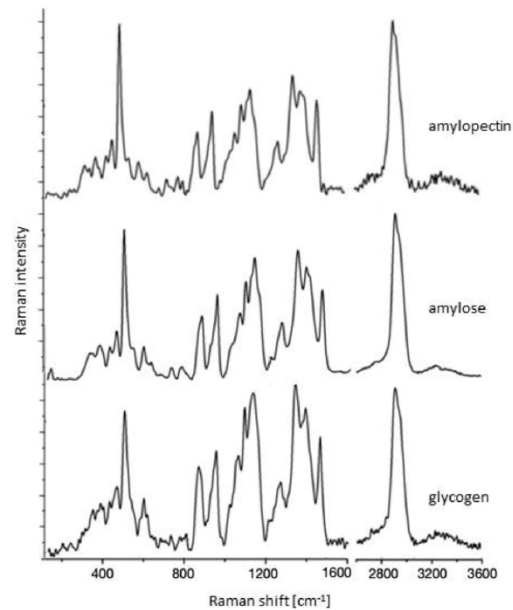
Table 3 shows that the different yeasts can be distinguished with great certainty. In contrast to bacteria, the Raman bands differed significantly in the three yeast types studied. However, here too, there was no direct analysis of the yeast in wine. Yeasts were tested (Petri dishes) and examined.^[56] A beer sample with harmful yeast must be taken and incubated at $\sim 30^\circ\text{C}$ for 48 to 72 h. Although Raman spectroscopy is in itself a rapid method for identifying substances, sample preparation is relatively time-consuming.^[56]

Carbohydrates

α -Glucan. Carbohydrates in the form of α -glucans come mainly from malt in the form of starch as amylose and amylopectin. These can enter the finished beer if starch is insufficiently converted into valuable sugars during the mashing process and the yeast cannot process them during fermentation. It is also possible that α -glucans originate directly from the yeast and occur as glycogen when reserve substances are released from the yeast cell or released via autolysis. These carbohydrates can impair the colloidal stability of beer and cause what is known as paste turbidity. This makes the beer more susceptible to infection and biological instability.^[68, 83]

Carbohydrates have been examined using FT-Raman spectroscopy.^[76, 84] Raman spectra of amylopectin, amylose and glycogen in solid form are shown in Figure 17. The spectroscopy was performed with a laser with a wavelength of 1064 nm and a resolution of 4 cm^{-1} . It can be seen that these three substances differ only slightly in their Raman bands.^[84]

Amylose and amylopectin are almost identical in their Raman spectra as well as in NIR spectra.^[84] At wave numbers of about 850 cm^{-1} and 520 cm^{-1} , which are based on a symmetrical valence oscillation of the COC group and ring-breathing - an oscillation within an aromatic ring - the bands vary and the carbohydrates can be distinguished. It

**Figure 17.** Raman spectra of amylopectin/amylose/glycogen as a solid.^[84] [adapted].

plays only a minor role for the investigation of beer turbidity whether it is amylose or amylopectin. Both types of carbohydrates would occur with paste clouding. They are due to poor mashing or poor malt quality.^[68]

Glycogen is similar in structure to amylopectin, since both carbohydrates are α -(1-4)-glycosidically bound and have α -(1-6)-glycosidically bound branches. However, the degree of branching is almost twice as high for glycogen as for amylopectin.^[84] For this reason, the Raman spectra are very similar and can only be distinguished in a few areas or by the ratio between different bands.

The bands at 484 cm^{-1} and 1130 cm^{-1} for glycogen and the bands at 479 cm^{-1} and 1131 cm^{-1} for amylopectin serve as examples. If the ratio of the relative intensities is calculated for these bands, a higher value results for glycogen than for amylopectin:

$$\text{amylopectin} : \frac{I_{479}}{I_{1131}} \approx 1$$

$$\text{glycogen} : \frac{I_{484}}{I_{1130}} \approx 1.6$$

It is therefore possible to distinguish glycogen from amylopectin, even if this is associated with greater effort. Differentiation plays an important role in the identification. It was possible to determine whether paste turbidity was caused by poor quality malt or insufficient brewhouse work, or whether it was due to poor yeast management.^[84] In contrast to amylopectin and amylose, glycogen was also investigated in aqueous solution and was excited at a wavelength of 532 nm. The Raman spectra of glycogen in solid state and

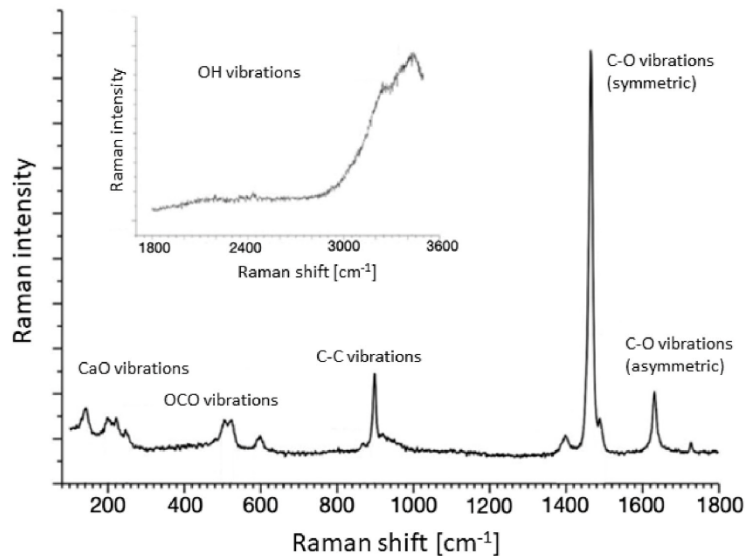


Figure 18. Raman spectrum of calcium oxalate.^[91] [adapted].

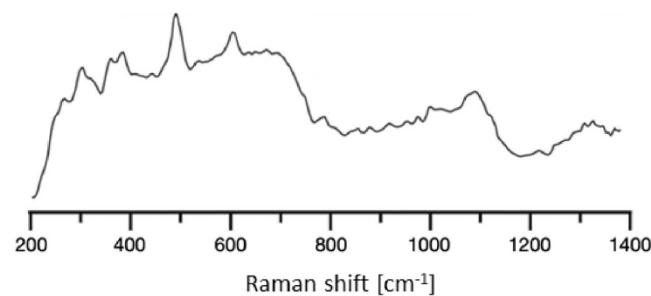


Figure 19. Raman spectrum of kieselguhr.^[92] [adapted].

in solution vary only slightly. Striking bands can be found here at wave numbers of 482, 942, 1088, 1129, 1339, 1381 cm^{-1} . Their causes are valence and deformation oscillations. The mentioned bands differ at most by 4 cm^{-1} from the peaks in the solid state and can be traced back to the same oscillations.^[85]

β -Glucan. The β -glucans are found both in the cell walls of the malt used and in the cell walls of the yeast. The majority of these polysaccharides, derived from barley or wheat, can survive malting and the beer production process unchanged and enter into the finished beer. It is possible that β -glucans from a molecular weight of 250 kDa and a concentration of 400 mg/L after filtration cause paste turbidity.^[86]

Like the α -glucans, the β -glucans have already been examined by FT-Raman spectroscopy and have been identified.^[87] However, it is difficult to determine the origin of the β -glucan present. Whether an impairment of colloidal

stability is due to poorly dissolved malt or insufficient yeast management cannot be deduced from this. Stress reactions release not only β -glucan but also other substances such as glycogen, mannan, and a small amount of trehalose from the yeast cell.^[68] These can be used to identify a yeast-conditioned β -glucan turbidity. Although mannan is also a reserve carbohydrate of many other plants, it does not play a role in the raw materials of beer and cannot be introduced into beer. It must therefore come from yeast. Mannan, like β -glucan, was examined by Raman spectroscopy, and it can be detected in an aqueous solution such as beer.^[88,89] The examination of a sample for mannan can show whether paste clouding is caused by the yeast.

Pentosan/arabinoxylan

Pentosan can cause turbidity in beer due to poor malting or mashing. As already shown in Figure 16, arabinoxylan from

Table 4. Overview of substances that actively cause turbidity and the possibility to identify them by Raman spectroscopy (RS = Raman spectroscopy; RMS = Raman micro-spectroscopy; cRMS = confocal Raman micro-spectroscopy; FT-RS = FT-Raman spectroscopy; ROA = Raman optical activity).

Turbidity active substances	Identification	Investigated substance	Raman	Description	Source
prolamine/hordein	microscopic (eosin yellow); enzymatic (pepsin)	solid	cRMS	Identifiable as solid; not yet in aqueous solutions	[63]
proline	microscopic (eosin yellow)	solid, aqueous resolution	RMS	Identifiable as a solid and in aqueous solutions	[58,59, 65, 69,70]
glutamine	microscopic (eosin yellow)	watery resolution	RMS	Identifiable as solid; in aqueous solutions; fluorescence problem	[59]
catechin	microscopic (methylene blue)	solid, wine	FT-RS; RS	identifiable as solid; general content of phenolic components quantifiable in wine	[52,53, 55, 60, 75]
proanthocyanidins	microscopic (methylene blue)	wine	–	No specific proanthocyanidins with RS; fluorescence problem;	[55, 57]
ferulic acid	microscopic (methylene blue)	solid	cRMS; FT-RS	identifiable as solid	[60, 76–78]
microorganism	microscopic	aqueous resolution	RS; RMS	Identifiable in aqueous solution after incubation	[8, 54, 56]
α-glucan	microscopic (thionine); enzymatic (amyloglucosidase); GPC	solid; aqueous resolution	RS; FT-RS; ROA	Identifiable and distinguishable as solids and in aqueous solution, but hardly any differences in spectra	[84,85]
β-glucan	microscopic (thionine, calcofluor); enzymatic (amyloglucosidase); GPC	solid; aqueous resolution	FT-RS	Identifiable as solid; Difficult to detect origin	[87, 89]
arabinoxylans	microscopic (thionine); enzymatic (amyloglucosidase); GPC	Solid	RMS	Identifiable as solid	[76]
calcium oxalate	microscopic	Solid	RS; RMS	Identifiable as solid and in aqueous solution; hydrate forms distinguishable	[24, 90]
inorganic substances (label remnants, filter aids, stabilizers, etc.)	microscopic (iodine solution)	beer, water, solid	cRMS; RS; FT-RS	Dependent on the investigated particles; microplasty, kieselguhr, silica gel, PVPP identifiable; e.g. problems with fluorescence	[42, 91, 93,94]

the cell walls of wheat grains can be analyzed by Raman spectroscopy.^[76] Water-extractable arabinoxylan was spectroscopically analyzed. The Raman micro-spectrometer used was equipped with a helium neon laser operating in the red spectrum. However, the sample was not analyzed in an aqueous solution, but the cell wall of the endosperm was examined as a solid. Arabinoxylan consists of the aldopentoses, xylose, and arabinose and can be clearly identified by a double band using Raman microscopy. At wave numbers of 898, 1090 and 1124 nm, a specific arabinoxylan vibration occurs in the cell wall of endosperm. This pentosan has not yet been investigated as a suspension in liquids such as beer, but only as a solid in wheat grains.^[76]

Calcium oxalate

Beer turbidity caused by calcium oxalate is relatively rare in beer because it is present early in the brewing process.^[68] Calcium oxalate can be formed with the remaining oxalic acid by adding water that contains calcium during filtration. This precipitates in crystalline form and leads to turbidity and sediments when the beer is briefly stored.^[68] As already mentioned, substances in solid or crystalline form can be investigated and identified well using Raman spectroscopy.^[56] This also applies to calcium oxalate, which forms small crystals in beer.^[83]

Calcium oxalate can appear as monohydrate, dihydrate and trihydrate, with the former occurring most frequently. The three hydrates can be distinguished by Raman spectroscopy, although this is not relevant for the analysis, identification or determination of the cause of turbidity. The monohydrate, which is called whewellite, and the dihydrate, which is called weddellite, have very similar Raman spectra that vary in their wave numbers and are therefore easily distinguishable.^[24] In practice, calcium oxalate samples were excited with a helium neon laser with a wavelength of 633 nm and a resolution of 2 cm⁻¹.^[90] In a wavelength range of 1200–1800 cm⁻¹, the most conspicuous band is based on a valence oscillation of the C–O group of the calcium oxalate. Whewellite has the band at a wave number of 1493 cm⁻¹ and the weddellite at 1475 cm⁻¹. A valence oscillation of the C–C group occurs in a range of 800 and 1100 cm⁻¹. The band lies at a wave number of 909 cm⁻¹ for both the monohydrate and the dihydrate. Thus it is very difficult to distinguish the two hydrates in this range. In a small wave number range of 100–700 cm⁻¹, bands appear that make it possible not only to identify calcium oxalate, but also its two hydrates. A band can be recognized for both forms at approx. 505 cm⁻¹ that is due to a symmetrical deformation oscillation of the OCO group. Further intense bands can be found in a range of 100–300 cm⁻¹. Distinct bands for whewellite and weddellite can be found at a wave

number of 259, 220, 188 and 162 cm^{-1} and are probably caused by valence and deformation oscillations of the CaO group.^[24] The differences between the hydrates are most obvious with the OH-oscillation in a wave-number-range of $2000\text{--}4000\text{ cm}^{-1}$. This is based on crystal-water, that occurs bound in the oxalate-crystals, and whose oscillation can be determined. For weddellite the bands are at 3467 and 3266 cm^{-1} . The whewellite has a strong peak at 3462 cm^{-1} and somewhat weaker bands, at 3359 , 3248 and 3067 cm^{-1} .^[24] Figure 18 shows the Raman spectrum of a calcium oxalate monohydrate, the whewellite. In this study the sample was irradiated by a laser with a wavelength of 532 nm and has a resolution of 1.2 cm^{-1} . Since a different wavelength is used here than in the Raman spectrum described above, the wave numbers of the respective oscillations also deviate from those mentioned above. However, it can be seen that they are in a similar range. Calcium oxalate can also be clearly identified here.^[90]

As can be seen from the work of Frost and of Hug et al., different oxalates can be analyzed by Raman spectroscopy.^[24, 90] Calcium oxalate and its hydrate forms were also investigated and the possibility of differentiation to other oxalates. It can be assumed that it is possible to identify beer turbidity caused by calcium oxalate in bottled beer by examination with a Raman micro-spectrometer. Calcium oxalate is very difficult to dissolve in water and beer and so oxalate should be easily detectable and a non-invasive process.

Inorganic substances

Some inorganic substances in beer in connection with turbidity do not originate from the raw materials, but rather could be dirt particles or filter aids and stabilizers that have broken through. Diatomaceous earth, or kieselguhr, is one of the most frequently used substances in the filtration of beer, and a trap filter generally ensures that it does not reach the finished beer. If no trap filter is present, or if errors occur during filtration, kieselguhr can be introduced into the beer and impair colloidal stability.^[68]

Confocal Raman micro-spectroscopy has already been used to examine various types of kieselguhr. The spectrometer is equipped with a helium neon laser at a wavelength of 632.8 nm . For the analysis, siliceous earth samples were washed out with water, dried, crushed and then examined in a glass cuvette. Figure 19 shows the Raman spectrum of diatomaceous earth at room temperature.^[91]

The two bands with the highest intensity were at a wave number of 493 and 607 cm^{-1} . These are due to the molecular vibrations of O_3SiOH and $(\text{SiO})_3$ and are specific for all kieselguhrs, regardless of their type and origin. If a residue of beer turbidity is obtained, it can be examined by Raman microscopy. If the turbidity is due to kieselguhr, it should be possible to detect it using these bands.

Silica gel, which is used for protein-side stabilization (i.e., for improved colloidal stability) of beer can also enter beer as a result of process errors and cause turbidity.^[92] This has been investigated in various studies using normal Raman spectroscopy and FT-Raman spectroscopy.^[42, 91] The spectra

show strong bands at about 495 and 605 cm^{-1} , which have the same origin as diatomaceous earth. The difference between the two substances is shown by a strong peak at about 910 cm^{-1} for silica gel, which is not very pronounced or only very weakly present in diatomaceous earth samples. This is due to the vibration of a SiH molecule. By this oscillation different types of diatomaceous earth can be distinguished.^[42, 91]

In beer and water samples, Raman micro-spectroscopy can be used to identify fibers of plastic particles (i.e., micro-plastics and cellulose).^[93] The samples were passed through a cellulose nitrate filter with a membrane pump, dried, and analyzed directly on the filter. An ND:YAG laser with green light and a wavelength of 532 nm was used as the illumination source. Using this method, fibers were found in all of the investigated beer and water samples. These fibers could be identified and consisted mainly of cellulose, polyethylene and polystyrene. Polyethylene terephthalate (PET) could not be detected. However, it also contained fibers that could not be examined due to a high fluorescence tendency.^[93]

Summary

The aim of this review was to determine whether and how turbidity-relevant substances in beer can be examined with the aid of Raman spectroscopy. This paper discussed what effort is involved in spectroscopy with regard to sample preparation and what technical equipment is required. It has been found that most of the substances that affect the colloidal stability of beer can be identified by Raman spectroscopy. Some substances such as the protein fraction prolamine or the proanthocyanidins procyanidin B3 and prodelphinidin B3 have not yet been investigated. For other substances, spectroscopy is difficult. This is true for glutamic acid. In the study of glutamine, fluorescence is strongly excited and covers the Raman bands. It is therefore difficult to obtain a meaningful Raman spectrum. The investigated substances were mainly analyzed in their pure form or in solution. A direct examination of beer or other beverages is difficult due to the fluorescence.^[12] Beverages contain numerous different substances which can strongly hinder the uptake of the Raman spectrum and therefore require complex sample preparation, e.g., by centrifugation and recovery of turbidity residues. While there are very few studies for beer in connection with Raman spectroscopy, wine has already been the subject of many studies in this field. Wine was analyzed for phenolic constituents, which can also cause turbidity in beer. However, no specific substances, such as catechin or epicatechin, could be differentiated in those investigations; a distinction was made only with regard to non-specific polyphenols, anthocyanins and tannins.

To date, beer has so far only been examined for micro-plastics using Raman microscopy. After relatively uncomplicated sample preparation, plastic fibers could be spectroscopically examined on a filter. Wine-spoiling micro-organisms have also already been investigated using this method. The analyzed yeasts and bacteria have many

similarities with beer-spoiling organisms. However, all investigations required complex sample preparation. Turbidity residues first had to be obtained and then incubated for three days in order to obtain a sufficient amount of sample material. Spectroscopy itself produced good results. Different yeast and bacterial genera could be very well differentiated and identified, but the analysis was not as good for different species identification. Substances such as calcium oxalate and various carbohydrates, which can cause turbidity in beer, were investigated as solids and partly in dissolved form, and identification was possible without major problems. It is often difficult to determine a clear cause for paste opacities that can be caused by α - and β -glucans. It is difficult to distinguish whether the turbidity is caused by poor quality raw materials, has technological reasons or is the result of inadequate yeast management.

An overview of turbidity-relevant substances and the possibility of examining them using Raman microscopy or other methods based on the Raman effect is shown in Table 4.

Table 4 shows that substances that actively cause turbidity such as proline and proline-rich proteins can be successfully investigated with RS. Limits occur due to fluorescence, which requires time-consuming sample preparation. However, this problem can be solved with suitable methods and the use of lasers with wavelengths in the near-infrared or infrared range. Most of the investigated origins of turbidity must first be isolated and analyzed as solids or in aqueous solutions in order to avoid superposition by other substances and fluorescence.

RS has enormous potential to determine turbidities in beer and other alcoholic and non-alcoholic beverages and is a time-saving and reliable method. The uncomplicated sample preparation and fast analysis means that a non-invasive analysis of beer may also be possible, and errors can be easily detected. Inline RS is conceivable through targeted further developments. This would allow real-time analysis during the process, and errors in chemical-physical stability could be detected immediately.

By using suitable wavelengths, adapted to the different turbidity-relevant substances, it should be possible to limit the problems caused by RS. The biggest obstacle — fluorescence — can already be localized with the help of suitable lasers and the use of fluorescence reduction methods. In combination with optical tweezers, particles can be singled out, specifically analyzed and identified without interfering with surrounding particles. By applying such a concept in conjunction with other methods, such as coherent anti-Stokes Raman scattering, or further development of existing techniques, problems should be continuously reduced and efficiency increased. Combining appropriate techniques could reduce undesirable turbidity and increase the shelf life of beer.

Outlook

In this review (Part 2), the different methods of Raman spectroscopy were discussed and related to analysis of substances related to beer turbidity discussed in the previous

review (Part 1). With the help of the TI-RMS (Turbidity Identification - Raman Micro-Spectroscopy), the issue of beer as a medium will be investigated in further research work. An appropriate methodology for sample preparation must first be established to combine these two basic topics in order to develop a novel robust approach to turbidity analysis.

Disclosure statement

No potential conflict of interest was reported by the author(s).

ORCID

Eva-Maria Kahle  <http://orcid.org/0000-0001-8371-3361>

Literature cited

- [1] Back, W. *Ausgewählte Kapitel Der Brauereitechnologie*; Hans Carl Fachverlag: Nürnberg, 2008.
- [2] Narziß, L.; Back, W.; Gastl, M.; et al. *Abriss Der Bierbrauerei*; Wiley: Weinheim, 2017; pp 361–414.
- [3] Steiner, E.; Gastl, M.; Becker, T. Die Identifizierung von Trübungen in Bier (1). *Brauwelt* 2011, 151, 161–166.
- [4] MEBAK (ed). Würze, Bier, Biermischgetränke (Band 2): Methodensammlung der Mitteleuropäischen Brautechnischen Analysenkommission, 2012.
- [5] Dele-Dubois, M.; Dhamelincourt, P.; Poirot, J.; Schubnel, H. Differentiation between Gems and Synthetic Minerals by Laser Raman Microspectroscopy. *J. Mol. Struct.* 1986, 143, 135–138. DOI: 10.1016/0022-2860(86)85222-X.
- [6] Gremilich, H.; Yan, B. *Infrared and Raman Spectroscopy of Biological Materials*; Marcel Dekker: New York, 2001.
- [7] Petry, R.; Schmitt, M.; Popp, J. Raman Spectroscopy-A Prospective Tool in the Life Sciences. *Chemphyschem* 2003, 4, 14–30. DOI: 10.1002/cphc.200390004.
- [8] Stöckel, S.; Kirchhoff, J.; Neugebauer, U.; Rösch, P.; Popp, J. The Application of Raman Spectroscopy for the Detection and Identification of Microorganisms. *J. Raman Spectrosc.* 2016, 47, 89–109. DOI: 10.1002/jrs.4844.
- [9] Gauglitz, G.; Vo-Dinh, T. *Handbook of Spectroscopy*; Wiley: Hoboken, 2006.
- [10] Bolwien, C.; Sulz, G. Raman-Mikroskopometer Zur Untersuchung Biologischer Proben. tm-Technisches Messen Plattform Für Methoden. *Systeme Und Anwendungen Der Messtechnik* 2010, 77, 437–444.
- [11] Puppels, G. J.; de Mul, F. F.; Otto, C.; Greve, J.; Robert-Nicoud, M.; Arndt-Jovin, D. J.; Jovin, T. M. Studying Single Living Cells and Chromosomes by Confocal Raman Microspectroscopy. *Nature* 1990, 347, 301–303. DOI: 10.1038/347301a0.
- [12] Kahle, E.-M.; Zarnkow, M.; Jacob, F. Substances in Beer That Cause Fluorescence: Evaluating the Qualitative and Quantitative Determination of These Ingredients. *Eur. Food Res. Technol.* 2019, 245, 2727–2737. DOI: 10.1007/s00217-019-03394-x.
- [13] Smith, E.; Dent, G. *Modern Raman Spectroscopy: A Practical Approach*; Wiley: Hoboken, 2005.
- [14] Dieing, T.; Hollrichter, O.; Toporski, J. *Confocal Raman Microscopy*; Springer: Berlin, Heidelberg, 2011.
- [15] Cox, G.; Sheppard, C. J. R. Practical Limits of Resolution in Confocal and Non-Linear Microscopy. *Microsc. Res. Tech.* 2004, 63, 18–22. DOI: 10.1002/jemt.10423.
- [16] Smith, E.; Dent, G. *Modern Raman Spectroscopy: A Practical Approach*; Wiley: NJ, USA, 2013.
- [17] König, N.; Schmitt, R. Optische Oberflächenmessverfahren zur Charakterisierung von Mikro- und Nanostrukturen, 2018. <https://www.inspect-online.com/topstories/automation/optische->

- oberflaechenmessverfahren-zur-charakterisierung-von-mikro-und-nanostr (accessed 2019).
- [18] Schmitt, M.; Popp, J. Raman Spectroscopy at the Beginning of the Twenty-First Century. *J. Raman Spectrosc.* **2006**, *37*, 20–28. DOI: 10.1002/jrs.1486.
- [19] Raman, C. V.; Krishnan, K. S. A New Type of Secondary Radiation. *Nature* **1928**, *121*, 501–502. DOI: 10.1038/121501c0.
- [20] Singh, R. CV Raman and the Discovery of the Raman Effect. *Phys. Perspect.* **2002**, *4*, 399–420. DOI: 10.1007/s000160200002.
- [21] Anger, P. M.; von der Esch, E.; Baumann, T.; Elsner, M.; Niessner, R.; Ivleva, N. P. Raman Microspectroscopy as a Tool for Microplastic Particle Analysis. *Trac, Trends Anal. Chem.* **2018**, *109*, 214–226. DOI: 10.1016/j.trac.2018.10.010.
- [22] Gewert, B.; Plassmann, M. M.; MacLeod, M. Pathways for Degradation of Plastic Polymers Floating in the Marine Environment. *Environ. Sci. Process. Impacts.* **2015**, *17*, 1513–1521. DOI: 10.1039/c5em00207a.
- [23] WITEC. Appendix System Description - Confocal Raman Microscopy. Ulm, **2017**.
- [24] Frost, R. L. Raman Spectroscopy of Natural Oxalates. *Anal. Chim. Acta* **2004**, *517*, 207–214. DOI: 10.1016/j.aca.2004.04.036.
- [25] Evans, C. L.; Sunney, X. X. Coherent Anti-Stokes Raman Scattering Microscopy: Chemical Imaging for Biology and Medicine. *Annu. Rev. Anal. Chem.* **2008**, *1*, 883–909.
- [26] Wiesheu, A. C. Raman-Mikrospektroskopie zur Analyse von organischen Bodensubstanzen und Mikroplastik, Technische Universität München, **2017**.
- [27] Spektrum. Argon-Ionenlaser, **2019**. <https://www.spektrum.de/lexikon/physik/argon-ionenlaser/749>.
- [28] Universität Göttingen. Helium-Neon-Laser. <https://lp.uni-goettingen.de/get/text/1804> (accessed Jun 24, **2019**).
- [29] Rheinisch Westfälische Technische Hochschule Aachen. ND:YAG Laser, **2019**. https://institut2a.physik.rwth-aachen.de/de/teaching/praktikum/Anleitungen/B_FK08-Nd-YAG_Teil1_12-03-2012.pdf.
- [30] Demtröder, W. *Laserspektroskopie 2: Experimentelle Techniken*; Springer-Verlag: Berlin, **2013**.
- [31] Spektrum. Krypton-Ionenlaser, **2019**. <https://www.spektrum.de/lexikon/physik/krypton-ionenlaser/8592>.
- [32] Ferdinand Braun Institut. Zwei-Wellenlängen-Diodenlaserlichtquelle bei 785 nm für die Raman-Spektroskopie, **2019**. <https://www.fbh-berlin.de/forschung/forschungsnews/detail/750-mw-zwei-wellenlaengen-diodenlaserlichtquelle-bei-785-nm-fuer-die-raman-spektroskopie>.
- [33] Chemgapedia. Einführung in die Interpretation von IR- und Raman-Spektren, **2016**. http://www.chemgapedia.de/vsengine/vlu/vsc/de/ch/3/anc/ir_spek/allg_interpretation.vlu.html (accessed June 10, 2019).
- [34] Socrates, G. *Infrared and Raman Characteristic Group Frequencies: Tables and Charts*; Wiley: Chichester, UK, **2004**.
- [35] Cherney, D. P.; Harris, J. M. Confocal Raman Microscopy of Optical-Trapped Particles in Liquids. *Annu. Rev. Anal. Chem. (Palo Alto Calif.)* **2010**, *3*, 277–297. DOI: 10.1146/annurev-anchem-070109-103404.
- [36] Krishna, R.; Unsworth, T. J.; Edge, R. *Raman Spectroscopy and Microscopy*; Elsevier: Manchester, UK, **2016**.
- [37] Wu, M.-Y.; Ling, D.-X.; Ling, L.; Li, W.; Li, Y.-Q. Stable Optical Trapping and Sensitive Characterization of Nanostructures Using Standing-Wave Raman Tweezers. *Sci. Rep.* **2017**, *7*, 42930. DOI: 10.1038/srep42930.
- [38] Horiba. What Laser Wavelengths are Used for Raman Spectroscopy? **2019**. <http://www.horiba.com/uk/scientific/products/raman-spectroscopy/raman-academy/raman-faqs/what-laser-wavelengths-are-used-for-raman-spectroscopy/>.
- [39] Salzer, R.; Thiele, S.; Suemmenchen, L. Raman Probenvorbereitung, **2019**. http://www.chemgapedia.de/vsengine/vlu/vsc/de/ch/3/anc/ir_spek/raman_probenvorb.vlu/Page/vsc/de/ch/3/anc/ir_spek/raman_spektroskopie/ra_probenvorbereitung/ra_7_1/ravorb_m13ht0603.vscml.html
- [40] Renishaw. Advantages of Raman Spectroscopy, **2019**. <https://www.renishaw.com/en/why-we-use-raman-spectroscopy-25803>.
- [41] Odziemkowski, M.; Koziel, J. A.; Irish, D. E.; Pawliszyn, J. Sampling and Raman Confocal Microspectroscopic Analysis of Airborne Particulate Matter Using poly(dimethylsiloxane) Solid-Phase Microextraction Fibers. *Anal. Chem.* **2001**, *73*, 3131–3139. DOI: 10.1021/ac001141m.
- [42] Matsui, K.; Satoh, H.; Kyoto, M. Raman Spectra of Silica Gel Prepared from Triethoxysilane and Tetraethoxysilane by the Sol-Gel Method. *Nippon. Seramikkusu. Kyokai. Gakujutsu. Ronbunshi.* **1998**, *106*, 528–530. DOI: 10.2109/jcersj.106.528.
- [43] Pedeche, S.; Simon, P.; Matzen, G.; Moulin, B.; Blanchard, K.; Querel, G. Probing Gas Bubbles inside Industrial Glasses by Raman Scattering. *J. Raman Spectrosc.* **2003**, *34*, 248–252. DOI: 10.1002/jrs.984.
- [44] Skoog, D. A.; Leary, J. J. *Instrumentelle Analytik: Grundlagen-Geräte-Anwendungen*; Springer-Verlag: Berlin, **2013**.
- [45] Sikorska, E.; Górecki, T.; Khmelinskii, I. V.; Sikorski, M.; De Keukeleire, D. Fluorescence Spectroscopy for Characterization and Differentiation of Beers. *J. Inst. Brew.* **2004**, *110*, 267–275. DOI: 10.1002/j.2050-0416.2004.tb00621.x.
- [46] Sikorska, E.; Górecki, T.; Khmelinskii, I. V.; Sikorski, M.; Koziol, J. Classification of Edible Oils Using Synchronous Scanning Fluorescence Spectroscopy. *Food Chem.* **2005**, *89*, 217–225. DOI: 10.1016/j.foodchem.2004.02.028.
- [47] Sikorska, E.; Górecki, T.; Khmelinskii, I. V.; Sikorski, M.; De Keukeleire, D. Monitoring Beer during Storage by Fluorescence Spectroscopy. *Food Chem.* **2006**, *96*, 632–639. DOI: 10.1016/j.foodchem.2005.02.045.
- [48] Potma, E. O.; Evans, C. L.; Xie, X. S. Heterodyne Coherent Anti-Stokes Raman Scattering (CARS) Imaging. *Opt. Lett.* **2006**, *31*, 241–243. DOI: 10.1364/ol.31.000241.
- [49] Fechner, P. Raman-Spektroskopie Und Atmosphärische Rasterelektronenmikroskopie-Charakterisierung Pharmazeutischer Hilfsstoffe. Doktorarbeit, Universität Halle, **2005**.
- [50] Chase, B. Fourier Transform Raman Spectroscopy. *Anal. Chem.* **1987**, *59*, 881A–890A. -DOI: 10.1021/ac00141a001.
- [51] Agarwal, U. P.; Atalla, R. H. FT Raman Spectroscopy: What It is and What It Can Do for Research on Lignocellulosic Materials. In: Proc. 8th Intl. Symp. Wood Pulp. Chem., Vol 8, **1995**; pp 67–72.
- [52] dos Santos, C. A. T.; Pascoa, R. N.; Lopes, J. A. A Review on the Application of Vibrational Spectroscopy in the Wine Industry: From Soil to Bottle. *Trac, Trends Anal. Chem.* **2017**, *88*, 100–118. DOI: 10.1016/j.trac.2016.12.012.
- [53] Gallego, Á. L.; Guesalaga, A. R.; Bordeu, E.; Gonzalez, Á. S. Rapid Measurement of Phenolics Compounds in Red Wine Using Raman Spectroscopy. *IEEE Trans. Instrum. Meas.* **2011**, *60*, 507–512. DOI: 10.1109/TIM.2010.2051611.
- [54] Rodriguez, S. B.; Thornton, M. A.; Thornton, R. J. Discrimination of Wine Lactic Acid Bacteria by Raman Spectroscopy. *J. Ind. Microbiol. Biotechnol.* **2017**, *44*, 1167–1175. DOI: 10.1007/s10295-017-1943-y.
- [55] Silva, M. A.; Ky, I.; Jourdes, M.; Teissedre, P.-L. Rapid and Simple Method for the Quantification of Flavan-3-Ols in Wine. *Eur. Food Res. Technol.* **2012**, *234*, 361–365. DOI: 10.1007/s00217-011-1628-0.
- [56] Rodriguez, S. B.; Thornton, M. A.; Thornton, R. J. Raman Spectroscopy and Chemometrics for Identification and Strain Discrimination of the Wine Spoilage Yeasts *Saccharomyces cerevisiae*, *Zygosaccharomyces bailii*, and *Brettanomyces bruxellensis*. *Appl. Environ. Microbiol.* **2013**, *79*, 6264–6270. DOI: 10.1128/AEM.01886-13.
- [57] Mandrile, L.; Zeppa, G.; Giovannozzi, A. M.; Rossi, A. M. Controlling Protected Designation of Origin of Wine by Raman Spectroscopy. *Food Chem.* **2016**, *211*, 260–267. DOI: 10.1016/j.foodchem.2016.05.011.
- [58] Johannessen, C.; Kapitán, J.; Collet, H.; Commeyras, A.; Hecht, L.; Barron, L. D. Poly(L-proline) II Helix Propensities in Poly(L-lysine) Dendrigrift Generations from Vibrational Raman

- Optical Activity. *Biomacromolecules* **2009**, *10*, 1662–1664. DOI: 10.1021/bm9002249.
- [59] Zhu, G.; Zhu, X.; Fan, Q.; Wan, X. Raman Spectra of Amino Acids and Their Aqueous Solutions. *Spectrochim Acta A Mol. Biomol. Spectrosc.* **2011**, *78*, 1187–1195. DOI: 10.1016/j.saa.2010.12.079.
- [60] Pompeu, D. R.; Larondelle, Y.; Rogez, H.; et al. Caractérisation et Discrimination Des Composés Phénoliques à L'aide de la Spectroscopie Raman à Transformée de Fourier et Des Outils Chimométriques. *Biotechnologie. Agronomie, Société et Environnement* **2018**, *22*, 13–28.
- [61] Täufel, A.; Ternes, W.; Tunger, L.; et al. *Lebensmittel-Lexikon*; Behrs Verlag: Hamburg/Germany, **1993**.
- [62] Osborne, T. B. *The Proteins of the Wheat Kernel*; Carnegie Institution of Washington: Washington, DC, **1907**.
- [63] Guo, Y.; Cai, W.; Tu, K.; Tu, S.; Wang, S.; Zhu, X.; Zhang, W. Infrared and Raman Spectroscopic Characterization of Structural Changes in Albumin, Globulin, Glutelin, and Prolamin during Rice Aging. *J. Agric. Food Chem.* **2013**, *61*, 185–192. DOI: 10.1021/jf303345r.
- [64] Gorinstein, S.; Zemser, M.; Vargas-Albores, F.; Ochoa, J.-L.; Paredes-Lopez, O.; Scheler, C.; Salmikow, J.; Martin-Belloso, O.; Trakhtenberg, S. Proteins and Amino Acids in Beers, Their Contents and Relationships with Other Analytical Data. *Food Chem.* **1999**, *67*, 71–78. DOI: 10.1016/S0308-8146(99)00071-0.
- [65] Walton, A. G.; Rippon, W. B.; Koenig, J. L. Raman Spectroscopy of Proline Oligomers and poly-L-Proline. *J. Am. Chem. Soc.* **1970**, *92*, 7455–7459. DOI: 10.1021/ja00728a034.
- [66] Wu, C.-S. *Handbook of Size Exclusion Chromatography and Related Techniques: Revised and Expanded*; CRC Press: New York, **2003**; Vol. 91.
- [67] Biologie-Lexikon. Brownsche Molekularbewegung, **2019**. http://www.biologie-lexikon.de/lexikon/browsnsche_molekularbewegung.php.
- [68] Narziß, L.; Back, W.; Gastl, M.; et al. *Abriss Der Bierbrauerei*; Wiley: Weinheim, **2017**.
- [69] Herlinger, A. W.; Long, T. V. Laser-Raman and Infrared Spectra of Amino Acids and Their Metal Complexes. 3. Proline and bisprolinato complexes. *J. Am. Chem. Soc.* **1970**, *92*, 6481–6486. DOI: 10.1021/ja00725a016.
- [70] Culka, A.; Jehlička, J.; Edwards, H. G. M. Acquisition of Raman Spectra of Amino Acids Using Portable Instruments: Outdoor Measurements and Comparison. *Spectrochim. Acta A Mol. Biomol. Spectrosc.* **2010**, *77*, 978–983. DOI: 10.1016/j.saa.2010.08.034.
- [71] Bunaciu, A. A.; Aboul-Enein, H. Y.; Hoang, V. D. Raman Spectroscopy for Protein Analysis. *Appl. Spectrosc. Rev.* **2015**, *50*, 377–386. DOI: 10.1080/05704928.2014.990463.
- [72] Siebert, K. J. Haze Formation in Beverages. *LWT-Food Sci. Technol.* **2006**, *39*, 987–994. DOI: 10.1016/j.lwt.2006.02.012.
- [73] Poeschl, M. Die Kolloidale Stabilität Untergäriger Biere-Einflussmöglichkeiten Und Vorhersagbarkeit. Dissertation, Freising-Weihenstephan, **2009**.
- [74] Gerhäuser, C.; Becker, H. Phenolic Compounds of Beer. In *Beer in Health and Disease Prevention* Preedy, V. R. editor; Academic Press: MA, USA, **2011**, pp 124–144.
- [75] Su, W.-H.; Sun, D.-W. Fourier Transform Infrared and Raman and Hyperspectral Imaging Techniques for Quality Determinations of Powdery Foods: A Review. *Compr. Rev. Food Sci. Food Saf.* **2018**, *17*, 104–122. DOI: 10.1111/1541-4337.12314.
- [76] Piot, O.; Autran, J.-C.; Manfait, M. Investigation by Confocal Raman Microspectroscopy of the Molecular Factors Responsible for Grain Cohesion in *Thetriticum aestivum* Bread Wheat. Role of the Cell Walls in the Starchy Endosperm. *J. Cereal Sci.* **2001**, *34*, 191–205. DOI: 10.1006/jcrs.2001.0391.
- [77] Ram, M. S.; Dowell, F. E.; Seitz, L. M. FT-Raman Spectra of Unsoaked and NaOH-Soaked Wheat Kernels, Bran, and Ferulic Acid. *Cereal Chem.* **2003**, *80*, 188–192. DOI: 10.1094/CCHEM.2003.80.2.188.
- [78] Prats Mateu, B.; Hauser, M. T.; Heredia, A.; Gierlinger, N. Waterproofing in Arabidopsis: Following Phenolics and Lipids in Situ by Confocal Raman Microscopy. *Front. Chem.* **2016**, *4*, 10. DOI: 10.3389/fchem.2016.00010.
- [79] Papp, A.; Winnewisser, W.; Geiger, E.; Briem, F. Influence of (+)-Catechin and Ferulic Acid on Formation of Beer Haze and Their Removal through Different Polyvinylpyrrolidone-Types. *J. Inst. Brew.* **2001**, *107*, 55–60. DOI: 10.1002/j.2050-0416.2001.tb00080.x.
- [80] Benesch, T. *Schlüsselkonzepte Zur Statistik: Die Wichtigsten Methoden, Verteilungen, Tests Anschaulich Erklärt*; Springer-Verlag: Berlin, **2012**.
- [81] Back, W. *Colour Atlas and Handbook of Beverage Biology*. Fachverlag Hans Carl: Nurnberg, **2005**.
- [82] Back, W. *Farbatlas Und Handbuch Der Getränkebiologie Teil 2*; Verlag Hans Carl: Nurnberg, **1994**.
- [83] Steiner, E.; Becker, T.; Gastl, M. Turbidity and Haze Formation in Beer - Insights and Overview. *J. Inst. Brew.* **2010**, *116*, 360–368. DOI: 10.1002/j.2050-0416.2010.tb00787.x.
- [84] Wiercigroch, E.; Szafraniec, E.; Czamara, K.; Pacia, M. Z.; Majzner, K.; Kochan, K.; Kaczor, A.; Baranska, M.; Malek, K. Raman and Infrared Spectroscopy of Carbohydrates: A Review. *Spectrochim. Acta A Mol. Biomol. Spectrosc.* **2017**, *185*, 317–335. DOI: 10.1016/j.saa.2017.05.045.
- [85] Dudek, M.; Zajac, G.; Szafraniec, E.; Wiercigroch, E.; Tott, S.; Malek, K.; Kaczor, A.; Baranska, M. Raman Optical Activity and Raman Spectroscopy of Carbohydrates in Solution. *Spectrochim. Acta A Mol. Biomol. Spectrosc.* **2019**, *206*, 597–612. DOI: 10.1016/j.saa.2018.08.017.
- [86] Speers, R. A.; Jin, Y.-L.; Paulson, A. T.; Stewart, R. J. Effects of β -Glucan, Shearing and Environmental Factors on the Turbidity of Wort and Beer. *J. Inst. Brew.* **2003**, *109*, 236–244. DOI: 10.1002/j.2050-0416.2003.tb00164.x.
- [87] Mikkelsen, M. S.; Jespersen, B. M.; Møller, B. L.; Laerke, H. N.; Larsen, F. H.; Engelsen, S. B. Comparative Spectroscopic and Rheological Studies on Crude and Purified Soluble Barley and Oat/Beta-Glucan Preparations. *Food Res. Int.* **2010**, *43*, 2417–2424. DOI: 10.1016/j.foodres.2010.09.016.
- [88] Leiper, K. A.; Miedl, M. *Colloidal Stability of Beer*; In *Beer: A Quality Perspective*, ed. C.W.Bamforth, pp 111–161. Academic Press: Burlington, MA, **2008**.
- [89] Noothalapati, H.; Sasaki, T.; Kaino, T.; Kawamukai, M.; Ando, M.; Hamaguchi, H.-O.; Yamamoto, T. Label-Free Chemical Imaging of Fungal Spore Walls by Raman Microscopy and Multivariate Curve Resolution Analysis. *Sci. Rep.* **2016**, *6*, 27789. DOI: 10.1038/srep27789.
- [90] Hug, S.; Grohe, B.; Jalkanen, J.; Chan, B.; Galarreta, B.; Vincent, K.; Lagugné-Labarthe, F.; Lajoie, G.; Goldberg, H. A.; Karttunen, M.; Hunter, G. K. Mechanism of Inhibition of Calcium Oxalate Crystal Growth by an Osteopontin Phosphopeptide. *Soft Matter* **2012**, *8*, 1226–1233. DOI: 10.1039/C1SM06232H.
- [91] Yuan, P.; He, H. P.; Wu, D. Q.; Wang, D. Q.; Chen, L. J. Characterization of Diatomaceous Silica by Raman Spectroscopy. *Spectrochim. Acta A Mol. Biomol. Spectrosc.* **2004**, *60*, 2941–2945. DOI: 10.1016/j.saa.2004.02.005.
- [92] Hartmann, K. Bedeutung Rohstoffbedingter Inhaltsstoffe Und Produktionstechnologischer Einflüsse Auf Die Trübungsproblematik im Bier. Technische Universität München, **2006**.
- [93] Wiesheu, A. C.; Anger, P. M.; Baumann, T.; Niessner, R.; Ivleva, N. P. Raman Microspectroscopic Analysis of Fibers in Beverages. *Anal. Methods* **2016**, *8*, 5722–5725. DOI: 10.1039/C6AY01184E.
- [94] Lang, P. L.; Katon, J. E.; O'Keefe, J. F.; Schiering, D. W. The Identification of Fibers by Infrared and Raman Microspectroscopy. *Microchem. J.* **1986**, *34*, 319–331. DOI: 10.1016/0026-265X(86)90127-X.

PART 3

2.4 Substances in beer that cause fluorescence: evaluating the qualitative and quantitative determination of these ingredients.

Fluorochromes can weaken investigation results or, because of their common recurrence (sub-atomic vibrations) totally superimpose significant signals and make estimations unthinkable. This is particularly valid for non-obtrusive, optical estimating techniques such as Raman micro-spectroscopy, which reach their cut-off points when fluorochromes are available. Beer contains numerous fluorescent substances, e.g. amino acids, nutrients and phenolic mixes. Consequently, in this investigation, eight unique beers (ale lager, dim ale, Pilsner brew, Radler lager, wheat lager, dull wheat lager, non-alcoholic ale brew, and liquor free wheat brew) were analyzed for their fluorescent ingredients. Utilizing the PARAFAC model, it was possible to clarify the fluorescence of the eight lagers for three components. By comparing the results with existing information, these parts could be subjectively attributed to the natural substances DOM (dissolved organic matter), DOC (dissolved organic carbon) or CDOM (colored dissolved organic matter) and OC (organic carbon). The discharge and termination spectra assisted with building up these natural substances as the three fragrant amino acids phenylalanine, tryptophan and tyrosine, iso- α -corrosive, phenolic mixes and the nutrient B gathering. What's more, relationships with the fluorescence forces from the EEM (excitation–emission matrix) information were recognized in the mixtures in the lager investigations. Accordingly, a connection emerged between the fluorescence power and iso- α -corrosive. The fluorescent amino acids phenylalanine, tryptophan and tyrosine indicated only slight connections with the fluorescent power. The results indicated that fluorescence spectroscopy combined with the acquired EEM information could be used to estimate organic components and enables sensitive monitoring to identify fluorescent substances in brewing tests. Subjective investigation in conjunction with the PARAFAC examination is likewise invaluable to distinguish the primary components.

Authors/Authorship contribution:

Kahle, E-M.: Literature search, writing, review conception and design; **Zarnkow, M.:** critical review of draft, discussion of data; **Jacob F.:** Supervised the project



Substances in beer that cause fluorescence: evaluating the qualitative and quantitative determination of these ingredients

Eva-Maria Kahle¹ · Martin Zarnkow¹ · Fritz Jacob¹Received: 10 July 2019 / Accepted: 19 October 2019 / Published online: 31 October 2019
© Springer-Verlag GmbH Germany, part of Springer Nature 2019

Abstract

Fluorochromes can impair analysis results or, due to their natural frequency (molecular vibrations) completely superimpose important signals and make measurements impossible. This is especially true for non-invasive, optical measuring methods such as Raman microspectroscopy, which reach their limits when fluorochromes are present. Beer contains many fluorescent substances, e.g., amino acids, vitamins and phenolic compounds. Therefore, in this study, eight different beers (lager beer, dark lager, Pilsner beer, Radler beer, wheat beer, dark wheat beer, alcohol-free lager beer, and alcohol-free wheat beer) were examined for their fluorescent ingredients. Using the PARAFAC model, the fluorescence of the eight beers could be explained for three components. By comparing with existing database literature, these components could be qualitatively assigned to the organic substances DOM (dissolved organic matter), DOC (dissolved organic carbon) or CDOM (colored dissolved organic matter) and OC (organic matter). The emission and extinction spectra helped to establish these organic substances as the three aromatic amino acids phenylalanine, tryptophan and tyrosine, iso- α -acid, phenolic compounds and the vitamin B group. In addition, correlations with the fluorescence intensities from the EEM (excitation–emission matrix) data were detected in combination with beer analyses. A correlation between the fluorescence intensity of origin and iso- α -acid could therefore be shown. The fluorescent amino acids phenylalanine, tryptophan and tyrosine showed only slight correlations with the fluorescent intensity. The calculated data showed that fluorescence spectroscopy with the obtained EEM represents a powerful real-time measurement, which offers sensitive monitoring for the identification of fluorescent substances in beer samples. Qualitative analysis combined with the PARAFAC analysis is also advantageous to identify the main components.

Keywords Fluorescence spectroscopy · Fluorescing substances · EEM · Amino acid · Vitamins · Phenolics · Iso- α -acid · PARAFAC

Introduction

Beer is a highly complex medium comprising more than 450 ingredients [1–3]. Many of these substances are fluorescing, but the primary components of water, ethanol and carbohydrates have no influence on the fluorescence [4]. Various ranges of the fluorescence spectra can be assigned to specific ingredients by comparing known fluorescing compounds of beer. Amino acids, vitamins and phenolic compounds are the main contributors to fluorescence [4–7]. The predominantly organic ingredients cause primary fluorescence, also

known as autofluorescence. These compounds—referred to as fluorochromes—can affect analysis results or fully overlay important signals as a result of their natural frequency (molecular vibrations), making measurement impossible [8–11]. This is especially true for non-invasive, optical measurement methods such as Raman microspectroscopy, which reach their limits if fluorochromes are present.

Fluorescence is described as the light spontaneously emitted when an electronically excited system returns to a lower energy state. Fluorescence occurs when light of a specific wavelength reaches a molecule. Photons are absorbed and electrons in the molecule are boosted, or excited, to an energetically higher orbital. If they then fall back to their original level, the energy released is emitted as heat and photons [8, 12–14]. The critical intermolecular, energetic processes during fluorescence can be explained using the Jabłoński diagram (see Fig. 1) [14–17].

✉ Eva-Maria Kahle
eva.maria.kahle@tum.de

¹ Forschungszentrum Weihenstephan für Brau- und Lebensmittelqualität, Technische Universität München, Alte Akademie 3, 85354 Freising-Weihenstephan, Germany

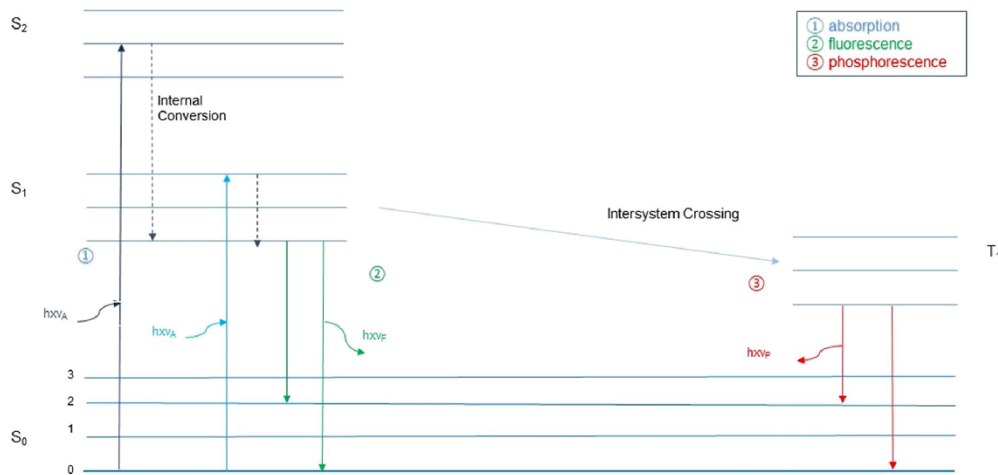


Fig. 1 Jablonski diagram: ① absorption (stimulation); ② fluorescence; ③ phosphorescence; S₀ ground singlet state, S₁, S₂ excited singlet states, T₁ triplet state; vibration states 0, 1, 2 and 3; internal conversion (IC); intersystem crossing (ISC); [15], adaption

Table 1 The key fluorescing substances: amino acids, vitamins, phenolic compounds and iso- α -acid and their extinction and emission ranges in (nm) [4–6, 21–27]

Substance	Emission λ (nm)	Extinction λ (nm)
Amino acids	284–400	258–300
Vitamins	393–520	270–450
Phenolic compounds	320–460	260–340
Iso- α -acid	395–450	300–350

In this study, different beer types were investigated using fluorescence spectroscopy for their fluorescing ingredients (lager beer = lb, dark lager = dl, Pilsner beer = pb, Radler beer = rb, wheat beer = wb-lb, wheat beer dark = wb-d, alcohol-free lager beer = af-lb, and alcohol-free wheat beer = af-wb). The following Table 1 shows the substances causing fluorescence and their extinction and emission values. Using this method of analysis, these ingredients could be presented as an emission and excitation spectrum (EEM, excitation–emission matrix) and evaluated as part of beer testing performed at the same time. Each beer displays different characteristics in the fluorescence spectra, which can be used for quantitative and qualitative analyses [4, 18–20]. Parallel factor analysis (PARAFAC) was used to evaluate the obtained data.

Amino acids

The amino acids account for a very large proportion of fluorescence. They lie in the emission range 284–400 nm and

the extinction range 258–300 nm. According to Sikorska et al., three amino acids are involved in fluorescence: phenylalanine, tryptophan and tyrosine [28]. Their emission and extinction ranges are: for phenylalanine ~ EM: 279 nm, EX: 258 nm; tryptophan ~ EM: 354 nm, EX: 278 nm and tyrosine ~ EM: 303 nm, EX: 275 nm.

Vitamins

Vitamins are another fluorescing substance group. The following vitamins were evaluated: vitamin B₂ (riboflavin), vitamin B₃ (niacin), vitamin B₅ (pantothenic acid), vitamin B_{5_{Ca}} (Ca-pantothenate), vitamin B₇ (biotin) and vitamin B₉ (folate). The vitamins lie in an emission range of 393–520 nm and an extinction range of 270–450 nm. The emission bands at ~450/500–600 nm can be attributed to riboflavin, flavin mononucleotide (FMN) and flavin adenine dinucleotide (FAD) and other phenolic compounds. Substances from the vitamin B₆ group (pyridoxine, pyridoxal, pyridoxamine, pyridoxic acid and pyridoxal-5-phosphate) emit in the 385–400 nm range. Vitamin B₂ (riboflavin) lies in an emission range of around 518 nm and an extinction range of 353–443 nm [5, 6, 21, 23–25, 28–31]. The vitamins come from the malt as well as the yeast.

Phenolic compounds

The next group of substances that causes fluorescence are the phenolic compounds. The phenolic compounds are

associated with the emission range of 320–460 nm and an extinction range of 260–340 nm. Analyses of phenolic compounds were performed on: flavonoids, polyphenols, phenols, xanthohumol, iso-xanthohumol, ferulic acid and coumaric acid. Ferulic acid falls in the extinction range around 340 nm and an emission range of 460 nm. Phenolic compounds are extracted from malt and hops in different quantities in the wort according to the technological method used. Depending on the structure and molecular size, they can greatly influence different beer properties such as color, flavor, foam, and chemical and physical stability. Unfavorable conditions, such as a high level of polymerizable or condensable compounds, and atmospheric oxygen, may cause derivatives to be produced that are high in protein and undesirable for flavor [32].

Iso- α -acid (isohumulone)

Iso- α -acids represent another substance group that increases fluorescence and is present in hops [6]. This chemical compound is largely responsible for the level of bittering units in beer. Iso- α -acid is converted from α -acid during the isomerization process in brewing and lies in the emission range of 395–450 nm and the extinction range of 300–350 nm [4, 31, 33].

Materials and methods

Biological replicates: beer preparation and treatment for fluorescence spectroscopy

Eight different beer varieties were used in total to measure fluorescence. According to Apperson et al., beer samples should be diluted for fluorescence spectroscopy and so all samples were diluted in a 1:10 ratio [6]. Carbon dioxide was eliminated from the samples, which were then filtered using vacuum membrane filtration, diluted with Milli-Q water and transferred to sterile 50 mL swing-top bottles. In the membrane filtration, the beers were filtered at a pore size of 0.45 μ m. Samples were prepared in triplicate for the biological replicates.

Fluorescence spectroscopy

The fluorescence measurements in this study were taken using the fluorescence spectrometer AqualogTM of HORIBA Scientific, Kyoto/Japan. The fluorimeter simultaneously measures excitation, emission and absorption spectra along with transmission. Using a 1 cm quartz cuvette, the fluorescence measurements were determined on an AqualogTM spectral fluorimeter. Before each measurement series, a device-specific validation experiment was performed using

Milli-Q water in a separate validation cuvette to calibrate the device. The Raman peak of water is also measured during validation. According to Lawaetz and Stedmon, the area of the Raman peak can be useful to standardize the measured fluorescence intensity. Fluorescence intensities can vary greatly according to the used device, the built-in components, and the experiment settings. It is therefore important to standardize the intensity to make it possible to compare these results with other fluorescence measurements. This standardization enables the original intensity of a diluted sample to be determined, by multiplying the dilution factor [34].

The test parameters of integration time, CCD gain, the ranges of the extinction spectrum and the scanning rate of the emission measurement can be set in the AqualogTM software. These settings have a direct influence on the duration and quality of the experiment. The suitable parameters with which to measure undiluted and diluted beer samples with identical settings were approximately determined at the start of the measurement series using test measurements. A dilution series of lager beer was also measured to establish the linearity of concentration and fluorescence intensity.

The settings for the fluorescence spectroscopy and the ranges used were: integration time 0.5 s, extinction spectrum 230–700 nm; 3.00 nm steps, emission spectrum 156–933 nm; 1.64 nm steps (4 pixels) and CCD gain at medium range.

A blank sample with Milli-Q water was measured before each measurement series. Using the software, the blank sample used to correct the Raman scattering can be automatically removed from the sample spectra. Excitation and emission spectra are presented in a three-dimensional matrix (EEM). The fluorescence measurements were taken as per the recommendations of HORIBA Scientific.

Technical replicates: beer analyses

All the analyses of the eight beer varieties were carried out in double determination ($n=2$), except for the vitamin analysis ($n=1$), and conducted according to the following test methods (see Table 2).

Data analysis

The data material was evaluated using statistical analysis with Excel 2016 (Microsoft, CA, USA) and using Origin 2019 (OriginLab Corporation, USA). The data had been calculated in statistical analyses using the correlation coefficient R , the coefficient of determination R^2 and one-way ANOVA. ANOVA was used with 95% confidence intervals and the statistical significance value was set to $p < 0.05$ both for ANOVA and the comparative analysis. The values are given as means of the standard deviation.

Table 2 Chemical–technical and microbiological test methods for the eight beer varieties with their units; all analyses in double determination ($n=2$) except for the vitamin analysis ($n=1$); WBBM = wort, beer, beer-mixed beverages [35–37]

Characteristics	Unit	Method
Amino acids	(mg/L)	MEBAK WBBM 2.6.4.1.2
Vitamin B ₂ : riboflavin	(mg/L)	DIN EN 14152, HPLC/FI
Vitamin B ₃ : niacin	(mg/L)	AOAC 944.13, Microbiology
Vitamin B ₅ : pantothenic acid	(mg/L)	AOAC 945.74, Microbiology
Vitamin B ₅ : Ca-pantothenate	(mg/L)	AOAC 945.74, Microbiology
Vitamin B ₇ : biotin	(mg/L)	SOP M 655, Microbiology, <i>L. plantarum</i>
Vitamin B ₉ : folate	(mg/L)	DIN EN 14131:2003, Microbiology
Flavonoids	(mg/L)	EBC 9.12
Polyphenols	(mg/L)	EBC 2.16.1
Phenols	(mg/L)	MEBAK vol. II 2.26
Iso- α -acid	(mg/L)	EBC 9.47
Xanthohumol	(mg/L)	MEBAK Raw materials vol. 4.3.3.1
Iso-xanthohumol	(mg/L)	MEBAK Raw materials vol. 4.3.3.1
Ferulic acid	(mg/L)	MEBAK WBBM 2.21.3.2
Coumaric acid	(mg/L)	MEBAK WBBM 2.21.3.2

The data were analyzed using the Solo + MIA 2019 program (Eigenvector Research, USA). The PARAFAC analysis was used to find a suitable model to describe the connections between the eight beers [38].

Results and discussion

Substances causing fluorescence using the EEM

Evaluation of the lager beer type

Multi-dimensional EEM was charted with the above-specified settings for all eight beers. The extinction wavelength (EX) in [nm] is plotted on the x-axis and the emission wavelength (EM) in [nm] on the y-axis. The intensity, with no units, [–] of the fluorescence radiation (FI) is shown as a color scale, where blue represents the lowest (0.000) and red the highest intensity (8800) [5, 19, 20]. The virtually diagonal line next to the emission peak can be attributed to Rayleigh scattering. Rayleigh scattering describes the emission of light of the same wavelength as the excitation light. The electrons of the molecules vibrate at the same frequency as the light, emitting electromagnetic waves of the same wavelength [39]. These inner filter effects are removed using the Solo + MIA software.

Based on the volume of data, the EEM for all of the analyzed types is described using the lager beer variety as an example. The individual components are presented in Fig. 2.

Figure 2 shows the EEM of the lager beer divided up into the most important ranges for the fluorescing substances. The volume of EEM data (Origin 2019) for the eight beer types, and the extinction and emission spectra of the four

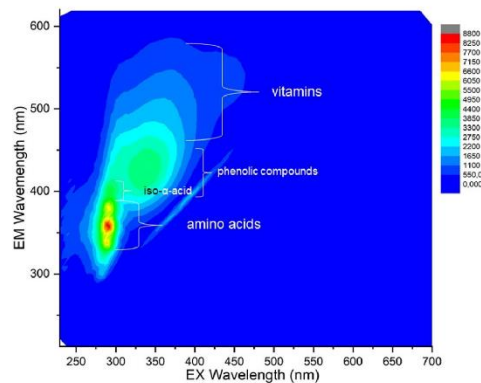


Fig. 2 Two-dimensional contour diagram of the lager beer as an emission and extinction spectrum (EEM) showing the most important ranges of fluorescing substances, vitamins, phenolic compounds, amino acids and iso- α -acid

substances (amino acids, vitamins, phenolic compounds and iso- α -acid) were used to calculate their contents and statistically evaluate them based on the fluorescence intensities (FI) (see Table 4).

Beer analyses: fluorescing properties of the tested beers in correlation with simultaneous analyses

The beer samples were analyzed for different characteristics (see Tables 3, 4) and tested for their correlation with the fluorescence spectra.

Table 3 Analysis results for the eight beer types, mean \bar{x} ($n=2$) with repeatability r (95%)

Characteristics	Unit	Repeatability r (95%)	Lager beer (lb)	Dark lager (dl)	Pilsner beer (pb)	Radler beer (rb)	Wheat beer (wb-lb)	Wheat beer dark (wb-d)	Alcohol-free lager beer (af-lb)	Alcohol-free wheat beer (af-wb)
Σ amino acids	(mg/L)	± 0.51	122.0	120.0	128.0	61.0	131.0	115.0	133.0	122.0
Σ vitamins	(mg/L)	n.s.	26.9	38.4	22.8	14.7	26.5	20.8	36.1	26.7
Σ phenolic compounds	(mg/L)	n.s.	160.4	196.2	175.1	109.8	90.6	167.3	188.5	114.8
Iso- α -acid	(mg/L)	$\pm 0.34\%$	18.8	23.2	32.4	5.8	9.7	9.5	21.0	9.2

n.s. not specified

Data evaluation using the PARAFAC model for qualitative determination

Following data preparation and pre-processing in the Solo + MIA program, the PARAFAC model is used to identify the number of main fluorescing components of the samples (see Fig. 3). The following calculations are important for evaluating the data:

Variance explained

The percentage of variance explained, which is taken from the results table of the PARAFAC model, provides information on how the model breaks down the data. It is calculated according to the following equation [40]:

$$\text{Variance explained}[\%] = 100 \times \left(1 - \frac{\sum_{ijk} e_{ijk}^2}{\sum_{ijk} x_{ijk}^2} \right), \quad (1)$$

where E_{ijk} represents the introduced residues and x_{ijk} is the data matrix. Variance can be a good indicator of how much noise there is in the data set and how accurately the model presents the data. Stedmon and Bro state that a meaningful variance is $> 99\%$, however, it depends on the respective data set [41].

Core consistency (Tucker3 model)

Core consistency describes how well the PARAFAC model fits a Tucker3 model that uses the same components that were found by the PARAFAC model, and how trilinear the model is. A three-way PARAFAC model can be described by the following function:

$$X = AT^{(F \times FF)}(CB)^T, \quad (2)$$

where X is the model output matrix. A , B and C are the parameter matrices that contain the parameters of the previous PARAFAC model. F is equivalent to the number of components. T ($F \times FF$) is the developed two-dimensional matrix that comes from a three-dimensional nucleus array. The three dimensions of this array are presented by $d=1$ to F , $e=1$ to F and $f=1$ to F . The superdiagonal elements of this three-dimensional matrix are shown by ones, whereas the remainder is zero. This means that each element of the matrix T $d=e=f=1$ and the rest is zero [40].

In the next step, a Tucker3 model is calculated, using the same parametrization (A , B and C) as the PARAFAC model. It is adjusted by minimizing the smallest square of the nuclear matrix G of the Tucker3 model.

$$\sigma(G) = IIX - AG(CB)^TII \quad (3)$$

Table 4 Results of the data evaluation of the beer analyses (lager beer = lb, dark lager = dl, Pilsner beer = pb, Rüdler beer = rb, wheat beer = wb-lb, wheat beer dark = wb-d, alcohol-free lager beer = af-lb, alcohol-free wheat beer = af-wb) and the fluorescence intensities (FI) of the EEM of amino acids, vitamins, phenolic compounds and Iso- α -acid; statistical evaluation using mean \bar{x} , standard deviation, confidence interval (p value) α , coefficient of determination R^2 , correlation coefficient R and the slope

Beer types	Amino acids			Vitamins			Phenolic compounds			Iso- α -acid		
	Σ FI [–]	Σ Phe (mg/L)	Σ Trp (mg/L)	Σ Tyr (mg/L)	Σ Vitamins (mg/L)	Σ FI [–]	Σ phenol. V. (mg/L)	Σ FI [–]	Σ Iso- α -acid (mg/L)			
lb	2.7E+06	79.00	39.00	71.00	7.3E+06	26.90	5.4E+06	160.40	1.5E+05	18.80		
dl	3.3E+06	83.00	33.00	78.00	7.1E+06	38.40	6.0E+06	196.20	1.4E+05	23.20		
pb	5.1E+06	84.00	36.00	74.00	6.7E+06	23.00	7.3E+06	175.10	1.3E+05	32.40		
rb	6.7E+06	41.00	19.00	38.00	1.1E+07	14.70	1.0E+07	109.80	1.9E+05	5.80		
wb-lb	2.9E+06	78.00	47.00	71.00	1.4E+07	26.50	7.0E+06	90.60	2.3E+05	9.70		
wb-d	4.2E+06	63.00	47.00	65.00	1.3E+07	20.80	8.0E+06	167.30	2.0E+05	9.50		
af-lb	4.4E+06	92.00	38.00	83.00	1.1E+07	36.10	7.8E+06	188.50	1.8E+05	21.00		
af-wb	4.3E+06	70.00	47.00	64.00	1.1E+07	26.70	7.7E+06	114.80	1.8E+05	9.20		
Statistics												
Arithmetic mean \bar{x}	3.4E+07	590.00	306.00	544.00	8.1E+07	213.00	5.9E+07	1202.80	1.4E+06	129.60		
Standard deviation	1.2E+06	14.90	8.90	12.80	2.6E+06	7.20	1.4E+06	37.20	3.1E+04	8.60		
Confidence interval (p value) α	8.4E+05	10.30	6.20	8.80	1.8E+06	5.00	9.4E+05	25.70	2.2E+04	5.90		
Coefficient of determination R^2	0.38	0.44	0.45	0.45	0.08	0.08	0.16	0.16	0.63	0.63		
Correlation coefficient R	-0.62	-0.66	-0.67	-0.67	-0.29	-0.29	-0.40	-0.40	-0.80	-0.80		
Slope	-7.63E-06	-4.87E-06	-7.09E-06	-8.00E-07	-1.10E-05	-2.19E-04	-1.10E-05	-1.10E-05	-1.10E-05	-2.19E-04		

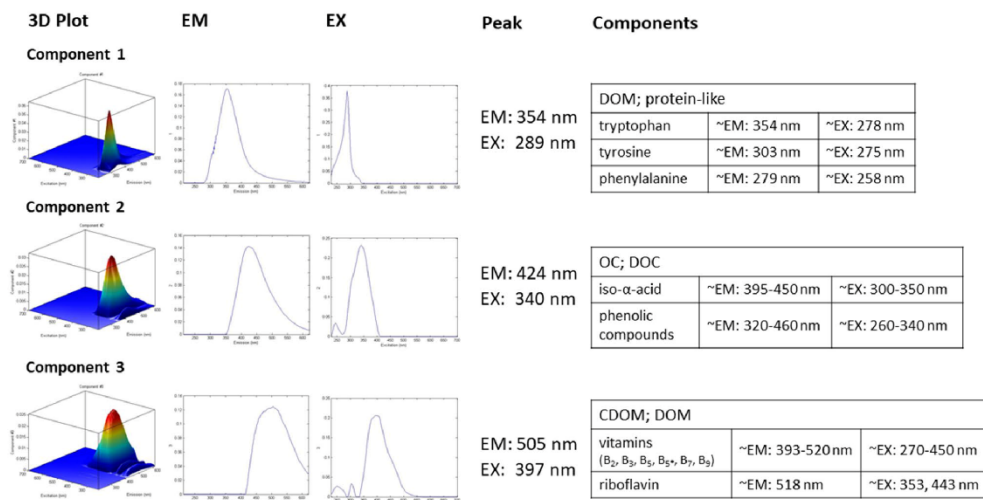


Fig. 3 PARAFAC model of the eight beers with 3D plot, EM, EX, peak and components [4, 5, 21, 23–25, 28–30, 33]

X is equivalent to the data set. G is the previously explained equivalent to T . However, it only equals T if a perfect fit can be achieved—a core consistency of 100%. The deviation, which corresponds to the difference of the PARAFAC model to a Tucker3 model, can be calculated as the core consistency using the following equation [40]:

$$\text{Core consistency}[\%] = 100 \times \left(1 - \frac{\sum_{d=1}^F \sum_{e=1}^F \sum_{f=1}^F (G_{def} - T_{def})^2}{F} \right) \quad (4)$$

The core consistency can range from 100 to $<0\%$, where 100% indicates the best fit. According to Bro and Kiers, a value $>90\%$ means that the model is trilinear, a value of around 50% means that the model is partially trilinear and partially models trilinear phenomena, and a value of 0% or less implies that the model is invalid as it does not describe trilinear variations. For EEM data, trilinear means no variation in the excitation spectra across the emission wavelengths and the opposite, as well as a virtually linear increase in the fluorescence signal with concentration [42]. The deficit in the core consistency cannot be identified visually by observing the different peaks, but the core consistency can be used to find the right number of components for a model. It usually starts at 100% and declines with increasing components. The correct quantity of components can often be found before or during this decrease together with other tools such as the explained variance [42, 43].

Split-half analysis

The split-half analysis is a useful tool to validate a model, by dividing the random samples of the data set into two separate sets. These sets are then used to calculate a single PARAFAC model [43]. The result is a percentage of the similarity of the models. Randomization, which is performed more than once, can provide information on stability. This can demonstrate that the model is representative for all samples and the right components were found [43].

Maximum fluorescence intensity (F_{\max}) calculation

The maximum fluorescence intensity (F_{\max}) is calculated to obtain relative quantitative information on the variation in the different components in different samples [42, 44].

$$F_{\max}[\text{R.U.}] = \text{Score}_n \times \text{EM}_n(\lambda_{\max}) \times \text{EX}_n(\lambda_{\max}) \quad (5)$$

The score (fluorescence intensity FI) is related to the quantitative value of a component for the sample n , calculated from the PARAFAC model. $\text{EM}_n(\lambda_{\max})$ is the maximum value in the emission spectra of the PARAFAC model and $\text{EX}_n(\lambda_{\max})$ is the maximum value in the excitation spectra [42, 44]. As the EEMs were standardized to the daily Raman peak, the unit of the F_{\max} value is described as Raman units (R.U.). As the fluorescence volume is different for a specific concentration of each component as a result of different quantum yields, the F_{\max} value cannot be used to compare the concentration of different components in a

sample. It is possible that F_{\max} is higher for a component than that for another component in the same sample but with the absolute concentration being lower.

To produce further dilution effects or assess the variation of the constituents in different samples, it is useful to analyze the relative proportion of the different components in the samples [42]. Hence,

$$\text{Share Ci [-]} = \frac{F_{\max,i}[\text{R.U.}]}{\sum_{j=1}^n F_{\max,j}[\text{R.U.}]}, \quad (6)$$

where Ci and i are the components contained in a random sample and n is the total number of components.

The PARAFAC model calculation of the eight beers gave a variance explained by 99%, a core consistency of 88% and a split-half analysis of 99%. Based on the values achieved, a suitable model can be assumed.

Three primary components could be found using the model calculations and these are shown in the following Fig. 3.

The peaks of the model can be found in Fig. 3. These could be identified using the OpenFluor database [45]. The determination of component 1 as DOM (dissolved organic matter) results in three different compounds in this case, which could be identified as being similar to protein. DOM consists of aromatic and aliphatic hydrocarbons, including amide, carboxyl, hydroxyl, ketone and other functional groups. The fluorescence of DOM can be classified into two groups, of humic-like and protein-like substances [46]. The total quantity of DOM is related to the DOC (dissolved organic carbon). It is assumed that component 1 is related to phenylalanine, tryptophan and tyrosine. The second components are attributed to OC (organic matter) and DOC compounds. DOC is the portion of the TOC (total organic matter) that can pass through a 0.45 μm filter. While organic matter (OM) in a sample is assigned to the TOC, the DOM is linked to the DOC [46]. Component 2 can be associated with iso- α -acid and the phenolic compounds. The third component was identified as CDOM (colored dissolved organic matter) or DOM. This assumes that component 3 belongs to the vitamins, riboflavin from the vitamin B group in particular.

Split-half analysis

Split-half analysis is used to verify whether the model is reliable. Values ~60% are assumed as minimum [43]. The value for the split-half analysis can be taken from the calculations of the Solo + MIA program as 98.6%. It shows that the model works very reliably and can be used.

Maximum fluorescence intensity (F_{\max}) calculation

The following Table 5 gives the relative percentages of the different components in the samples.

Table 5 shows the percentage amounts as Share Ci [%]. This shows the ratios of the respective components in the samples.

Correlation calculation for the quantitative determination with Origin and ANOVA

Using Origin, statistical evaluations were performed using the calculated totals of FI and the analysis values of all beer types. There was a significant correlation ($R^2=0.63$) between the iso- α -acid concentrations of the beer types and the calculated FI from Origin (see Table 4 and Fig. 4). The graphical representation of the correlation of all beer types shows the relationship between iso- α -acid and the calculated FI. The FI was obtained from the EEM graphs by narrowing the respective extinction and emission ranges and thus calculating the amount of data.

From the calculation using the one-way ANOVA, this gave a statistical significance of the p value $< \alpha = 0.005$ (p value: 0.00408). The slope is significantly different from zero.

From the correlations of the amino acid concentrations with the FI, the following correlations were found for the three amino acids (see Table 6):

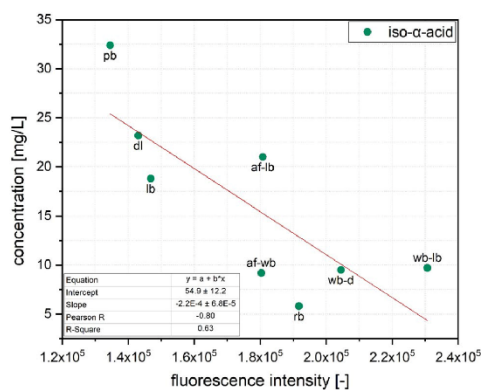
According to the literature, the aromatic amino acids phenylalanine, tryptophan and tyrosine are primarily involved in fluorescence [4, 25, 28, 31].

According to the ANOVA calculation, there was no significant correlation between the relevant amino acids and the FI of the beers despite p values $< \alpha = 0.005$ (phenylalanine $p=0.0008$; tryptophan $p=0.0009$; tyrosine $p=0.0004$). However, a relationship can be assumed based on the trend (phenylalanine: $R^2=0.38$; tryptophan: $R^2=0.44$; tyrosine: $R^2=0.45$).

If the phenolic compounds ferulic acid, coumaric acid and iso-xanthohumol are considered individually, there are no correlations with the fluorescence intensities (FI). There were also no significant correlations for the three phenolic compounds according to the ANOVA calculation (ferulic acid: $p=0.1157$; coumaric acid $p=0.0159$; iso-xanthohumol $p=0.0371$). The other phenolic compounds shall be disregarded as a result of too little correlation. The vitamin analysis also only showed slight correlation.

Table 5 Results of the calculations of components 1, 2 and 3 with the score (FI), EM, EX, F_{\max} and share Ci values with the eight beer types

	Score _n	EM _n (λ_{\max})	EX _n (λ_{\max})	F_{\max} [R.U.]	Share Ci [%]
Component 1					
Lager beer (lb)	1.09E+11	1.49E-03	2.08E-03	3.37E+09	6.99
Dark lager (dl)	1.32E+05	1.49E-03	2.08E-03	4.10E-01	0
Pilsner beer (pb)	5.63E+11	1.49E-03	2.08E-03	1.74E+09	36.17
Radler beer (rb)	2.57E+11	1.49E-03	2.08E-03	7.97E+09	16.52
Wheat beer (wb-lb)	1.66E+11	1.49E-03	2.08E-03	5.13E+09	10.64
Wheat beer dark (wb-d)	1.17E+11	1.49E-03	2.08E-03	3.63E+09	7.53
Alcohol-free lager beer (af-lb)	1.74E+11	1.49E-03	2.08E-03	5.40E+08	11.2
Alcohol-free wheat beer (af-wb)	1.70E+11	1.49E-03	2.08E-03	5.29E+09	10.96
Component 2					
Lager beer (lb)	1.18E+11	6.96E-03	2.25E-03	1.85E+09	7.55
Dark lager (dl)	1.12E+16	6.96E-03	2.25E-03	1.75E+09	7.14
Pilsner beer (pb)	8.27E+11	6.96E-03	2.25E-03	1.29E+07	52.74
Radler beer (rb)	1.39E+11	6.96E-03	2.25E-03	2.17E+09	8.84
Wheat beer (wb-lb)	1.64E+10	6.96E-03	2.25E-03	2.56E+08	1.04
Wheat beer dark (wb-d)	1.99E+11	6.96E-03	2.25E-03	3.11E+09	12.68
Alcohol-free lager beer (af-lb)	1.43E+10	6.96E-03	2.25E-03	2.23E+09	0.91
Alcohol-free wheat beer (af-wb)	1.42E+11	6.96E-03	2.25E-03	2.23E+09	9.08
Component 3					
Lager beer (lb)	3.53E+11	3.05E-02	2.65E-132	2.86E-122	13.09
Dark lager (dl)	3.13E+16	3.05E-02	2.65E-132	2.53E-122	11.58
Pilsner beer (pb)	1.12E+11	3.05E-02	2.65E-132	9.03E-123	4.14
Radler beer (rb)	5.19E+11	3.05E-02	2.65E-132	4.20E-122	19.24
Wheat beer (wb-lb)	7.25E+10	3.05E-02	2.65E-132	5.87E-123	2.69
Wheat beer dark (wb-d)	1.03E+11	3.05E-02	2.65E-132	8.30E-123	3.81
Alcohol-free lager beer (af-lb)	6.11E+11	3.05E-02	2.65E-132	4.94E-122	22.64
Alcohol-free wheat beer (af-wb)	6.16E+11	3.05E-02	2.65E-132	4.98E-122	22.82

**Fig. 4** Graphical representation of the correlation of all beer types (lager beer=lb, dark lager=dl, Pilsner beer=pb, Radler beer=rb, wheat beer=wb-lb, wheat beer dark=wb-d, alcohol-free lager beer=af-lb, alcohol-free wheat beer=af-wb) with the analysis concentrations of iso- α -acid (mg/L) and the FI [-] and statistical evaluation: Pearson R and R^2 **Table 6** Pearson R and coefficient of determination R^2 of phenylalanine, tryptophan, tyrosine

Amino acid	R	R^2
Phenylalanine	-0.62	0.38
Tryptophan	-0.66	0.44
Tyrosine	-0.67	0.45

Conclusion

Diverse fluorescing beer ingredients could be assigned using fluorescence spectroscopy based on emission and extinction ranges. Using the PARAFAC analysis, a specific model was created that identified the three main components of the fluorescing substances. These components could be qualitatively assigned to the organic substances DOM, DOC or CDOM and OC by comparing with existing database literature. Using the emission and extinction spectra, these ranges could be assigned to the three aromatic amino acids phenylalanine, tryptophan and tyrosine, iso- α -acid, phenolic compounds, and the vitamin B group. The PARAFAC model explained the fluorescence of the

eight beers with a variance of 98.7% for three components. The F_{\max} and Share Ci evaluation divided the beers quantitatively into the relative percentage amounts of the different components.

In addition, correlations to the fluorescence intensities FI could be evidenced from the EEM data by incorporating beer analyses. In particular, the correlation with the FI from Origin software could be shown for iso- α -acid ($R^2 = 0.63$). This resulted in a statistical significance of the p value $< \alpha = 0.005$ (p value: 0.00408). For the fluorescing amino acids phenylalanine, tryptophan and tyrosine, only slight correlations could be shown with the FI. There were no correlations for the phenolic compounds ferulic acid, coumaric acid and isoxanthohumol. This was also shown in the EEM spectra, as only slight differences were determined in the color ranges. The same trend was evidenced in the quantitative evaluation of the vitamins.

It can be concluded that fluorescence spectroscopy with the obtained EEM data presents a powerful measurement that offers sensitive monitoring to identify fluorescence substances in beer samples. Only general sample preparation and processing needs to be observed for beer samples. Qualitative evaluation using the PARAFAC analysis is also advantageous to identify the primary components. A quantitative evaluation appears to be difficult.

For future research purposes, additional beer analyses should be taken into account, for example, for hydroxymethylfurfural. HMF is another substance suspected of being involved in fluorescence [47]. Further, beers could therefore be investigated using fluorescence spectroscopy combined with analysis.

Acknowledgements Special thanks go to Dr. Carolin Heim from the Chair of Urban Water Systems Engineering, Garching (TUM), as we were able to carry out our measurements on the fluorescence spectroscopy there.

Compliance with ethical standards

Conflict of interest Eva-Maria Kahle, Martin Zarnkow and Fritz Jacob declare that they have no conflict of interest.

Compliance with ethics requirements The authors Eva-Maria Kahle, Martin Zarnkow and Fritz Jacob hereby confirm that this manuscript was prepared according to and follows the COPE guidelines and has not already been published nor is it under consideration for publication elsewhere. This article does not contain any studies with human or animal subjects.

References

- Steiner E, Gastl M, Becker T (2011) Die Identifizierung von Trübungen in Bier (2). *Brauwelt* 7:193–205
- Steiner E, Gastl M, Becker T (2011) Die Identifizierung von Trübungen in Bier (1). *Brauwelt* 05(06):161–166
- Steiner E, Arendt EK, Gastl M, Becker T (2011) Influence of the malting parameters on the haze formation of beer after filtration. *Eur Food Res Technol* 233(4):587–597
- Sikorska E, Görecki T, Khmelinskii IV, Sikorski M, de Keukeleire D (2004) Fluorescence spectroscopy for characterization and differentiation of beers. *J Inst Brew* 110(4):267–275
- Christensen J, Nørgaard L, Bro R, Engelsen SB (2006) Multivariate autofluorescence of intact food systems. *Chem Rev* 106(6):1979–1994
- Apperson K, Leiper KA, McKeown IP, Birch D (2002) Beer fluorescence and the isolation, characterisation and silica adsorption of haze-active beer proteins. *J Inst Brew* 108(2):193–199
- Noack D, Lachenmeier D (2019) Nachweis einer Megasphaera-Kontamination bei Schankbier mittels fluoreszenzmarkierter-types Gensonden
- Demčenko AP (2015) Introduction to fluorescence sensing, 2nd edn. Cham, Heidelberg, New York, Dordrecht, London
- Baschong W, Landmann L (2006) Fluorescence microscopy. In: Baschong W, Landmann L (Hrsg.) Cell biology Chapter 1—Fluorescence microscopy
- Huang YY, Beal CM, Cai WW, Ruoff RS, Terentjev EM (2010) Micro-Raman spectroscopy of algae. Composition analysis and fluorescence background behavior. *Biotechnol Bioeng* 105(5):889–898
- Huang Y-S, Karashima T, Yamamoto M, Ogura T, Hamaguchi H (2004) Raman spectroscopic signature of life in a living yeast cell. *J Raman Spectrosc* 35(7):525–526
- Borlinghaus RT (2016) Konfokale Mikroskopie in Weiß. Optische Schnitte in allen Farben, Berlin, Heidelberg
- Kubitschek U (2017) Fluorescence microscopy. From principles to biological applications. Weinheim
- Brand L, Johnson ML (Hrsg.) (2008) Fluorescence spectroscopy. Amsterdam
- Lakowicz JR (2010) Principles of fluorescence spectroscopy, Third edition, corrected at 4. printing. New York, NY
- Wedler G, Freund H-J (2012) Lehrbuch der physikalischen Chemie, 6., vollst. überarb. und aktualisierte Aufl. Weinheim
- Valeur B, Berberan-Santos MN (2012) Molecular fluorescence. Principles and applications, 2. ed. Weinheim
- Gordon R, Cozzolino D, Chandra S, Power A, Roberts J, Chapman J (2017) Analysis of Australian beers using fluorescence spectroscopy. *Beverages* 3(4):57
- Guilbault, G. G.: Practical fluorescence (1999)
- Ndou TT, Warner IM (1991) Applications of multidimensional absorption and luminescence spectroscopies in analytical chemistry. *Chem Rev* 91(4):493–507
- Christensen J, Ladefoged AM, Nørgaard L (2005) Rapid determination of bitterness in beer using fluorescence spectroscopy and chemometrics. *J Inst Brew* 111(1):3–10
- Friedrich W (1988) Vitamin B12 und verwandte Corrinoiden. In: Walter de Gruyter, Berlin, New York
- Gorinstein S, Goshev I, Moncheva S, Zemser M, Weisz M, Caspi A, Libman I, Lerner HT, Trakhtenberg S (2000) Intrinsic tryptophan fluorescence of human serum proteins and related conformational changes. *J Protein Chem* 19(8):637–642
- Gorinstein S, Zemser M, Vargas-Albores F, Ochoa J-L, Paredes-Lopez O, Scheeler C, Salnikow J, Martin-Belloso O, Trakhtenberg S (1999) Proteins and amino acids in beers, their contents and relationships with other analytical data. *Food Chem* 67(1):71–78
- Sikorska E, Gliszczynska-Swiglo A, Insińska-Rak M, Khmelinskii I, Keukeleire de D, Sikorski M (2008) Simultaneous analysis of riboflavin and aromatic amino acids in beer using fluorescence and multivariate calibration methods. *Anal Chim Acta* 613(2):207–217

26. Chen J, LeBoeuf EJ, Dai S, Gu B (2003) Fluorescence spectroscopic studies of natural organic matter fractions. *Chemosphere* 50(5):639–647
27. Viñas P, Balsalobre N, López-Erroz C, Hernández-Córdoba M (2004) Liquid chromatographic analysis of riboflavin vitamins in foods using fluorescence detection. *J Agric Food Chem* 52(7):1789–1794
28. Sikorska E, Górecki T, Khmelinskii IV, Sikorski M, de Keukeleire D (2006) Monitoring beer during storage by fluorescence spectroscopy. *Food Chem* 96(4):632–639
29. Duyvis MG, Hilhorst R, Laane C, Evans DJ, Schmedding DJM (2002) Role of riboflavin in beer flavor instability. Determination of levels of riboflavin and its origin in beer by fluorometric apoprotein titration. *J Agric Food Chem* 50(6):1548–1552
30. Shahidi F, Naczek M (2004) Phenolics in food and nutraceuticals. Fla. Boca Raton
31. Sikorska E, Górecki T, Khmelinskii IV, Sikorski M, Koziol J (2005) Classification of edible oils using synchronous scanning fluorescence spectroscopy. *Food Chem* 89(2):217–225
32. Narziß L, Back W (2012) Die Bierbrauerei. Band 2: Die Technologie der Würzerebereitung
33. Andrés-Lacueva C, Mattivi F, Tonon D (1998) Determination of riboflavin, flavin mononucleotide and flavin-adenine dinucleotide in wine and other beverages by high-performance liquid chromatography with fluorescence detection. *J Chromatogr A* 823(1–2):355–363
34. Lawaetz AJ, Stedmon CA (2009) Fluorescence intensity calibration using the Raman scatter peak of water. *Appl Spectrosc* 63(8):936–940
35. MEBAK (Hrsg.) (2012) Würze, Bier, Biermischgetränke (Band 2): Methodensammlung der Mitteleuropäischen Brautechnischen Analysenkommission
36. Anger H-M (2006) Brautechnische Analysemethoden. Rohstoffe
37. Convention EB (1992) *Analytica EBC. Method 9.12. 3. J Inst Brew* 98:21–22
38. Geddes CD (Hrsg.) (2018) *Reviews in fluorescence 2017*. Cham
39. Harris DC, Werner G, Werner T (Hrsg.) (2014) *Lehrbuch der Quantitativen Analyse*. Berlin
40. Bro R, Kiers HAL (2003) A new efficient method for determining the number of components in PARAFAC models. *J Chemom J Chemom Soc* 17(5):274–286
41. Stedmon CA, Bro R (2008) Characterizing dissolved organic matter fluorescence with parallel factor analysis. A tutorial. *Limnol Oceanogr Methods* 6(11):572–579
42. Murphy KR, Stedmon CA, Graeber D, Bro R (2013) Fluorescence spectroscopy and multi-way techniques. PARAFAC. *Anal Methods* 5(23):6557–6566
43. Andersen CM, Bro R (2003) Practical aspects of PARAFAC modeling of fluorescence excitation-emission data. *J Chemom J Chemom Soc* 17(4):200–215
44. Prasad M, Kumar A, Atta DK, Ramanathan L (2014) Spectrofluorometric analysis of organic matter in the Sundarban mangrove, Bangladesh
45. Lablicate GmbH 2019: openfluor data base. URL: <https://openfluor.lablicate.com/>. Abrufdatum 12.06.2019
46. Leenheer JA, Croué J-P (2003) Peer reviewed. Characterizing aquatic dissolved organic matter
47. Walmsley TA, Lever M (1982) Fluorometric measurement of furfural and 5-hydroxymethylfurfural. *Anal Biochem* 124(2):446–451

Publisher's Note Springer Nature remains neutral with regard to jurisdictional claims in published maps and institutional affiliations.

PART 4

2.5 Investigation and identification of foreign turbidity particles in beverages via Raman micro-spectroscopy

This study considers two main sources of external influences. Raman micro-spectroscopy (RMS) was used to detect, evaluate and validate filter aids, stabilizers and various microplastic (MP) particles. A suitable sample preparation was developed, membrane filters were tested, and a filtration method for isolating the individual particles was established and implemented. To identify particles with RMS and for better representation, a few particles were selected and the results were validated using cluster analysis and the similarity matrix. The different media influences were identified by analyzing particles both dry, in water and beer. The filtration residue after membrane filtration was also analyzed. A two-dimensional image scan of the particles served to determine particle homogeneity. The spectra were then recorded with single-point scans. The polyvinylpyrrolidone (PVPP) spectra in the different media showed similarities greater than 80 %, usually greater than 95 %. The cellulose spectra showed no differences between the different media, but consistently high average similarities of 94.5 %. This investigation should show that foreign particles can be detected and evaluated by RMS with suitable sample preparation and recording.

Authors/Authorship contribution:

Kahle, E-M.: Literature search, writing, review conception and design; **Zarnkow, M.:** critical review of draft, discussion of data; **Jacob F.:** Supervised the project



Investigation and identification of foreign turbidity particles in beverages via Raman micro-spectroscopy

Eva-Maria Kahle¹ · Martin Zarnkow¹ · Fritz Jacob¹Received: 1 September 2020 / Revised: 24 October 2020 / Accepted: 31 October 2020
© Springer-Verlag GmbH Germany, part of Springer Nature 2020

Abstract

Cloudiness, opalescence or a milky appearance in beverages is usually undesirable and lead the consumers to assume that the product is of lower quality. Many different types of formation and entry can lead to cloudiness and these causes can be divided into two major categories: beverage-specific, where the ingredients cause an interaction, and external influences such as process errors or particles interacting with the medium. This study considers two main sources of external influences. Raman micro-spectroscopy (RMS) was used to detect, evaluate and validate filter aids, stabilisers and various microplastic (MP) particles. A suitable sample preparation was developed, membrane filters were tested, and a filtration method for isolating the individual particles was established and implemented. To identify particles with RMS and for better representation, a few particles were selected and the results were validated using cluster analysis and the similarity matrix. The different media influences were identified by analysing the particles both dry, in water and beer. The filtration residue after membrane filtration was also analysed. A two-dimensional image scan of the particles served to determine particle homogeneity. The spectra were then recorded with single-point scans. The polyvinylpyrrolidone (PVP) spectra in the different media showed similarities greater than 80%, usually greater than 95%. The cellulose spectra showed no differences between the different media, but consistently high average similarities of 94.5%. This investigation should show that foreign particles can be detected and evaluated by RMS with suitable sample preparation and recording.

Keywords Turbidity · Beer · Beverages · Filter aids and stabilisers · Microplastic · Raman

Introduction

In addition to the turbidity that occurs due to the raw material, the colloids that cause turbidity must also be taken into account, which are caused by particles that are foreign to beer. The presence of beer-extraneous turbidity particles usually indicates errors in process control, e.g. when particles from filter aids or stabilising agents break through the filter medium due to pressure surges. In addition to filter aids and stabilisers, other particles with the potential to form turbidity can also occur in breweries [1–4]. In this context, label fibres, lubricant residues from the lids of beer cans as well as plastic abrasion or microplastics from conveyor belts, membranes, valves, pipes or seals should be mentioned. The

MP particles can cause turbidity from the product interacting with the packaging [4, 5]. With the development of new analytical methods and techniques, it is possible to analyse raw materials and food during operation. Especially in the case of beverage samples, there is usually no risk of MP being introduced via the raw materials due to the frequently filtration steps in the closed process. Instead, most particles in beverages can be attributed either to exposure through process plastic during production or to subsequent contamination as a result of unsuitable sampling and treatment methods [6]. The plastic can enter the beer during the process, e.g. through the manual addition of additives and raw materials, contaminated water in the brewhouse and fermentation cellar. It can also enter the beer during transport and storage by dissolving crown cork compound materials or PET from the wall of a plastic bottle [7, 8]. According to the definition of the National Oceanic and Atmospheric Administration, MP are plastic particles with a size of 0.1–5000 µm [9].

Inorganic substances can cause turbidity and may include filter aids that have penetrated or label residues.

✉ Eva-Maria Kahle
eva.maria.kahle@tum.de

¹ Forschungszentrum Weihenstephan für Brau- und Lebensmittelqualität, Technische Universität München, Alte Akademie 3, 85354 Freising, Weihenstephan, Germany

It is also possible for organic substances of microbiological or non-microbiological origin to impair the colloidal stability of beer [4]. Turbidity of non-microbiological origin can also be distinguished as cold turbidity, permanent turbidity and turbidity from foreign substances [10]. As is the case for non-alcoholic beverages, turbidity can occur in beer in three different ways: Particles already contained in beer or its raw materials can coagulate, and turbidity can also arise from substances introduced during beer production. Last but not least, foreign particles can enter the beer before or during filling and cause turbidity [4]. Figure 1 lists various types of turbidity and shows their origins. The overview categorises the different origins of turbidity. In this study, the beer-extraneous turbidity particles are a particular focus and will be explained in more detail in the following sections. By means of Raman micro-spectroscopy (RMS), numerous filter aids (cellulose, kieselguhr, perlite) and stabilisers (PVPP, silica gel like xerogel) as well as the most common MP particles (UP, PA, PE, PF, PMMA, PS, PVC, PP, PVDF, PTFE, PEEK, PET) were detected, evaluated and validated. At the beginning, a suitable sample was prepared with filtration equipment and a filter validation was performed to detect the foreign particles also in the liquid medium.

Materials and methods

The focus of this work is on the identification and characterisation of non-beer turbidity particles. Beer is a highly complex medium comprising more than 450 ingredients [11–14]. This complex matrix often makes the analysis of different particles difficult using Raman spectroscopy, since the substances to be analysed are often overlaid by other ingredients [15]. Therefore, it is important to establish a suitable sample preparation in advance of the analysis to solve these matrix problems. Three various filter aids and stabilisers as well as twelve plastics were analysed, which are described in detail in the following. Samples were prepared in five-fold determination ($n=5$) for the replicates.

Filter aids and stabilisers

In terms of filter aids, kieselguhr (Dicalite Speedflow), perlite (Dicalite MF2) and cellulose fibres (CelluFluxx P 50) were used as sample materials, which were provided by Erbslöh GmbH, Geisenheim. The kieselguhr used is a preparation of medium fineness. Dicalite MF2 is a medium to coarse perlite and CelluFluxx P 50 is an extra-long cellulose fibre. All preparations were stored in a dry and dark location at room temperature. Preparations from various manufacturers were used for the stabilisers. We analysed a non-regenerable

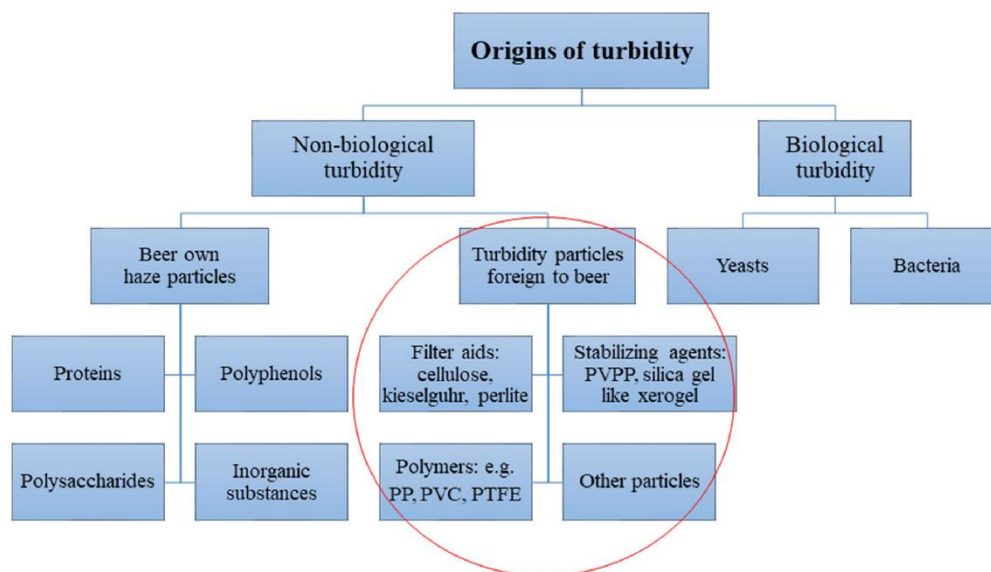


Fig. 1 Various origins of turbidity. For this investigation the turbidity particles foreign to beer are relevant

PVPP from Erbslöh GmbH, Geisenheim and used the PVPP preparation Stabiclear from Stabifix Brauerei-Technik KG and also used the silica gel Stabifix Extra. This is a hydrated xerogel. All preparations were stored in a dry place and protected from light at room temperature.

Sample preparation of filter aids and stabilisers

To investigate the influence of different media on the Raman spectra, the PVPP preparations of both manufacturers (Stabifix and Erbslöh), as well as the cellulose preparation were analysed as a dry powder, a suspension in water, a suspension in beer and as a filtration residue after membrane filtration. To prepare the suspension in water, 2 mg each of the dry PVPP and cellulose preparation was weighed and suspended in 1000 µL sterile water using a vortex mixer. The suspension in beer was prepared in the same way using beer instead of water. The beer was first decarbonised by shaking. Furthermore, a standing time of two hours before starting measurement to allow for possible enrichment of the PVPP particles with polyphenols from the beer. To analyse the filtration residue, a suspension in beer was also prepared. A suspension of 7.5 mg PVPP was suspended in 150 mL beer, which corresponds to a dose of 5 g/hL. In the case of the cellulose preparation, 37.5 mg cellulose fibres were suspended in 150 mL beer, which corresponds to a dosage of 25 mg/hL.

Polymers (MP particles)

To cover the widest possible range of plastic classes, a collection of plastic samples from PlasticsEurope Deutschland e.V. were used. PET samples in different trade forms were also provided by Forum PET for this study. Table 1 lists the plastic workpieces and shows an overview of all the examined plastic samples, product samples and materials, as well as the origin of the samples.

Sample preparation of polymers

To validate the analytical method, the existing plastic samples were crushed by rubbing them with different grades of sandpaper. The resulting spectra were stored so that the polymer spectra could be corrected if necessary. The consequential particles were then transferred to screw-top test tubes as storage containers and could be removed with a spatula if necessary. The abrasive paper was previously segmented to avoid cross-contamination of the polymer types. At the beginning, no uniform particle size distribution was required, so the plastic dusts could be used as internal quality standards. To avoid interfering signals, the sandpaper material was examined microscopically and spectroscopically. The resulting spectra were stored so that the polymer spectra could be corrected if necessary. The microplastic preparations produced in this way are shown in Fig. 2 in the sequence shown in Table 1, at fourfold magnification.

Filtration and validation

The membrane filters were cut into quarters for microscopic and spectroscopic validation of the filter surface and fixed between two uncoated slides. In doing so, alignment had to be observed so as not to confuse the front and back sides of the gold-coated membrane filters. To analyse the polymer samples on the filter surfaces, 20 mL screw-top test tubes were cleaned according to the procedure described above and stored upside down in a fume cupboard for drying until use. Subsequently, 100 mg of each of the various particle dusts was weighed into the screw-top test tubes and filled with 10.0 mL of double-distilled water [9]. The tops were screwed on to the tubes, which were suspended in a vortex mixer directly before being transferred for filtration. The vacuum pump was then switched off and the membrane filter was transferred to a slide using special tweezers.

Table 1 Analysed polymer types and their origin

Sample no.	Material	Abbreviation	Origin
1	Unsaturated polyester resin	UP	PlasticsEurope
2	Polyamide	PA	PlasticsEurope
3	Polyethylene	PE	PlasticsEurope
4	Phenolic resin	PF	PlasticsEurope
5	Polymethyl methacrylate	PMMA	PlasticsEurope
6	Polystyrene	PS	PlasticsEurope
7	Polyvinyl chloride	PVC	PlasticsEurope
8	Polypropylene	PP	Reed valve housing #1
9	Polyvinylidene fluoride	PVDF	Reed valve housing #3
10	Polytetrafluoroethylene	PTFE	valve #6
11	Polyetheretherketone	PEEK	Seat gasket #8
12	Polyethyleneterephthalate	PET	Forum PET

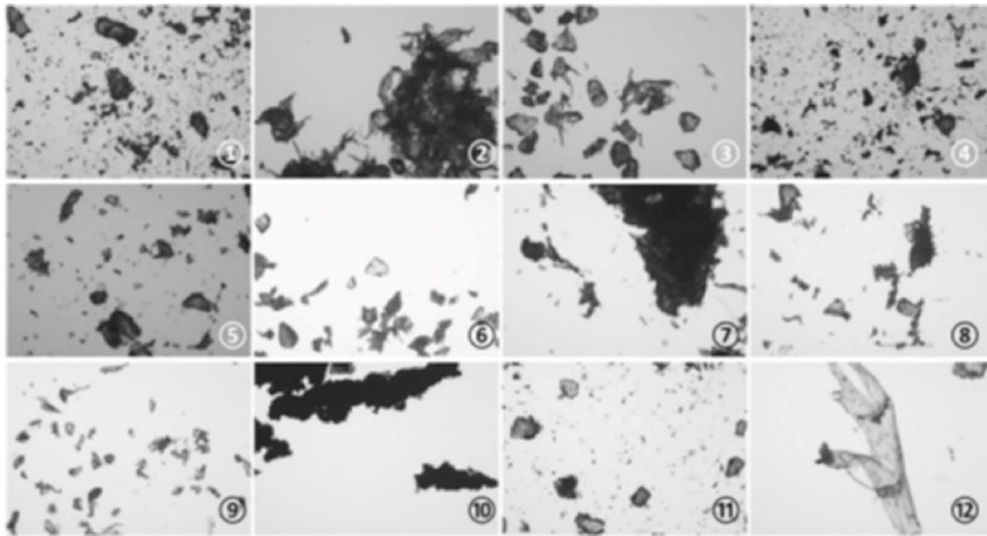


Fig. 2 Microscopic images of the plastic samples used at 4x magnification; labelling according to Table 1

To check the suitability of the membrane filters for routine analysis, all filters were examined microscopically and spectroscopically. First, the requirements for the filter membranes were checked for each filter type. For this purpose the filters were analysed for irregularities in their surface structure using bright-field microscopy with the 20 \times lens. The Raman spectra of the individual filters were then recorded. The same settings were selected as for the polymer reference spectra. The thermal stability of the filters was also qualitatively determined. To determine the maximum laser intensities and thus the thermal stability of the individual filter types and materials, Raman spectra of the filters were recorded at 2, 5, 10, 20 and 40 mW laser power. The thermal resistance was defined and validated.

Sampling and preparation

The principle of due diligence applies in particular to the process steps for obtaining and preparing samples, as well as all other steps preceding the analysis. The theoretical analysis limits of the common analysis methods for microplastics are currently between 20 μm (FTIR), 10 μm (NIR) and 1 μm (RS) [15, 16].

Evaluation of membrane filters

Some pre-analysis preparation is necessary for smaller MP particle sizes, for example, filtering the particles and

removing the sample matrix. To avoid interfering signals superimposing on the particle Raman signals, high demands are placed on the filter material and the filter parameterisation. Depending on the complexity of the sample, filter specifications and analysis parameters and smaller particle sizes can be measured.

Membrane filtration

To validate suitable filter materials and surfaces, five membrane filter types were tested from Analytische Produktions-, Steuerungs- und Controlgeräte GmbH (APC) and three membrane filter types from i3 Membrane GmbH. These eight membrane filters had different filter materials, as well as different layer thicknesses or the arrangement of the gold coating. The membrane filters were stored in the storage containers provided and protected from light and contamination. The relevant specifications of the tested filters are listed in Table 2.

The membrane filters used, however, had a diameter of 25 mm due to given test parameters. The sample preparation and a suitable filtration attachment was designed and manufactured. The requirements placed on the workpiece are listed in Table 3.

The preliminary design drawing is shown in Fig. 3. For the basic construction, standardised stainless steel components of the company Martin Wagner "WAGNERINOX" were used. Subsequently, a tapered stainless steel work

Table 2 Material, coating properties and manufacturer of the validated membrane filters

No	Description	Filter carrier material	Arrangement of the coating	Manufacturer
1	APC Thicker Type	Polycarbonate	40/20	APC GmbH
2	APC PET	Polyethyleneterephthalate	40/20	APC GmbH
3	APC Folie 1	Filter film 1	40/20	APC GmbH
4	APC Folie 2	Filter film 2	40/20	APC GmbH
5	APC PC	Polycarbonate	0/0	APC GmbH
6	I3 Trackpor Gold	Polycarbonate	40/20	i3 Membrane GmbH
7	I3 Trackpor Gold	Polycarbonate	40/0	i3 Membrane GmbH
8	I3 Flexipor	Aluminium oxide	0/0	i3 Membrane GmbH

Table 3 Requirements for membrane filtration

Requirement	Solution
Fit for Ø25 mm membrane filter	More favourable design due to standardised component
Stainless steel body	No plastic parts on the retentate part → No additional source of contamination
Smooth, non-static surface	Electrochemical properties of plastic particles → Adhesion, falsification of results
Compatibility	Can be adapted to existing membrane filtration systems
Fast filtration, few steps	Work to exclude contamination as much as possible

piece was attached to the upper part, which serves as a filling funnel and increases the maximum sample volume of the component. The individual components are placed on top of each other in sequence and fastened with a two-bar clamp. The filtration attachment was mounted on a pressure-stable vacuum bottle made by Schott AG and connected to a water jet pump made by Diagonal GmbH & Co. KG. For safety reasons, the vacuum bottle was additionally covered with a splinter protection net.

Raman micro-spectroscopy (RMS)

A Raman spectroscopy system of the model alpha300R from WiTec GmbH was connected to the confocal research microscope. Two laser units generated monochromatic light at the wavelengths 532 nm and 785 nm. These laser beams entered the microscope via two connected optical fibre cables. There, the beams were directed onto the sample and the spectroscopy detects the emitted photons. After the scattering process, the emitted photons were focused using a pinhole aperture and transmitted to the spectroscopy. Two spectroscopies were available for particle measurements, one each for a laser unit and a wavelength range. For analyses with the 532 nm laser, a UHTS series (Ultra-High Throughput Spectrometer) spectroscopy from WiTec GmbH was used. These were specially developed for high-resolution Raman spectra with short measuring times. The model used, a UHTS 300 VIS, is designed for excitation wavelengths in the visible range (approx. 450–700 nm).

When using the 785 nm laser, a spectroscopy of the model UHTS 400 NIR is used. This spectroscopy is specially adapted to the wavelength range of 650–1300 nm and thus to the near infrared range. However, since the efficiency of the CCD detectors is directly dependent on the wavelength of the laser, and the Raman signal decreases by four times the power of the laser wavelength, the acquisition of Raman spectra with the 785 nm laser requires a longer measurement time than the 532 nm laser. Furthermore, the theoretically possible resolution of the laser increases with increasing wavelength, which contradicts a quantitative analysis [17, 18]. For this reason, the 785 nm laser is not used in this paper. Gratings scatter the detected Raman signal over the CCD detectors. The number of ridges per millimetre determines the resolution of the Raman signals and the absolute measuring time. The higher the number of ridges, the higher the resolution and the longer the analysis time. With the existing system it was possible to choose between two gratings (600 and 1800 g/mm). Due to the homogeneity of the samples and the measurement duration, only the 600 g/mm grating was used. The scattered photons were then recorded by two CCD detectors from WiTec GmbH. These convert the detected photons into electrical signals and feed the software with the data of the Raman signals. By cooling down to a working temperature of -60°C , interfering signals (e.g. noise or dark current) are avoided. The standard intensity of the 532 nm laser was set at 2.0 mW and increased to 5.0 mW if necessary. The integration time per recorded spectrum

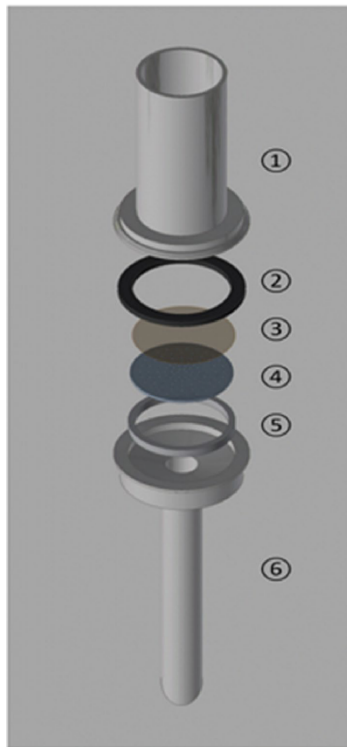


Fig. 3 Construction drawing of the filtration attachment (CAD image file): ① The upper part is composed of a stainless steel hollow cylinder (DN25) and a clamp weld-on socket ② The sealing ring provides the necessary contact pressure of the membrane filter ③ The membrane filter is inserted between the sealing ring and filter frit ④ The filter frit serves as a carrier surface for the membrane filter and defines the flow volume ⑤ The carrier ring serves as a support and fixation of the filter frit ⑥ The lower part is composed of a bevelled stainless steel hollow cylinder (DN10) and a clamp welding socket

was 0.4 s at 50 accumulations. This results in an absolute measurement duration of 20 s/particle. To obtain significant reference spectra, five individual spectra of each substance were recorded at different positions within a sample and an average spectrum was generated. Video images of each substance were stored to be able to make comparisons during later microscopic analyses. The images were acquired with the WiTec software Control 5.1, which directly links the video images with the acquired spectra. The programme also stores the position and parameters of the single spectra, line scans and image scans. During the later evaluation the video images can be combined with the spectral data and the results can be visualized.

 Springer

Data analysis and statistical evaluation

All analyses and measurements were controlled and performed with the WiTec Control FIVE 5.1 software. The quantitative data evaluation and processing was carried out by the WiTec software Project FIVE 5.1. The data material was evaluated using the software BioNumerics 7.6.3. Applied Maths N.V., Belgium. The determined average spectra of the reference samples, all spectra as well as the cluster data sets from the image scans were imported into the database and processed. A five-fold determination ($n=5$) of all analysed samples was carried out, each with three different particles in the sample. Due to the size of the particles, the five-fold determination of the samples was carried out at three different positions within a particle. Each individual spectrum was automatically formed from the mean value of ten repeated measurements using the WITec Control software.

Results and discussion

Filter aids and stabilisers

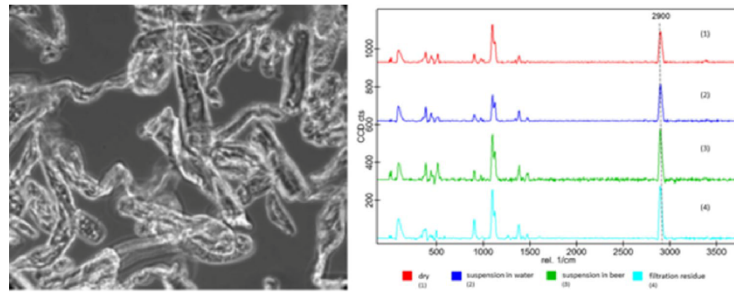
The first peak in the Raman spectra at a wavenumber of approx. 0 rel. cm^{-1} can be neglected, since this peak represents the laser [19]. For a better overview, only one of the Raman spectra from each of the five samples is shown below, unless otherwise described.

Samples containing cellulose and silicon dioxide

The cellulose fibres were analysed in dry state, as suspension in water, as suspension in beer and as filtration residue. Although cellulose fibres have no adsorption capacity, it is necessary to check the particles from the filtration residue to determine whether a change in the Raman spectra can be detected as a result of a possible deposition of beer constituents. Figure 4 shows a microscope image of the cellulose fibres at $60\times$ magnification and the corresponding spectra.

The Raman spectra of cellulose fibres show a peak at approx. $2900 \text{ rel. cm}^{-1}$. At this wave number, the C-H compounds from the hydrocarbon chains of cellulose oscillate [17, 19]. However, a characteristic oscillation frequency in the range of $2900\text{--}3500 \text{ rel. cm}^{-1}$ was found for OH groups, so that these are also reflected in the measured Raman spectra at approx. $2900 \text{ rel. cm}^{-1}$ [17]. The other peaks in the range of about $600\text{--}1500 \text{ rel. cm}^{-1}$ can generally be assigned to aliphatic hydrocarbons ($600\text{--}1300 \text{ rel. cm}^{-1}$) and organic carbon ($1300\text{--}1700 \text{ rel. cm}^{-1}$) [17, 19]. The spectra show similarities of at least 89.6% to each other. No other groups

Fig. 4 Microscope image of cellulose fibres in bright field with white light source at 60x magnification (left); Raman spectra of cellulose fibres at different sample preparations [(dry (1); suspension in water (2); suspension in beer (3); filtration residue (4) (colour-coded)], $n=10$, $\lambda=532$ nm (right)



can be identified with regard to the different sample preparations, which is also confirmed by the dendrogram shown in Fig. 5.

Figure 5 shows that, due to the high similarities across all individual spectra, no clusters are formed according to the different sample preparations. The spectra shows an average of at least 94.5% similarity to each other. Thus, although cellulose fibres in different media and states cannot be distinguished from each other, all spectra show a similar Raman spectrum. Figure 6 shows microscopic images of particles of the silica gel, kieselguhr and perlite

preparations investigated. The spectra each have a peak at approx. 925 rel. cm^{-1} and a slightly lower peak at approx. 460 rel. cm^{-1} . In the literature, oscillation frequencies at 450–550 rel. cm^{-1} and 900–1100 rel. cm^{-1} are assigned to the silicon oxides [17, 19].

Table 4 shows the SiO_2 contents of hydrated xerogel, flux-calcined kieselguhr, perlite, and borosilicate glass.

It is evident that all materials have a high proportion of SiO_2 in common. The spectra of the different materials are at least 91.2% similar to each other. The Table 4 also shows that the particle spectra in particular do not show

Fig. 5 Evaluation of Raman spectra of cellulose fibres at different sample preparations (colour-coded) using a hierarchical cluster analysis, $\lambda=532$ nm

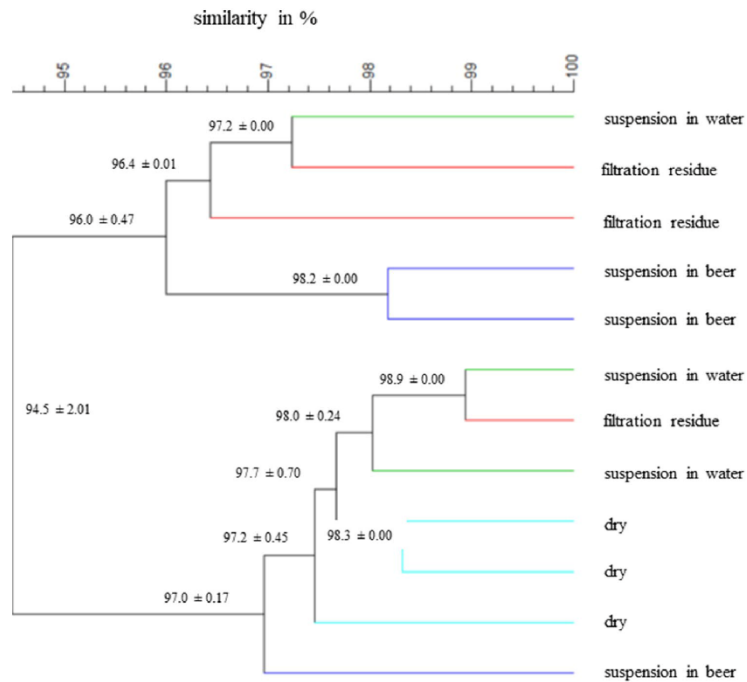


Fig. 6 Microscope images of silica gel (a), kieselguhr (b) and perlite particles (c) in bright field with white light source at 60x magnification and Raman spectra of silica gel (1), perlite (2), kieselguhr (3) and borosilicate glass (4) (colour-coded), $n = 10$, $\lambda = 532$ nm

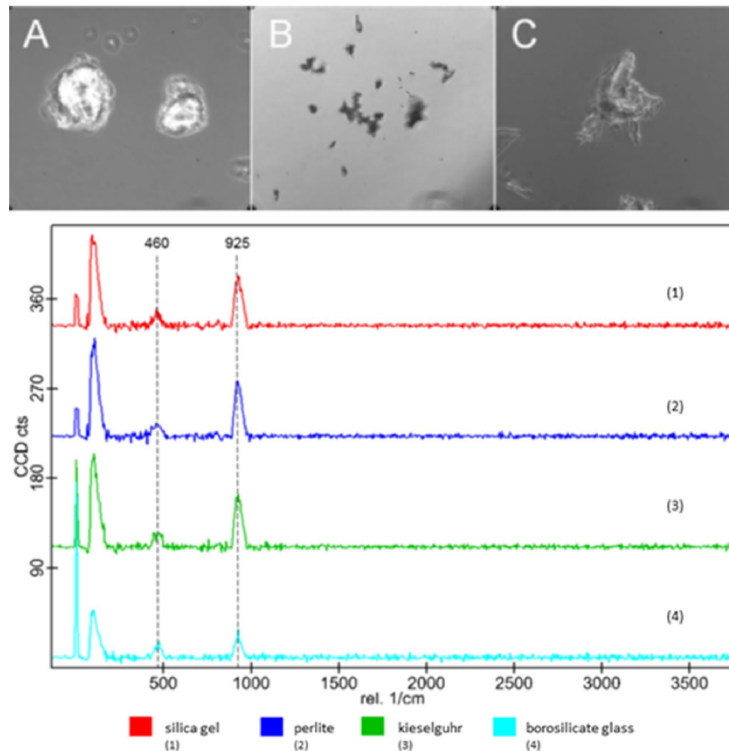


Table 4 Silicon dioxide contents of various materials in %

	SiO ₂ content [%]
Hydrated xerogel (Stabifix 2015)	55–62
Flux-calcined kieselguhr (Römpf 2007)	88–92
Perlite (Römpf 2010)	68–75
Borosilicate (Römpf 2009a)	70–80

any tendency to cluster formation. This is illustrated by the hierarchical cluster analysis, as shown in Fig. 7.

Due to the similarity of the silica gel, kieselguhr and perlite spectra to those of borosilicate glass, it is not possible to judge whether the spectra reflect the material properties of the particles or the slide. For this reason, no further analyses of these particles in different media were carried out. For future measurements, slides made of other materials such as calcium fluoride (CaF₂) should be used instead of borosilicate [20, 21].

PVPP (polyvinylpyrrolidone)

Figure 8 presents a microscope image of PVPP particles at 60x magnification and the corresponding spectrum of PVPP at different sample preparations. The microscope images show particle agglomerates of different sizes. When viewed purely optically there are no differences between the two preparations. The spectra each show a prominent peak at approx. 2930 rel. cm⁻¹, as well as a region with several consecutive peaks at approx. 700–1700 rel. cm⁻¹. The peak at approx. 2930 rel. cm⁻¹ can be assigned to the oscillations of the C–H compounds (2800–3100 rel. cm⁻¹) [19]. C–H compounds are found in PVPP both in the hydrocarbon chain as well as in the cyclic amide structure. The oscillations of the N–H compounds, as well as the carbonyl group from the amide group of PVPP, show peaks in the Raman spectrum at a wave number of about 1550–1700 rel. cm⁻¹ [17]. Especially the carbonyl group, which is usually located at approx. 1700 rel. cm⁻¹, can be identified in the spectra shown at a wavelength of approx. 1660 rel. cm⁻¹ [17, 22]. This peak is lower in the samples

Fig. 7 Evaluation of Raman spectra of silica gel, perlite, kieselguhr and borosilicate glass using a hierarchical cluster analysis, $\lambda=532$ nm

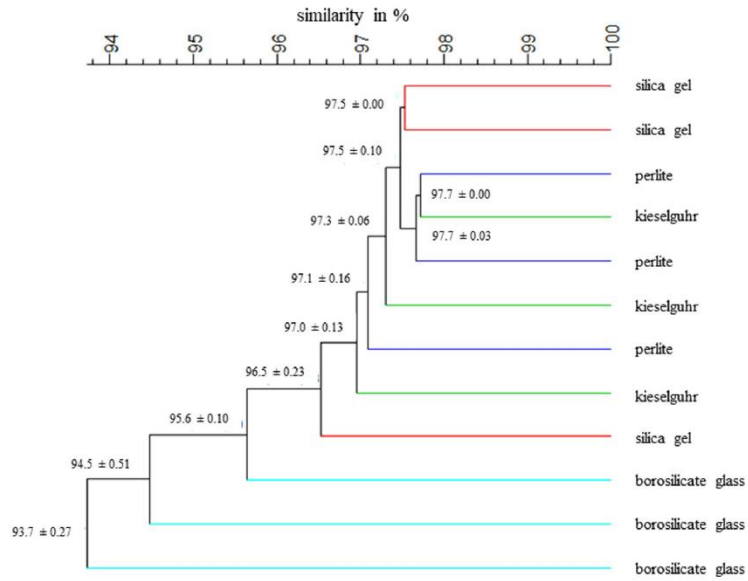
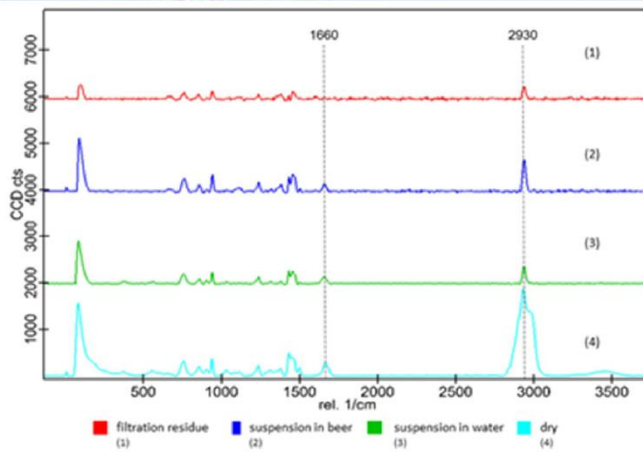
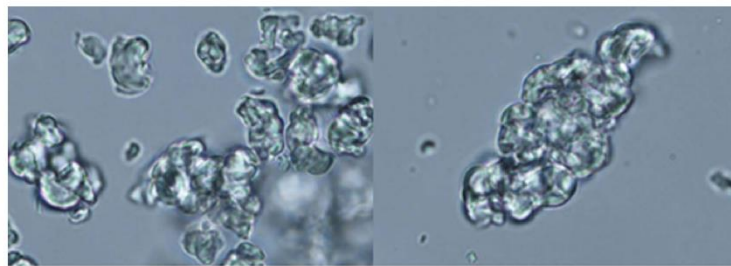


Fig. 8 Microscope images of PVPP particles in bright field with white light source at $\times 100$ magnification and Raman spectra of PVPP at different sample preparations: filtration residue (1), suspension in beer (2), suspension in water (3), dry (4) (colour-coded); $n = 10$, $\lambda = 532$ nm



from the filtration residue compared to the other samples. This could be due to a shift in charge conditions at the carbonyl group caused by the hydrogen bonds that form there with the polyphenols. The remaining peaks in the range of approx. 700–1700 rel. cm^{-1} were generally assigned in the literature to aliphatic hydrocarbons (600–1300 rel. cm^{-1}) and organic carbon (1300–1700 rel. cm^{-1}) [17, 19]. The bands below 1800 rel. cm^{-1} [19] and 1500 rel. cm^{-1} [17] also characterise the molecule as a whole. This range is also referred to as the "fingerprint" of the molecule [17, 19, 22].

Figure 8 also shows that the dry state spectrum differs from that in suspension (beer and water) and from the filtration residue. The peak at a wave number of approx. 2930 rel. cm^{-1} is particularly noticeable here, being higher and wider in the dry sample compared to the other samples. The Raman spectra of PVPP in dry state are at least 96.8% similar, whereas the similarities to the spectra of the other samples are between 51.2–59.9%. Furthermore, the spectra of the other samples also show high similarities. The spectra of samples suspended in water are at least 99.6% similar, those of samples suspended in beer at least 95.2% similar and those from the filtration residue at least 89.4% similar. Furthermore, it can be seen that the samples from the filtration residue and those suspended in beer are at least 86.7% similar and that the samples suspended in water are at least 83.0% similar to those suspended in beer. However, when

comparing the samples from the filtration residue with those from the water suspension, the spectra only show a similarity of 71.9–76.1%. This may be attributed to polyphenol adsorption by the PVPP particles. Further analyses are necessary to verify this assumption. The similarity ratios of the Raman spectra can also be determined by means of a hierarchical cluster analysis: The cluster analysis shows four clusters, each consisting of the different particle variants. As in the similarity matrix, the cluster analysis shows only a low average similarity of 56.4% for the dry particles compared to the remaining particles, whereas the clusters of the remaining PVPP particles are, on average, at least 80.7% similar.

Polymers

Five individual spectra of each polymer type were recorded at several points within a sample and an average spectrum was generated. Reference spectra for the following experiments were to be recorded and spectral series were used to determine the intensity maxima of the polymers to empirically determine and confirm the general test parameters. For a better overview, only three of the respective individual spectra of the polymers are shown in Fig. 9.

The polymer samples 1–7 and 12 were the most common types of plastic and two additional polymer types (UP and PF). Finally, it was possible to generate the spectral data of

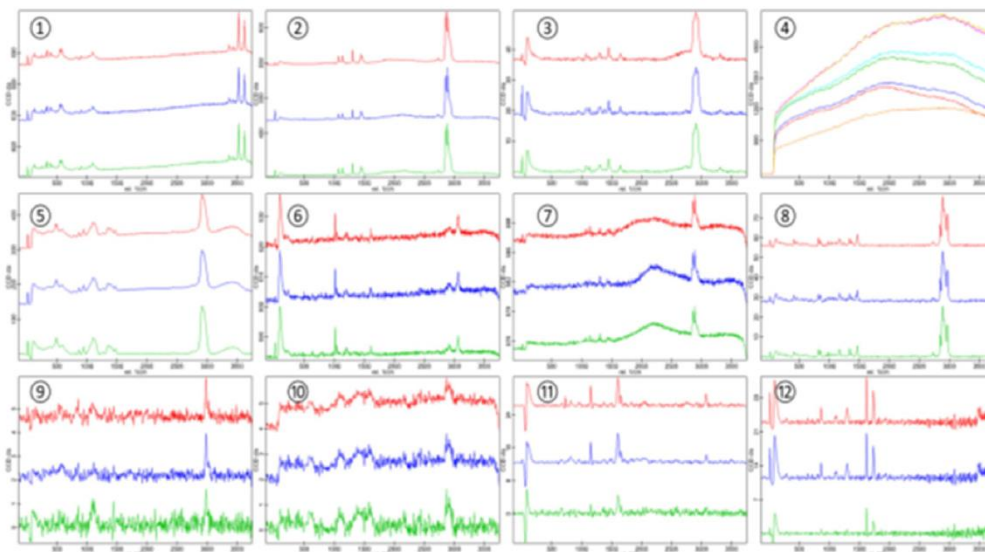


Fig. 9 Reference spectra of the polymer samples (①=UP ②=PA ③=PE ④=PF ⑤=PMMA ⑥=PS ⑦=PVC ⑧=PP ⑨=PVDF ⑩=PTFE ⑪=PEEK ⑫=PET)

all polymers except the PF sample ④. However, due to fluorescence signals, the defined experimental parameters often had to be varied and adjusted accordingly. To get an overview of the laser intensity level at which the individual polymers tended to emit fluorescence signals, the intensity spectral series of the polymers were recorded. Figure 10 shows such an iterative spectral series. Using the standard parameters, the spectrum of the examined PA sample showed strong interference signals between 1500 and 4000 rel. cm^{-1} . The laser intensity was then reduced and the number of accumulation cycles increased. The green graph shows, at 1 mW and 100 accumulation cycles, a maximum of peaks in the relevant fingerprint area at relatively low fluorescence signals. In the next iteration step (0.5 mW) the signal strength of the individual peaks decreased again, therefore the intensity optimum of this sample was set at 1 mW.

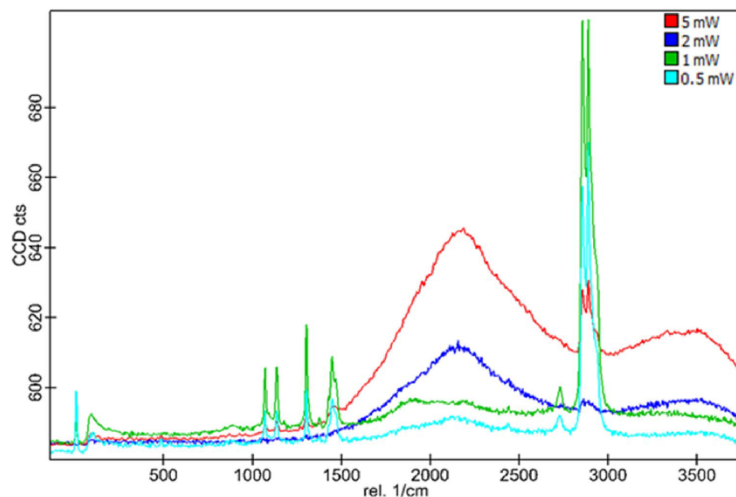
With the help of the Sub BG function of the Project FIVE 5.1 software some of the fluorescence superimposed spectra could also be restored or cleaned up. However, the identifiability of the respective substance spectra also decreased. By means of this processing function, all acquired Raman signals are attenuated down to a common baseline. The substance-specific peaks should therefore be clearly identifiable in advance. Otherwise, the signal-to-noise ratio (SNR) may be too low, resulting in unidentifiable spectra. The partial images ⑤, ⑩ and ⑫ in Fig. 10 show polymer spectra which demonstrate a very low SNR value after using the Sub BG function. In the PF sample, the interference signals could not be reduced even at the lowest intensity level of 0.1 mW and ultimately led to the fact that the reference spectra could not be recorded. On the one hand, this may be due to the deep black colour of the sample, on the other hand, it may also

be due to the unknown composition or possible additives. Specific information about the composition of the sample was not available, so this hypothesis remains unconfirmed. The microscopic examination showed no thermal damage whatsoever to the particles examined. Other samples were also dark or black in colour (e.g. PVC, PEEK) and yet the Raman spectra of these samples could be detected, even though they were very weak. It must therefore be assumed that unknown fluorophoric substances are present in the PF sample. In the end, the PF sample was the only polymer sample from which no spectra could be recorded and was therefore not investigated further in the subsequent experiments. Based on the results of the filter validations, the range of laser intensity levels to be tested was set at 0.1 to 10 mW. The recorded spectra had to be clear enough to be used to identify the polymers and at the same time not show any thermally induced impairment of the analysis results. The minimum value was set at the value at which the particle under investigation could be identified perfectly using the resulting spectrum.

Conclusion

In this study a method for the identification of particles in beverages was established, tested and validated using standard suspensions. The confocal Raman micro-spectroscopy (RMS) system served as the analytical method. To make the results reproducible and comparable, the standard test parameters were determined and tested empirically. The conception of the method included the preparation of particle standards, the design of a sampling

Fig. 10 Spectral series of the PA sample after iterative modification of the test parameters



or preparation procedure, the selection of suitable membrane filters and the validation of the measuring method. Different filter aids and stabilising agents as well as different polymer samples of the most common types of plastics and some high-performance plastics from food production were investigated. The polymers were manually comminuted to generate the spectral data of the respective substances in the dry state. These served as reference spectra in later experiments. The substance-specific peaks were compared with corresponding literature values and included in the existing database. In addition, the thermal load capacity of each polymer sample was checked by iterative intensity increase of the laser power. Based on the given experimental parameters, a filtration apparatus was designed and manufactured. Different filter types were analysed to select suitable membrane filters. These differed in the carrier material, the filter thickness and the coating of the filter surface. The sampled filters were validated on the basis of a requirement profile created from the previous literature research. The filters were tested for their tendency to emit fluorescent signals and their thermal load capacity. This also served to empirically determine the analysis parameters necessary for the automatic analysis and identification of unknown particles. During the analysis of the particle samples on the selected membrane filters, small particles within the sample were manually located and focused. Video images and image scans of these particles were created, which were then evaluated using the programme functions Cluster Analysis and True Component Analysis. During the evaluation of the data, it was noticed that mainly polymer samples that tended to emit fluorescent signals could be detected by the Cluster Analysis. These primarily included dyed and pigmented polymers that exhibited strong fluorescence signals even at low intensity. The other polymers showed higher intensities only in some subranges or at significantly stronger laser settings, which were suitable for generating average spectra. To test the suitability of the analysis and the final selection of the most suitable membrane filter type, the spectra of the polymer particles on the previously validated filters were compared with the reference spectra of the dry polymer samples and presented in similarity matrices. In conclusion, the ability to characterise foreign particles, which can cause turbidity in beverages, using RMS has been successfully established.

Acknowledgements The authors want to thank Ludwig Gerlinger and Luis Raihofer for their excellent practical and theoretical work as part of their master's theses.

Compliance with ethical standards

Conflict of interest Eva-Maria Kahle, Martin Zarnkow and Fritz Jacob declare that they have no conflict of interest.

Compliance with ethics requirements The authors Eva-Maria Kahle, Martin Zarnkow and Fritz Jacob hereby confirm that this manuscript is performed according to and follows the COPE guidelines and has not already been published nor is it under consideration for publication elsewhere. This article does not contain any studies with human or animal subjects.

References

- Basarova G (1990) The structure-function relationship of polymeric sorbents for colloid stabilization of beer. *Food Struct* 9(3):1
- Hartmann K, Kreis S, Zarnkow M et al (2004) Identifizierung von Filterhilfsmitteln nach den einzelnen Filtrationsschritten. *Der Weihenstephaner* 4:141–143
- Leiper KA, Miedl M (2008) Colloidal stability of beer. Academic Press, Burlington
- Steiner E, Becker T, Gastl M (2010) Turbidity and haze formation in beer—insights and overview. *J Inst Brew* 116(4):360–368. <https://doi.org/10.1002/j.2050-0416.2010.tb00787.x>
- Sharpe FR, Channon PJ Beer Haze Caused by Can Lid Lubricant. *Institute of Brewing* 1987(Vol. 93): 163
- OBmann BE, Sarau G, Holtmannspötter H et al (2018) Small-sized microplastics and pigmented particles in bottled mineral water. *Water Res* 141:307–316
- Kaiser W (2015) *Kunststoffchemie für Ingenieure: Von der Synthese bis zur Anwendung*. Carl Hanser Verlag GmbH Co KG
- Schymanski D, Goldbeck C, Humpf H-U et al (2018) Analysis of microplastics in water by micro-Raman spectroscopy: release of plastic particles from different packaging into mineral water. *Water Res* 129:154–162. <https://doi.org/10.1016/j.watres.2017.11.011>
- Arthur C, Baker J, Bamford H (2008) International research workshop on the occurrence, effects, and fate of microplastic marine debris. In: *Conference Proceedings*, pp 9–11
- Mastanjević K, Krstanović V, Lukinac J et al (2018) Beer—the importance of colloidal stability (non-biological haze). *Fermentation* 4(4):91
- Steiner E, Gastl M, Becker T (2011) Protein changes during mashing and brewing with focus on haze and foam formation: a review. *Eur Food Res Technol* 232(2):191–204. <https://doi.org/10.1007/s00217-010-1412-6>
- Steiner E, Gastl M, Becker T (2011) Die Identifizierung von Trübungen in Bier (1). *Brauwelt* 2011(Ausgabe 05/06): 161–166
- Steiner E, Gastl M, Becker T Die Identifizierung von Trübungen in Bier (2). *Brauwelt* 2011(Ausgabe 7): 193–205
- Steiner E, Arendt EK, Gastl M et al (2011) Influence of the mashing parameters on the haze formation of beer after filtration. *Eur Food Res Technol* 233(4):587–597. <https://doi.org/10.1007/s00217-011-1547-0>
- Kahle E-M, Zarnkow M, Jacob F (2019) Substances in beer that cause fluorescence: evaluating the qualitative and quantitative determination of these ingredients. *Eur Food Res Technol* 7(06):193. <https://doi.org/10.1007/s00217-019-03394-x>
- Erni-Cassola G, Gibson MI, Thompson RC et al (2017) Lost, but found with Nile Red: a novel method for detecting and quantifying small microplastics (1 mm to 20 μm) in environmental samples. *Environ Sci Technol* 51(23):13641–13648
- Smith E, Dent G (2005) *Modern Raman spectroscopy: a practical approach*. Hoboken, John Wiley & Sons
- Anger PM, von der Esch E, Baumann T et al (2018) Raman microspectroscopy as a tool for microplastic particle analysis. *TrAC, Trends Anal Chem* 109:214–226
- Dieing T, Hollricher O, Toporski J (2011) *Confocal raman microscopy*. Springer, Berlin, Heidelberg

20. El-Mashtoly SF, Petersen D, Yosef HK et al (2014) Label-free imaging of drug distribution and metabolism in colon cancer cells by Raman microscopy. *Analyst* 139(5):1155–1161
21. Tolstik T, Marquardt C, Matthäus C et al (2014) Discrimination and classification of liver cancer cells and proliferation states by Raman spectroscopic imaging. *Analyst* 139(22):6036–6043
22. Smith E, Dent G (2013) *Modern Raman spectroscopy: A practical approach*. John Wiley & Sons

Publisher's Note Springer Nature remains neutral with regard to jurisdictional claims in published maps and institutional affiliations.

PART 5

2.6 Identification and differentiation of haze substances using Raman micro-spectroscopy

The identification of turbidity or haze is an important part of brewery analytics. Haze can be caused by various issues throughout the brewing process and identifying the composition can pinpoint the origin. Haze analytics are commonly based on enzymatic or microscopic methods, which can be inaccurate or laborious. Raman micro-spectroscopy (RMS) presents a promising alternative for detecting haze particles. It is fast, easy to use and requires little sample preparation. Here, the applicability of RMS at 532 nm and 785 nm to identify potentially haze-forming particles has been evaluated. At 532 nm, measurements were taken using standard microscope slides. Due to the high fluorescent background of normal glass at an excitation wavelength of 785 nm, fused quartz microscope slides were used at this wavelength. Starch, arabinoxylan, cellulose, yeast β -glucan, barley β -glucan, gliadin, ferulic acid, proline, glutamine, calcium oxalate and PVPP were identified at 532 nm. The same substances when analyzed at 785 nm resulted in problems with weak carbohydrate spectra of the β -glucans and arabinoxylan. All the other substances could be analyzed at 785 nm. Catechin, which produced fluorescence noise at 532 nm could be identified at 785 nm. Although there is an issue with the intense fluorescence noise of some beer components, Raman micro-spectroscopy has great potential in haze analysis and potentially in wider brewery analyses.

Authors/Authorship contribution:

Kahle, E-M.: Literature search, writing, review conception and design; **Zarnkow, M.:** critical review of draft, discussion of data; **Jacob F.:** Supervised the project



Research article

Received: 14 July 2020

Revised: 9 September 2020

Accepted: 14 September 2020

Published online in Wiley Online Library

(wileyonlinelibrary.com) DOI 10.1002/jib.627

Identification and differentiation of haze substances using Raman microspectroscopy

Eva-Maria Kahle,*  Martin Zarnkow and Fritz Jacob

The identification of turbidity or haze is an important part of brewery analytics. Haze can be caused by various issues throughout the brewing process and identifying the composition can pinpoint the origin. Haze analytics are commonly based on enzymatic or microscopic methods, which can be inaccurate or laborious. Raman microspectroscopy (RMS) presents a promising alternative for detecting haze particles. It is fast, easy to use and requires little sample preparation. Here, the applicability of RMS at 532 nm and 785 nm to identify potentially haze-forming particles has been evaluated. At 532 nm, measurements were taken with standard microscope slides. Due to the high fluorescent background of normal glass at an excitation wavelength of 785 nm, fused quartz microscope slides were used at this wavelength. Starch, arabinoxylan, cellulose, yeast β -glucan, barley β -glucan, gliadin, ferulic acid, proline, glutamine, calcium oxalate and PVPP were identified at 532 nm. The same substances when analysed at 785 nm resulted in problems with weak carbohydrate spectra of the β -glucans and arabinoxylan. All the other substances could be analysed at 785 nm. Catechin, which produced fluorescence noise at 532 nm could be identified at 785 nm. Although there is an issue with the intense fluorescence noise of some beer components, Raman microspectroscopy has great potential in haze analysis and potentially in wider brewery analyses. © 2020 The Authors. Journal of the Institute of Brewing published by John Wiley & Sons Ltd on behalf of The Institute of Brewing & Distilling

Keywords: beer haze; identification; Raman microspectroscopy

Introduction

Beer is a complex beverage and contains an almost unlimited variety of different substances (1,2). Under certain conditions, some of these substances (Table 1) can interact chemically and physically with each other, which can lead to lasting changes in beer properties. For example, beer colour and taste can change over time. It is also possible that dissolved or suspended substances become visible and form a cloudy precipitate. Most of these reactions are undesirable and are associated with the ageing of the product. Accordingly, there is an increasing focus on the prediction and prevention of these reactions to increase the shelf life of beer. Cloudiness of the product can also be caused by other factors (3–6). The methods of analysis used for particle identification are often complex, imprecise and time consuming, and a new, rapid and reliable method would be advantageous.

The aim of this work was to verify the potential of Raman microspectroscopy (RMS) as a method for the rapid and simple particle identification of haze particles. Turbidity particles and substances related to turbidity formation in beer are excited and characterised using a Raman microscope at different excitation wavelengths for Raman scattering. In RMS, scattering molecules are excited by radiation sources with a very small frequency range. They reach higher or lower energy levels and then release part of their energy to the irradiated photons. The frequency or energy difference between exciting and emitted radiation is detected and is unique for each group of molecules. Peaks of the respective molecular groups are imaged on the frequency spectra. These 'fingerprints' can then be used to identify unknown substances (7). Problems that arise and possible solutions are presented.

Materials and methods

The focus of this work was on the identification and characterisation of particles in beer which can lead to an optical or analytically detectable haze. Beer is a complex medium comprising more than 450 ingredients (1,8). This matrix makes it difficult to analyse different particles using RMS, since the substances to be analysed are often overlaid by other ingredients (9). Accordingly, samples need extensive preparation with methods or substances that reduce fluorescence. In surface enhanced Raman scattering (SERS), the analytes are brought into direct proximity to metal nanoparticles. The electromagnetic amplification is based on surface plasmon resonance. SERS can amplify the Raman signal by up to 10^{15} (10). As a first step, different slides were examined and validated.

Slides

Before the samples were analysed, the suitability of quartz (ThermoFisher, Germany) and normal glass (Th. Geyer, Germany)

* Correspondence to: Eva-Maria Kahle, Forschungszentrum Weihenstephan für Brau- und Lebensmittelqualität, Technische Universität München, Alte Akademie 3, 85354 Freising-Weihenstephan, Germany. E-mail: eva.maria.kahle@tum.de

Forschungszentrum Weihenstephan für Brau- und Lebensmittelqualität, Technische Universität München, Alte Akademie 3, 85354, Freising-Weihenstephan, Germany

This is an open access article under the terms of the Creative Commons Attribution License, which permits use, distribution and reproduction in any medium, provided the original work is properly cited.

**Table 1.** Composition of standard beer (6,30)

Component	Concentration	Number of different substances	Origin
Water	90 – 94%	1	-
Ethanol	3 – 5% v/v	1	Yeast, malt
Carbohydrates	1 – 6% w/v	approx. 100	Malt
Carbon dioxide	3.5 – 4.5 g/L	1	Yeast, malt
Inorganic salts	500 – 4000 mg/L	approx. 25	Water, malt
Total nitrogen	300 – 1000 mg/L	approx. 100	Yeast, malt
Organic acids	50 – 250 mg/L	approx. 200	Yeast, malt
Higher alcohols	100 – 300 mg/L	80	Yeast, malt
Aldehydes	30 – 40 mg/L	approx. 50	Yeast, hop
Esters	25 – 40 mg/L	approx. 150	Yeast, malt, hop
Sulphur compounds	1 – 10 mg/L	approx. 40	Yeast, malt, hop
Hop derivatives	20 – 60 mg/L	> 100	Hop
Vitamin B compounds	5 – 10 mg/L	13	Yeast, malt

slides as substrates for RMS was evaluated. For this purpose, spectra described by the slides were recorded and compared ($n = 5$).

Preparation of gold indium tin oxide slides for SERS

Special slides for SERS according to Shan et al. (11) were required, some of which were produced in-house. Glass slides coated with the semiconductor material indium tin oxide were purchased. Furthermore, a 1% (w/v) solution of sodium citrate, a 30 mM silver nitrate solution and a 10 mM ascorbic acid solution were prepared. For germ synthesis, 25 mL of chloroauric acid germ solution and 25 μ L 1 M hydrogen chloride was heated to boiling in a 100 mL Erlenmeyer flask, then 3.75 mL of the sodium citrate solution was added. 1 mL of silver nitrate and 500 μ L of ascorbic acid solution was then added simultaneously. If prepared correctly, the colour of the suspension turns from red to blue.

Production of turbidity particles from forcibly aged beer

A pale export beer was used to produce forcibly aged beer samples. The beer was filtered but not treated with PVPP. The beer was incubated at 60°C for four weeks to produce haze. In a second batch, hydrogen peroxide (2 mL) was added to the beer. The bottle (0.5 L) was then resealed and incubated for two weeks. After the incubation period, both beer samples were cooled to room temperature, transferred to a 2 L glass bottle and degassed by shaking by hand. 400 mL of each sample was cooled and split into 8 \times 50 mL centrifuge tubes and centrifuged at 1683 g for 5 min (Centrifuge Z 366 K). The pellets were then combined, washed twice with distilled water and centrifuged at 1683 g for 5 min. The washed pellet was transferred to a glass flask and dried at 50°C water temperature in a vacuum rotary evaporator.

Preparation of polyphenolic extract from beer

Haze relevant polyphenols were isolated from a light export beer using a Discovery DPA 65 SPE column (Supelco, USA) according to Dvorakova et al. (12). The column contains a polyamide resin which selectively adsorbs -OH groups of phenolic substances, which are present in an aqueous or methanolic solution. Before extraction, the beer was degassed by manually shaking in a 2 L glass bottle. The column was filled with 5 mL methanol and then with 10 mL distilled water. 100 mL of the beer was acidified with 36% (v/v)

hydrochloric acid to pH 1.5 and passed through the column. The bound phenolic substances were then eluted with acetone (12 mL) and collected in a round bottom flask. The eluate was dried in a rotary vacuum evaporator at 50°C.

Production of protein extract from beer

A tannin precipitation was used to extract the haze relevant proteins from beer (13). Beer (180 mL) was degassed by shaking and then mixed with 20 mL of 2% (v/v) tannin solution. The mixture was incubated for 1 h at 10°C. The resulting suspension was divided into 50 mL centrifuge tubes and centrifuged at 1683 \times g for 5 min (Centrifuge Z 366 K). The pellets were combined, distilled water was added, and the samples were re-centrifuged. The pellet was suspended in 20 mL of 0.3% (v/v) caffeine solution to separate protein and tannin (14), stirred and incubated for 10 min. The suspension was centrifuged for 10 min at 1683 \times g and the pellet discarded. The protein in the supernatant was dried in a rotary vacuum evaporator at 50°C.

Production of protein-polyphenol complex

Beer like protein-polyphenol complexes were produced with gliadin as the protein and tannin as the polyphenol component. Gliadin was dissolved in water and then precipitated with tannin at a gliadin:tannin ratio of 3:1. The resulting suspension was centrifuged at 1683 \times g for 5 min (Centrifuge Z 366 K). The pellet was re-suspended twice with distilled water, centrifuged and dried at 50°C in a rotary vacuum evaporator.

Generation of artificial beer turbidity

To produce artificially clouded beer samples, insoluble substances were suspended in beer (50 mL). The concentration of the substances are shown in Table 2 and were selected so that haze was clearly visible to the naked eye. Before processing, the preparations were incubated for at least 15 minutes.

Extraction of haze substances from artificially clouded beer

To extract haze particles from artificially hazy beer, the samples were transferred to 50 mL centrifuge tubes and centrifuged for 10 min at 748 \times g (Centrifuge Z 366 K). The resulting pellet was



Identifying haze substances using Raman microspectroscopy

Table 2. Selected suspended solids added to beer

Substances	Concentration (g/50 mL)
PVPP	0.05
Starch	0.25
Yeast β -glucan	0.005
Barley β -glucan	0.005
Arabinoxylans	0.01
Calcium oxalate	0.05
Cellulose	0.05

treated twice with distilled water and centrifuged again. The pellet was washed with 1 mL distilled water into a 1.5 mL reaction tube and centrifuged for 10 min at 21,382 x g (benchtop centrifuge Mikro 200). The supernatant was removed and discarded. The pellet was dried for 2 h at 60°C in a thermal mixer (Eppendorf, Hamburg).

RMS

A Raman spectroscopy system, model alpha300R from WiTec GmbH, was connected to a confocal microscope. Two laser units generated monochromatic light at the wavelengths 532 nm and 785 nm. These laser beams entered the microscope via two connected optical fibre cables. Two spectroscopes were available for particle measurements, one each for a laser unit and wavelength range. For analyses with the 532 nm laser, a UHTS series spectroscope from WiTec GmbH was used. These were specially developed for high-resolution Raman spectra with short measuring times. A UHTS 400 NIR spectroscope was used for the 785 nm laser. Gratings scatter the detected Raman signal over the CCD detectors. The number of ridges per millimetre determined the resolution of the Raman signals and the absolute measuring time. These convert the detected photons into electrical signals and feed the software with the data of the Raman signals.

Raman spectra 532 nm

The measurements of the Raman spectra at 532 nm were performed as described above. The spectrometer was operated with the spectral centre at 2050 rel. cm^{-1} . The burr settings were G1: 600 g mm^{-1} and BLZ = 500 nm. The prepared slides were placed with the sample side down on the microscope stage and fixed with metal clamps. The 40x objective was used to search for and focus on particles. The entire measurement took 100 seconds divided into 100 accumulations each with 1 s exposure time.

Verification of pure substance spectra at 532 nm

The spectra of the pure substances recorded by Raman microspectroscopy at 532 nm were verified using literature data and databases (9,15,16). In addition, cluster analysis was used check that the spectra correlated with each other and where $n=5$.

Data analysis

All analyses and measurements were controlled and performed using WiTec Control FIVE 5.1 software. Quantitative data evaluation and processing was carried out using the WiTec software Project FIVE 5.1. The spectra were identified using the KnowItAll

software (BioRad, USA), and data material was evaluated using the software BioNumerics 7.6.3, Applied Maths N.V., Belgium and Origin 2019b, OriginLab, USA.

Results and discussion

Slides

Slides and cover glasses of conventional glass and pure quartz were tested for their suitability for Raman analysis. Both materials consist of silicon dioxide, with additional minerals being added to conventional glass during manufacturing. Figure 1 shows Raman spectra of glass and quartz slides at 532 nm. Although there are similarities, there are significant differences in the spectra of the two materials. Both materials show different, broad peaks from 0–1200 rel. cm^{-1} , with those of glass being particularly pronounced between 600 and 1200 rel. cm^{-1} . The use of a confocal microscope in Raman microscopy can help to minimise these peaks, since the focus is not on the slide but on the sample itself. In addition, the intense peaks of the slides do not significantly disturb the fingerprint region of the spectrum. The spectra of glass and quartz were reproducible in five repeat scans. For reasons of cost and sample preparation, all measurements at an excitation wavelength of 532 nm were performed using glass.

However, a different picture emerges for measurements at 785 nm (Figure 2). In Raman analyses at an excitation wavelength of 785 nm, the glass slides showed a strong fluorescence band between 1000 and 2200 rel. cm^{-1} . Strong fluorescence can superimpose over peaks and thus compromise the Raman spectrum. Fluorescence also occurs when the laser is focused exclusively on the sample. Due to the strong fluorescence using conventional glass slides, only quartz slides were used at 785 nm. The spectra were easily reproducible confirming the work of Tuschel (17).

Spectra of pure substances at 532 nm: starch, wheat arabinoxylan and ferulic acid

High molecular weight starch is a potent haze agent that can be found in beer through insufficient mashing or over-heating. The identification of starch as a cause of turbidity can be an important step in process optimisation. The spectrum recorded at the excitation wavelength of 532 nm (Figure 3) was identified as soluble starch with 96.8% agreement using the KnowItAll database software (Bio-Rad, USA). The spectra of the five different preparations showed a very high similarity, which suggests good reproducibility. In contrast, arabinoxylan only plays a minor role in haze formation, but if malting or mashing is inadequate, an increased arabinoxylan concentration can lead to turbidity in beer or to filtration problems (4,18). In addition, the phenolic compound - ferulic acid - can be found in haze particles, although it is not considered a major contributor (19). Arabinoxylan showed a weak Raman signal with difficult-to-differentiate peaks, which was characterised by some diversity in the five scans (Figure 3). The research of Philippe et al. (16) showed that the Raman spectra of arabinoxylan from wheat are subject to fluctuation depending on the stage of development and the cell layer from which the material originates. This is partly due to the varying composition of arabinoxylan, which is composed of arabinose and xylose units. However, the spectra recorded here show a strong optical correlation to the data published by Philippe et al. (16). If the arabinoxylan originates from the aleurone layer of the wheat grain, peaks at 1630 rel. cm^{-1} and 1603 rel. cm^{-1} also clearly show phenolic components that indicate

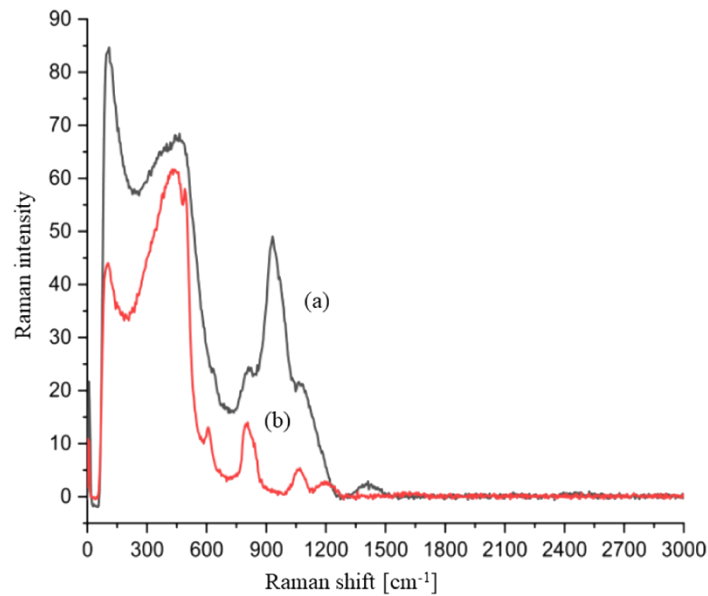


Figure 1. Raman spectra of glass (a) and quartz (b) slides at 532 nm ($n=5$); The spectrum was recorded at 50 mW laser intensity in 100 accumulations with an exposure time of 1 s each over a wave range of 0–3000 rel. cm^{-1} . The two spectra are clearly similar, but the spectrum of the quartz is weaker with differences between 600 and 1200 rel. cm^{-1} . [Colour figure can be viewed at wileyonlinelibrary.com]

the linkage of the arabinoxylan with ferulic acid (16). These peaks cannot be found in Figure 3, since the material used was purified. However, the peaks noted above are visible in the ferulic acid spectrum. This spectrum could be identified by the database algorithm with agreement of 98.9%. Furthermore, the five replicates show a high similarity to each other, which suggests that the identification

of ferulic acid is highly reproducible with the Raman microspectroscopy. Using the results of Philippe et al. (16), it is also possible to identify ferulic acid linked to arabinoxylan, a form that occurs naturally in cereals.

β -glucan

In most cases, the occurrence of β -glucans in beer, which include cellulose, yeast β -glucan and barley β -glucan, have various causes. Cellulose can enter beer via filter breakthrough of filtration aid. Yeast β -glucan in beer originates from the yeast cell wall. Barley β -glucan reflects inadequate malting or mashing. It is important to identify these substances in order to identify the possible origin. The Raman spectrum of cellulose (Figure 4) showed an agreement of 96.7% with the reference spectrum. Furthermore, cellulose showed a high uniformity in the five replicates, which confirms good reproducibility of identification by Raman microspectroscopy.

Comparison of the cellulose spectrum with the two β -glucans, showed a similar spectra (Figure 4). This is probably due to the structural similarity of the substances. However, there is a clear difference in the peak at about 1100 rel. cm^{-1} , which is much more defined in the case of cellulose. While the yeast β -glucan spectra were highly reproducible in the experiment, the barley β -glucan spectra were poorly reproducible. In addition to possible impurities in the sample, this may be due to the very weak Raman signals of individual samples, which were neglected by the clustering algorithm. However, the two different groups that correlate with each other can be clearly seen but there is no rapid method to distinguish yeast from barley β -glucan. However, the separate observation of the wave range of 1000–1200 rel. cm^{-1} showed in all five

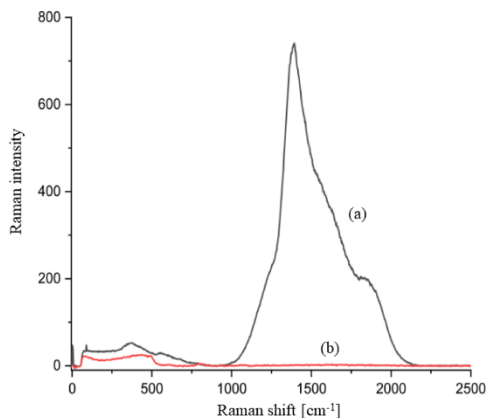


Figure 2. Raman spectra of glass (a) and quartz (b) slides at 785 nm ($n=5$); The spectrum was recorded at 80 mW laser intensity in 100 accumulations, with an exposure time of 1 s each over a wave range of 0–3000 rel. cm^{-1} . The two spectra differ significantly. The intense fluorescence between 1000 and 2200 rel. cm^{-1} is clearly visible. [Colour figure can be viewed at wileyonlinelibrary.com]



Identifying haze substances using Raman microspectroscopy

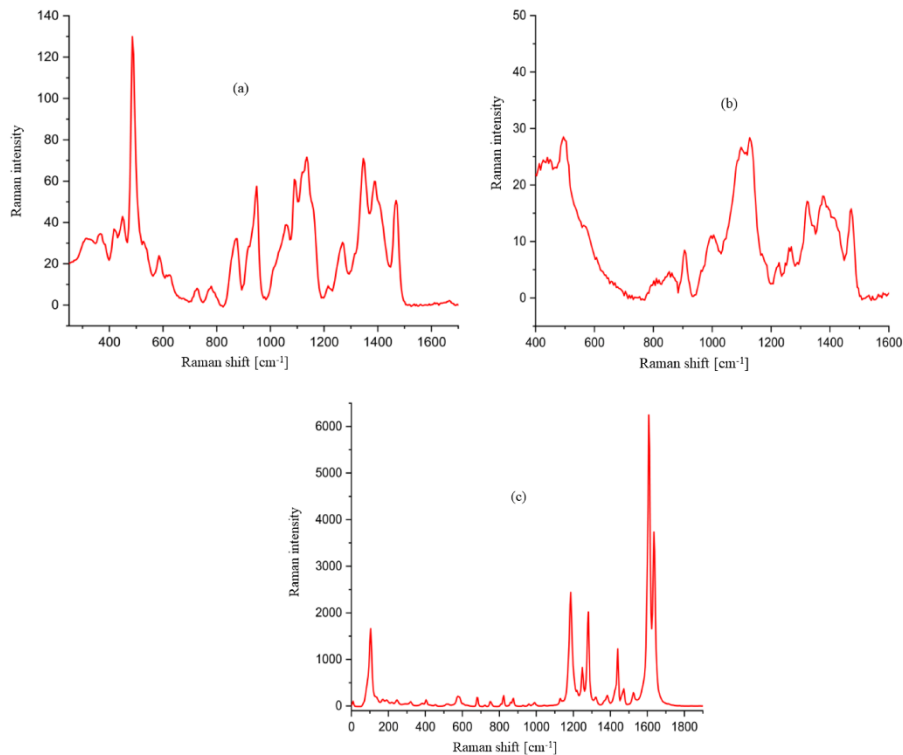


Figure 3. Raman spectrum of starch (a) at 532 nm ($n=5$); The spectrum was recorded at 50 mW laser intensity in 100 accumulations with an exposure time of 1 s each. The wave range shown is from 250–1700 rel. cm^{-1} . Raman spectrum of wheat arabinoxylan (b) at 532 nm ($n=5$); The spectrum was recorded at 50 mW laser intensity in 100 accumulations with an exposure time of 1 s each. The wave range from 400–1600 rel. cm^{-1} is shown. Raman spectrum of ferulic acid (c) at 532 nm ($n=5$); The spectrum was recorded at 30 mW laser intensity in 100 accumulations with an exposure time of 1 s each. The wave range from 0–1900 rel. cm^{-1} is shown. [Colour figure can be viewed at wileyonlinelibrary.com]

repeat measurements a differing shoulder height of the double peak, which both β -glucan types show in this range (Figure 5). Barley β -glucan shows a peak in the higher wave number range with a less intense shoulder than in the lower wave number range. This is reversed for barley β -glucan. This phenomenon is also confirmed by previous spectra of the different β -glucans (15, 20). This small difference in the spectra could be useful in the rapid differentiation of the two substances.

Gliadin and catechin

Although gliadin and catechin are not by themselves haze particles, they are the basis for protein-polyphenol turbidity. Gliadin is a protein fraction of wheat (equivalent to hordein in barley), which has a high content of the amino acids, glutamine and proline. Catechin is a phenolic substance frequently found in beer, which forms di- or trimers, referred to as oligomeric proanthocyanidins. These two substances are capable of forming insoluble haze particles by cross-linking with each other (4). The identification of these particles is a helpful tool to find the origin of haze in the brewing process and to target possible solutions for solving such a problem.

The spectrum of the pure gliadin fraction recorded by RMS showed a weak signal with many small and broad peaks (Figure 6). The KnowItAll algorithm was able to assign the spectrum with 98.1% agreement to zein, the equivalent of the gliadin fraction in maize, and with 96.3% agreement to human hair, which is composed of proline and 4-hydroxy-proline.

Zhu et al. (21) showed that the amino acid proline (among other amino acids) can be identified from a protein spectrum. Conversely, it might be possible to identify proteins and polypeptides with a high proline or glutamine content by means of the corresponding amino acid spectra. The Raman spectra of the amino acids proline and glutamine show very clearly defined peaks (Figure 6). Both spectra were clearly identified by the database algorithm (proline 83.2%; glutamine 96.6%). The spectra of both amino acids were reproducible, but with proline showing some deviations in measurement.

This is most likely due to the sample material used. In this work, a racemic mixture of the two enantiomers D-proline and L-proline was used. The Raman spectra of enantiomers can be distinguished from each other. Thus, Raman spectroscopy can be a simple method to differentiate between enantiomers that are otherwise difficult to distinguish (22). Glutamine and especially proline are binding partners of catechin and its polymers in the formation of



E.-M. Kahle et al.

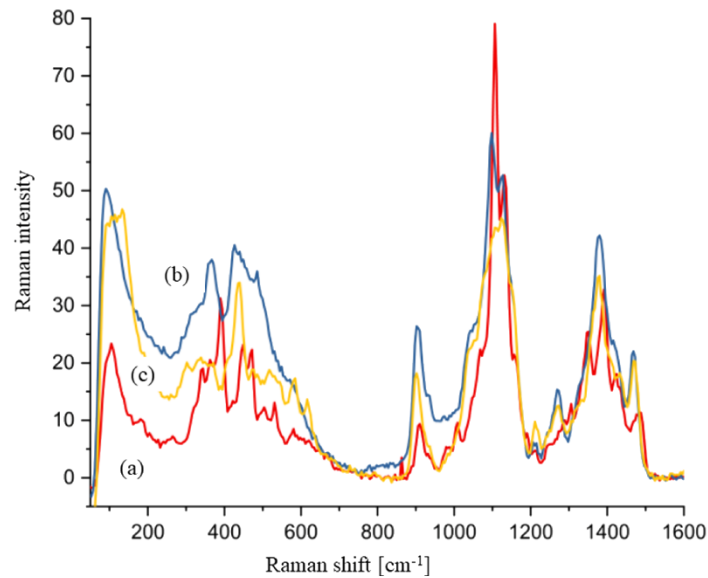


Figure 4. Raman spectra of cellulose ((a), red), barley β -glucan ((b), blue) and yeast β -glucan ((c), yellow) compared at 532 nm ($n=5$); The spectra were recorded at 50 mW laser intensity in 100 accumulations with an exposure time of 1 s each and show the wave range from 50–1600 rel. cm^{-1} . The three spectra show a very high similarity. However, the intense cellulose peak at about 1100 rel. cm^{-1} , which distinguishes cellulose from the other β -glucans, is clearly visible. Other, but much less marked differences can also be seen. [Colour figure can be viewed at wileyonlinelibrary.com]

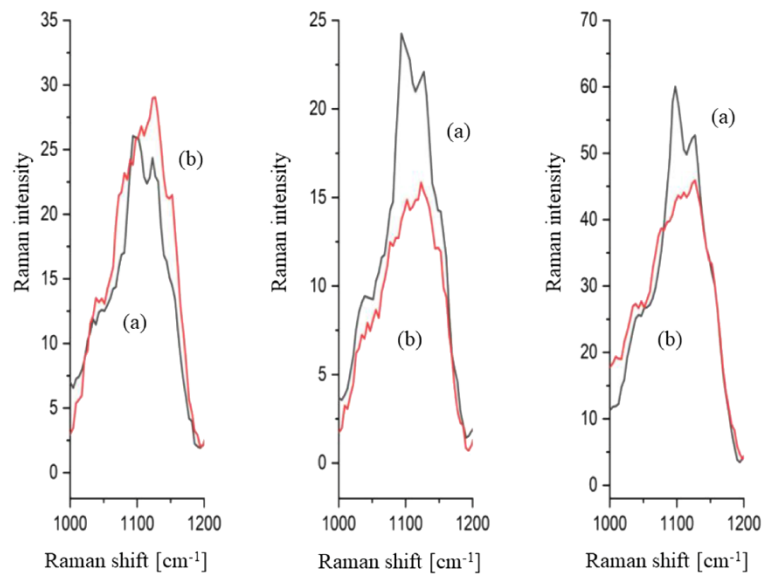


Figure 5. Difference in Raman spectra of barley β -glucan and yeast β -glucan at 532 nm ($n=5$); The spectra were recorded at 50 mW laser intensity in 100 accumulations with an exposure time of 1 s each and show the wave range from 1000–1200 rel. cm^{-1} . It can be clearly seen that the double peak in barley β -glucan ((a), black) has a higher intensity in the lower wave range and in yeast β -glucan ((b), red) in the higher wave range. [Colour figure can be viewed at wileyonlinelibrary.com]



Identifying haze substances using Raman microspectroscopy

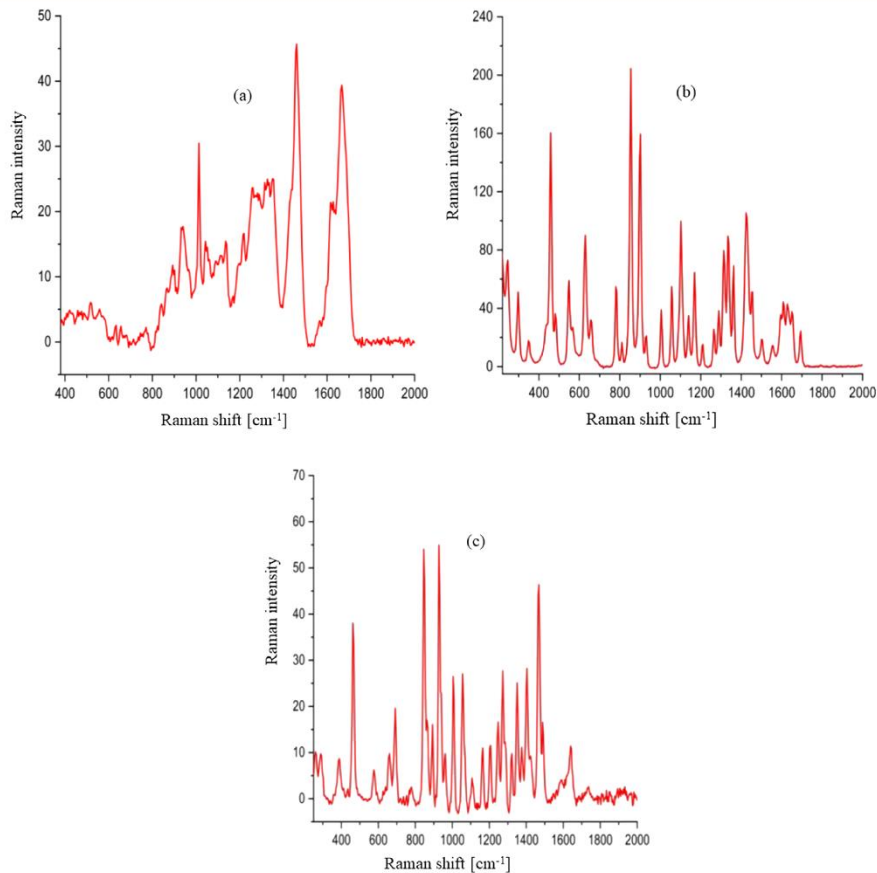


Figure 6. Raman spectrum of gliadin (a) at 532 nm ($n=5$); The spectrum was recorded at 50 mW laser intensity in 100 accumulations with an exposure time of 1 s each. The wave range from 400–2000 rel. cm^{-1} is shown. Raman spectra of L-glutamine (b) and D/L-proline (c) at 532 nm ($n=5$); The spectra were recorded at 50 mW laser intensity in 100 accumulations with an exposure time of 1 s each and show the wave range from 280–2000 rel. cm^{-1} . [Colour figure can be viewed at wileyonlinelibrary.com]

insoluble protein-polyphenol complexes. However, it is very difficult to identify catechin using RMS at 532 nm partly due to the fluorescence signal that completely overlays the weak Raman spectrum. Another problem is even small amounts of fluorescent polyphenols are sufficient to make Raman measurements of protein-polyphenol complexes impossible. The Raman spectrum of the catechin recorded in this work is completely superimposed by fluorescence and therefore has no value. Importantly, it was also impossible to investigate the haze particles produced by the forced ageing of beer due to the fluorescence that occurs.

PVPP

In beer stabilisation, it is important to minimise the protein-crosslinking polyphenols, typically catechin and its polymers, which can cause problems in beer. Polyvinylpyrrolidone (PVPP) is used to remove these polyphenols. The structure of PVPP imitates the amino acid proline or a polyproline peptide which is

frequently found in proteins that cause turbidity and to which catechin binds during haze formation (23). However, PVPP itself can also contribute turbidity by entering the beer stream from filter breakthrough. PVPP as a pure substance provides a good Raman spectrum with clearly differentiated peaks (Figure 7). The PVPP showed 98.6% agreement with the reference spectrum from the database and reproducibility of the spectra. PVPP can be identified with a high degree of certainty using the Raman microscope.

Calcium oxalate can lead not only to particles in beer, but also to other phenomena such as gushing (24). The Raman spectra recorded by calcium oxalate showed clearly separated, narrow peaks and thus good spectra, which could be clearly identified at 98.4% agreement with the reference spectrum (Figure 7). Despite the intense spectra, the measurement of calcium oxalate was poorly reproducible. All spectra showed similar peaks, but there were always small differences. Nevertheless, each spectrum could be clearly identified as calcium oxalate, which occurs in different hydrations. The spectra of monohydrate and dihydrate differ slightly.

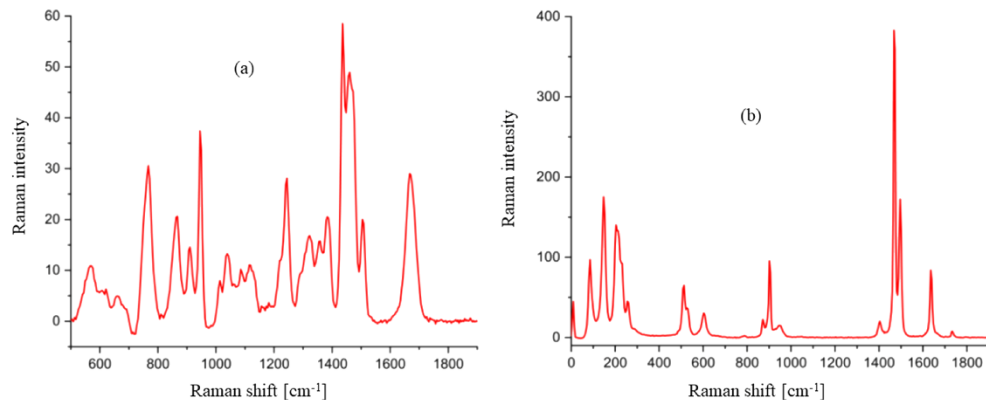


Figure 7. Raman spectrum of PVPP (a) and calcium oxalate (b) at 532 nm ($n=5$); The spectrum was recorded at 50 mW laser intensity in 100 accumulations with an exposure time of 1 s each. The wave range from 0–2000 rel. cm^{-1} is shown. [Colour figure can be viewed at wileyonlinelibrary.com]

The peak at about 1480 rel. cm^{-1} is particularly striking and a narrow double peak for monohydrate and a single peak for dihydrate (25).

Spectra of pure substances at 785 nm

The spectra of pure substances recorded by RMS at 785 nm were also verified by means of literature data and databases (9,15,16). In addition, the correlation of the five repeated spectra was checked by cluster analysis. If the spectra were comparable with the results obtained, these results are not discussed any further. However, in general, recording spectra at an excitation wavelength of 785 nm takes considerably more time, is technically difficult, and requires an optimised laser focus. The spectra are also much weaker in most cases.

Conclusions

This work shows that RMS can be a useful method for the identification and differentiation of various haze substances. Most of the particles can be detected by excitation wavelengths at 532 nm even after contact with beer. In some cases, the use of an alternative wavelength (785 nm) can be advantageous. For the full range of haze particles in beer to be covered, it is required to minimise the autofluorescence of some haze particles or to bypass background fluorescence. Particles with complex and unknown composition recovered from beer caused major problems in this respect. The identification and differentiation of particles by means of peak matching-based cluster analysis can cause problems that can be quickly detected by visually inspecting the spectra. If visual inspection of the data is dispensed with, an alternative is the use of a database algorithm that compares the spectra with reference spectra on the basis of different characteristics.

Raman microspectroscopy is a useful extension to conventional turbidity analysis. In particular, the differentiation of structurally closely related carbohydrates is comparatively easy with this method. As studies show, RMS can be used to detect and identify particles and a wide variety of microorganisms (26–29). In combination with a complete turbidity analysis, a considerable proportion

of brewery and beverage analysis could be carried out with RMS, using one instrument and without extensive sample preparation. However, to achieve this goal, it is necessary to eliminate the fluorescence problems that occur with some substances and in biological material. Furthermore, a way must be found to distinguish and identify spectra with high statistical significance. This creates the need for establishing a corresponding spectra database.

The haze material extracted from forcibly aged beer could not be analysed due to the variety of organic components and the resulting fluorescence. Should it be possible to reduce this fluorescence, it might be possible to determine the components of the particles by Raman analysis. For this purpose, however, the spectra of the pure substances contained in the haze particles must be known in order to interpret the mixed spectra of the haze substances. Due to the heterogeneity of haze particles in different beers, it will be necessary to investigate the influence of the different chemical components on the mixed spectrum of haze particles. For this purpose, artificial particles with different compositions could be produced and examined in preliminary tests. At the moment, RMS must be regarded as a method for large laboratories, as the equipment requires substantial acquisition costs. However, the cost of a single analysis are comparatively low due to the uncomplicated sample preparation and the short time required. Should it be possible to automate Raman analysis with automatic particle recognition, it could evolve into a high-throughput method.

Author contributions

Eva-Maria Kahle: conceptualisation, methodology, validation, formal analysis, investigation, writing – original draft, visualisation. Martin Zamkow: writing – review and editing, supervision. Fritz Jacob: supervision

Acknowledgements

The authors want to thank Joseph Heintges for his excellent practical and theoretical work as part of his Master's thesis. Open access funding enabled and organized by Projekt DEAL.



Identifying haze substances using Raman microspectroscopy

Conflict of interest

The authors declare there are no conflicts of interest.

References

- Steiner E, Arendt EK, Gastl M, Becker, T. 2011. Influence of the malting parameters on the haze formation of beer after filtration. *Eur Food Res Technol* 233:587-597. <https://doi.org/10.1007/s00217-011-1547-0>
- Steiner E, Gastl M, Becker, T. 2010. Turbidity and haze formation in beer - insights and overview. *J Inst Brew* 116:360-368. <https://doi.org/10.1002/j.2050-0416.2010.tb00787.x>
- Bamforth CW. 2017. Progress in brewing science and beer production. *Annu Rev Chem Biomol Eng* 8:161-176. <https://doi.org/10.1146/annurev-chembioeng-060816-101450>
- Bamforth CW. 1999. Beer haze. *J Am Soc Brew Chem* 57:81-90. <https://doi.org/10.1094/ASBCJ-57-0081>
- Bamforth CW. 2016. Haze measurement, p 251-256, In Bamforth CW (ed), *Brewing Materials and Processes*, Elsevier. <https://doi.org/10.1016/B978-0-12-799954-8.00012-5>
- Buiatti S. 2009. Beer composition: An overview, p 213-225, In Preedy VR (ed), *Beer in Health and Disease Prevention*, Elsevier, London, UK. <https://doi.org/10.1016/B978-0-12-373891-2.00020-1>
- Smith E, Dent, G. 2013. *Modern Raman Spectroscopy: A Practical Approach*, John Wiley & Sons, New Jersey, USA.
- Steiner E, Gastl M, Becker, T. 2011. Protein changes during malting and brewing with focus on haze and foam formation. *Eur Food Res Technol* 232:191-204. <https://doi.org/10.1007/s00217-010-1412-6>
- Kahle E-M, Zarnkow M, Jacob, F. 2019. Substances in beer that cause fluorescence. *Eur Food Res Technol* 245:2727-2737. <https://doi.org/10.1007/s00217-019-03394-x>
- Anger PM, Esch E von der, Baumann T, Elsner M, Niessner R, Ivleva, NP. 2018. Raman microspectroscopy as a tool for microplastic particle analysis. *Trends Analyt Chem* 109:214-226. <https://doi.org/10.1016/j.trac.2018.10.010>
- Shan F, Zhang X-Y, Fu X-C, Zhang L-J, Su D, Wang S-J, Wu J-Y, Zhang, T. 2017. Investigation of simultaneously existed Raman scattering enhancement and inhibiting fluorescence using surface modified gold nanostars as SERS probes. *Sci Rep* 7:1-10. <https://doi.org/10.1038/s41598-017-07311-8>
- Dvorakova M, Hulín P, Karabin M, Dostalek, P. 2007. Determination of polyphenols in beer by an effective method based on solid-phase extraction and high performance liquid chromatography with diode-array detection. *Czech J Food Sci* 25:182-188
- Pöschl M, Bauer S, Leal L, Illing S, Stretz D, Wellhoener U, Tenge C, Geiger, E. 2007. The influence of fermentation-control on the colloidal stability and the reducing power of the resulting bottom fermented beers. *Brew Sci July/Aug*:96-108
- Mejbaum-Katzenellenbogen W, Dobryszczyka W, Boguslavska-Jaworska J, Morawiecka, B. 1959. Regeneration of protein from insoluble protein-tannin compounds. *Nature* 184:1799-1800.
- Mikkelsen MS, Jespersen BM, Møller BL, Lærke HN, Larsen FH, Engelsen, SB. 2010. Comparative spectroscopic and rheological studies on crude and purified soluble barley and oat β -glucan preparations. *Food Res Int* 43:2417-2424. <https://doi.org/10.1016/j.foodres.2010.09.016>
- Philippe S, Barron C, Robert P, Devaux M-F, Saulnier L, Guillon, F. 2006. Characterization using Raman microspectroscopy of arabinoxylans in the walls of different cell types during the development of wheat endosperm. *J Agric Food Chem* 54:5113-5119. <https://doi.org/10.1021/jf060466m>
- Tuschel D. 2016. Selecting an excitation wavelength for Raman spectroscopy. *Spectrosc* 37:14-23
- Coote N, Kirsop, BH. 1976. A haze consisting largely of pentosan. *J Inst Brew* 82:34 <https://doi.org/10.1002/j.2050-0416.1976.tb03718.x>
- Gerhäuser C, Becker, H. 2009. Phenolic compounds in beer, p 124-144, In Preedy VR (ed), *Beer in Health and Disease Prevention*, Elsevier, London, UK
- Novák M, Sinytsya A, Gedeon O, Slepíčka P, Procházka V, Sinytsya A, Blahovec J, Hejlová A, Čopíková, J. 2012. Yeast $\beta(1-3)(1-6)$ -D-glucan films. *Carbohydr Polym* 87:2496-2504. <https://doi.org/10.1016/j.carbpol.2011.11.031>
- Zhu G, Zhu X, Fan Q, Wan, X. 2011. Raman spectra of amino acids and their aqueous solutions. *Spectrochim Acta A* 78:1187-1195.
- Norris L, Rathmell C, Mattley, Y. 2012. Raman spectroscopy as a quantitative tool for industry. *J Spectrosc* 27:2916-2926.
- Siebert KJ, Lynn PY, Siebert, KJ. 1997. Mechanisms of beer colloidal stabilization. *J Am Soc Brew Chem* 55:73-78. <https://doi.org/10.1094/ASBCJ-55-0073>
- Gastl M, Zarnkow M, Werner, B. 2009. Gushing - a multicausal problem! *Brauwelt Int* 27:16-20.
- Edwards HGM, Farwell DW, Jenkins R, Seaward, MRD. 1992. Vibrational Raman spectroscopic studies of calcium oxalate monohydrate and dihydrate in lichen encrustations on Renaissance frescoes. *J Raman Spectrosc* 23:185-189. <https://doi.org/10.1002/jrs.1250230310>
- Araujo CF, Nolasco MM, Ribeiro AMP, Ribeiro-Claro, PJA. 2018. Identification of microplastics using Raman spectroscopy. *Water Res* 142:426-440. <https://doi.org/10.1016/j.watres.2018.05.060>
- Käppler A, Fischer D, Oberbeckmann S, Schernewski G, Labrenz M, Eichhorn K-J, Voit, B. 2016. Analysis of environmental microplastics by vibrational microspectroscopy. *Anal Bioanal Chem* 408:8377-8391. <https://doi.org/10.1007/s00216-016-9956-3>
- Rösch P, Schmitt M, Kiefer W, Popp, J. 2003. The identification of microorganisms by micro-Raman spectroscopy. *J Mol Struct* 661:363-369. <https://doi.org/10.1016/j.molstruc.2003.06.004>
- Stöckel S, Kirchoff J, Neugebauer U, Rösch P, Popp, J. 2016. The application of Raman spectroscopy for the detection and identification of microorganisms. *J Raman Spectrosc* 47:89-109. <https://doi.org/10.1002/jrs.4844>
- Hardwick WA. 1995. The properties of beer, p 551-587, In Hardwick WA (ed), *Handbook of Brewing*, Marcel Dekker, New York, USA

3 Discussion

Turbidity identification is an important part of brewery analysis. Turbidity in beer can have many causes, and originate from a wide variety of places in the brewing process [11, 78–80]. To find this origin, it is important to identify the type of turbidity. The vibrational spectroscopic technique of RMS could offer a promising alternative to conventional analysis. It offers the advantages of a fast and straightforward method without time-consuming sample preparation [81–89]. There are no studies to date that address the identification of beer turbidity using Raman micro-spectroscopy. However, work exists in the field of wine production [90–95]. Although these scientific studies are not designed for turbidity, conclusions can be drawn about turbidity-active constituents. The main components of turbidity-active substances are polyphenols and proline-rich proteins and there are some studies on these for identification using Raman spectroscopy [96–98].

The main focus in this work has been on the particles that can cause the strongest and also most intense turbidity. The differentiation of the ingredients into the main categories described above is intended to simplify the classification of the turbidity-causing substances. Among the beverage-specific ingredients which are primarily considered by scientists to be the "top" turbidity-causing substances are: Polyphenols, proteins, β -glucans, calcium oxalates and starch. Among these, again, there are gradations and sub-substances. One of the most important representatives was chosen: The polyphenol catechin and the protein fraction gliadin. Although gliadin and catechin are not turbidity particles in themselves, they form the basis for the very common protein-polyphenol turbidity [99]. Gliadin is a protein fraction of wheat (equivalent to hordein in barley) that is high in the amino acids glutamine and proline. Catechin is a phenolic substance commonly found in beer that often forms di- or trimers called oligomeric proanthocyanidins. These two classes of substances are capable of forming insoluble turbidity particles by cross-linking with each other [11]. Identification of the particles is a useful tool to find the origin of turbidity in the brewing process and a possible starting point for solving the turbidity problem. Among the next beverage-specific substances are β -glucans. The occurrence of β -glucans in beer, which include the potentially turbid substances cellulose, yeast β -glucan and barley β -glucan, in most cases has various causes. Cellulose, for example, can enter the beer via the remnants of a paper label or as a filter breakthrough from a filtration aid. Yeast- β -glucan in beer often comes from yeast. Barley- β -glucan may be present

in beer if malt production or mashing operations are inadequate. It is important to identify these substances to narrow down their possible origin. Calcium oxalate is a substance that can lead not only to turbidity in beer, but also to other phenomena such as gushing. High molecular weight starch is a strong turbidity agent that can enter the beer, for example, due to insufficient mashing or excessive heating. Here, the arabinoxylans were investigated, which are known as cell wall polysaccharides whose turbidity potential, however, is not known exactly.

The second classification of causes of turbidity is due to external influences such as process defects or particles interacting with the medium. In addition to the raw material-related turbidity, the turbidity-causing colloids caused by particles foreign to the beer must also be taken into account. The presence of non-beer turbidity particles usually indicates errors in process control, e.g. when particles from filter aids or stabilizers break through the filter medium due to pressure surges. In addition to filter aids and stabilizers, other particles can also occur in breweries that have the potential to form turbidity [79, 100–102]. In this context, label fibers, lubricant residues from beer can lids, and plastic debris or microplastics from conveyor belts, membranes, valves, lines, or seals should be mentioned [79, 103]. The MP particles can cause turbidity due to the interaction of the product with the packaging. With the development of new analytical methods and techniques, it is possible to analyze raw materials and food products during operation. For beverage samples in particular, there is usually no risk of MP being introduced via the raw materials due to the frequent filtration steps in the closed process. Instead, most particles in beverages are due to either exposure from process plastic during production or subsequent contamination as a result of inappropriate sampling and handling methods [6]. The plastic can enter the beer during the process, e.g., through the manual addition of additives and raw materials, contaminated water in the brewhouse and fermentation cellar. It can also enter the beer during transportation and storage by crown cork joints or PET detaching from the wall of a plastic bottle [104, 105]. Numerous filter aids (cellulose, diatomaceous earth, perlite) and stabilizers (PVPP, silica gel such as Xerogel) as well as the most common MP particles (UP, PA, PE, PF, PMMA, PS, PVC, PP, PVDF, PTFE, PEEK, PET) were detected, evaluated and validated.

The first part of this dissertation addressed the diverse fluorescing beer ingredients. The predominantly organic ingredients cause primary fluorescence. These compounds can affect analysis results or fully overlay important signals as a result of their natural frequency (molecular vibrations), making measurement impossible [32, 106–109]. This is especially true for non-invasive, optical measurement methods such as RMS, which reach their limits if fluorochromes are present. With the aid of a fluorescence spectroscope, the fluorescent compounds were analyzed and identified [110, 111]. Using the PARAFAC analysis, a specific model was created that identified the three main components of the fluorescing substances [112, 113]. These components could be qualitatively assigned to the organic substances DOM, DOC or CDOM and OC by comparing with existing database literature. Using the emission and extinction spectra, these ranges could be assigned to the three aromatic amino acids phenylalanine, tryptophan and tyrosine, as well as to iso- α -acid, phenolic compounds, and the vitamin B group. The PARAFAC model explained the fluorescence of eight beers with a variance of 98.7% for three components. In addition, correlations to the fluorescence intensities (FI) could be evidenced from the EEM data by incorporating beer analyses. In particular, the correlation with the FI from Origin software could be shown for iso- α -acid ($R^2 = 0.63$). This resulted in a statistical significance of the p value $< \alpha = 0.005$ (p value: 0.00408). For the fluorescing amino acids phenylalanine, tryptophan and tyrosine, only slight correlations could be shown with the FI. There were no correlations for the phenolic compounds ferulic acid, coumaric acid and isoxanthohumol. This was also shown in the EEM spectra, as only slight differences were determined in the color ranges. The same trend was evidenced in the quantitative evaluation of the vitamins. The objective of this analysis was to study several beers and discover which organic compounds show fluorescence. In further research, some methods to avoid fluorescence were applied to ensure interference-free analysis.

Two different slide types were available for selection for analysis in further studies on this topic. Conventional glass slides showed no problems when analyzed at 532 nm. In contrast they showed strong interference spectra, when excited at 785 nm. The glass produced a strong fluorescent background that made analysis difficult. This fluorescence background could be completely avoided by using slides made of pure quartz [114]. Therefore, quartz slides are recommended for measurements at 785 nm, while conventional glass slides can be

used for measurements at 532 nm [115]. At an excitation wavelength of 532 nm, many potentially beer-clouding substances could be detected reliably and reproducibly as pure substances. These included the carbohydrates starch, wheat arabinoxylan, cellulose, yeast β -glucan and barley β -glucan. It is of particular note that RMS could distinguish the yeast and barley β -glucans, as well as cellulose. Furthermore, gliadin could be detected as a turbidity-relevant protein fraction, as well as calcium oxalate and PVPP as additional turbidity formers. The amino acids proline and glutamine, which are very frequently found in turbidity-forming proteins, as well as ferulic acid, which is also a frequent component of turbidity particles, were also reliably detected. Pure substances that are insoluble in beer (starch, cellulose, arabinoxylan, yeast β -glucan, barley β -glucan, calcium oxalate, PVPP) were used to produce artificially cloudy beer. After extracting these substances from the beer, they could still be detected without fluorescence.

Catechin as a turbidity-relevant polyphenol [116, 117], which was not detectable in the 532 nm measurements due to strong fluorescence, was easily detected using the 785 nm laser. The already weak carbohydrate spectra of barley and yeast β -glucan, as well as arabinoxylan, could hardly be evaluated at 785 nm. The trub particles extracted directly from force-aged beer could not be analyzed with neither the 532 nm laser nor the 785 nm laser due to strong fluorescence. In addition to identifying trub substances, it is also very important to differentiate them. Beer contains a large number of different substances which can interfere with Raman measurement by autofluorescence [32]. Artificial beer turbidity was created with the substances that are difficult to dissolve or which are insoluble in beer. These substances were subsequently removed from the beer. The aim of this method was to test whether the particles were still easily identifiable after contact with beer or whether any fluorescent impurities adsorbed onto them and impaired the measurement. Similarity matrices and dendrograms were created to identify the particles, each comparing a 5-fold determination ($n = 5$) of beer particles with uncontaminated pure substances. In addition, spectra were identified using the KnowItAll algorithm.

Particles of arabinoxylan, cellulose, starch, yeast β -glucan, barley β -glucan, PVPP and calcium oxalate were investigated. Arabinoxylan, yeast β -glucan, and barley β -glucan could not be identified by the algorithm, as in the validation of the pure substance spectra, but showed

high similarities with comparable spectra in literature [57-59]. It was also possible to distinguish the three β -glucans by the double peak between 1000 and 1200 $\text{rel. } 1/\text{cm}$. Good agreement with the reference spectra was observed for starch (97.0 %), cellulose (96.7 %), calcium oxalate (97.92 %), and PVPP (96.6 %). With exception of the cellulose and calcium oxalate spectra, all recorded data from the beer contact samples showed high uniformity within their substance class. However, the lack of uniformity of the calcium oxalate spectra is due to the presence of the monohydrate and dihydrate forms, each of which split into uniform groups. The poor reproducibility of the cellulose spectra is possibly due to the ability of the material to adsorb a wide variety of organic and inorganic materials [63]. These impurities could produce single, small peaks that still allow unambiguous identification of the substance but lead to peak matching discrepancies in a direct comparison.

To differentiate the particles, a cluster analysis was carried out with all the data on the spectra of the pure substances and on the pure substances after contact with beer. The aim of the analysis was to test to what extent and with what certainty the individual particles can be distinguished. The cluster analysis is based on peak matching. Similarities and differences are thus represented primarily on the basis of common peaks.

The dendrogram created from the cluster analysis (Figure 6) shows that especially PVPP (violet), starch (brown) and calcium oxalate (light blue) form compact groups that are clearly distinguishable from all other substances. The group of β -glucans is also clearly visible, consisting of yeast β -glucan, barley β -glucan and cellulose, grouped at the upper branches of the dendrogram. Closely grouped below are the other carbohydrates arabinoxylan and starch. The peak matching algorithm can distinguish the carbohydrates from each other as far as possible. Starch, in particular, can be clearly distinguished from all the others. Only the individual outliers show problems, with representatives from each carbohydrate group settling in the dendrogram between calcium oxalate and PVPP. Such outliers are especially possible in spectra with very weak signal strength, since here peaks often hardly stand out from the signal noise and are thus not detected. On the other hand, it is also possible that noise is detected as a peak.

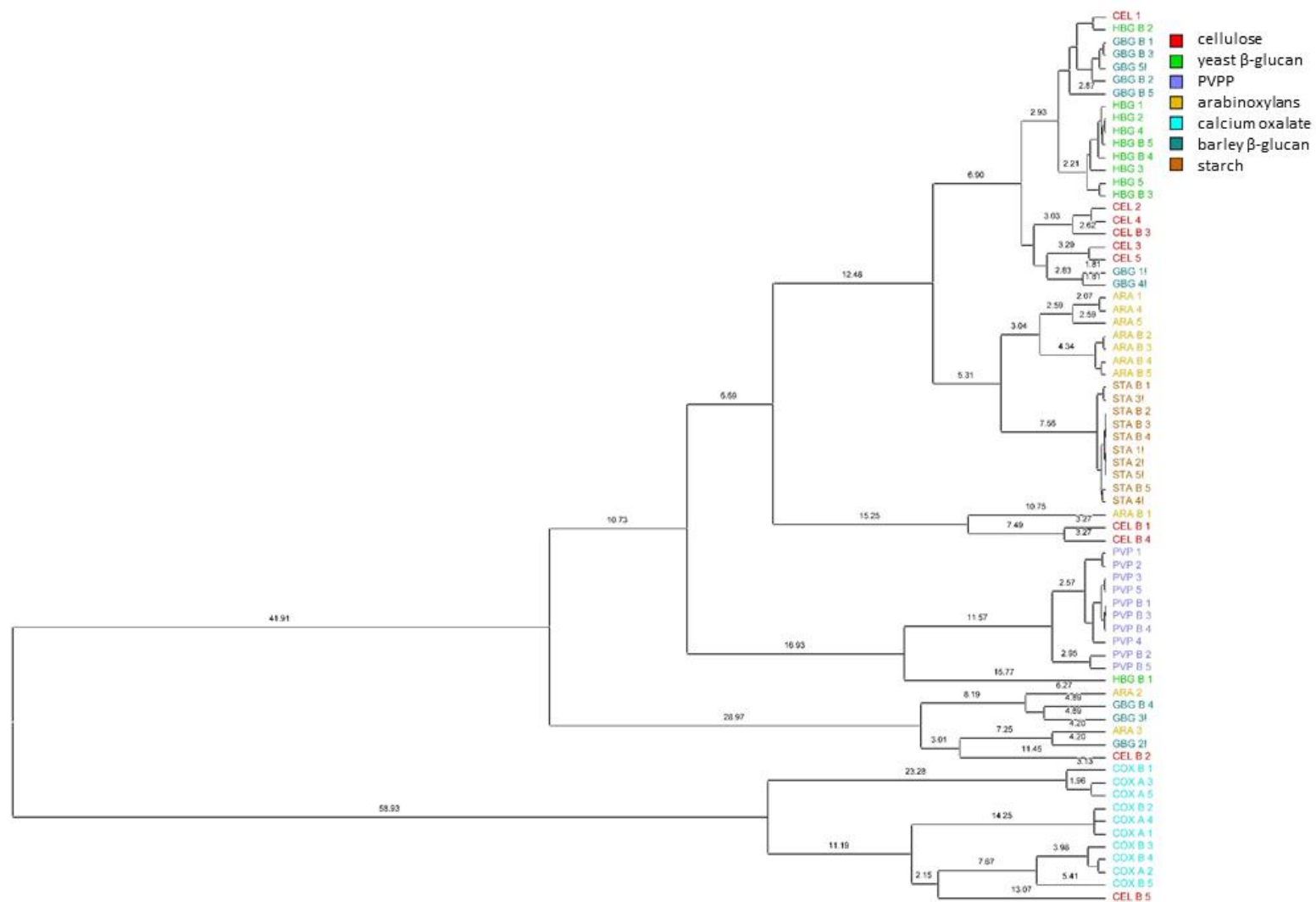


Figure 6 Dendrogram of all pure substance and beer contact spectra at 532 nm

Due to the more intense Raman scattering at shorter wavelengths, the spectra recorded at 532 nm were usually much more intense. Nevertheless, some substances can also be detected reproducibly at 785 nm. In this work, however, the 785 nm laser was only indispensable for the analysis of catechin (see Table 2).

Table 2 Quality of pure substance spectra

substance	λ 532 nm	λ 785 nm
starch	[++]	[++]
cellulose	[++]	[+]
barley β -glucan	[+]	[-]
yeast β -glucan	[+]	[-]
arabinoxylans	[+]	[-]
gliadin	[++]	[-]
bentonite	[- -]	[- -]
catechin	[- -]	[++]
proline	[++]	[++]
glutamine	[++]	[++]
ferulic acid	[++]	[++]
calcium oxalate	[++]	[++]
PVPP	[++]	[++]

The analysis of some substances proved to be very difficult with the 785 nm laser. In particular, the weak carbohydrate spectra caused problems. While starch and cellulose could still be identified with reproducible results, arabinoxylan, barley β -glucan and yeast β -glucan could not be analyzed. Despite long optimization trials and summed exposure times of up to 300 s, no analyzable spectra were obtained. Although the available reference spectra made it possible to roughly classify the investigated substances as carbohydrates, no reliable identification could be made due to the very poor signal to noise ratio. In addition, the results were hardly reproducible. Similar problems arose in the analysis of gliadin. Although a similarity of 87.6 % with the reference spectrum of wool (collagen) could be determined, these results were also not reproducible to a sufficient degree.

Furthermore, in this work, attention was paid to the non-beer particles: A method to identify microplastics in beverages was established, tested and validated using polymer standard suspensions. In order to make the results reproducible and comparable, the standard test parameters were empirically determined and tested. The design of the methodology included the preparation of polymer standards, the design of a sampling/preparation procedure, the selection of suitable membrane filters, and the validation of the measurement method. Various polymer samples of the most common types of plastics were tested, as well as some high-performance plastics from food production. The polymers were manually crushed to generate spectral data of the respective substances in the dry state. These served as reference spectra in later experiments. The substance-specific peaks were matched with corresponding literature values and included in the existing database.

The thermal load capacity of each polymer sample was also checked by iteratively increasing the intensity of the laser power. Based on the given experimental parameters, a filtration apparatus was designed and fabricated. Different types of filters were analyzed to select suitable membrane filters. These differed in the substrate material, the filter thickness and the coating of the filter surface. The sampled filters were validated against a requirements profile drawn up from the previous literature research. To this end, the filters were tested for their tendency to emit fluorescence signals and for their thermal load capacity. This also served to empirically determine the analysis parameters required for the automatic analysis and identification of unknown polymer particles. The procedure for automatic particle detection was created via the imaging software and realized by saturation differentiation of neighboring pixels. Adaptation to various particle parameters, such as shape or size of the particles or visibility in transmitted light, was performed on a sample-specific basis. The inverted design of the microscope resulted in a relatively large area in the Z-direction between the slides used, which was clearly outside the focal plane. This allowed particles of all sizes to fall out of the focal plane and thus falsify the results. Furthermore, penetrations and displacements of the filter membranes in the X-Y-Z direction occurred as a result of the filter fixation between the slides. The automatic particle detection was strongly influenced by these factors and had to be adjusted and limited accordingly. During the analysis of the polymer samples on the selected membrane filters, small particles within the sample were manually approached and focused. Video images and image scans were created of these particles,

which were then evaluated using the Cluster Analysis and True Component Analysis program functions. When evaluating the data, it became apparent that Cluster Analysis mainly detected polymer samples that tended to emit fluorescence signals. These included primarily the dyed and pigmented polymers, which showed strong fluorescence signals even at a low intensity. The remaining polymers showed higher CCD-counts only in some subregions or at significantly stronger laser settings, which were suitable for generating average spectra. For the suitability test of the analysis as well as the final selection of the most suitable membrane filter type, the spectra of the polymer particles on the previously validated filters were compared with the reference spectra of the dry polymer samples and plotted in similarity matrices. Similarity values ranging from 0 % to 92.26 % were found. However, due to the analogous structural makeup of many polymers, the unambiguous identification of unknown particles is necessary to detect possible sources of contamination within manufacturing processes.

The results of this work show that Raman micro-spectroscopy can be a potent technique for the identification and differentiation of a wide variety of beer-turbid substances. Most particles can be easily detected by excitation at 523 nm even after contact with beer. In some cases, the use of alternative wavelengths may also be advantageous. If the full range of beer-turbid particles is to be covered, measures are needed to minimize the autofluorescence of some turbid particles or to bypass the fluorescence. In particular, particles extracted from beer with complex and unknown composition pose problems in this regard.

Identification and differentiation of particles via peak matching based cluster analysis can lead to cases that can be quickly detected by visual inspection of the spectra. If visual inspection of the data is to be dispensed with, a database algorithm that compares the spectra with reference spectra on the basis of various features can be a useful alternative, or a good addition. Already, Raman microspectroscopy is a useful extension of conventional turbidity analysis. In particular, the differentiation of structurally closely related carbohydrates is comparatively easy using this method. In the future, the acquisition of Raman spectra could completely replace conventional turbidity analysis. Combined with complete turbidity analysis, a significant portion of brewery and beverage analysis could be performed quickly and without much sample preparation using only one instrument.

However, to achieve this aim, it is necessary to eliminate the fluorescence problems that occur with some substances and often in biological material. In addition, a way must be found to distinguish and identify spectra with high statistical significance. This creates the need for the construction of an appropriate spectra database.

The main goal of this dissertation was to show how beer-inherent and non-beer turbidity particles can be detected and identified. Numerous turbidity-active substances can be investigated and identified using Raman micro-spectroscopy. Depending on the method and the type of particles investigated, this can be done without much sample preparation or even non-invasively. However, for some samples, problems arise due to fluorescence. For other substances, turbidity residues must first be obtained and examined in solid form, or in the case of microbiological turbidity, samples must first be obtained and incubated. Confocal Raman micro-spectroscopy could be well suited to determine turbidity in beer and other alcoholic and non-alcoholic beverages in the future in a time-saving and reliable way. By using suitable wavelengths matched to the different turbidity-relevant substances, it would be possible to examine bottled beverages non-invasively and to initiate countermeasures at an early stage in order to avoid impairments of the colloidal stability and to extend the shelf life of beverages. In summary, the identification was successful.

5 Appendix

5.1 Oral presentations with first authorship

Kahle, E.M., Zarnkow, Martin; Jacob, Fritz: "Trübungsidentifizierung in Bier" BrauBeviale 2019, Nürnberg, 12.11.2019

Kahle, E.M., Zarnkow, Martin, Jacob, Fritz: "Trübungsidentifizierung in Bier" BrauBeviale 2019, Nürnberg, 13.11.2019

Kahle, E.M., Zarnkow, Martin, Jacob, Fritz: "Trübungsidentifizierung in Bier" BrauBeviale 2019, Nürnberg, 14.11.2019

Kahle, E.M., Zarnkow, Martin, Jacob, Fritz: "Trübungspaket -Mikroskopie, Enzymatik und Raman" 14. Weihenstephaner Praxisseminar, Bayreuth, 25.10.2019

Kahle, E.M., Zarnkow, Martin, Jacob, Fritz: "Turbidity Identification in Beer via Raman Micro Spectroscopy (TI-RMS)" Young Scientist Symposium, Bitburg, 14. September 2018

Kahle, E.M., Zarnkow, Martin, Jacob, Fritz: "Raman Mikroskopie" 6. Seminar Hefe und Mikrobiologie, Freising-Weihenstephan, 13.–14. März 2018

5.2 Poster presentations with first authorship

Kahle, E.M., Zarnkow, Martin; Jacob, Fritz: "Turbidity identification in beer via Raman micro spectroscopy (RMS)" 37th EBC Congress 2019 Antwerp, Belgium

5.3 Non-reviewed papers

Schneiderbanger, H., Kahle, E.M., Zarnkow, M., Coelhan, M., Jacob, F.: "N-Nitrosodimethylamin in Malz: Blick auf Gerstensorten und Anbauggebiete". Brauwelt 49: 1446-1450, 2017

E.-M. Kahle, J. Heintges, M. Zarnkow, F. Jacob: "Bierspezifische Trübungen und deren Identifizierung mittels Raman-Mikrospektroskopie – Eine Übersicht der Möglichkeiten" Der Weihenstephaner S. 30-32

5.4 Permission of publishers for imprints of publications

Kahle, E.M., Zarnkow, M., Jacob, F. (2019) **“Substances in beer that cause fluorescence: evaluating the qualitative and quantitative determination of these ingredients.”** European Food Research and Technology, 245(12), 2727-2737
DOI: 10.1007/s00217-019-03394-x

Kahle, E.M., Zarnkow, M., Jacob, F. (2020) **“Investigation and identification of foreign turbidity particles in beverages via Raman micro-spectroscopy”** European Food Research and Technology
DOI: 10.1007/s00217-020-03647-0

Von: [Thomas Henle](#)
An: [Kahle, Eva-Maria](#)
Betreff: Re: Permission of publication
Datum: Donnerstag, 19. November 2020 14:25:35
Anlagen: [image001.png](#)

OK, permission granted...

Best regards,
Thomas Henle

--

Prof. Dr. Thomas Henle
Technische Universität Dresden
Chair of Food Chemistry
Chemistry Building, Room 412
Bergstrasse 66
D-01062 Dresden, Germany
Tel.: +49(0)351-463-34647
Fax: +49(0)351-463-34138
E-mail: thomas.henle@tu-dresden.de
Internet: <http://www.chm.tu-dresden.de/lc1/>

Von: "Kahle, Eva-Maria" <eva.maria.kahle@tum.de>
Datum: Donnerstag, 19. November 2020 um 14:21
An: "Thomas.Henle@chemie.tu-dresden.de" <Thomas.Henle@chemie.tu-dresden.de>
Betreff: Permission of publication

Dear Mr. Professor Henle,

I would like to ask for permission to use my published paper (DOI: 10.1007/s00217-020-03647-0 and DOI: 10.1007/s00217-019-03394-x) as secondary publication in my dissertation.

Thank you,
best regards
Eva-Maria Kahle

Dipl.-Ing. Eva-Maria Kahle
Forschung und Entwicklung
Research and Development

[Forschungszentrum Weihenstephan
für Brau- und Lebensmittelqualität](#)
Alte Akademie 3
85354 Freising-Weihenstephan
DEUTSCHLAND / GERMANY
Tel. / Phone: +49 8161 71-5627

Kahle, E.M., Zarnkow, M., Jacob, F. (2020) “**Beer Turbidity Part 1: A Review of Factors and Solutions**” Journal of the American Society of Brewing Chemists, DOI: 10.1080/03610470.2020.1803468

Kahle, E.M., Zarnkow, M., Jacob, F. (2020) “**Beer Turbidity Part 2: A Review of Raman Spectroscopy and Possible Future Use for Beer Turbidity Analysis**” Journal of the American Society of Brewing Chemists, DOI: 10.1080/03610470.2020.1800345

Von: [Sonnie, Laura](#)
An: [Inge Russell](#)
Cc: [Kahle, Eva-Maria; jasbceditor@gmail.com \(jasbceditor@gmail.com\)](#)
Betreff: RE: Permission for publication - just double checking on that OK to put her PhD thesis
Datum: Montag, 19. Oktober 2020 16:03:36
Anlagen: [image001.png](#)
[AcceptedAuthorPublishingAgreement_JASBC_1803468.pdf](#)

Correct. No written permission is needed for this purpose. Eva-Maria, attached is the author agreement with the list of full rights in case you need it (see Sec 4. viii).

Best,
Laura Sonnie
Production Supervisor

From: Inge Russell <irussell@Alltech.com>
Sent: Monday, October 19, 2020 9:30 AM
To: Sonnie, Laura <laura.sonnies@taylorandfrancis.com>
Cc: eva.maria.kahle@tum.de; jasbceditor@gmail.com (jasbceditor@gmail.com)
<jasbceditor@gmail.com>
Subject: FW: Permission for publication - just double checking on that OK to put her publication into her PhD thesis

Hi Laura,
Can you confirm that Eva-Maria does not need any additional permission from us to include her own two publications in her PhD thesis.
I know I have asked this question before but just want to confirm that I remember correctly to ensure she does not run into any issues.
Cheers
Inge

Eva-Maria – double checking for you – Inge

From: Kahle, Eva-Maria <eva.maria.kahle@tum.de>
Sent: Saturday, October 17, 2020 7:11 AM
To: Inge Russell <irussell@Alltech.com>
Subject: Permission for publication

Dear Inge,

I would like to ask for permission to use my published papers as secondary publication in my dissertation. Can you help me?

<https://doi.org/10.1080/03610470.2020.1803468>
<https://doi.org/10.1080/03610470.2020.1800345>

Thank you,
best regards
Eva-Maria Kahle

Kahle, E.M., Zarnkow, M., Jacob, F. (2020) “**Identification and differentiation of haze substances using Raman microspectroscopy**” Journal of the Institute of Brewing, DOI 10.1002/jib.627

Von: [jib.journal](#)
An: [Kahle, Eva-Maria](#)
Betreff: Re: Permission of publication
Datum: Montag, 19. Oktober 2020 13:21:23
Anlagen: [image001.png](#)

Dear Dr. Kahle,

Thank you for your email. You can use it as a reference in your dissertation.

Regards,

Nandhinie Kalaivanan
Editorial Assistant
Journal of the Institute of Brewing

From: Kahle, Eva-Maria <eva.maria.kahle@tum.de>
Sent: Saturday, October 17, 2020 10:55 AM
To: jib.journal <jib.journal@wiley.com>
Subject: Permission of publication

This is an external email.

Dear Nandhinie Kalaivanan,

I would like to ask for permission to use my published paper (DOI 10.1002/jib.627) as secondary publication in my dissertation.

Thank you,
best regards
Eva-Maria Kahle

Dipl.-Ing. Eva-Maria Kahle
Forschung und Entwicklung
Research and Development

Forschungszentrum Weihenstephan
für Brau- und Lebensmittelqualität
Alte Akademie 3
85354 Freising-Weihenstephan
DEUTSCHLAND / GERMANY
Tel. / Phone: +49 8161 71-5627
Fax: +49 8161 71-4181
Email: eva.maria.kahle@tum.de
Internet: <http://www.blq-weihenstephan.de>

References

1. Back W (2008) Ausgewählte Kapitel der Brauereitechnologie. Hans Carl Fachverlag, Nürnberg
2. Narziß L, Back W, Gastl M et al. (2017a) Das fertige Bier: Abriss der Bierbrauerei. Abriss der Bierbrauerei:361–414
3. Kahle E-M, Zarnkow M, Jacob F (2020) Beer Turbidity Part 1: A Review of Factors and Solutions. ASBCJ:1–16. <https://doi.org/10.1080/03610470.2020.1803468>
4. MEBAK (ed) (2012) Würze, Bier, Biermischgetränke (Band 2): Methodensammlung der Mitteleuropäischen Brautechnischen Analysenkommission.
5. Diniz P., Menzel V, Nüter C et al. Trübungsanalyse: Aktuelle Methoden und neue Möglichkeiten. Brauerei Forum November 2013:12–15
6. Nimwegen F (2017) Trübungsmessung in Kompaktbauform. Brauwelt 157:51–52
7. Bamforth CW (2016) Haze measurement. In: Bamforth CW (ed) Brewing Materials and Processes. Elsevier, pp 251–256
8. Hartmann K (2006) Bedeutung rohstoffbedingter Inhaltsstoffe und produktionstechnologischer Einflüsse auf die Trübungsproblematik im Bier, Technische Universität München
9. Kusche M (2005) Kolloidale Trübungen in untergärigen Bieren – Entstehung, Vorhersage und Stabilisierungsmaßnahmen
10. Mastanjević K, Krstanović V, Lukinac J et al. (2018) Beer-The Importance of colloidal stability (non-biological haze). Fermentation 4:91
11. Steiner E, Gastl M, Becker T (2010) Turbidity and haze formation in beer - insights and overview. J Inst Brew 116:360–368. <https://doi.org/10.1002/j.2050-0416.2010.tb00787.x>
12. Hartmann K (2006) Bedeutung rohstoffbedingter Inhaltsstoffe und produktionstechnologischer Einflüsse auf die Trübungsproblematik im Bier
13. Butler HJ, Ashton L, Bird B et al. (2016) Using Raman spectroscopy to characterize biological materials. Nature protocols 11:664–687
14. Tolstik T, Marquardt C, Matthäus C et al. (2014) Discrimination and classification of liver cancer cells and proliferation states by Raman spectroscopic imaging. Analyst 139:6036–6043
15. Colomban P, Tournie A, Bellot-Gurlet L (2006) Raman identification of glassy silicates used in ceramics, glass and jewellery: A tentative differentiation guide. J Raman Spectrosc 37:841–852. <https://doi.org/10.1002/jrs.1515>
16. Bolwien C, Sulz G (2010) Raman-Mikrospektrometer zur Untersuchung biologischer Proben. tm-Technisches Messen Plattform für Methoden, Systeme und Anwendungen der Messtechnik 77:437–444. <https://doi.org/10.1524/teme.2010.0037>
17. Dele-Dubois, M., P. Dhamelincourt, J. Poirot, H. Schubnel (1986) Differentiation between gems and synthetic minerals by laser Raman microspectroscopy. Journal of Molecular Structure:135–138
18. Kong L, Zhang P, Li Y-q et al. (2011) Multifocus confocal Raman microspectroscopy for rapid single-particle analysis. Journal of biomedical optics 16:120503
19. Thygesen LG, Løkke MM, Micklander E et al. (2003) Vibrational microspectroscopy of food. Raman vs. FT-IR. Trends in Food Science & Technology 14:50–57
20. Raman CV, Krishnan KS (1928) A new type of secondary radiation. Nature 121:501–502
21. Ferraro JR (2003) Introductory raman spectroscopy. Elsevier
22. Ferraro, JR, Nakamoto K, Brown CW (2003) Book Introductory Raman Spectroscopy. Amsterdam, The Netherland

23. Stiles PL, Dieringer JA, Shah NC et al. (2008) Surface-enhanced Raman spectroscopy. *Annu. Rev. Anal. Chem.* 1:601–626
24. Schröder B (1985) *Physikalische Methoden in der Chemie*. VCH
25. Käßler A, Fischer D, Oberbeckmann S et al. (2016) Analysis of environmental microplastics by vibrational microspectroscopy: FTIR, Raman or both? *Anal Bioanal Chem* 408:8377–8391. <https://doi.org/10.1007/s00216-016-9956-3>
26. Schmitt M, Popp J (2006) Raman spectroscopy at the beginning of the twenty-first century. *J. Raman Spectrosc.*
27. Schmitt M, Popp J *Raman-Spektroskopie - ein leistungsstarkes Werkzeug für biomedizinische Forschung*
28. Schmitt M, Popp J *Raman-Spektroskopie - Biomedizinische Diagnostik*
29. Petry R, Schmitt M, Popp J (2003) Raman Spectroscopy—A Prospective Tool in the Life Sciences. *Chemphyschem*:14–30
30. Smekal A (1923) Zur quantentheorie der dispersion. *Naturwissenschaften* 11:873–875
31. Turrell G, Corset J (1996) *Raman microscopy: developments and applications*. Academic Press
32. Kahle E-M, Zarnkow M, Jacob F (2019) Substances in beer that cause fluorescence: Evaluating the qualitative and quantitative determination of these ingredients. *Eur Food Res Technol* 245:2727–2737. <https://doi.org/10.1007/s00217-019-03394-x>
33. Smith E, Dent G (2005) *Modern raman spectroscopy: A practical approach*. Hoboken, John Wiley & Sons
34. Smith E, Dent G (2013) *Modern Raman spectroscopy: A practical approach*. John Wiley & Sons, New Jersey, USA
35. Hesse M, Meier H, Zeeh B et al. (2016) *Spektroskopische Methoden in der organischen Chemie, 9., überarbeitete und erweiterte Auflage*. Georg Thieme Verlag, Stuttgart, New York
36. WITEC (2017b) *Solutions for High-Resolution - Confocal Raman Microscopy*. Ulm.
37. Calin MA, Parasca SV, Savastru R et al. (2013) Optical techniques for the noninvasive diagnosis of skin cancer. *Journal of cancer research and clinical oncology* 139:1083–1104
38. Jenkins AL, Larsen RA, Williams TB (2005) Characterization of amino acids using Raman spectroscopy. *Spectrochimica Acta Part A: Molecular and Biomolecular Spectroscopy* 61:1585–1594
39. Larkin P (2017) *Infrared and Raman spectroscopy: principles and spectral interpretation*. Elsevier
40. Wiercigroch E, Szafraniec E, Czamara K et al. (2017) Raman and infrared spectroscopy of carbohydrates: A review. *Spectrochimica Acta Part A: Molecular and Biomolecular Spectroscopy* 185:317–335
41. Förster T (1982) *Fluoreszenz organischer verbindungen*. Vandenhoeck & Ruprecht
42. Sikorska E, Górecki T, Khmelinskii IV et al. (2004) Fluorescence Spectroscopy for Characterization and Differentiation of Beers. *Journal of the Institute of Brewing* 110:267–275. <https://doi.org/10.1002/j.2050-0416.2004.tb00621.x>
43. Sikorska E, Górecki T, Khmelinskii IV et al. (2006) Monitoring beer during storage by fluorescence spectroscopy. *Food Chemistry* 96:632–639. <https://doi.org/10.1016/j.foodchem.2005.02.045>
44. Sikorska E, Górecki T, Khmelinskii IV et al. (2005) Classification of edible oils using synchronous scanning fluorescence spectroscopy. *Food Chemistry* 89:217–225. <https://doi.org/10.1016/j.foodchem.2004.02.028>

45. Sikorska E, Gliszczyńska-Swigło A, Insińska-Rak M et al. (2008) Simultaneous analysis of riboflavin and aromatic amino acids in beer using fluorescence and multivariate calibration methods. *Anal Chim Acta* 613:207–217. <https://doi.org/10.1016/j.aca.2008.02.063>
46. Sikorska E, Khmelinskii I, Sikorski M (2009) Fluorescence methods for analysis of beer. In: *Beer in Health and Disease Prevention*. Elsevier, pp 963–976
47. Druet SAJ, Taran J-PE (1981) CARS spectroscopy. *Progress in quantum Electronics* 7:1–72
48. Wiesheu AC (2017) Raman-Mikrospektroskopie zur Analyse von organischen Bodensubstanzen und Mikroplastik, Technische Universität München
49. Kühler P (2015) Oberflächenverstärkte Spektroskopie mit plasmonisch gekoppelten Goldnanopartikeln, Imu
50. Song L, Hennink EJ, Young IT et al. (1995) Photobleaching kinetics of fluorescein in quantitative fluorescence microscopy. *Biophysical journal* 68:2588–2600
51. am Macdonald, Wyeth P (2006) On the use of photobleaching to reduce fluorescence background in Raman spectroscopy to improve the reliability of pigment identification on painted textiles. *Journal of Raman Spectroscopy: An International Journal for Original Work in all Aspects of Raman Spectroscopy, Including Higher Order Processes, and also Brillouin and Rayleigh Scattering* 37:830–835
52. Wei D, Chen S, Liu Q (2015) Review of fluorescence suppression techniques in Raman spectroscopy. *Applied Spectroscopy Reviews* 50:387–406
53. Horiba: (2019) What laser wavelengths are used for Raman spectroscopy? <http://www.horiba.com/uk/scientific/products/raman-spectroscopy/raman-academy/raman-faqs/what-laser-wavelengths-are-used-for-raman-spectroscopy/>
54. Horiba: (2019) [Duplikat] What laser wavelengths are used for Raman spectroscopy? <http://www.horiba.com/uk/scientific/products/raman-spectroscopy/raman-academy/raman-faqs/what-laser-wavelengths-are-used-for-raman-spectroscopy/>
55. Horiba: (2019) What are the advantages and disadvantages of ultra-violet (UV) lasers for Raman? <https://www.horiba.com/uk/scientific/products/raman-spectroscopy/raman-academy/raman-faqs/what-are-the-advantages-and-disadvantages-of-ultra-violet-uv-lasers-for-raman/>
56. Bright FV, Hieftje GM (1986) A new technique for the elimination of fluorescence interference in Raman spectroscopy. *Appl Spectrosc* 40:583–587
57. Johnson G, Donnelly BJ, Johnson DK (1968) The chemical nature and precursors of clarified apple juice sediment. *Journal of Food Science* 33:254–257
58. Siebert KJ, Lynn PY, Siebert KJ (1997) Mechanisms of beer colloidal stabilization. *J Am Soc Brew Chem* 55:73–78. <https://doi.org/10.1094/ASBCJ-55-0073>
59. Asano K, Shinagawa K, Hashimoto N et al. (1982) Characterization of haze-forming proteins of beer and their roles in chill haze formation. *Journal of the American Society of Brewing Chemists* 40:147–154
60. Siebert KJ (1999) Effects of protein- polyphenol interactions on beverage haze, stabilization, and analysis. *J Agric Food Chem* 47:353–362. <https://doi.org/10.1021/jf980703o>
61. Siebert KJ, Carrasco A, Lynn PY (1996) Formation of protein- polyphenol haze in beverages. *J Agric Food Chem* 44:1997–2005
62. Siebert KJ, Lynn PY (2000) Effect of protein-polyphenol ratio on the size of haze particles. *ASBCJ* 58:117–123
63. Siebert KJ, Lynn PY (2008) On the mechanisms of adsorbent interactions with haze-active proteins and polyphenols. *ASBCJ* 66:48–54

64. Siebert KJ, Lynn PY (2003) Effects of alcohol and pH on protein-polyphenol haze intensity and particle size. *ASBCJ* 61:88–98
65. Siebert KJ, Lynn PY (1998) Comparison of polyphenol interactions with polyvinylpyrrolidone and haze-active protein. *Journal of the American Society of Brewing Chemists*:24–31
66. Thompson CC, Forward E (1969) European Brewery convention: haze and foam group. Towards the chemical prediction of shelf life. *Journal of the Institute of Brewing* 75:37–42
67. Kuchel L, Brody AL, Wicker L (2006) Oxygen and its reactions in beer. *Packaging Technology and Science: An International Journal* 19:25–32
68. Bamforth CW (1999) Beer haze. *J Am Soc Brew Chem* 57:81–90. <https://doi.org/10.1094/ASBCJ-57-0081>
69. Letters R (1969) Haze and foam group origin of carbohydrate in beer sediments. *Journal of the Institute of Brewing* 1969:54–60
70. Lewis MJ, Poerwantaro WM Release of Haze Material from the Cell Walls of Agitated Yeast, vol 1991
71. Gjertsen P (1966) Beta-glucans in malting and brewing. I. Influence of beta-glucans on the filtration of strong beers. In: *Proceedings. Annual meeting-American Society of Brewing Chemists*, vol 24, pp 113–120
72. Bamforth CW (2009) Current perspectives on the role of enzymes in brewing. *Journal of cereal science* 50:353–357
73. Bamforth CW, Martin HL (1983) The degradation of β -glucan during malting and mashing: The role of β -Glucanase. *Journal of the Institute of Brewing* 89:303–307
74. Greif P, Schildbach R (1978) Investigations on the oxalic acid problem in the brewery. *Monatsschr. Brauwiss* 31:275–280
75. Gastl M, Zarnkow M, Werner B (2009) Gushing-a multicausal problem! *Brauwelt International* 27:16–20
76. Steiner E, Gastl M, Becker T (2011) Die Identifizierung von Trübungen in Bier (1). *Brauwelt* 2011:161–166
77. Steiner E, Gastl M, Becker T Die Identifizierung von Trübungen in Bier (2). *Brauwelt* 2011:193–205
78. Bishop LR (1975) HAZE-AND FOAM-FORMING SUBSTANCES IN BEER. *Journal of the Institute of Brewing* 81:444–449
79. Steiner E, Arendt EK, Gastl M et al. (2011) Influence of the malting parameters on the haze formation of beer after filtration. *Eur Food Res Technol* 233:587–597. <https://doi.org/10.1007/s00217-011-1547-0>
80. Asano K, Ohtsu K, Shinagawa K et al. (2014) Affinity of Proanthocyanidins and Their Oxidation Products for Haze-forming Proteins of Beer and the Formation of Chill Haze. *Agricultural and Biological Chemistry* 48:1139–1146. <https://doi.org/10.1080/00021369.1984.10866300>
81. Bunaciu AA, Aboul-Enein HY, Hoang VD (2015) Raman spectroscopy for protein analysis. *Applied Spectroscopy Reviews* 50:377–386
82. Agarwal UP, Atalla RH (1995) FT Raman spectroscopy: What it is and what it can do for research on lignocellulosic materials. In: *Proc. 8th Intl. Symp. Wood Pulp. Chem*, vol 8, pp 67–72
83. Noothalapati H, Sasaki T, Kaino T et al. (2016) Label-free chemical imaging of fungal spore walls by Raman microscopy and multivariate curve resolution analysis. *Scientific reports* 6:27789

84. Anger PM, Esch E von der, Baumann T et al. (2018) Raman microspectroscopy as a tool for microplastic particle analysis. *Trends Analyt Chem* 109:214–226. <https://doi.org/10.1016/j.trac.2018.10.010>
85. Wiesheu AC, Anger PM, Baumann T et al. (2016) Raman microspectroscopic analysis of fibers in beverages. *Anal. Methods* 8:5722–5725. <https://doi.org/10.1039/c6ay01184e>
86. Araujo CF, Nolasco MM, Ribeiro AMP et al. (2018) Identification of microplastics using Raman spectroscopy: Latest developments and future prospects. *Water Res* 142:426–440. <https://doi.org/10.1016/j.watres.2018.05.060>
87. Soares FLF, Ardila JA, Carneiro RL (2017) Thin-layer chromatography-surface-enhanced Raman spectroscopy and chemometric tools applied to Pilsner beer fingerprint analysis. *J Raman Spectrosc* 48:943–950. <https://doi.org/10.1002/jrs.5168>
88. Piot O, Autran J-C, Manfait M (2001) Investigation by confocal Raman microspectroscopy of the molecular factors responsible for grain cohesion in *thriticum aestivum* bread wheat. Role of the cell walls in the starchy endosperm. *Journal of cereal science* 34:191–205
89. Prasad M, Kumar A, Atta DK et al. (2014) Spectrofluorometric analysis of organic matter in the Sundarban mangrove, Bangladesh
90. dos Santos CAT, Pascoa RN, Lopes JA (2017) A review on the application of vibrational spectroscopy in the wine industry: From soil to bottle. *TrAC Trends in Analytical Chemistry* 88:100–118
91. Gallego ÁL, Guesalaga AR, Bordeu E et al. (2010) Rapid measurement of phenolics compounds in red wine using Raman spectroscopy. *IEEE Transactions on Instrumentation and Measurement* 60:507–512
92. Mandrile L, Zeppa G, Giovannozzi AM et al. (2016) Controlling protected designation of origin of wine by Raman spectroscopy. *Food Chemistry* 211:260–267
93. Rodriguez SB, Thornton MA, Thornton RJ (2013) Raman spectroscopy and chemometrics for identification and strain discrimination of the wine spoilage yeasts *Saccharomyces cerevisiae*, *Zygosaccharomyces bailii*, and *Brettanomyces bruxellensis*. *Appl. Environ. Microbiol.* 79:6264–6270
94. Rodriguez SB, Thornton MA, Thornton RJ (2017) Discrimination of wine lactic acid bacteria by Raman spectroscopy. *Journal of industrial microbiology & biotechnology* 44:1167–1175
95. Silva MA, Ky I, Jourdes M et al. (2012) Rapid and simple method for the quantification of flavan-3-ols in wine. *Eur Food Res Technol* 234:361–365
96. Johannessen C, Kapitán J, Collet H et al. (2009) Poly (L-proline) II helix propensities in poly (L-lysine) dendrigraft generations from vibrational Raman optical activity. *Biomacromolecules* 10:1662–1664
97. Zhu G, Zhu X, Fan Q et al. (2011) Raman spectra of amino acids and their aqueous solutions. *Spectrochim Acta A* 78:1187–1195
98. Pompeu DR, Larondelle Y, Rogez H et al. (2018) Caractérisation et discrimination des composés phénoliques à l'aide de la spectroscopie Raman à transformée de Fourier et des outils chimiométriques. *Biotechnologie, Agronomie, Société et Environnement* 22:13–28
99. Steiner E, Gastl M, Becker T (2011) Protein changes during malting and brewing with focus on haze and foam formation: A review. *Eur Food Res Technol* 232:191–204. <https://doi.org/10.1007/s00217-010-1412-6>
100. Basarova G (1990) The structure-function relationship of polymeric sorbents for colloid stabilization of beer. *Food structure* 9:1

101. Hartmann K, Kreis S, Zarnkow M et al. (2004) Identifizierung von Filterhilfsmitteln nach den einzelnen Filtrationsschritten. *Der Weihenstephaner* 4:141–143
102. Leiper KA, Stewart GG, McKeown IP (2003) Beer Polypeptides and Silica Gel Part I. Polypeptides Involved in Haze Formation. *Journal of the Institute of Brewing* 109:57–72. <https://doi.org/10.1002/j.2050-0416.2003.tb00594.x>
103. Sharpe FR, Channon PJ Beer Haze Caused by Can Lid Lubricant. *Institute of Brewing* 1987:163
104. Kaiser W (2015) *Kunststoffchemie für Ingenieure: Von der Synthese bis zur Anwendung*. Carl Hanser Verlag GmbH Co KG
105. Schymanski D, Goldbeck C, Humpf H-U et al. (2018) Analysis of microplastics in water by micro-Raman spectroscopy: Release of plastic particles from different packaging into mineral water. *Water Research* 129:154–162. <https://doi.org/10.1016/j.watres.2017.11.011>
106. Demčenko AP (2015) *Introduction to fluorescence sensing*, Second edition. Springer, Cham, Heidelberg, New York NY, Dordrecht, London
107. BASCHONG W, LANDMANN L (eds) (2006) *Cell Biology Chapter 1 - Fluorescence Microscopy*. Elsevier
108. Huang YY, Beal CM, Cai WW et al. (2010) Micro-Raman spectroscopy of algae: Composition analysis and fluorescence background behavior. *Biotechnol Bioeng* 105:889–898. <https://doi.org/10.1002/bit.22617>
109. Huang Y-S, Karashima T, Yamamoto M et al. (2004) Raman spectroscopic signature of life in a living yeast cell. *J Raman Spectrosc* 35:525–526. <https://doi.org/10.1002/jrs.1219>
110. Antonov M, Lenhardt L, Manojlović D et al. (2016) Changes of Color and Fluorescence of Resin Composites Immersed in Beer. *J Esthet Restor Dent* 28:330–338. <https://doi.org/10.1111/jerd.12232>
111. Apperson K, Leiper KA, McKeown IP et al. (2002) Beer Fluorescence and the Isolation, Characterisation and Silica Adsorption of Haze-Active Beer Proteins. *Journal of the Institute of Brewing* 108:193–199. <https://doi.org/10.1002/j.2050-0416.2002.tb00540.x>
112. Andersen CM, Bro R (2003) Practical aspects of PARAFAC modeling of fluorescence excitation-emission data. *Journal of Chemometrics: A Journal of the Chemometrics Society* 17:200–215
113. Gordon R, Cozzolino D, Chandra S et al. (2017) Analysis of Australian Beers Using Fluorescence Spectroscopy. *Beverages* 3:57. <https://doi.org/10.3390/beverages3040057>
114. Kerr LT, Hennelly BM (2016) A multivariate statistical investigation of background subtraction algorithms for Raman spectra of cytology samples recorded on glass slides. *Chemometrics and Intelligent Laboratory Systems* 158:61–68. <https://doi.org/10.1016/j.chemolab.2016.08.012>
115. Tuschel D (2016) Selecting an excitation wavelength for Raman spectroscopy. *Spectroscopy* 31:14–23
116. Walters MT, Heasman AP, Hughes PS (1997) Comparison of (+)-catechin and ferulic acid as natural antioxidants and their impact on beer flavor stability. Part 2: Extended storage trials. *J. Am. Soc. Brew. Chem* 55:91–98
117. Shahidi F, Naczk M (2004) *Phenolics in food and nutraceuticals*. CRC Press, Boca Raton, Fla.